

Bowley, Hannah E. (2013) Iodine dynamics in the terrestrial environment. PhD thesis, University of Nottingham.

Access from the University of Nottingham repository:

http://eprints.nottingham.ac.uk/13241/1/Iodine_dynamics_in_the_terrestrial_environment_-_Hannah_Bowley.pdf

Copyright and reuse:

The Nottingham ePrints service makes this work by researchers of the University of Nottingham available open access under the following conditions.

- Copyright and all moral rights to the version of the paper presented here belong to the individual author(s) and/or other copyright owners.
- To the extent reasonable and practicable the material made available in Nottingham ePrints has been checked for eligibility before being made available.
- Copies of full items can be used for personal research or study, educational, or not-for-profit purposes without prior permission or charge provided that the authors, title and full bibliographic details are credited, a hyperlink and/or URL is given for the original metadata page and the content is not changed in any way.
- Quotations or similar reproductions must be sufficiently acknowledged.

Please see our full end user licence at:

http://eprints.nottingham.ac.uk/end_user_agreement.pdf

A note on versions:

The version presented here may differ from the published version or from the version of record. If you wish to cite this item you are advised to consult the publisher's version. Please see the repository url above for details on accessing the published version and note that access may require a subscription.

For more information, please contact eprints@nottingham.ac.uk

**IODINE DYNAMICS
IN THE TERRESTRIAL ENVIRONMENT**

HANNAH E. BOWLEY MChem (hons.), MSc.

**Thesis submitted to the University of Nottingham
for the degree of doctor of philosophy**

JULY 2013

ABSTRACT

The aim of this work was to investigate the effect of soil properties on soil iodine dynamics and uptake to plants. Soil and vegetation samples were collected from across eastern Northern Ireland (NI) to form the basis of most experimental work; samples from the Rothamsted Park Grass archive were used to investigate the role of changing soil chemistry through time and due to selected fertiliser applications; and iodine dynamics in humic acid (HA) were studied to improve understanding of the role of organic matter in soils. Input of iodine in rainfall was considered in the context of samples from both locations, and the additional influences of coastal proximity, soil type and underlying geology were reviewed for the NI samples. Total iodine analysis was carried out using extraction with TMAH and quantification by ICP-MS; aqueous iodine speciation was determined using HPLC and SEC coupled with ICP-MS.

The most important iodine inputs to both soil and vegetation were found to be directly from the sea in coastally-exposed locations, and from rainfall in other cases. Soil organic matter (measured as soil organic carbon, SOC) was determined to be involved in both retaining a portion of recalcitrant iodine in soil and HA, and in promoting sorption of both iodide and iodate in highly organic soils. Metal oxides (Fe, Mn and Al) were found to be important in rapid sorption of iodate to soils with $\text{SOC} \leq 38\%$, and there was an indication that they may be involved in promoting the reaction of iodide with organic matter.

Replenishment of a transient phyto-available pool was essential for provision of iodine to vegetation. The availability of recently added iodine (as $^{129}\text{IO}_3^-$) in the pot experiment was controlled by its sorption onto the solid phase, and near-constant input from irrigation water was the major source of vegetation iodine in most cases. Rainfall was shown to be important in controlling vegetation iodine concentrations in field situations. In soils collected from very coastally-exposed locations, the soil iodine concentration was extremely high and therefore a greater proportion of labile native iodine was available for uptake; irrigation sources were much less important.

This work improves understanding of soil iodine dynamics and the important factors controlling iodine speciation and availability to plants. Results can be used to inform practices regarding provision of iodine to crops for both humans and grazing animals.

ACKNOWLEDGEMENTS

First and foremost I would like to say thank you to my husband Neil, for having the vision and belief in me to suggest that I do a PhD in the first place, and for all his love, support, encouragement, and most of all understanding through the tough times. Thank you to my parents for their constant love and support, for nodding and smiling when I try to explain the technical stuff to them, and for being proud of me even when it's not clear exactly what I'm doing. Thank you to Lyn and Steve for looking after me during my trips to Nottingham in the last 6 months.

Of course I could not have completed this PhD without the help of my supervisors. So, thank you to Scott for almost always having the time to answer queries and discuss ideas; to Liz, for your technical and very important pastoral support; to Michael, for encouraging me to have confidence and take control when necessary; to Neil, for being enthusiastic about my modelling even when lab work 'got in the way', and for interpreting the slightly cryptic OpenModel error codes for me; and to Louise, for explaining the wonders of Arc GIS, and for an enjoyable sampling trip to Northern Ireland. Thank you all for helping this PhD progress satisfactorily despite there being six of us being involved!

Finally thanks go to Vicky Moss-Hayes at BGS Keyworth for providing the organic carbon measurements on the Northern Ireland samples; to Darren Hepworth and John Corrie for providing technical support; and for administrative support, to Emma Hooley, Sue Golds and at BGS, June Wright.

TABLE OF CONTENTS

Abstract.....	2
Acknowledgements	3
Table of contents	4
Table of figures.....	9
Table of tables	19
Glossary.....	22
1 INTRODUCTION.....	24
1.1 Iodine deficiency.....	24
1.1.1 Preventing IDD's	26
1.1.2 Understanding iodine dynamics	28
1.2 Iodine in the environment.....	28
1.2.1 Iodine in soil.....	30
1.2.1.1 Volatilisation.....	32
1.2.1.2 Microbial influence on soil iodine	32
1.2.2 Iodine uptake by plants.....	32
1.3 Aims.....	34
2 MATERIALS AND METHODS	35
2.1 Introduction.....	35
2.2 Northern Ireland sample collection.....	35
2.2.1 Sample processing and storage.....	35
2.3 Iodine analysis	36
2.3.1 Iodine extraction.....	36
2.3.2 ICP-MS for iodine quantification.....	38
2.3.3 Solution phase iodine speciation	40
2.3.4 Solid phase iodine speciation	41
2.4 Characterisation methods.....	41
2.4.1 Soil pH.....	41
2.4.2 Soil organic carbon.....	41
2.4.3 Dissolved organic carbon	42
2.4.4 Extraction of metal oxides from soil	42
2.4.5 Total iodine extraction.....	42
2.5 Use of ¹²⁹ I.....	43

2.6	ICP-MS analysis	43
2.6.1	Analysis for metal oxides	44
2.6.2	Iodine analysis	44
2.6.2.1	Total iodine	44
2.6.2.2	Iodine speciation	44
3	TOTAL IODINE IN NORTHERN IRELAND FIELD SAMPLES	46
3.1	Introduction.....	46
3.2	Materials and methods	47
3.3	Results and discussion	47
3.3.1	Total iodine in soil.....	52
3.3.2	Total iodine in vegetation.....	57
3.3.3	Total iodine in rainfall	63
3.3.4	Site-specific inputs of iodine	68
3.4	Conclusions.....	68
4	IODINE DYNAMICS IN NORTHERN IRELAND SOILS	70
4.1	Introduction.....	70
4.1.1	Aims	71
4.2	Materials and methods	71
4.3	Results and discussion	72
4.3.1	Organic iodine in solution	75
4.3.2	Transformation between inorganic species	78
4.4	Modelling iodine dynamics	79
4.4.1	Model structure and fitting	79
4.4.2	Model development	81
4.4.3	Results of modelling.....	81
4.5	Linking model parameters to soil properties	90
4.5.1	Parameters related to reaction mechanisms.....	90
4.5.2	Fate of iodide	92
4.5.2.1	Instantaneous partitioning to solid	92
4.5.2.2	Equilibrium with iodine on solid.....	94
4.5.2.3	Equilibrium with OrgI in solution.....	94
4.5.3	Fate of iodate	95

4.5.3.1	Instantaneous partitioning to the soil solid phase	96
4.5.3.2	Instantaneous partitioning to OrgI in solution	97
4.5.3.3	Reduction to iodide	98
4.5.4	Model predicting iodine dynamics from soil properties.....	99
4.6	Conclusions.....	105
5	IODINE DYNAMICS IN HUMIC ACID	107
5.1	Introduction.....	107
5.1.1	Aims	108
5.2	Materials and methods	108
5.3	Results and discussion	109
5.3.1	Rates of reaction	114
5.3.2	Production of Org ¹²⁹ I.....	118
5.4	Modelling iodine dynamics in humic acid.....	123
5.4.1	Model development	123
5.4.2	Final model description	124
5.4.3	Results of modelling.....	129
5.4.3.1	Unavailable iodine	129
5.4.3.2	Comparison to soil dynamics	130
5.5	Conclusions.....	130
6	POT TRIAL TO MEASURE UPTAKE OF IODINE FROM NORTHERN IRELAND SOILS BY RYEGRASS	132
6.1	Introduction.....	132
6.1.1	Aims	134
6.2	Materials and methods	134
6.2.1	Pot trial structure	134
6.2.1.1	Growing conditions and maintenance.....	134
6.2.1.2	Grass harvesting	135
6.2.2	Grass and soil analysis.....	135
6.2.2.1	Total iodine analysis	136
6.2.2.2	Iodine speciation	136
6.2.2.3	Dissolved organic carbon (DOC).....	136

6.3	Results and discussion	136
6.3.1	Total iodine in soil and grass.....	136
6.3.2	Effect of yield on iodine concentration	143
6.3.3	Spike / non-spike ratios in grass and soil	146
6.3.4	Contribution of irrigation water to phyto-available iodine.....	149
6.3.5	Comparison of concentration ratios measured in the field and pot trial 157	
6.3.6	Spike / non-spike ratios in soil solution	159
6.3.7	Iodine speciation in soil solution.....	162
6.3.8	Phyto-availability of solution iodine	170
6.4	Modelling uptake from soil to grass	171
6.4.1	Preliminary model structure and fitting.....	172
6.4.2	Model development	175
6.4.3	Final grass uptake model	176
6.4.4	Discussion of fitted results	181
6.5	Conclusions.....	184
7	TOTAL IODINE IN SOILS AND VEGETATION FROM THE ROTHAMSTED PARK GRASS EXPERIMENT	187
7.1	Introduction.....	187
7.2	Materials and methods	187
7.2.1	Sample characterisation.....	189
7.3	Results and discussion	191
7.3.1	Soil pH.....	194
7.3.2	Soil iodine concentration	194
7.3.3	Vegetation iodine.....	201
7.4	Stepwise regression to predict vegetation iodine.....	210
7.5	Conclusions.....	211
8	CONCLUSIONS.....	213
8.1	Iodine interactions with soil.....	213
8.2	Iodine uptake by grass	214
8.3	Implications for provision of dietary iodine	215
8.4	Future work.....	216
	REFERENCES	217
	Appendix 1: Northern Ireland sampling information.....	230

Appendix 2: Results of soil iodine dynamics experiment	238
Appendix 3: Soil iodine dynamcis model	246
Appendix 4: Soil iodine dynamcis array model	249
Appendix 5: Results of iodine dynamics experiment in humic acid	254
Appendix 6: Humic acid iodine dynamics model	259
Appendix 7: Grass uptake model	263

TABLE OF FIGURES

Figure 3.1. Geological Survey of Northern Ireland Tellus survey iodine topsoil map showing soil, vegetation and rainfall sampling locations (after Smyth and Johnson, 2011). Also locations of some geographical features noted in text.....	48
Figure 3.2. Relationship between coastal proximity and total iodine in Northern Irish soil (I_S); samples arranged in descending coastal proximity. Error bars represent standard error ($n = 3$). Axis for total iodine has been limited to 50 mg I kg^{-1} in order to show lower concentrations. Values for NI05 and NI08 exceed the scale and are 274 and 127 mg I kg^{-1} respectively.	53
Figure 3.3. Soil iodine content (I_S) as a function of soil type. I_S values are mean of three replicates for measurement of each soil within the class (comprising ‘n’ soils) and error bars show standard error of the same. The two coastal soils (NI05 and NI08) are excluded.....	54
Figure 3.4. Soil iodine content (I_S) as a function of soil texture (field observation) and ordered by increasing I_S . I_S values are mean of three replicates for measurement of each soil within the class (comprising ‘n’ soils) and error bars show standard error of the same. The two coastal soils (NI05 and NI08) are excluded.	55
Figure 3.5. Relationship between total soil iodine (I_S) and soil organic carbon (SOC). The two coastal soils (NI05 and NI08) are excluded.	56
Figure 3.6. Relationship between total soil iodine (I_S) and soil pH. The two coastal soils (NI05 and NI08) are excluded.....	56
Figure 3.7. Relationship between total iodine in soil (I_S) and total iodine in (unwashed) vegetation (I_V). Error bars show the standard error of triplicate analyses. The two coastal soils (NI05 and NI08) are excluded.	61
Figure 3.8. Relationship of vegetation iodine concentration (I_V) with A) soil organic carbon (SOC) and B) soil pH. The two coastal soils (NI05 and NI08) are excluded.	62
Figure 3.9. Relationship between rainfall volume and iodine concentration in rain (I_R).	65
Figure 3.10. Relationship between total annual rainfall and soil iodine (I_S) concentration. Error bars show standard error of three replicates. The two coastal soils (NI05 and NI08) are excluded.....	65
Figure 4.1. Change in the concentration of spike iodine in solution ($^{129}I_L$) with time, following addition equivalent to $500 \mu\text{g }^{129}\text{I kg}^{-1}$ as iodide. Data points represent	

individual soils; error bars show standard error of triplicate measurements for each soil. 74

Figure 4.2. Change in the concentration of spike iodine in solution ($^{129}\text{I}_L$) with time, following addition equivalent to $500 \mu\text{g } ^{129}\text{I kg}^{-1}$ as iodate. Data points represent individual soils; error bars show standard error of triplicate measurements for each soil. 74

Figure 4.3. Relationship between DOC and native iodine in solution ($^{127}\text{I}_L$), following addition of $500 \mu\text{g } ^{129}\text{I kg}^{-1}$ as iodide and iodate. Data points represent individual soils and species incubated for 1, 3, 7 or 24 hr; error bars show standard error of triplicate measurements for each sample. 75

Figure 4.4. Change in the concentration of ^{129}I species in solution with time, following addition of $500 \mu\text{g } ^{129}\text{I kg}^{-1}$ as iodide (left-hand column) or iodate (right-hand column). Species measured include iodide ($^{129}\text{I}_L$; A and B), iodate ($^{129}\text{IO}_3^-$; C and D) and organic iodine (Org ^{129}I ; E and F). Soils are classed as ‘coastal’ (blue circles), ‘organic’ (orange circles) and ‘mineral’ (black circles). Data points represent individual soils; error bars show standard error of triplicate measurements for each soil. Notice that Y-axis scales are unique to each graph. 77

Figure 4.5. Relationship between DOC and spike iodine in solution ($^{129}\text{I}_L$), following addition of $500 \mu\text{g } ^{129}\text{I kg}^{-1}$ as iodide and iodate. Data points represent individual soils and species added after 24 hr incubation; error bars show standard error of triplicate measurements for each sample. Box encloses samples from soil NI20. 78

Figure 4.6. Conceptual model describing iodine dynamics in soil. 80

Figure 4.7. Comparison of measured and modelled concentrations of iodine species for **Model A**. Solid and open symbols denote iodide- and iodate-spiked soils respectively. Data includes measurements made after 1 hr (\circ, \bullet), 3 hr (\square, \blacksquare), 7 hr (Δ, \blacktriangle) and 24 hr (\diamond, \blacklozenge). The solid line represents a 1:1 relation. 85

Figure 4.8. Comparison of measured and modelled concentrations of iodine species for **Model B**. Solid and open symbols denote iodide- and iodate-spiked soils respectively. Data includes measurements made after 1 hr (\circ, \bullet), 3 hr (\square, \blacksquare), 7 hr (Δ, \blacktriangle) and 24 hr (\diamond, \blacklozenge). The solid line represents a 1:1 relation. 86

Figure 4.9. Results of modelling data for soil NI01 applying Models A and B to both iodide- and iodate-spiked suspensions, as indicated. The three variables measured and modelled are $^{129}\text{I}_L$ (closed circles; solid line), $^{129}\text{IO}_3^-$ (shaded circles; dotted line) and

$^{129}\text{I}^-_{\text{L}}$ (open circles; dashed line). Error bars show mean coefficient of variance on measured values.....	87
Figure 4.10. Results of modelling data for soil NI03 applying Models A and B to both iodide- and iodate-spiked suspensions, as indicated. The three variables measured and modelled are $^{129}\text{I}_{\text{L}}$ (closed circles; solid line), $^{129}\text{IO}_3^-_{\text{L}}$ (shaded circles; dotted line) and $^{129}\text{I}^-_{\text{L}}$ (open circles; dashed line). Error bars show mean coefficient of variance on measured values.	88
Figure 4.11. Results of modelling data for soil NI05 applying Models A and B to both iodide- and iodate-spiked suspensions, as indicated. The three variables measured and modelled are $^{129}\text{I}_{\text{L}}$ (closed circles; solid line), $^{129}\text{IO}_3^-_{\text{L}}$ (shaded circles; dotted line) and $^{129}\text{I}^-_{\text{L}}$ (open circles; dashed line). Error bars show mean coefficient of variance on measured values.	89
Figure 4.12. Comparison of relationship between A) fitted kd and pH, and B) fitted log(kd) and pH.....	93
Figure 4.13. Relationship between fitted values of kd2 and kd3 for Model B.....	95
Figure 4.14. Comparison of relationship between A) fitted kd2 and pH, and B) fitted log(kd2) and pH.....	97
Figure 4.15. Relationship between fitted k5 and Al content of soils.....	99
Figure 4.16. Comparison of measured and modelled concentrations of (A) $^{129}\text{I}_{\text{L}}$, (B) $^{129}\text{I}^-_{\text{L}}$ and (C) $^{129}\text{IO}_3^-_{\text{L}}$ for the Array Model using soil properties to predict rate parameters and partition coefficients. Spiked ^{129}I was added as iodide (solid symbols) or iodate (open symbols); equilibration times were 1 hr (circles), 3 hr (squares), 7 hr (triangles) and 24 hr (diamonds). The solid line is the 1:1 relationship.....	102
Figure 4.17. Array Model fits for soil NI01, utilising optimised rate parameters and partition coefficients determined by soil properties: A) iodide added, B) iodate added. Data and model fits include: $^{129}\text{I}_{\text{L}}$ (closed circles; solid line), $^{129}\text{IO}_3^-_{\text{L}}$ (shaded circles, dotted line) and $^{129}\text{I}^-_{\text{L}}$ (open circles, dashed line). Error bars show mean coefficient of variance on measured values. Error bars not visible are within the symbol.	103
Figure 4.18. Array Model fits for soil NI03, utilising optimised rate parameters and partition coefficients determined by soil properties: A) iodide added, B) iodate added. Data and model fits include: $^{129}\text{I}_{\text{L}}$ (closed circles; solid line), $^{129}\text{IO}_3^-_{\text{L}}$ (shaded circles, dotted line) and $^{129}\text{I}^-_{\text{L}}$ (open circles, dashed line). Error bars show mean coefficient of variance on measured values. Error bars not visible are within the symbol.	104

Figure 4.19. Array Model fits for soil NI05, utilising optimised rate parameters and partition coefficients determined by soil properties: A) iodide added, B) iodate added. Data and model fits include: $^{129}\text{I}_L$ (closed circles; solid line), $^{129}\text{IO}_3^-_L$ (shaded circles, dotted line) and $^{129}\text{I}^-_L$ (open circles, dashed line). Error bars show mean coefficient of variance on measured values. Error bars not visible are within the symbol. 105

Figure 5.1. Change in ^{129}I concentrations with time following spiking with ^{129}I as **iodide** at a range of concentrations: A) $22.1 \mu\text{g I L}^{-1}$ added, B) $44.1 \mu\text{g I L}^{-1}$ added, C) $88.2 \mu\text{g I L}^{-1}$ added. Species measured included $^{129}\text{I}^-$ (red symbols), $^{129}\text{IO}_3^-$ (yellow symbols) and Org^{129}I (blue symbols); the purple and red lines represent the measured and expected sum of ^{129}I species respectively. Error bars show standard error of triplicate measurements. 111

Figure 5.2. Change in ^{129}I concentrations with time following spiking with ^{129}I as **equal concentrations of iodide and iodate** at a range of total concentrations: A) $22.1 \mu\text{g I L}^{-1}$ added, B) $44.1 \mu\text{g I L}^{-1}$ added, C) $88.2 \mu\text{g I L}^{-1}$ added. Species measured included $^{129}\text{I}^-$ (red symbols), $^{129}\text{IO}_3^-$ (yellow symbols) and Org^{129}I (blue symbols); the purple and red lines represent the measured and expected sum of ^{129}I species respectively. Error bars show standard error of triplicate measurements. 112

Figure 5.3. Change in ^{129}I concentrations with time following spiking with ^{129}I as **iodate** at a range of concentrations: A) $22.1 \mu\text{g I L}^{-1}$ added, B) $44.1 \mu\text{g I L}^{-1}$ added, C) $88.2 \mu\text{g I L}^{-1}$ added. Species measured included $^{129}\text{I}^-$ (red symbols), $^{129}\text{IO}_3^-$ (yellow symbols) and Org^{129}I (blue symbols); the purple and red lines represent the measured and expected sum of ^{129}I species respectively. Error bars show standard error of triplicate measurements. 113

Figure 5.4. Change in concentration of Org^{129}I with time following addition of ^{129}I as iodide (red symbols), iodate (yellow symbols) and a mixed spike (blue symbols). Total concentrations of added ^{129}I include: A) $22.1 \mu\text{g I L}^{-1}$, B) $44.1 \mu\text{g I L}^{-1}$ and C) $88.2 \mu\text{g I L}^{-1}$. Error bars show standard error of triplicate measurements. Note that y axis scales differ. 116

Figure 5.5. Change in the ratio of (measured iodide)/(added iodide) with time, following addition of iodide (red symbols) and mixed iodide/iodate ^{129}I spikes (blue symbols). Total concentrations of ^{129}I added were: $22.1 \mu\text{g I L}^{-1}$ (circles), $44.1 \mu\text{g I L}^{-1}$ (squares) and $88.2 \mu\text{g I L}^{-1}$ (triangles). Error bars show standard error of triplicate measurements. 117

Figure 5.6. Change in ratio of (measured iodate)/(added iodate) with time, following addition of iodate (yellow symbols) and mixed iodide/iodate ^{129}I spikes (blue symbols). Total concentrations of ^{129}I added were: $22.1 \mu\text{g I L}^{-1}$ (circles), $44.1 \mu\text{g I L}^{-1}$ (squares) and $88.2 \mu\text{g I L}^{-1}$ (triangles). Error bars show standard error of triplicate measurements. 117

Figure 5.7. Size exclusion chromatograms of humic acid incubated for 26 hr with $88.2 \mu\text{g }^{129}\text{I L}^{-1}$ as A) iodide, B) a mixed spike of iodide and iodate and C) iodate. Black lines show ^{127}I ; coloured lines show ^{129}I . Both isotopes have been background corrected. Lines are moving averages of detected values, over 20 points. 120

Figure 5.8. Size exclusion chromatograms of humic acid incubated for 26 hr with $88.2 \mu\text{g }^{129}\text{I L}^{-1}$ as A) iodide, B) a mixed spike of iodide and iodate and C) iodate. Black lines show ^{127}I , coloured dots show ratio of $^{127}\text{I}/^{129}\text{I}$ at each time point. Red line shows overall ratio of $^{127}\text{I}/^{129}\text{I}$ in the sample. Values have been background corrected. 121

Figure 5.9. Size exclusion chromatograms of humic acid incubated for 1855 hr with $88.2 \mu\text{g }^{129}\text{I L}^{-1}$ as A) iodide, B) a mixed spike of iodide and iodate, and C) iodate. Black lines show ^{127}I , coloured dots show ratio of $^{127}\text{I}/^{129}\text{I}$ at each time point. Red line shows overall ratio of $^{127}\text{I}/^{129}\text{I}$ in sample. Values have been background corrected. 122

Figure 5.10. Conceptual model describing iodine transformations in the presence of HA. Spike and native iodine allowed independent description of their dynamic behaviour. 123

Figure 5.11. Results of Model 4 when $^{129}\text{I}^-$ was added at concentrations of $22.1 \mu\text{g I L}^{-1}$ (20 ppb, circles), $44.1 \mu\text{g I L}^{-1}$ (40 ppb, squares) and $88.2 \mu\text{g I L}^{-1}$ (80 ppb, triangles); see Table 5.1. Measured data and modelled lines are shown for ^{127}I (closed symbols, solid lines) and ^{129}I (open symbols; dashed lines). Species include iodide (red symbols), iodate (yellow symbols) and OrgI (blue symbols). Error bars show coefficient of variance on measured values; where not visible they are within the symbol. 125

Figure 5.12. Results of Model 4 when $^{129}\text{IO}_3^-$ was added at concentrations of $22.1 \mu\text{g I L}^{-1}$ (20 ppb, circles), $44.1 \mu\text{g I L}^{-1}$ (40 ppb, squares) and $88.2 \mu\text{g I L}^{-1}$ (80 ppb, triangles); see Table 5.1. Measured data and modelled lines are shown for ^{127}I (closed symbols, solid lines) and ^{129}I (open symbols; dashed lines). Species include iodide (red symbols), iodate (yellow symbols) and OrgI (blue symbols). Error

bars show coefficient of variance on measured values; where not visible they are within the symbol.	126
Figure 5.13. Results of Model 4 when equal concentrations of $^{129}\text{I}^-$ and $^{129}\text{IO}_3^-$ were added at total concentrations of $22.1 \mu\text{g I L}^{-1}$ (20 ppb, circles), $44.1 \mu\text{g I L}^{-1}$ (40 ppb, squares) and $88.2 \mu\text{g I L}^{-1}$ (80 ppb, triangles); see Table 5.1. Measured data and modelled lines are shown for ^{127}I (closed symbols, solid lines) and ^{129}I (open symbols; dashed lines). Species include iodide (red symbols), iodate (yellow symbols) and OrgI (blue symbols). Error bars show coefficient of variance on measured values; where not visible they are within the symbol.	127
Figure 5.14. Comparison of modelled and measured concentrations of iodine when ^{129}I was added at total concentrations of $22.1 \mu\text{g I L}^{-1}$ (circles), $44.1 \mu\text{g I L}^{-1}$ (squares) and $88.2 \mu\text{g I L}^{-1}$ (triangles) as iodide, iodate and a mixed spike; see Table 5.1. Isotopes are ^{127}I (closed symbols) and ^{129}I (open symbols) measured as the species: iodide (red symbols), iodate (yellow symbols) and OrgI (blue symbols).	128
Figure 6.1. Concentrations of $^{127}\text{I}_G$ for each ryegrass cut; the LOD ($0.0139 \text{ mg I kg}^{-1}$) is shown by a red line. Error bars represent the standard error of triplicate pots for each soil.	140
Figure 6.2. Concentrations of $^{129}\text{I}_G$ for each ryegrass cut; the LOD ($0.0005 \text{ mg I kg}^{-1}$) is shown by a red line. Error bars represent the standard error of triplicate pots for each soil.	141
Figure 6.3. Relationship between ^{127}I iodine in grass ($^{127}\text{I}_G$) and in soil ($^{127}\text{I}_S$). Error bars show standard error of three replicates for each soil and each cut.	142
Figure 6.4. Relationship between ^{129}I in grass ($^{129}\text{I}_G$) and soil ($^{129}\text{I}_S$). Error bars show standard error of three replicates for each soil and each cut.	143
Figure 6.5. Grass yield for each soil and each cut. Error bars show standard error of triplicate pots.	144
Figure 6.6. Relationship between ^{127}I in grass ($^{127}\text{I}_G$) and growth rate (GR). Samples in box are from NI05 (cuts 1 – 4) and NI08 (cuts 1 and 4). Error bars show standard error of triplicate measurements.	145
Figure 6.7. Relationship between ^{129}I in grass ($^{129}\text{I}_G$) and growth rate (GR). Error bars show standard error of triplicate measurements.	145
Figure 6.8. Grass/soil ratio for each cut: $\text{I}_{G/S} = (^{129}\text{I}_G / ^{127}\text{I}_G) / (^{129}\text{I}_S / ^{127}\text{I}_S)$. Error bars represent standard error of three replicates for each cut and soil.	148

Figure 6.9. Estimated percentage of iodine in grass originating from irrigation water ($I_{G(Ir,E)}$). Mean $I_{G(Ir,E)}$ values for each cut from three replicates of 17 soils (standard deviation shown by error bars): NI01 – NI20 excluding NI05 and NI08 (all values negative) and NI16 (not included in experiment).....	151
Figure 6.10. Comparison of the actual iodine provision from irrigation water ($I_{G(Ir,A)}$) and estimated irrigation contribution to total iodine in grass ($I_{G(Ir,E)}$), both expressed as a percentage of the total iodine uptake. Error bars show triplicate values for each soil, for cut 4 only. Negative values have been omitted for clarity.....	153
Figure 6.11. Comparison of ^{127}I -CR and ^{129}I -CR for each soil, for each of four cuts. Error bars show standard error of triplicate pots. Note y-axis scales.....	156
Figure 6.12. Relationship between concentration ratios of ^{127}I in pot and field samples. Error bars show standard error of three pots (pot samples) and triplicate measurements (field samples).	157
Figure 6.13. Solution/soil ratio ($I_{L/S}$) for each soil. Error bars show standard error of three replicates. Dashed line is at $I_{L/S} = 1$	160
Figure 6.14. Relationship between $^{129}\text{I}_G / ^{127}\text{I}_G$ and $^{129}\text{I}_L / ^{127}\text{I}_L$ for cut 4 values. The box includes values for NI10 and NI17; the dashed box includes values from NI05 and NI08; red line is the 1:1 trend.....	162
Figure 6.15. Examples of typical size exclusion chromatograms for ^{127}I . Chromatograms are offset by 0.1×10^4 counts per second to allow clear comparison. Red – NI13a; blue – NI17a; green – NI20a.....	164
Figure 6.16. Examples of typical size exclusion chromatograms for ^{129}I . Chromatograms are offset by 0.1×10^4 counts per second to allow clear comparison. Red – NI02a; blue – NI04a; green – NI05a.....	164
Figure 6.17. Relationship between $^{127}\text{I}_L$ and DOC in soil solution (NI05 not shown: DOC = 93.2 mg I L^{-1} , $^{127}\text{I} = 1210 \text{ } \mu\text{g I L}^{-1}$).	165
Figure 6.18. Size exclusion chromatograms of ^{127}I in soil solution with four clear organic peaks. Chromatograms are offset by 1×10^4 counts per second to allow clear comparison. Red – NI08a; blue – NI07a; green – NI05a.	167
Figure 6.19. Size exclusion chromatograms of ^{127}I in soil solution where separation within organic peak is suggested. Chromatograms are offset by 0.2×10^4 counts per second to allow clear comparison. Red – NI11a; blue – NI15a.	168
Figure 6.20. Size exclusion chromatograms of ^{127}I in soil solution from soil not used in pot experiment: four clear organic peaks less clear. Chromatograms are offset by 1	

x 10 ⁴ counts per second to allow clear comparison. Red – NI08a; blue – NI07a; green – NI05a.	169
Figure 6.21. Relationship between grass/soil ratio for cut 4 ($I_{G/S}$) and liquid/soil ratio ($I_{L/S}$). Red line is 1:1 line. Solid box includes NI05 and NI08.	171
Figure 6.22. Conceptual model of iodine dynamics in a soil-grass system. $^{127}\text{IO}_3^-$ is not represented in solution as it was never observed. $^{129}\text{IO}_3^-$ in solution is included as it was the form in which ^{129}I was added for the pot trial. The values of the coefficients a, b, and c depended on the isotope and were varied as part of method development, as described in the main text.	172
Figure 6.23. Conceptual model of iodine dynamics in a soil-grass system, showing optimised rate parameters.	176
Figure 6.24. Change in the cumulative amount of iodine in grass with time, for Iodine-129 ($^{129}\text{I}_{G,C}$; A and C) and Iodine-127 ($^{127}\text{I}_{G,C}$; B and D), following ryegrass cultivation on soil spiked with 64.1 g $^{129}\text{I ha}^{-1}$ as iodate. Results for NI01 (A and B), a mineral soil; and NI03 (C and D), an example of a soil with a relatively poor fit to the model. Error bars show standard error of triplicate measurements for each harvest. Notice that Y-axis scales are unique to each graph.	178
Figure 6.25. Change in the cumulative amount of iodine in grass with time, for Iodine-129 ($^{129}\text{I}_{G,C}$; A and C) and Iodine-127 ($^{127}\text{I}_{G,C}$; B and D), following ryegrass cultivation on soil spiked with 64.1 g $^{129}\text{I ha}^{-1}$ as iodate. Results for NI05 (A and B), a coastal soil; and NI09 (C and D), an organic soil. Error bars show standard error of triplicate measurements for each harvest. Notice that Y-axis scales are unique to each graph.	179
Figure 6.26. Comparison of modelled and measured weights of ^{127}I and ^{129}I in grass ($^{127}\text{I}_{G,C}$ and $^{129}\text{I}_{G,C}$ respectively) as labelled, at the four harvest times: cut 1 (672 hr; blue diamonds), cut 2 (1032 hr; red squares), cut 3 (1560 hr; green triangles), cut 4 (2448 hr; purple circles). Inset shows detail of graph close to the origin.	180
Figure 6.27. Comparison of regressed (based on soil properties) and fitted (from plant uptake model) values of A) k_{pS} and B) k_{pN}	183
Figure 7.1. Effect of liming as a function of time on soil pH in control plot 3. Data from A. Macdonald (pers. comm.) with additional values from Silvertown (2006).	194
Figure 7.2. Schematic diagram showing relative locations of individual plots. Soil iodine concentrations (mg I kg^{-1} with standard error of three replicates given in	

brackets) are given for 1876 and 2008 sub plots (a-d). Values in italics are soil pH at the indicated date.....	195
Figure 7.3. Soil iodine concentration (I_S) as a consequence of liming (liming started 1903). Control plot 3 results only. Error bars show standard error of 3 replicate measurements (error bars are within the data point if not shown). Uncertainty due to sampling is unknown.....	196
Figure 7.4. Variation in soil iodine concentration across the site in “d” (unlimed) plots, where plot ‘location’ refers to the position of the plot, starting from 1 at the far south-western end (Figure 7.2). ‘P’ numbers are plot names. Error bars are the standard error of three replicates (1876 error bars are within the size of the circles). Lines show significant positive correlations.	197
Figure 7.5. Relationship between soil iodine (I_S) and vegetation iodine concentrations (I_V) for all samples. Error bars show standard error of 3 replicate measurements....	201
Figure 7.6. Relationship between I_S and I_V for all samples. Each bin is defined by soil iodine concentration, with the number of samples (n) in each bin shown as open circles, quantified on the secondary y axis. Mean vegetation iodine (I_V) is calculated as the mean of n samples, with error bars representing the standard error of the mean.	202
Figure 7.7. Relationship between vegetation iodine concentration (I_V) and vegetation yield (Y). All samples.....	203
Figure 7.8. Relationship between vegetation yield and vegetation/soil iodine ratio. All samples.....	203
Figure 7.9. Correlation between growing season rainfall (GSR) and annual vegetation iodine off-take (I_{off}) in control plot 3. Error bars show standard error of 3 replicate measurements.	205
Figure 7.10. Effect of time and liming treatment on vegetation iodine concentration in samples from control plot 3. Error bars show standard error of 3 replicate measurements. Lines are added for clarity but do not represent a temporal trend....	206
Figure 7.11. Vegetation yield (Y, $t\ ha^{-1}$) from cut 1, 1870 to 2008 for limed and unlimed sub-plots of plot 3. Lines are added for clarity but do not represent a temporal trend.....	207
Figure 7.12. Relationship between annual vegetation iodine off-take (I_{off}) and soil pH for 2008 samples.....	207

Figure 7.13. Schematic diagram of influences on vegetation iodine concentration and off-take, with linear correlations observed for the various sample groups. 209

Figure 7.14. Relationship between regressed (predicted from regression results) and measured vegetation iodine concentrations (I_V). Error bars show the standard error of three replicates originating from I_V measurement. Samples shown are those where both soil and vegetation samples were available for analysis. 210

Figure 7.15. Relationship between regressed (predicted from regression results) and measured vegetation iodine off-take (I_{off}). Error bars show the standard error of three replicates originating from I_V measurement. Samples shown are those where both soil and vegetation samples were available for analysis. 211

TABLE OF TABLES

Table 3.1. Measured chemical characteristics of soils, total iodine in soil and vegetation, and site-specific information distance to coast and total annual rainfall. Values in brackets show the number of replicates for determination of each value. ND = not detected.	49
Table 3.2. Geology, soil type and field textural observations at each sampling location. Soil descriptions are those of Cruickshank (1997).	50
Table 3.3. Total iodine concentrations in vegetation (I_V), and concentration ratios (CR) grown under field conditions, from published studies. ‘NR’ = not recorded, or not possible to calculate from given data.	58
Table 3.4. Rainfall volumes and iodine concentrations (I_R) in samples collected in Hillsborough, NI. All were collected over a period of seven days. I_R was measured in the presence/absence of 0.1 % TMAH matrix and the mean of the two values calculated. NR = volume not recorded, or insufficient sample to analyse.	64
Table 3.5. Iodine mass balance calculations: annual input from rainfall (I_{in}); the amount of soil iodine per hectare (I_{tot}); estimated annual iodine off-take by vegetation (I_{off}); the number of years to reach current values of I_S (Yr), assuming full retention of incoming rainfall iodine; and I_{off} as a percentage of I_{tot}	67
Table 3.6. Site-specific iodine inputs recorded during sampling.	68
Table 4.1. Fitted parameters for Model A . RSS is residual sum of squares from best model fit. S. D. is the standard deviation of the associated parameter value.	83
Table 4.2. Fitted parameters for Model B . RSS is residual sum of squares from best model fit. S. D. is the standard deviation of the associated parameter value.	84
Table 4.3. Parameters for the array model, predicting iodine dynamics from soil properties. Regressed parameter values were determined in Sections 4.5.2 and 4.5.3; optimised values are the result of the fitted array model.	101
Table 5.1. Details of humic acid solutions incubated in triplicate with ^{129}I as iodide, iodate and both inorganic species together.	109
Table 5.2. Details of HA-iodine dynamics models trialled and comparison of overall relative sum of squares (RSS). Parameters refer to those shown in Figure 5.10; where only $k_1 - k_5$ were used, $k_8 = k_2$ and $k_7 = k_3$. RSS per species was calculated by dividing RSS by the number of fitted species.	124
Table 5.3. Optimised parameter values describing HA-iodine dynamics in Model 4.	124

Table 6.1. Total soil iodine content: mean and standard error of three replicates....	138
Table 6.2. Total ^{127}I and ^{129}I measured in grass harvested during experiment. Mean and standard error of three replicates. Values below LOD are underlined.	139
Table 6.3. Estimated contribution of grass iodine from irrigation water, as a concentration ($^{127}\text{I}_{\text{G(Ir)}}$, mg I kg^{-1}), and as a percentage of total iodine in grass ($\text{I}_{\text{G(Ir,E)}}$, %). ‘Neg’ indicates that a negative value was calculated and so the calculation of $\text{I}_{\text{G(Ir,E)}}$ is invalid.	150
Table 6.4. Concentration ratios for pot experiment (^{127}I -CR cuts 1 – 4) and field samples (^{127}I). Standard error represents variation in three replicates.	154
Table 6.5. Spike concentration ratios for pot experiment (^{129}I -CR cuts 1 – 4). Standard error represents variation in three replicates.	155
Table 6.6: Concentration ratios ($\text{CR} = \text{I}_V / \text{I}_S$) from published studies of iodine uptake from soil in pot experiments grown indoors.....	158
Table 6.7. Total concentrations in soil solution of ^{129}I ($^{129}\text{I}_L$), ^{127}I ($^{127}\text{I}_L$), and dissolved organic carbon (DOC). Mean and standard error of three replicates, except for soils NI05 and NI15 ($n = 2$).	159
Table 6.8. Speciation of soil solution. Individual species are presented as a percentage of sum of species. Sum of species quantified is quoted as percentage of measured total iodine concentration. Replicates a and b for each soil. Values where none of that isotope was measured by SEC are indicated by -	163
Table 6.9. Summary of fitting results for NI01 plant uptake, as the rate coefficient describing uptake varied, sometimes including reciprocal dependence on time, t . The ‘rate coefficients’ listed were substituted for k_p in Eqns. 6.10 (^{129}I) and 6.11 (^{127}I) as shown for each model. ‘ k_{pS} ’ and ‘ k_{pN} ’ are fitted parameters for ^{129}I and ^{127}I respectively, which form part of the rate coefficient for each isotope.	175
Table 6.10. Parameter values for the plant uptake model, individually fitted to all soils used in the pot experiment. Mean and standard deviation values calculated by OpenModel. RSS is the residual sum of squares when $^{127}\text{I}_{\text{G,C}}$ and $^{129}\text{I}_{\text{G,C}}$ were fitted.	177
Table 7.1. Details of soil treatments. Codes are those defined in Rothamsted Research (2006). Application rates quoted are from Macdonald, A. (pers. comm.) or Warren and Johnston (1963).	188
Table 7.2. Summary of archived soil and vegetation samples used (*). Individual plot treatments details are given in Table 7.1.	189

Table 7.3. Control plot results: iodine concentration in soil (I_S) and vegetation (I_V) with vegetation yields from cut 1 (Y) and resulting total soil iodine (I_{tot}) and annual vegetation iodine off-take (I_{off}).....	192
Table 7.4. 2008 results: iodine concentration in soil (I_S) and vegetation (I_V) with vegetation yields from cut 1 (Y) and resulting total soil iodine and vegetation iodine off-take (I_{off}).	193
Table 7.5. Total iodine measured in fertiliser samples applied to treated plots, and the number of samples analysed in each case.	199
Table 7.6. Iodine contributed by chalk applications, to all plots, between 1881 and 2009. Mean iodine input calculated using mean iodine concentration in chalk (Table 7.5). Some lime was added to plots before liming treatments started, hence sub-plot d ('unlimed') does have some historical lime input.	199
Table 7.7. Iodine contributed by treatments analysed. Iodine content is mean of measured values (Table 7.5). Notes: * Fertilisers unavailable to sample; ^a 4-yearly inputs calculated as mean annual additions; ^b additions between 1870 and 1955; ^c additions from 1959 onwards; ^d additions from 2003 onwards.....	200
Table 7.8. Results of stepwise regression to predict iodine vegetation concentration (I_V) and off-take (I_{off}) from soil properties pH, SOC (%), I_S (mg I kg^{-1}) and GSR (mm) and Y ($\text{t ha}^{-1} \text{ cut}^{-1}$). Includes all samples analysed. Any predictors not appearing in 'relative influence' column did not significantly influence the response; values in brackets are the significance of including that predictor.....	210

GLOSSARY

ANOVA	Analysis of variance
c.	Circa
CR	Concentration ratio (dimensionless): iodine concentration in vegetation / iodine concentration in soil
CR _F	Concentration ratio for field samples
CR _p	Concentration ratio for pot trial samples
DOC	Dissolved organic carbon
FYM	Farmyard manure
GR	Growth rate (g day ⁻¹)
GSR	Growing season rainfall (mm)
HA	Humic acid
HPLC	High pressure liquid chromatography
I ⁻	Iodide
ICP-MS	Inductively coupled plasma - mass spectrometry
ICPS	Integrated counts per second
IDD	Iodine deficiency disease(s)
¹²⁷ I _{Ir}	¹²⁷ I in irrigation water (μg I L ⁻¹)
¹²⁷ I _{Ir,t}	Addition of ¹²⁷ I in irrigation water through time (μg I hr ⁻¹)
¹²⁹ I _{meas} and ¹²⁷ I _{meas}	Measured concentrations of ¹²⁹ I and ¹²⁷ I respectively, usually before some form of correction
I _G	Iodine in grass (mg I kg ⁻¹)
I _{G(Ir)}	Iodine in grass originating from irrigation water (mg I kg ⁻¹)
I _{G(Ir,A)}	Total amount of iodine provided by irrigation water during pot experiment, expressed as a percentage of the iodine uptake in grass (%)
I _{G(Ir,E)}	Estimated percentage of iodine in grass originating from irrigation water (%)
I _{G(S)}	Iodine in grass originating from soil (mg I kg ⁻¹)
I _{G/S}	Grass/soil ratio: ¹²⁹ I/ ¹²⁷ I in grass divided by the equivalent ratio in soil
I _{in}	Annual iodine input from rainfall (g I ha ⁻¹ yr ⁻¹)
I _L	Iodine in solution (subscript 'L' also used to indicate concentrations of species in solution)
I _{L/S}	Liquid/soil ratio: ¹²⁹ I/ ¹²⁷ I in soil solution divided by the equivalent ratio in whole soil
IO ₃ ⁻	Iodate

I_{off}	Iodine off-take by vegetation ($\text{g I ha}^{-1} \text{ yr}^{-1}$)
I_{R}	Iodine in rain ($\mu\text{g I L}^{-1}$)
I_{S}	Iodine in soil (mg I kg^{-1})
I_{solid}	Iodine bound to solid
I_{tot}	Total weight of iodine in each hectare of soil (g I ha^{-1})
I_{V}	Iodine in vegetation (mg I kg^{-1})
LOD	Limit of detection
MCF	Mass correction factor
MQ water	Milli-Q purified water
MW	Molecular weight
NI	Northern Ireland
NI01 - NI20	Individual labels for twenty soils collected in NI
OM	Organic matter
OrgI	Organically bound iodine
ppb	Parts per billion
RSS	Residual sum of squares
RT	Retention time (min)
S. D.	Standard deviation
S. E.	Standard error
SEC	Size exclusion chromatography
SOC	Soil organic carbon
SOM	Soil organic matter
TAR	Total annual rainfall (mm)
t_{G}	Growth time (days)
v	Volume of water in system (L, used in modelling)
V_{Ir}	Mean volume of irrigation water provided (L day^{-1})
V_{R}	Volume of rain ($\text{L ha}^{-1} \text{ yr}^{-1}$)
W_{S}	Weight of soil in top 20 cm (kg ha^{-1} , assumed to be $2,500,000 \text{ kg ha}^{-1}$)
Y	Yield (g)

1 INTRODUCTION

Iodine is a naturally occurring element, present at trace concentrations in rocks and soils (average concentrations c. $0.24 \text{ mg I kg}^{-1}$ in igneous rocks, 2.0 mg I kg^{-1} in sedimentary rocks, 5 mg I kg^{-1} in soil (Fuge and Johnson, 1986)). The largest store (c. 70 %) of iodine is considered to be marine sediments, due to the seawater iodine concentration of $58 \mu\text{g I L}^{-1}$; seawater is considered to be the largest source of iodine to the terrestrial biosphere (Fuge and Johnson, 1986; Muramatsu and Wedepohl, 1998). Iodine has one stable isotope (^{127}I) and various non-stable isotopes, the longest-lived of which is ^{129}I , $t_{1/2} = 1.7 \times 10^7$ years (Fuge and Johnson, 1986; Royal Society of Chemistry). Iodine is usually present at one of three oxidation states: -1 (I^-), +5 (IO_3^-) and 0 (I_2) (Fuge and Johnson, 1986; Whitehead, 1984). Understanding its environmental behaviour is important because of its role in human and animal nutrition (Fordyce et al., 2003; Kelly, 1961; Lidiard, 1995; Orr et al., 1928; Watts et al., 2010) and because ^{129}I is a key component of radioactive waste and can be accidentally released by nuclear accidents (Beresford et al., 2012; Bostock et al., 2003; Endo et al., 2012; Hou et al., 2009; Knapp, 1964; Yoshida et al., 2007).

1.1 IODINE DEFICIENCY

Iodine deficiency has long been recognised as a problem (Fordyce et al., 2003) and until the 1950s, almost every country in the world suffered from problems due to iodine deficiency (Fuge, 2005). It is recognised by the World Health Organisation (WHO) as, “...the world’s most prevalent, yet easily preventable, cause of brain damage.” (World Health Organisation, 2009). Monitoring iodine deficiency worldwide and promoting research into prevention is therefore a focus of the WHO and UNICEF (Andersson et al., 2007a; de Benoist et al., 2003; de Benoist et al., 2008). The term ‘iodine deficiency disorder’ (or IDD) is used to describe illnesses attributed to a lack of iodine in the diet. Iodine is an essential part of hormones produced by the thyroid gland, and lack of iodine in humans can give rise to goitre, birth defects, decreased fertility, increased perinatal death and ‘cretinism’: deaf-mutism and reduced intelligence and physical development (ICCIDD, 2009b; Johnson et al., 2003; Stewart and Pharoah, 1996; Zimmermann, 2008; Zimmermann et al., 2008). Early treatments involved preparations of seaweed and even before the link between a lack of dietary iodine and goitre had been made, research into increasing iodine in plants by adding manure was being investigated (Orr et al., 1928; Stewart and Pharoah, 1996). Other

treatments include limiting intake of compounds that hinder uptake of iodine, termed 'goitrogens'. Suggested goitrogens include components of brassicas, Zn, thiocyanate from cassava, Se and minerals containing SO_3F and Li (Anke et al., 1995; Barry et al., 1983; Fuge, 1996; Stewart and Pharoah, 1996). Modern research into prevention and treatment of IDD focus on improving iodine provision (Andersson et al., 2007b; Rose et al., 2001; Zimmermann, 2008; Zimmermann et al., 2006).

Iodine sufficiency is important for animals as well as humans, with deficiency again resulting in impaired fertility and growth problems, even when no goitre is visible (Anke et al., 1995; Franke et al., 2009; Lidiard, 1995; Whitehead, 1975). As such, iodine supplementation for grazing animals may be necessary, depending upon the iodine content of pasture and other feed (Smith et al., 1999; Whitehead, 1979). Care must be taken, however, not to over-supplement, as there is a risk of providing too much iodine to the end consumers of dairy products (Schone et al., 2009).

In contrast to deficiency, iodine poisoning has also been recognised in human subjects, notably during early development of iodine treatments against cretinism (Stewart and Pharoah, 1996). Symptoms of poisoning include gastrointestinal illnesses, cardiovascular problems and cyanosis, and although less of a widespread problem than IDD, hyperthyroidism has been observed in cases where dietary iodine has been suddenly increased (Rose et al., 2001; Weng et al., 2009; Zimmermann, 2008).

The impact of IDD on a community can be serious, affecting economics as well as health through suboptimal performance of productive animals, or by reducing IQ in the human population (Zimmermann et al., 2008). Therefore the benefits of investing in iodine sufficiency cannot be measured solely in terms of health improvements or lives saved, but must be considered in a broader context (Alderman, 2010). The wide geographical distribution of communities suffering IDDs and the need to co-ordinate remedial measures resulted in formation of the International Council for the Control of Iodine Deficiency Disorders (ICCIDD), with the aim of increasing knowledge in order to tackle the problem (ICCIDD, 2009a). The need to improve communication between medics and environmental scientists to find the best approaches to IDD prevention was highlighted by Stewart and Pharoah (1996).

1.1.1 Preventing IDD

The simplest approach to preventing IDD is to increase dietary iodine. In this context the most important source of iodine is marine fish. Leafy vegetables, dairy products and meat may also contain beneficial concentrations of iodine (Bath et al., 2011; Dunn, 1993; Eckhoff and Maage, 1997; Fordyce, 2003). In developing countries access to foods which are naturally iodine-rich may be limited whereas in developed countries, food from a wide variety of sources is generally available, and a balanced diet can be chosen. Additionally, ‘adventitious iodine’ is often provided, for example in milk through the use of iodophors for teat cleaning in the dairy industry, or in food additives (Dunn, 1993; Fordyce, 2003; Johnson, 2003b; Zimmermann et al., 2008). By choosing ‘healthier’ options such as less-processed food or organic milk, people can unknowingly be reducing their iodine intake (Bath et al., 2011; Dahl et al., 2003; Fordyce, 2003) and recent reports suggest increasing IDD prevalence in developed countries without a mitigation strategy as a consequence. Further investigation to confirm this link and raise awareness has been called for (Vanderpump et al., 2011; Zimmermann, 2010).

Cows’ milk is an important source of iodine in the human diet, although its iodine content varies (Phillips, 1997; Schone et al., 2009; Vanderpump et al., 2011). Seasonal changes in cattle feed result in fluctuating milk iodine concentrations, as iodine-enriched fodder often replaces outdoor grazing pasture in the winter (Dahl et al., 2003; Dunn, 1993; Haldimann et al., 2005; Reid et al., 2008). Dahl et al. (2003) also reported geographical differences in milk iodine concentrations, which were more pronounced in summer when reliance on environmentally available iodine was greatest. Iodophors are not used for cleaning in the Norwegian dairy industry that was being studied and there was no significant correlation between soil iodine and milk iodine concentrations. Therefore differences in concentration by location were explained by variations in the length of time for which cattle were allowed to graze outside (Dahl et al., 2003). The influence of iodine availability from soil to pasture cannot be ruled out, however, as pasture iodine concentrations were not recorded.

Widespread iodisation of salt has been used as a cost effective and efficient method of increasing iodine intake (de Benoist et al., 2008; Phillips, 1997; Zimmermann, 2010). A programme of iodisation of all salt for human and animal consumption, ‘universal

salt iodisation', was implemented in 1993 (World Health Organisation, 2009). Recently the value of this approach has been questioned, as increasing numbers of people reduce their salt intake for health reasons (Andersson et al., 2007a; Dahl et al., 2003). In countries where salt iodisation is recommended, it does not always reach the intended population, with reasons including a preference for locally produced, cheaper salt (Cao et al., 1994; Dai et al., 2004; Hong et al., 2009; Smyth et al., 2011; Stewart, 1990; Zhu et al., 2003), the loss of iodine during cooking (Hong et al., 2009; Zhu et al., 2003) and mis-information in labelling (Zimmermann, 2010). Direct intervention is also commonly used to supply iodine to humans, delivered as tablets and/or injections given at regulated intervals (Zimmermann, 2008). While these may ensure correct iodine dosing to those who take them, such treatment is expensive, often logistically difficult, and not always readily accepted by the target populations (de Long, 2002; Mackowiak and Grossl, 1999; Rengel et al., 1999).

Biofortification can be an indirect method of increasing dietary iodine provision, by improving the nutrient content of vegetable-based foods (Blasco et al., 2008; Caffagni et al., 2011; Voogt et al., 2010). Uptake of elements including iodine varies according to plant species, and in some cases differences between plant species can be greater than the effect of fertilisation (Hong et al., 2009; White et al., 2012). Therefore the plant types chosen for biofortification need to be carefully considered to achieve optimum uptake of iodine present. To be widely useful, the plant should grow readily in a range of climatic conditions, and be easy to store and transport. The age and part of the plant that is eaten affects its iodine concentration, so the likely intake of that food, and time of harvesting, must also be correctly estimated to be effective (Landini et al., 2011; Mackowiak and Grossl, 1999; MacNaeidhe, 1995). Thus good knowledge of the typical diet of the target population is required (Haldimann et al., 2005).

Controlling iodine in the growing medium so that optimal plant uptake of iodine is achieved is likely to be a good long-term strategy towards reducing IDD. For example, adding iodine to irrigation water has been shown to be a cheap and simple method whereby long-lasting local improvements in iodine sufficiency in humans and animal populations can be achieved (Cao et al., 1994; de Long, 2002; Ren et al., 2008). One drawback of this approach is that adding too much iodine can result in

toxic effects to plants and waste money and resources (DeLong, 2002; Rengel et al., 1999), although Cao et al. (1994) argued that it would be difficult to add too much iodine by this method.

Underpinning all these treatments to prevent IDD is the fact that they should be directed to local populations, taking into account location, cultural and agricultural practices (Andersson et al., 2007b). However, treating the problem at source, for example by manipulating water and/or soil iodine concentrations, is more likely to have long-lasting, far-reaching impacts than treating people and animals individually.

1.1.2 Understanding iodine dynamics

Total iodine concentration in soil alone is not a good predictor of iodine availability to the food chain. For example Derbyshire, known historically for ‘Derbyshire neck’ or goitre, has soil iodine concentrations around 5 mg I kg⁻¹ in the limestone regions, which is high compared to global averages (Saikat et al., 2004). Furthermore, despite soil iodine concentrations that are typically high relative to global averages (Johnson, 2003a; Whitehead, 1979) endemic goitre was widespread in Britain until the 1960s (Fuge, 1996; Kelly and Snedden, 1960; Phillips, 1997). No correlation between environmental iodine concentrations and goitre was found by Stewart et al. (2003) after consideration of data sets from England and Wales, and Whitehead (1979) observed that soil iodine concentrations at farms where cattle IDD had been diagnosed were not low in the context of worldwide values. Despite this knowledge and extensive research into the medical effects of IDD and direct provision of iodine to affected populations, there had been little investigation into controls on iodine behaviour in the environment until the last decade (Johnson et al., 1999). Since then, links between concentrations in soil and water, and the iodine status of local populations outside the UK have been investigated (Fordyce et al., 2003; Johnson et al., 2002; Ren et al., 2008; Watts and Mitchell, 2009). It is evident from the available research that in order to optimise IDD prophylaxis, iodine dynamics in the terrestrial environment must be better understood (Johnson et al., 2003).

1.2 IODINE IN THE ENVIRONMENT

Unlike many other elements, soil iodine concentrations are not determined by the concentration in underlying rocks. It had been suggested that soil iodine is primarily

derived from rock weathering and influenced by movement of tectonic plates (Cohen, 1985; Stewart, 1990), but it is now understood that most iodine in the biosphere originates from the oceans (Fuge, 2005; Fuge and Johnson, 1986; Whitehead, 1984; Zimmermann et al., 2008). The marine origin of many sedimentary rocks is reflected in their iodine concentrations ($0.4 - 30 \text{ mg I kg}^{-1}$), which tend to be higher than igneous and metamorphic rocks ($0.005 - 0.2 \text{ mg I kg}^{-1}$), where high temperatures during formation may drive off iodine (Fuge and Johnson, 1986; Gerzabek et al., 1999; Hou et al., 2009; Johnson, 2003b; Muramatsu et al., 1994; Whitehead, 1984).

Volatilisation of iodine from the oceans is considered to be the major source of iodine to the atmosphere, being transferred via complex mechanisms dependent on weather and atmospheric conditions, but probably involving volatile species such as CH_3I and I_2 (Baker et al., 2000; Bloss and Ball, 2009; Martino et al., 2009; Muramatsu et al., 2004; Redeker et al., 2000). Recent research suggests that HOI and I_2 are also likely to be important in determining atmospheric concentrations (Carpenter et al., 2013). Volatilisation from some species of seaweed also contributes to iodine concentrations in the atmosphere and rainfall (Chance et al., 2009; Gilfedder et al., 2008; Nitschke et al., 2011; Saiz-Lopez et al., 2006). Contributions to the atmosphere from plankton, bacteria and algae have also been suggested (Campos et al., 1996; Chance et al., 2009; Nitschke et al., 2011; Smyth et al., 2011). Gaseous iodine species such as I_2 and organic molecules are short-lived (hours), and transport of sea-spray containing iodine is limited, so the marine influence on soil concentrations is mainly observed around the coast (Baker et al., 2000; Bloss and Ball, 2009; Gilfedder et al., 2007; Smyth and Johnson, 2011). Dry deposition of particulate iodine is also possible although this was considered by Truesdale and Jones (1996) to have minimal input to total soil iodine. Wet deposition is relatively much more important for transferring iodine from the air to ground and vegetation (Shaw et al., 2007).

Rain is an important transport mechanism of iodine, washing it from the atmosphere onto land. Therefore in areas where the atmospheric concentration is high, such as over oceans and around the coast, rainfall has a higher iodine concentration than further inland (Aldahan et al., 2009; Krupp and Aumann, 1999; Neal et al., 2007). The mean UK rainfall iodine concentration calculated from literature sources (Hou et al., 2009, Neal et al., 2007, Johnson, 2003b, Lidiard, 1995) is c. $2 \mu\text{g I L}^{-1}$. As well as

proximity to coast, variations in rainfall iodine concentration can be due to the length, intensity and frequency of showers. For example in drier seasons and when there has been a period of no rain, concentrations in rainfall are likely to be higher as there is a build-up of iodine in the atmosphere (Fuge and Johnson, 1986; Truesdale and Jones, 1996). Neal et al. (2007) reported that rainfall iodine concentration was inversely proportional to the volume of rain collected, supporting a 'wash-out' mechanism. The importance of rainfall as an iodine source to land is illustrated by the apparent presence of iodine 'rain shadows' on the leeward side of some mountains where rainfall is rarer (Aldahan et al., 2009; Fuge, 1996; Lidiard, 1995).

1.2.1 Iodine in soil

The concentration of iodine in soil and any subsequent uptake by plants represents a balance between input, retention and availability, the last two of which are determined by soil properties. In a database of over 2,000 soil iodine 'average' concentrations collated from global literature, Johnson (2003a) reported that the highest concentration measured was 150 mg I kg^{-1} , but that nearly half the soils contained $< 2.5 \text{ mg I kg}^{-1}$ iodine. In the UK, concentrations in soil have been reported as $0.5 - 98.2 \text{ mg I kg}^{-1}$ (Johnson, 2003a; Whitehead, 1984), with higher concentrations in coastal areas. A concentration of 660 mg I kg^{-1} was recorded for a coastal location in Northern Ireland by Smyth and Johnson (2011).

While the main inputs to soil are atmospheric deposition, rainfall and sea-spray, other mechanisms have been proposed for inland areas, including volatilisation from vegetation, paddies and wetlands (Aldahan et al., 2009), and 'land hopping' via volatilisation and re-deposition until soil properties result in the iodine becoming fixed (Fuge, 1996; Johnson, 2003b). This process requires that soil promotes the presence of free iodide which can be transformed to volatile species under ambient conditions, and if widespread, could reduce coastal iodine concentrations and increase inland concentrations. The highest soil iodine concentrations tend to be found in coastal areas due to greater and more consistent inputs. Local variations in soil properties affect how well incoming iodine is retained, however, resulting in a wider range of observed concentrations in coastal regions (Johnson, 2003a; Johnson et al., 2002; Smyth and Johnson, 2011).

Organic matter (soil organic carbon, SOC), metal oxides and soil pH are the most important factors in iodine retention. The link between high SOC and high iodine concentration has often been noted (Kashparov et al., 2005; Muramatsu et al., 2004; Whitehead, 1973a; Whitehead, 1974b) and it has been suggested that retention in organic matter may be by physical occlusion within the structure (Sheppard and Thibault, 1992). Recently, covalent bonding between iodine and organic carbon, usually at aromatic carbon sites, has been confirmed by X-ray absorption fine structure (XAFS) (Schlegel et al., 2006; Yamaguchi et al., 2010).

Several mechanisms by which metal oxides can be involved in iodine binding within soils have been proposed. Goldschmidt (1958) suggested that the highly polarisable nature of iodide may allow it to substitute for hydroxide ions in ferric hydroxides; while Whitehead (1984) suggested retention of iodine anions via bonding to localised positive charge on the oxide surface. Pure MnO₂ has been shown to encourage both reduction and oxidation of iodine, enhancing reaction with organic matter (Anschutz et al., 2000; Fox et al., 2009; Xu et al., 2011a). Although oxides of Fe and Mn are most commonly invoked, Al oxides can also be involved (Dai et al., 2004; Muramatsu et al., 1990; Whitehead, 1978). The rate of reaction between anionic iodine species and metal oxides is likely to be higher at low pH, due to reduced competition with hydroxide for positively charged sites (Dai et al., 2009; Hong et al., 2012; Whitehead, 1973a). Several authors have reported faster sorption to soils at lower pH, which may involve initial binding to metal oxides (Fox et al., 2009; Shetaya et al., 2012; Yoshida et al., 1992), however soils with high SOC also tend to have low pH thus it can be difficult to separate the relative effects of individual parameters.

Clays have also been linked to iodine retention (Fuge and Johnson, 1986; Gerzabek et al., 1999; Hong et al., 2012; Sheppard and Thibault, 1992), however Assemi and Erten (1994) noted that the effect was less important than retention by organic matter. Where it occurs, sorption by clays may be due to the presence of metals within clay minerals, as clay alone carries a negative charge and would therefore be expected to repel anionic forms of iodine (Bird and Schwartz, 1997).

1.2.1.1 Volatilisation

Iodine volatilisation from seawater is well-known but in soils, oxidation of iodide to volatile species such as I_2 and CH_3I is a necessary precursor to volatilisation (Fuge, 1990). Methyl iodide, CH_3I , is the most common form of iodine reported as volatilised from soil (Muramatsu and Yoshida, 1995; Muramatsu et al., 2004; Redeker et al., 2000) but the amount of iodine volatilised is suggested to be very small. After reviewing the available literature, Sheppard et al. (2006) estimated that 0.000058 of the total soil iodine concentration is volatilised per day, which is similar to the loss expected to leaching, but they also suggested that soil ‘degassing’ rates for individual soils may vary by a factor of up to 1000. The presence of plants may also play a role (Muramatsu and Yoshida, 1995; Redeker et al., 2000; Sheppard et al., 1994) but in the context of a whole soil-plant system, iodine volatilisation is likely to be negligible compared to losses to leaching. For example, Bostock et al. (2003) quoted a total loss of $\leq 0.01\%$ of spiked iodine from forest and grassland soils, compared to a loss to leaching of 1 – 6.5 %.

1.2.1.2 Microbial influence on soil iodine

Microbial activity may influence soil iodine dynamics by production of enzymes or changing soil pH (Amachi, 2008; Li et al., 2012; Muramatsu et al., 2004). The impact of microbial activity depends on the soil conditions and microbe species present (Amachi et al., 2010; Seki et al., 2013; Xu et al., 2011a). While these processes can be influential, Sheppard et al. (1996) reported that abiotic processes were more important in the soils they studied, and Shetaya et al. (2012) concluded that observed reaction rates were too fast to be significantly affected by microbial activity. Therefore microbial processes have not been investigated in this work, as soil chemistry is likely to predominate.

1.2.2 Iodine uptake by plants

Literature reports of vegetation iodine concentration are typically up to $500 \mu\text{g I kg}^{-1}$ in vegetables and grasses (Whitehead, 1984); but as low as 10 – $25 \mu\text{g I kg}^{-1}$ in vegetables growing in very low-iodine soils in Morocco (Johnson et al., 2002) and up to $3000 \mu\text{g I kg}^{-1}$ in vegetables grown in iodine-spiked soil in Canada (Sheppard et al., 1993). It is important to understand how soil properties affect the amount of iodine that is available to plants, the ‘phyto-available’ iodine, because plants are the link

between the source and receptors of iodine: the atmosphere and soil, and animals/humans in the food chain. Mechanisms of iodine uptake are still not clear; iodine is not believed to be essential for plant growth, therefore uptake is expected to be directly proportional to uptake of soil solution (Dai et al., 2006; Whitehead, 1973c). Whitehead (1973c), however, concluded that more iodine was taken up by ryegrass, timothy and clover grown hydroponically than would be expected from a purely passive uptake.

Uptake by plants can be via roots or leaves, and will vary depending upon species. The importance of stomatal conductance for foliar uptake was shown by Tschiersch et al. (2009), who reported that washing leaf samples had little effect on measured iodine concentration. Uptake through leaves is particularly relevant when considering pathways of radioactive iodine to humans from the atmosphere (Collins et al., 2004; Shaw et al., 2007; Tschiersch et al., 2009), but an investigation by Landini et al. (2011) confirmed the dominance of root uptake over foliar uptake for natural iodine. Soil chemistry, plant species and soil iodine content all interact to affect plant uptake via roots. Sheppard et al. (2010) and Hong et al. (2009) reported that uptake depended significantly on the plant species, although Whitehead (1973c) determined that the iodine content in a hydroponic solution influenced final vegetation iodine concentration more than plant species did. Iodine uptake has been shown to increase linearly from soils with concentrations up to c. 50 mg I kg⁻¹. Above these concentrations, the rate of uptake decreases (Weng et al., 2008a; Weng et al., 2008b). This non-linearity may be linked to the toxicity of iodine at high concentrations reducing the plant's growth rate (Blasco et al., 2011; Weng et al., 2008b), and should be considered in any iodine biofortification scheme that relies on the addition of iodine to soil.

Soil properties affect iodine speciation and hence the relative proportion that is available for plant uptake. This influence has been investigated, but with limited success (Kashparov et al., 2005). Various authors have explored the preference for uptake of one iodine species or another, but most compare which added species resulted in greatest uptake (Smith et al., 1999; Whitehead, 1975). Experiments in hydroponic solution, such as those by Mackowiak and Grossl (1999), Zhu et al. (2003) and Dai et al. (2006), yield information about which inorganic species is most readily

taken up by plants, but this does not take into account interactions between iodine and soil that may change the iodine speciation. Indeed iodide and iodate have been shown to be rapidly transformed in soil solution to organic-iodine species (Shetaya et al., 2012). If iodine uptake from soils is to be optimised, studies need to account for transformations before uptake. This would demonstrate whether manipulation of the soil may be possible to promote iodine uptake.

1.3 AIMS

Iodine is essential for human and animal health. Soil properties affect iodine speciation and therefore its availability to plants, however it is only recently that research into quantifying the influence of soil has been undertaken, with limited success. One place where the importance of soil in determining iodine provision is evident is Northern Ireland (NI). There is limited data relating to IDD in NI, but modern anecdotal evidence suggests that cattle farmers have to supplement their cows' diets with iodine, despite the non-low iodine concentrations that were measured across NI by Smyth and Johnson (2011). Kelly and Sneddon (1960) recognised that goitre was more common in rural areas of NI and less prevalent near the coast. To some extent this reflects the distribution of iodine in soil, but more importantly, at the time of the reports quoted by Kelly and Sneddon (1960), (published 1933 and 1942) it is likely that the rural populations relied more heavily than urban populations on food grown locally. Thus the observations of IDD in rural populations may well have been caused by the low iodine availability that is still evident today in cattle. Therefore this work uses NI as a case study to investigate iodine dynamics in the terrestrial environment, including the relationships between iodine availability and soil, and rainfall and coastal proximity in iodine provision. Predictive modelling based on soil properties has been used to enable results to be applied to other locations.

In this work, four main questions are explored:

1. How relatively important are metal oxides and soil organic carbon in retaining iodine in soil?
2. What are the main processes controlling soil iodine dynamics?
3. What role does soil play in regulating iodine uptake by plants?
4. How can information about the influence of soil properties be used to improve provision of dietary iodine, particularly for grazing cattle?

2 MATERIALS AND METHODS

2.1 INTRODUCTION

Samples from NI have been used for the main body of this work. They were collected in the field between 6th and 14th October 2010, and sample processing and storage are detailed below. Sampling locations and site observations are presented in Chapter 3. Samples from the Rothamsted Park Grass long-term experiment have been used to investigate the role of soil properties in determining iodine concentration over the long term. These were collected from the Rothamsted archive in 2010 and 2012 and processing is described in Chapter 7. This chapter describes methods used throughout the work to characterise soils, vegetation and waters, and analyse iodine.

2.2 NORTHERN IRELAND SAMPLE COLLECTION

Sites across eastern Northern Ireland were chosen to give samples with a range of soil properties, underlying geology and distance to the coast. The Geological Survey of Northern Ireland's geochemical survey (the "Tellus" Project) was used to select soil locations based upon soil pH, loss on ignition and total iodine concentrations (Smyth and Johnson, 2011). At each location an area representative of the location was chosen for sampling. Five topsoil (0-15 cm) sub-samples were collected using an auger at the corners and centre of a square approximately 20 m x 20 m. Topsoil sub-samples (c. 1 kg) were placed in paper 'Kraft' bags and roots were removed where possible. Vegetation was cut from as close as possible to the soil sampling locations using stainless steel scissors and loosely stored in paper 'Kraft' bags. Care was taken to exclude attached soil particles to minimise contamination. The work of Sheppard et al. (2010) suggests that these measures are likely to have been successful in preventing soil contamination. Soil and vegetation samples were stored at ambient temperature in ventilated crates to allow air movement around the samples during their return to the laboratory.

2.2.1 Sample processing and storage

Soil sub-samples from each location were combined to produce composite samples and dried in a cool greenhouse until sufficiently dry to sieve to < 4 mm. The wet, fibrous nature of NI16 (peat) meant that it was broken into small pieces rather than sieved. The majority of each sample was stored under aerobic conditions, at 4 °C.

Approximately 100 g of each soil was air dried and a portion was ground using a Retsch PM 400 agate ball mill at 300 rpm for 4 minutes. Dry samples were stored in the dark at room temperature in plastic zip lock bags.

Vegetation was combined to create composite samples for each location. Each sample was spread out with leaves facing in the same direction, split in half vertically then one half spread over the other. This process was repeated three times. On the last occasion half was placed into paper bags and the remaining portion washed three times in deionised water, before placing in paper bags. All samples (washed and unwashed) were oven dried at 30 °C for 3 days. Following drying, samples were cut into c. 1 – 2 cm pieces using clean stainless steel scissors then ground using a Retsch ZM 200 centrifugal mill. Ground samples were stored in the dark at room temperature in plastic zip-lock bags.

2.3 IODINE ANALYSIS

Accurate and precise detection of iodine species in a range of media is essential to understanding and predicting iodine dynamics (Downs and Adams, 1975; Fuge, 2005; Michalke, 2003). Analysis of iodine in natural samples must be sensitive enough to accurately determine trace concentrations, and may need to be selective for particular isotopes and/or species, depending on the application. Low detection limits are important for ^{129}I analysis, which is typically present at extremely low concentrations (Izmer et al., 2003).

Early methods for total iodine quantification used colorimetric detection (e.g. Sandell and Kolthoff (1937)), until instrumental techniques with lower detection limits and greater selectivity and sensitivity, such as high performance liquid chromatography – inductively coupled plasma – mass spectrometry (HPLC-ICP-MS), were developed (Buchberger et al., 2003). The accuracy of historical iodine measurements has been questioned, although Fuge and Johnson (1986) concluded that in light of results from modern techniques, they are likely to be reasonable.

2.3.1 Iodine extraction

The first step towards accurate quantification is extraction, ensuring that no iodine is lost during the process (Stark et al., 1997). Acid digestion and pyrohydrolysis have

been used to extract iodine from various matrices, however it is widely recognised that at low pH iodine may form volatile species such as I₂ and HI that can be lost (Haldimann et al., 2000; Izmer et al., 2003; Tagami et al., 2006). Alkaline extraction reduces volatilisation losses, and tetramethyl ammonium hydroxide (TMAH) has been successfully used, usually with heating, for quantification of iodine in soils (Tagami et al., 2010; Watts and Mitchell, 2009; Yuita et al., 2005), plants (Chen et al., 2007; Tagami et al., 2006; Wang and Jiang, 2008), and foodstuffs (Fecher et al., 1998; Reid et al., 2008). Good accuracy and precision for iodine determination in soil and sediment reference materials was reported by Watts and Mitchell (2009) using a single TMAH extraction step, while repeated extraction was required to ensure quantitative extraction of ¹²⁹I by Shetaya et al. (2012).

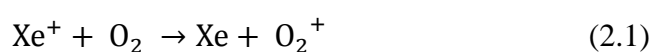
Phyto-available iodine is that which is available for uptake by plants from the growing medium. Attempts have been made to selectively chemically extract phyto-available iodine from soil, for example, Tagami et al. (2010) defined plant-available iodine as that which was extractable with TMAH, representing both water-soluble and organically-bound iodine. This was compared to the 'total' iodine content as measured by energy-dispersive X-ray fluorescence, but a statistically significant difference between the two measurements was only observed when total I < 5 mg I kg⁻¹. Results of other studies suggest that defining phyto-available iodine in this way would not accurately reflect the amount which is actually taken up, however, as reported concentration ratios are extremely low (Dai et al., 2006; Sheppard et al., 1993; Sheppard et al., 2010). Therefore alternative methods for investigating the phyto-available portion of soil iodine are required. Commonly, the concentration of iodine actually taken up by plants under specified growing conditions is measured, allowing comparison between soil types and vegetation species (Hong et al., 2009; Kashparov et al., 2005; Sheppard et al., 2010). In addition to usual considerations such as sample preparation and analytical procedure, this approach requires additional attention to factors such as: which plant parts to sample, when in the growing season to harvest, potential for soil contamination of plant matter, and growing conditions (MacNaoidhe, 1995). Further discussion of plant uptake experiments is in Chapter 6. After harvesting, an appropriate extraction method is required for total iodine determination. Extraction with TMAH has been used successfully by several groups

(Fecher et al., 1998; Johnson et al., 2002; Sheppard et al., 2010; Tagami et al., 2006), and this was the approach used in this study (Section 2.4.5).

2.3.2 ICP-MS for iodine quantification

ICP-MS is now commonly used for analysis of iodine in environmental samples, typically giving limits of detection of c. $1 \mu\text{g } ^{127}\text{I L}^{-1}$, and c. $0.3 \mu\text{g } ^{129}\text{I L}^{-1}$ (Brown et al., 2007; Popp et al., 2010; Shetaya et al., 2012). This allows ^{129}I to be used as a directly-detected tracer when added at low concentrations, in preference to isotopes such as ^{125}I which has a short half-life and requires gamma-detection. ICP-MS can also be coupled to HPLC to allow reliable detection of individual species (Section 2.3.3).

There are some complications when using ICP-MS for iodine analysis. The element's relatively high first ionisation potential (10.45 eV) reduces analytical sensitivity compared to many other elements, and ionisation efficiency can be further affected by the sample matrix (Dyke et al., 2009). Also, since detection depends on mass/charge (m/z) of species in the detector, other species with the same m/z can interfere with results. There are no singly-charged isotopes that affect ^{127}I measurement, although some isobaric interferences including $^{111}\text{Cd}^{16}\text{O}^+$, $^{113}\text{Cd}^{16}\text{O}^+$, $^{89}\text{Y}^{40}\text{Ar}$, $^{115}\text{In}^{14}\text{N}$ and MoO_2^+ may occur depending on the sample matrix (Haldimann et al., 2000; Hou et al., 2009; Reid et al., 2008). More importantly, interference of the argon impurity ^{129}Xe with ^{129}I is well documented (Beals et al., 1992; Brown et al., 2007; Haldimann et al., 2000). This can be overcome by applying a correction factor based on the natural abundances of ^{131}Xe and ^{129}Xe (Haldimann et al., 1998; Shetaya et al., 2012), or by use of an O_2 cell gas. The use of O_2 as a reaction gas has been shown to improve the signal:noise ratio, but may have a detrimental effect on repeatability of results (Brown et al., 2007; Izmer et al., 2003; Izmer et al., 2004; Reid et al., 2008; Wang and Jiang, 2008). Oxygen helps to remove the interference by charge transfer, with Xe^+ formed in preference to I^+ (Eqn. 2.1).



This renders ^{129}Xe neutrally charged and therefore undetectable (Izmer et al., 2004; Reid et al., 2008).

Internal standards account for small changes in sample introduction rate or detector drift throughout the run. To be successful, the internal standard should behave similarly to the analyte, not be naturally present in the sample, and be stable in the analytical matrix. Dyke et al. (2009) reviewed internal standards for iodine analysis, considering Ge, In and ^{129}I . Reliability of Ge was reduced in inhomogeneous samples and its mass is quite different from ^{127}I , which undermined its suitability. Although ^{115}In has low natural abundance and an atomic mass close to ^{127}I , its considerably lower ionisation potential resulted in underestimation of ^{127}I concentrations (Dyke et al., 2009). Unsurprisingly ^{129}I was found to be preferable, since isotopes of the same element should behave very similarly in ICP-MS analysis, with only minor mass discrimination effects (Dyke et al., 2009; Heumann, 1992; Heumann et al., 1994); however it would obviously be inappropriate where ^{129}I is used as a tracer. Alternative internal standards have included Sb, used for quantification of I and Mo in milk, soil and plant samples (Johnson et al., 2002; Reid et al., 2008); Re in waters and soils (Watts and Mitchell, 2009; Watts et al., 2010); and Te for dairy products, fish, soil and waters (Dahl et al., 2003; Eckhoff and Maage, 1997; Yuita et al., 2005). A strong benefit of using Te is that its ionisation energy is closer to that of I than those of Rh or In (Fecher et al., 1998), however isobaric interferences render it unsuitable, because for example $^{126}\text{Te H}^+$, $^{128}\text{TeH}^+$ and $^{130}\text{TeH}^+$ interfere with ^{127}I , ^{129}I and ^{131}Xe respectively. Since no single element was more favourable as an internal standard, a combination of In, Rh and Re were chosen for this work. The combination of all three compared to each one individually was investigated for each run and selection was based on that which resulted in most consistent calibration and accurate quantification of known reference materials. In practice, Re usually gave the best results (Section 2.6.2.1).

Where possible, the quantification of ^{129}I is carried out using ^{129}I standards (Brown et al., 2007; Izmer et al., 2003; Reid et al., 2008). However ^{129}I may be quantified relative to ^{127}I , in order to reduce analysis times or for isotopic dilution (Haldimann et al., 1998). In this case, a mass correction factor (MCF) is applied to account for differences in detection sensitivity between the two isotopes (Eqn. 2.2).

$$\text{MCF} = \frac{R_{\text{true}}}{R_{\text{exp}}} \quad (2.2)$$

where R_{true} = ratio of isotopes known to be present from certified concentrations and R_{exp} = ratio of isotopes measured. The magnitude and consistency of the MCF was shown by Haldimann et al. (1998) to vary between 0.97 and 1.05. Although the difference should be small for two isotopes with similar atomic weights, the particularly low concentrations in environmental samples make the correction important. When ^{127}I was used to quantify ^{129}I in this work, the MCF was measured at the beginning of each run and applied to results during processing.

2.3.3 Solution phase iodine speciation

Knowing iodine speciation in environmental samples is essential to understanding iodine dynamics and transformation mechanisms. Speciation in aqueous samples can frequently be undertaken without sample pre-treatment. Separation coupled to a detector such as UV-visible spectrophotometry or ICP-MS is the most common approach (Rodriguez-Gonzalez et al., 2005). Iodine speciation in milk, marine and estuarine waters, groundwaters, sewage effluent, drinking waters, extractions of soils and sediments and biological samples have all been studied (Buchberger et al., 2003; Hirsch et al., 2000; Hu et al., 2005; Kodama et al., 2006; Leiterer et al., 2001; Machado et al., 2001; Michalke and Schramel, 1999; Pansar-Kallio and Manninen, 1998; Stark et al., 1997; Wong and Cheng, 2008; Yang et al., 2007). When using HPLC coupled to ICP-MS compatible eluents must be selected to avoid suppression of the signal, nebuliser blockage, or damage to cones (Popp et al., 2010).

Organic iodine species are typically quantified by difference between total and sum of inorganic (iodide and iodate) species (e.g. Schwehr and Santschi (2003), Wong and Cheng (2008)). Size exclusion chromatography (SEC), which allows direct determination of organically-bound iodine, can also be used (Andersen et al., 2009; Andersen et al., 2008; Fernandez-Sanchez and Szpunar, 1999; Striegel et al., 2009; Yamada et al., 2002). Molecules are separated by size, although some separation on the basis of ionic interactions can occur, resulting also in separation of iodide and iodate (Dean, N., GE Healthcare, personal communication). SEC is therefore useful

for investigating iodine speciation in humic and fulvic substances, which can be related to behaviour in soil (Bostock et al., 2003; Warwick et al., 1993).

2.3.4 Solid phase iodine speciation

While iodine speciation in aqueous samples is now routine, identification and quantification of species extracted from the solid phase is not, as speciation may be affected by the extraction process (Chen et al., 2007; Michalke, 2003). Sequential extractions have been used for identification of iodine species but cannot unequivocally identify individual species (Hou et al., 2009; Young et al., 2006). Direct analysis of the solid phase, e.g. by X-ray absorption spectroscopy, is possible and has been applied to assess iodine speciation in soils and organic matter, but is also technically challenging (Schlegel et al., 2006; Shimamoto and Takahashi, 2008; Yamaguchi et al., 2010).

2.4 CHARACTERISATION METHODS

2.4.1 Soil pH

Soil pH was measured using a combined glass electrode with a Hanna Instruments pH meter 209. Measurements were made in MQ water and also in 0.01 M CaCl₂ to allow direct comparison to values from the Tellus survey. The electrode was calibrated using buffers at pH 7 and pH 4.01 before each set of measurements. Dry sieved soil (5.0 ± 0.1 g) was shaken with 12.5 ml of MQ water for 30 min. pH was noted when the reading was stable. For pH determinations in 0.01 M CaCl₂, 5.0 ± 0.1 g of dry, sieved soil was stirred, using a magnetic stirrer, with 12.5 ml of 0.01 M CaCl₂ for 5 min, allowed to settle for 15 min, then pH recorded when stable. Highly organic soils required a lower ratio of soil:solution, in order to obtain slurry that was suitable (typically 17.5 ml to 5.0 g soil). The pH values measured were all pH < 7 and therefore it was not considered necessary to measure carbonate content.

2.4.2 Soil organic carbon

Soil organic carbon was measured at BGS as total organic carbon. Air dried, ground soil (100 – 1000 mg) was further dried in silver foil cups (100-105 °C for at least 1.5 hr), treated with excess acid (HCl, 50 % v/v) to remove inorganic carbon, then dried again (100-105 °C for at least 1.5 hr). Analysis was carried out using an Elementar Vario Max C/N analyser, which measures production of CO₂ after

combustion of the sample at 1050 °C. Results were calculated using 'VarioMax' software on the instrument.

2.4.3 Dissolved organic carbon

Dissolved organic carbon in solution was analysed using a Shimadzu TOC-VCPH. Each sample was acidified with HCl to pH 2 - 3 to remove inorganic carbon, before the remaining (organic) carbon was detected as CO₂ by non-dispersive infrared detection after heating the sample to 720 °C with a platinum-coated alumina catalyst. Samples were quantified against standards of 2.125 g L⁻¹ potassium hydrogen phthalate (1000 mg C L⁻¹), diluted to appropriate concentrations using MQ water.

2.4.4 Extraction of metal oxides from soil

Extraction of Fe, Mn and Al oxides from soil was carried out in triplicate using a method adapted from Kostka and Luther (1994) and Anschutz et al. (1998). To 0.3 g of dry, ground soil 25 ml of a solution containing 0.22 M trisodium citrate, 0.11 M sodium hydrogen carbonate and 0.1 M sodium dithionite was added. Samples were shaken at 45 °C for 22 hr, with loosened lids, before being centrifuged for 20 min at 3000 rpm, filtered using 0.22 µm Millipore filters, and diluted 1 in 10 with 2 % trace analysis grade (TAG) HNO₃ before analysis. Soils NI03, NI17 and NI20 were further diluted to 1 in 100 using 2 % TAG HNO₃ immediately before analysis, due to flocculation at 1 in 10 dilution which would have affected ICP-MS results.

2.4.5 Total iodine extraction

An extraction trial was carried out using sample soils that had been dried and sieved or dried and ground, using TMAH concentrations between 0 and 25 %, heated at 20, 40 and 70 °C for 3 hr. Single and multiple extractions were compared. Results showed that heating to 70 °C was required but grinding was not. While multiple extraction with 25 % TMAH gave optimum results, there was little difference compared to results obtained from a single extraction using 5 % TMAH. In order to balance the requirement of reliable, accurate results with limitations of time and cost, a final method based on that of Watts and Mitchell (2009) was used.

TMAH (5 ml of 5 %) was added to 0.25 g of dried, ground sample. After heating for 3 hr at 70 °C, with shaking after 1.5 hr, 5 ml of MQ water was added to each sample

before shaking and immediate centrifugation at 3000 rpm for 50 minutes. Supernatant was poured off, and if necessary, stored at 4 °C before analysis. Where vegetation was extracted the supernatant was left overnight to allow any suspended plant material, not spun down by centrifugation, to settle. Samples were diluted to 1 % TMAH immediately before analysis, at which point extractions from soils with a high organic matter content were filtered to <0.45 µm using nylon acrodisc syringe filters.

2.5 USE OF ¹²⁹I

Spiking experiments were carried out with ¹²⁹I diluted from stocks obtained from the American National Institute of Standards (NIST). It was experimentally determined that the ¹²⁹I contained about 12 % ¹²⁷I, which was accounted for during processing of results for spiked samples, according to Eqns. 2.3 and 2.4.

$$^{129}\text{I}_{\text{Sp}} = ^{129}\text{I}_{\text{meas}} \times 1.12 \times \left(\frac{^{127}}{^{129}} \right) \quad (2.3)$$

$$^{127}\text{I}_{\text{N}} = ^{127}\text{I}_{\text{meas}} - 0.12 \times ^{129}\text{I}_{\text{meas}} \quad (2.4)$$

Where ¹²⁹I_{Sp} and ¹²⁷I_N are corrected concentrations of ¹²⁹I and ¹²⁷I, or ‘spiked’ and ‘non-spiked’ iodine, respectively (µg I L⁻¹); ¹²⁹I_{meas} and ¹²⁷I_{meas} are measured concentrations of the respective isotopes in solution (µg I L⁻¹); factors of 1.12 (Eqn. 2.3) and 0.12 (Eqn. 2.4) account for the presence of ¹²⁷I in ¹²⁹I; and 127/129 corrects the gravimetric concentration for the two isotopic masses. For ease of interpretation, ¹²⁹I_{Sp} and ¹²⁷I_N remain labelled as ¹²⁷I and ¹²⁹I throughout this thesis, and whenever concentrations are quoted, the corrections in Eqn. 2.3 and Eqn. 2.4 have been applied.

When ¹²⁹I was quantified against ¹²⁷I standards, a run-specific MCF was applied, having been calculated individually for each run according to Section 2.3.2.

2.6 ICP-MS ANALYSIS

Most ICP-MS analysis was carried out at university on a Thermo-Fisher Scientific X-series II in standard mode, using PlasmaLab software (version 2.5.1.276) for control and data processing. Total iodine in NI soil and vegetation was analysed at BGS using a VG Elemental PQ ExCell in standard mode, using PlasmaLab software version 1.06.

Unless otherwise specified, instruments were run in standard mode and samples were introduced to the concentric glass venturi nebuliser (Thermo-Fisher Scientific; 1 ml min⁻¹) through a T-piece to mix sample with internal standard.

2.6.1 Analysis for metal oxides

Soil extracts were analysed by ICP-MS in collision cell mode (7 % helium in hydrogen) with Sc, Ge and Rh internal standards and 2 % TAG HNO₃ wash. Calibration was carried out using 0 – 100 µg L⁻¹ Fe, Mn and Al standards from Multielement Solution 2 (SpexCertiPrep) diluted with 2 % TAG HNO₃. Concentrations of Al, Mn and Fe in solid (g kg⁻¹) were calculated from concentrations in solution (µg L⁻¹).

2.6.2 Iodine analysis

Stock standards for ¹²⁷I analysis were prepared at 1000 mg I L⁻¹ from oven-dried KI and KIO₃, and stored at 4 °C in 1 % TMAH. Standards for ¹²⁹I analysis were diluted from NIST stocks (Section 2.5). All standards were freshly diluted in 1 % TMAH or MQ water as required before each analytical run.

2.6.2.1 Total iodine

Internal standards of Rh, Re and In were added to the sample at approximately 10 µg L⁻¹ via a T-piece before the nebuliser. Sample and wash matrices were 1 % TMAH to ensure full wash-out of iodine between samples. Total iodine in rainwater and deionised water also used this method, but with a 0 % or 0.1 % TMAH matrix instead of 1 % TMAH.

2.6.2.2 Iodine speciation

Chromatography to separate iodine species used a Dionex ICS-3000 HPLC coupled to ICP-MS. The HPLC was controlled with a computer using Chromeleon software (Dionex, version 6.80SR12) and sample processing was carried out with Plasmalab software. Samples were introduced directly into the nebuliser from the chromatography column output. Working standards of ¹²⁷I⁻ and ¹²⁷IO₃⁻ (0 – 100 µg I L⁻¹) were diluted in MQ water from 1000 mg I L⁻¹ stocks (Section 2.6.2). Working standards of ¹²⁹I⁻ and ¹²⁹IO₃⁻ (0 – 50 µg I L⁻¹) were diluted in MQ water from NIST stocks (Section 2.5). Species-specific quantification was carried out with

standards of $^{127}\text{I}^-$, $^{127}\text{IO}_3^-$, $^{129}\text{I}^-$ and $^{129}\text{IO}_3^-$, and mean, isotope-specific, ‘ $\mu\text{g I L}^{-1}$ per ICPS (integrated counts per second)’ were calculated from iodide and iodate standards and used to quantify organic iodine. No internal standards were used during speciation; drift correction was applied using repeated standards through the run.

A Xe correction factor (typically around 1.08) was applied to all ^{129}I chromatography results, according to Eqn. 2.6. Calculation of the correction factor using the natural abundances of ^{131}Xe and ^{129}Xe (Section 2.3.2) was found to over-correct the ^{129}I signal. Therefore the correction was calculated individually for each run by iteration until the ^{129}I baseline for all chromatograms was on average at zero (Eqn. 2.6):

$$^{129}\text{I}_{\text{corr}} = ^{129}\text{I}_{\text{meas}} - (x \times ^{131}\text{Xe}_{\text{meas}}) \quad (2.6)$$

where $^{129}\text{I}_{\text{corr}}$ = corrected counts per second (CPS) for ^{129}I ; $^{129}\text{I}_{\text{meas}}$ = measured CPS for ^{129}I ; x = factor determined by iteration for each run; $^{131}\text{Xe}_{\text{meas}}$ = measured CPS for ^{131}Xe . Xenon correction was applied to ^{129}I chromatography results before peak integration. Iodine-129 peaks were manually integrated between the two points where the chromatogram crossed the baseline, using the baseline as the bottom of the peaks. Iodine-127 peaks were manually integrated between the two points where the chromatogram crossed a baseline that was consistent for each analysis run and deemed to represent the bottom of the observed peaks.

Inorganic iodine speciation (iodide and iodate) was carried out using a Hamilton PRP X-100 column (5 μm , 4.1 x 50 mm) using an isocratic method with 1.3 ml min^{-1} eluent (60 mM ammonium nitrate, 2 % methanol, 1×10^{-5} M EDTA, pH adjusted to 9.5 using TMAH) for 308 s and an injection volume of 25 μl .

Separation of organic iodine from iodide and iodate was carried out by SEC – ICP-MS using a Superose 12 10/300 GL column (GE Healthcare) with an isocratic method at 1 ml min^{-1} eluent (0.1 M tris(hydroxymethyl amine) with pH adjusted to 8.8 using 50 % TAG HNO_3) for 25 min and 25 μl injection volume.

3 TOTAL IODINE IN NORTHERN IRELAND FIELD SAMPLES

3.1 INTRODUCTION

The main source of iodine input to soil is the ocean, either directly e.g. as sea spray, or indirectly from rainfall which washes marine particulates out of the atmosphere (Neal et al., 2007; Truesdale and Jones, 1996). Fuge (1996) observed that soils within 20 km of the Welsh coast appeared to show elevated iodine concentrations as a consequence of these inputs, and the existence of a ‘coastal band’ of soils enriched in iodine extending as far inland as 50 km was proposed by Johnson (2003a) on the basis of a wider study.

Soil iodine concentration represents a balance between iodine input from rainfall and marine sources, and output through leaching and uptake by vegetation (Fuge, 1996; Fuge and Johnson, 1986), with soil properties determining the extent of retention. Factors which encourage retention in soils are likely to be the same ones that reduce iodine availability to vegetation. Iodine in vegetation originates from the medium in which it grows (e.g. Smoleń et al. (2011), Whitehead (1975), Tsukada et al. (2008) and Sheppard et al. (1993)), and from rainfall and direct aerial deposition (Schmitz and Aumann, 1994; Shaw et al., 2007; Sheppard et al., 1993; Tschiersch et al., 2009; Whitehead, 1984). It may therefore be expected that vegetation low in iodine and an associated increased prevalence of IDD is more likely in inland locations.

While IDD is frequently reported in remote continental regions (Fordyce et al., 2003; Johnson et al., 1999; Johnson et al., 2002; Watts and Mitchell, 2009), they are not exclusive to these areas (Kelly and Snedden, 1960). For example, instances of IDD have been reported in the UK, where soil iodine concentrations are not considered to be low (Phillips, 1997; Saikat et al., 2004). There is anecdotal evidence of cattle in Northern Ireland (NI) suffering from IDD despite soil iodine concentrations that are high in the context of European and worldwide values (Smyth and Johnson, 2011). Thus soil iodine concentration cannot alone be the only predictor of the likelihood of IDD and other factors must be involved (Saikat et al., 2004; Stewart et al., 2003).

This chapter investigates the role of soil properties, location and rainfall on iodine mobility and retention in soil and vegetation using NI as the study area. The balance between iodine inputs, outputs and soil properties has been investigated through the collection of soil and vegetation samples at a range of distances from the coast in areas that have different rainfall inputs and soil types. The variation in iodine concentrations of rainfall collected at a single location over time has also been investigated.

3.2 MATERIALS AND METHODS

Twenty soil and associated vegetation samples were collected from sites across NI, chosen to represent a range of soil properties and distances from the coast. Soil properties pH, loss on ignition and total iodine content measured by the Tellus survey of NI topsoils was used to aid site selection. Samples of rainfall were also collected over seven day periods at Hillsborough, Co. Down, NI, between January and June 2012 using permanently open bulk collectors. Soil and vegetation samples were processed and stored as described in Chapter 2, and soils were classified according to the descriptions in Cruickshank (1997). Total iodine was extracted from soil and vegetation samples as described in Section 2.4.5 except that supernatants containing high concentrations of organic matter (from soils where SOM > 10 %) were filtered through 0.45 µm nylon acrodisc syringe filters before dilution. Rainfall samples were stored unfiltered at 4 °C and analysed for total iodine with and without addition of 0.1% TMAH. Total iodine in rainfall, and soil and vegetation extracts was analysed as described in Section 2.6.2.1, with amendments described above. Soil characteristics including pH, SOC, and Fe, Mn and Al oxide concentrations were determined as described in Section 2.4.

3.3 RESULTS AND DISCUSSION

Sample locations are shown in Figure 3.1 overlaid on the Tellus iodine data for NI topsoils, and presented in Appendix 1 with site observations. Soil characteristics are given in Table 3.1 together with information on coastal proximity and annual rainfall. Soil classification, description, geology and texture (field observation) are presented in Table 3.2. Individual soil and vegetation descriptions from field observations are in Appendix 1. All soils were acidic, with pH (measured in water) between 2.84 and 5.90 (median pH = 4.76). Most soils had SOC < 30 %. Five had 38 % ≤ SOC ≤ 53 %,

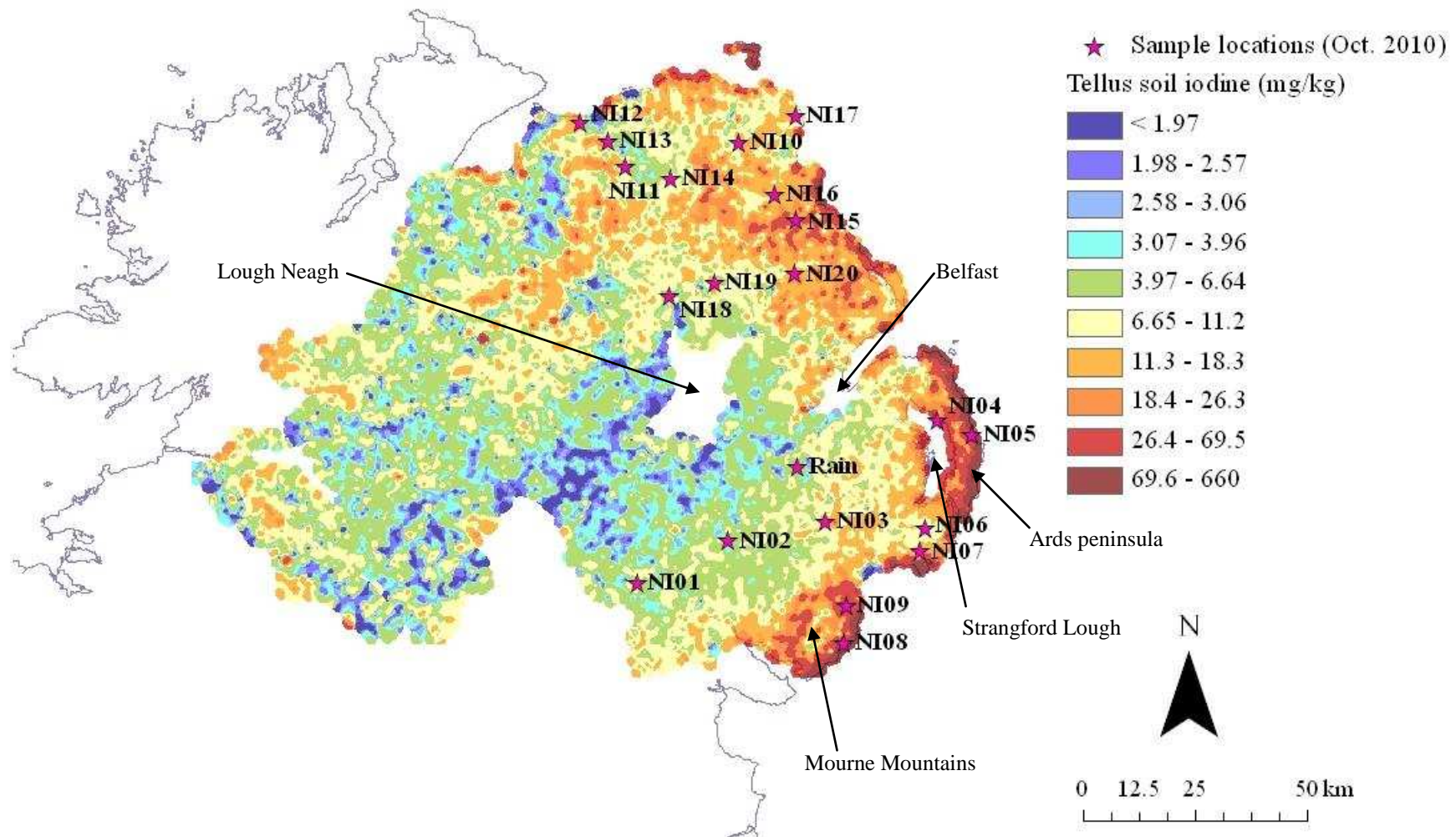


Figure 3.1. Geological Survey of Northern Ireland Tellus survey iodine topsoil map showing soil, vegetation and rainfall sampling locations (after Smyth and Johnson, 2011). Also locations of some geographical features noted in text.

Table 3.1. Measured chemical characteristics of soils, total iodine in soil and vegetation, and site-specific information distance to coast and total annual rainfall. Values in brackets show the number of replicates for determination of each value. ND = not detected.

Site	Distance to coast (km)	Total annual rainfall (mm)	pH (in H ₂ O) (n = 1)	Soil Organic Carbon (%) (n = 1)	Al (g kg ⁻¹) (n = 3)		Mn (g kg ⁻¹) (n = 3)		Fe (g kg ⁻¹) (n = 3)		Total iodine in soil (mg I kg ⁻¹) (n = 3)		Tellus soil iodine range (mg I kg ⁻¹)		Total iodine in washed veg (mg I kg ⁻¹) (n = 3)		Total iodine in unwashed veg (mg I kg ⁻¹) (n = 3)	
					Mean	S. E. (x 10 ⁻³)	Mean	S. E. (x 10 ⁻³)	Mean	S. E. (x 10 ⁻²)	Mean	S. E.	Min	Max	Mean	S. E. (x 10 ⁻²)	Mean	S. E. (x 10 ⁻³)
NI01	22.3	1129	4.71	4.81	1.25	28.6	0.132	1.32	9.01	0.751	2.89	0.0153	6.65	11.2	0.881	28.1	0.799	3.86
NI02	17.8	881	4.54	3.64	1.57	30.3	0.32	0.796	10.1	5.77	4.29	0.0204	3.97	6.64	0.205	0.794	0.185	3.31
NI03	12.5	1163	3.72	47.7	3.8	60.6	0.0103	0.0619	1.34	1.04	20.8	0.218	11.3	18.3	1.46	11.2	1.75	150
NI04	0.007	807	4.96	3.28	0.573	5.69	0.0547	0.479	4.55	7.33	9.29	0.138	6.65	11.2	1.74	15.6	1.59	54.9
NI05	0.257	807	5.49	4.76	1.72	32.4	0.162	1.35	8.11	5.43	274	14.9	69.6	660	2.61	11.7	3.62	200
NI06	4.7	835	4.78	3.59	1.74	40.5	0.526	8.32	13	12.0	9.38	0.254	6.65	11.2	0.62	1.44	0.51	11.5
NI07	2.5	845	5.89	3.98	1.29	20.6	0.23	2.24	10.2	6.89	14	0.36	11.3	18.3	0.818	2.9	0.716	34.5
NI08	0.981	1146	5.9	6.01	2.07	44.7	0.0757	1.38	9.29	7.57	127	2.63	69.6	660	1.42	2.04	1.21	15.2
NI09	3.16	1510	3.7	38.5	3.46	39.5	0.0107	0.114	2.01	3.03	32	0.776	26.4	69.5	2.2	8.04	2.31	26.2
NI10	10.8	1494	3.52	52.1	0.416	9.14	0.00704	0.0513	1.14	4.55	16.6	0.335	11.3	18.3	1.15	2.53	1.01	28.6
NI11	13	1016	4.8	9.58	4.03	79.2	0.358	7.38	18.2	60.3	10	0.22	3.97	11.2	0.641	2.13	0.82	3.06
NI12	1.65	1009	4.7	5.05	1.7	18.4	0.155	0.620	14.7	17.1	4.15	0.127	11.3	18.3	0.4	1.26	0.331	13.3
NI13	6.3	1054	5.74	12.1	2.56	80.6	0.372	8.50	18.7	39.6	7.46	0.292	11.3	18.3	0.297	0.375	0.465	14.7
NI14	20	1011	5.37	8.11	2.39	67.1	0.312	5.13	20.7	48.1	5.16	0.145	6.65	11.2	0.36	1.29	0.465	35.1
NI15	5.69	1387	4.28	22.9	8.34	254	0.619	9.70	18.6	11.1	27.4	0.455	18.4	26.3	0.356	0.943	0.434	1.25
NI16	7.93	1599	2.84	50.1	0.74	20.3	0.00649	0.0102	1.75	3.05	21.6	0.189	11.3	18.3	1.12	3.38	1.27	20.5
NI17	1.37	1322	3.49	53.4	0.295	12.8	ND	0.0081	0.358	0.0407	13.2	0.46	6.65	11.2	1.37	1.66	1.25	6.42
NI18	38.9	891	4.86	8.43	4.13	95.4	0.841	14.1	20.1	65.3	9.64	0.272	3.97	6.64	0.174	0.293	0.186	4.94
NI19	28.7	967	4.85	8.33	3.61	64.6	0.966	10.8	23.9	12.6	11.1	0.478	3.97	6.64	0.18	0.271	0.191	6.56
NI20	14.2	1353	4.73	29.7	10.7	101	0.0418	0.154	10.1	7.59	9.6	0.29	11.3	18.3	0.413	1.62	0.366	7.09

Table 3.2. Geology, soil type and field textural observations at each sampling location. Soil descriptions are those of Cruickshank (1997).

Classification	Description	Site	Observed texture	Underlying geology
Alluvium	Mineral soil with various textures.	NI11	Clayey silt	Upper basalt formation.
Brown Earth	Has A, B, C horizons, free draining, little visible differentiation between horizons, normally brown or reddish-brown throughout. B horizon weathered. Ap horizons not humic; usually cultivated.	NI01	Silty clay	On border of dolerite dyke and Gala group sandstone.
		NI06	Silt	Hawick group sandstone.
		NI15	Silt	Lower basalt formation.
		NI18	Clayey silt	Lower basalt formation.
Gley 1	Gley with good drainage at time of surveying and small point mottling. Tend to be 'relatively dry or just moist' even in winter. Moisture does not collect in floor of 1 m inspection pit. Includes groundwater and surface water gleys.	NI04	Sandy clay	Sherwood group sandstone.
		NI05	Silty sand	Gala group sandstone.
		NI13	Sandy clay	Upper basalt formation.
Gley 2	Gley with impeded drainage at time of surveying and usually large rusty mottles. Water collects in floor of dug pit; water table within ~70 cm of soil surface. Includes groundwater and surface water gleys.	NI07	Silt	Hawick group sandstone.
		NI14	Silty clay	Lower basalt formation.
		NI19	Clayey silt	Upper basalt formation.
Humic gley	Looks very peaty but is classified as humic gley.	NI20	Silt	Upper basalt formation.
Peat	Incorporates peat > 50 cm thick.	NI10	Peat	Psammite and semi-pelite (Altimore formation).
		NI16	Peat	Upper basalt formation.

Classification	Description	Site	Observed texture	Underlying geology
		NI17	Peat	Psammite and semi-pelite (Runabay formation).
Podzol	Free-draining, acid, well-leached. Visibly differentiated profile.	NI02	Silty clay	Gala group sandstone.
		NI08	Sandy silt	Hawick group sandstone.
Ranker	'Raw and undeveloped thin soils'. Less than 40 cm depth to parent material. No developed horizons. Mostly free draining. Includes humic rankers, where surface humic horizon is acid and < 40 cm thick. Often found in association with blanket peat.	NI03	Silt	Gala group sandstone.
		NI09	Silt	Granite dyke.
		NI12	Sandy clay	Upper basalt formation.

which was associated with low pH ≤ 3.7 , classified as either peat or ranker. Mn was typically $< 1 \text{ g kg}^{-1}$, with slightly more Al (median 1.90 g kg^{-1}) and considerably greater concentrations of Fe (median 10.1 g kg^{-1}).

3.3.1 Total iodine in soil

Soil iodine concentrations (I_s) varied substantially; most were in the range $2.89 - 32.0 \text{ mg I kg}^{-1}$, but two coastal soils contained substantially more iodine (NI05: 274 mg I kg^{-1} and NI08: 127 mg I kg^{-1}). The median concentration for all samples was $10.6 \text{ mg I kg}^{-1}$. Measured I_s values were in good agreement with those determined by XRFs as part of the Tellus survey (Table 3.1, Figure 3.1) (Smyth and Johnson, 2011). In the context of European and worldwide soil iodine values (European mean $5.56 \text{ mg I kg}^{-1}$, worldwide range $0.1 - 72 \text{ mg I kg}^{-1}$ and mean $5.09 \text{ mg I kg}^{-1}$), the I_s concentrations measured here were relatively high (Johnson, 2003a; Smyth and Johnson, 2011). They are also slightly higher than the reported range for UK soils ($0.5 - 98.2 \text{ mg I kg}^{-1}$, mean 9.2 mg I kg^{-1} , Whitehead (1979)), reflecting the relative proximity of the entire NI landmass to the coast.

Coastal proximity can be considered a proxy for the likely input of “marine-derived” iodine to soils and plants. Sites close to the sea will receive direct sea spray, and rainfall in coastal areas contains more iodine than that further inland (Aldahan et al., 2009). A comparison of soil iodine concentration with coastal proximity is shown in Figure 3.2. All samples were within 50 km of the coast, the majority within 20 km, and therefore within the ‘band’ where I_s concentrations should be elevated according to Fuge (1996) and Johnson (2003a). Selected samples showed elevated I_s concentrations, with the highest concentrations observed in samples closest to the coast. However, other samples at similar distances had lower I_s , and consequently the relationship between coastal proximity and I_s was not significant ($r = -0.339$, $p = 0.144$). Whitehead (1973b) also found no correlation between coastal proximity and I_s in a range of British soils despite finding that soils subject to marine influence were more likely have high I_s than inland soils. The greater range of I_s values observed in samples close to the coast, particularly within 5 km, suggests that despite potentially high inputs only some soils are able to retain the iodine. As soil organic carbon is the main sink of iodine in soils it might therefore be expected to control iodine retention in these coastal soils. Comparison of samples closest to the coast (NI04, NI05 and

NI08), which have similar organic carbon contents ($3 \leq \text{SOC} \leq 6\%$) but very different I_s concentrations ($9.29 \text{ mg I kg}^{-1}$, 274 mg I kg^{-1} and 127 mg I kg^{-1} respectively) suggests that other factors are also important. Site NI04 was on the west coast of the Ards peninsula on the edge of Strangford Lough, a sea lough, sheltered from direct sea winds (Figure 3.1). In contrast, NI05 and NI08 were sampled from the top of hills receiving direct sea spray. There is limited evidence to support an effect of location on I_s when results from samples along the west coast of the Ards Peninsula within the Tellus Survey are considered (Figure 3.1, Smyth and Johnson (2011)). These had lower I_s concentrations than those on the east coast which receives more direct sea-spray, despite the soil characteristics and rainfall being similar (Smyth and Johnson, 2011). Although NI05 and NI08 were not the only samples from close to the coast, they will be identified from this point onwards as the ‘coastal’ soils for ease of reference.

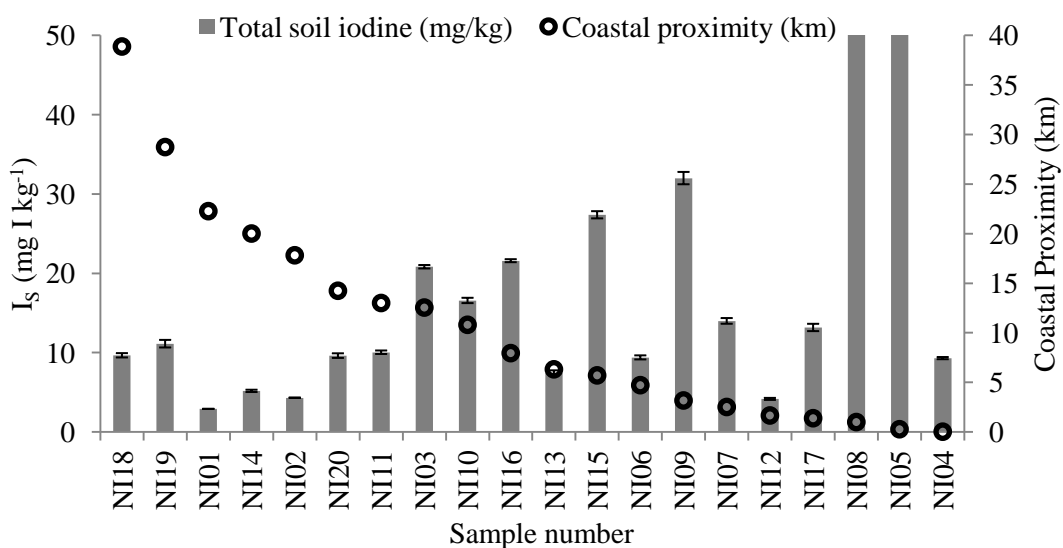


Figure 3.2. Relationship between coastal proximity and total iodine in Northern Irish soil (I_s); samples arranged in descending coastal proximity. Error bars represent standard error ($n = 3$). Axis for total iodine has been limited to 50 mg I kg^{-1} in order to show lower concentrations. Values for NI05 and NI08 exceed the scale and are 274 and 127 mg I kg^{-1} respectively.

According to the samples’ soil classifications (Table 3.1), half the soils were gleys or peats. Gleys are common across NI (covering 50.5 % of the land area), where annual rainfall typically exceeds annual evapotranspiration, resulting in surplus water in the soil and the formation of gleys and humic gleys (Cruickshank, 1997). Soil type (classification) effectively describes soils by their combination of characteristics, there was a significant difference in I_s according to soil type (analysis of variance, ANOVA,

$p = 0.019$) (Figure 3.3), which remained when the two high iodine soils (NI05 and NI08) were removed ($p = 0.023$). Highest iodine concentrations were observed in the peats and humic rankers where pH was low (2.8 – 3.7) and SOC was high (38 – 53 %), allowing retention of large amounts of incoming iodine (Keppler et al., 2003). The gley soils have lower iodine concentrations which may be due to waterlogging resulting in reducing conditions (Ashworth and Shaw, 2006b; Neal et al., 2007; Whitehead, 1984) and iodine transformation to iodide, which is less well adsorbed by metal oxides (Allard et al., 2009; Dai et al., 2009; Muramatsu et al., 1990). Reduction to iodide has been suggested as a mechanism for loss of iodine from complexes with organic molecules (Francois, 1987).

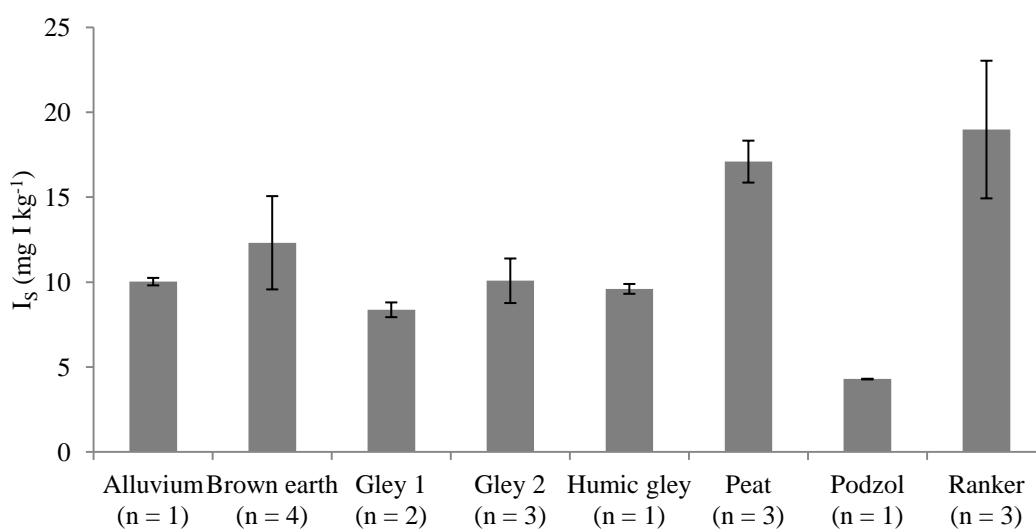


Figure 3.3. Soil iodine content (I_s) as a function of soil type. I_s values are mean of three replicates for measurement of each soil within the class (comprising ‘n’ soils) and error bars show standard error of the same. The two coastal soils (NI05 and NI08) are excluded.

Soil texture also had a significant effect on I_s (ANOVA, $p < 0.001$) (Table 3.2, Figure 3.4). Soils classified as peat and silt (on the basis of their location and formation) both have high SOC and consequently the highest I_s concentrations. Sandy and silty clay soils contained least iodine (Figure 3.4) because they are poor at retaining nutrients due to their relatively low concentrations of both organic matter and metal oxides that provide sorption sites (Gerzabek et al., 1999; Sheppard et al., 1996).

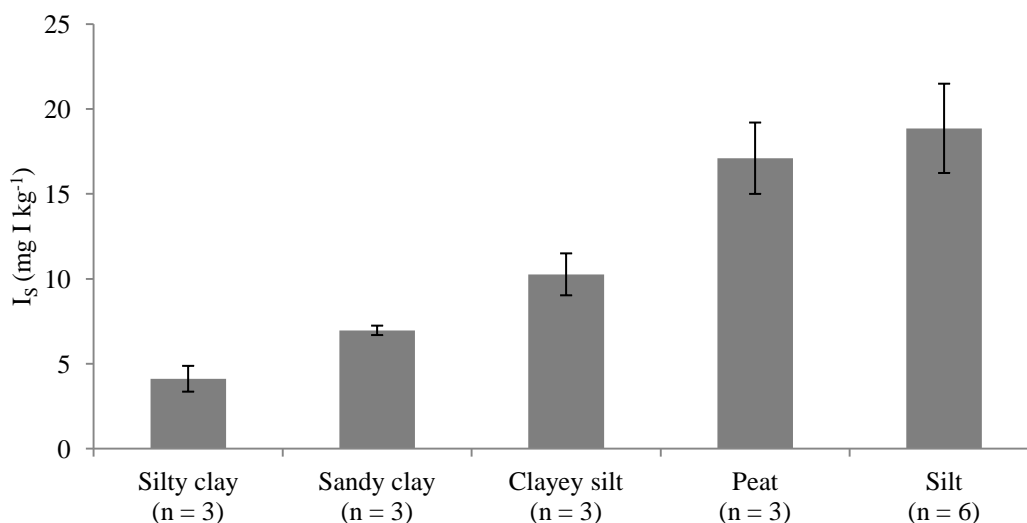


Figure 3.4. Soil iodine content (I_S) as a function of soil texture (field observation) and ordered by increasing I_S . I_S values are mean of three replicates for measurement of each soil within the class (comprising 'n' soils) and error bars show standard error of the same. The two coastal soils (NI05 and NI08) are excluded.

A significant positive correlation between SOC and I_S ($r = 0.642$, $p = 0.004$) was observed when the two high iodine coastal soils (NI05 and NI08) were excluded (Figure 3.5). A significant negative correlation between soil pH and I_S ($r = -0.584$, $p = 0.011$) was also observed (Figure 3.6). Organic matter has been shown to be the main sink for iodine in soils, binding it both in isolation and within the soil matrix (Kashparov et al., 2005; Moulin et al., 2001; Muramatsu et al., 2004; Sheppard et al., 1996; Sheppard and Thibault, 1992; Shetaya et al., 2012; Whitehead, 1984) (Figure 3.5). Soils with high SOC typically have low pH. The influence of soil pH on iodine retention has been investigated by various authors and shown to be complex (e.g. Fuge, 1990; Fuge and Johnson, 1986; Lidiard, 1995). Shetaya et al. (2012) demonstrated that low pH increases the instantaneous sorption of iodine to soil metal oxides with the sorbed iodine then undergoing slower transformation to organic forms. At high pH, $\text{OH}^-_{(\text{aq})}$ will be present, competing with iodine anions for positively charged sites, whereas at low pH there are more positively charged sites and therefore greater opportunity to bind anionic iodine (Allard et al., 2009; Whitehead, 1974b; Yoshida et al., 1992).

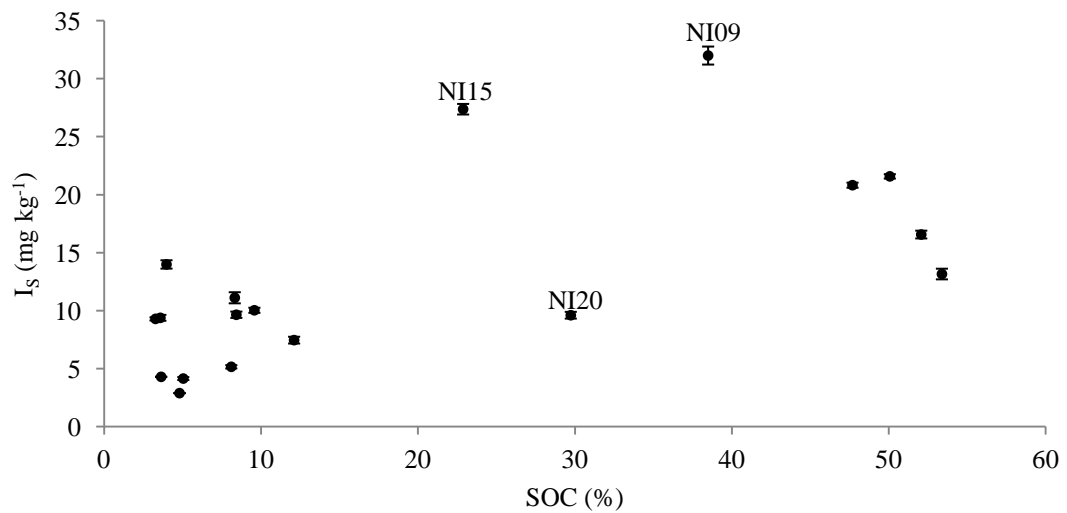


Figure 3.5. Relationship between total soil iodine (I_s) and soil organic carbon (SOC). The two coastal soils (NI05 and NI08) are excluded.

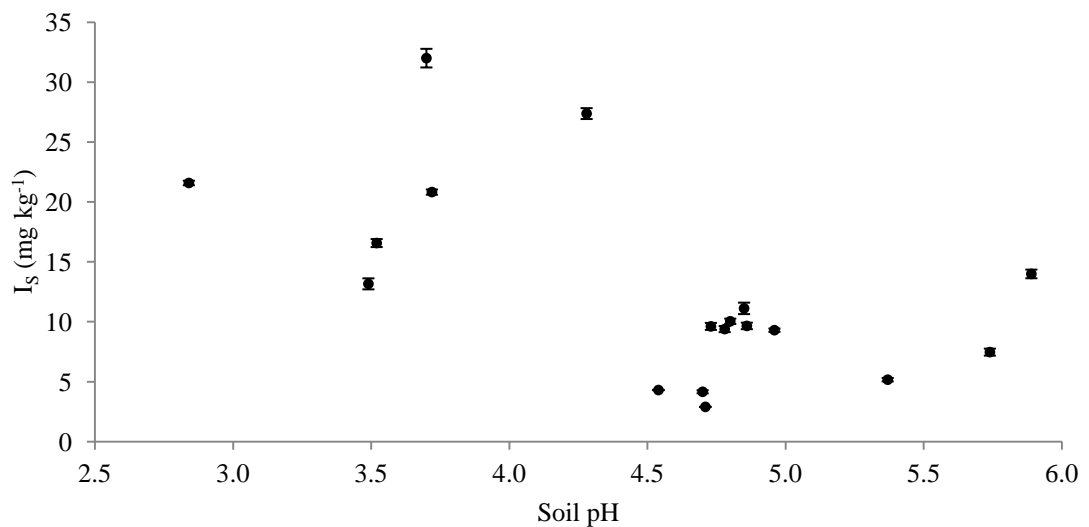


Figure 3.6. Relationship between total soil iodine (I_s) and soil pH. The two coastal soils (NI05 and NI08) are excluded.

No significant correlation between I_s and Al, Fe or Mn contents was observed for these soils. Metal oxides have been shown to be an important reservoir for native iodine in some soils, particularly at $\text{pH} < 5$ (Schmitz and Aumann, 1995; Whitehead, 1973a). However, in organic-rich soils, organic matter is more important at retaining iodine (Hansen et al., 2011; Sheppard and Thibault, 1992). Therefore, although the NI soils all have $\text{pH} < 6$, which is the region in which iodine sorption to metal oxides is promoted, they are also all relatively rich in organic matter, with SOC contents 3.28 –

53.4 %. Therefore it is likely that the role of organic matter in binding iodine masks any correlation that may be present with metal oxides.

3.3.2 Total iodine in vegetation

Vegetation iodine concentration (I_v , Table 3.1) was determined on both unwashed samples and the same samples washed in MQ water. Concentrations ranged between 0.185 – 3.62 mg I kg⁻¹ (median 0.758 mg I kg⁻¹) in unwashed samples and were similar in washed samples (0.174 – 2.61 mg I kg⁻¹; median 0.730 mg I kg⁻¹). There was no significant difference between the two sets of results (paired t-test, $p = 0.366$) therefore only unwashed vegetation values will be presented and discussed. The concentrations measured were within the ranges of those quoted in the literature for a variety of vegetation and soil types from field studies (Table 3.3). They were higher by a factor of ten than those observed by Johnson et al. (2002) in areas of Morocco where IDD's are common.

Table 3.3. Total iodine concentrations in vegetation (I_v), and concentration ratios (CR) grown under field conditions, from published studies. ‘NR’ = not recorded, or not possible to calculate from given data.

Author, date	Experimental details	Soil type	Vegetation type	I_v (mg I kg ⁻¹ dry weight)	CR*
Johnson et al. (2002)	Investigation of environmental iodine in Morocco. Ounein Valley: $I_s \sim 1 - 2$ mg I kg ⁻¹ , 3 – 7 % LOI, pH 7.5 – 7.7. Agadir: $I_s \sim 2 - 3$ mg I kg ⁻¹ , 3 – 5 % LOI, pH 7.5 – 7.6.	‘Poor sandy soil’ (Ounein)	Carrot	$18 - 31 \times 10^{-3}$	0.0075 – 0.0 358
			Runner bean	$<10 - 12 \times 10^{-3}$	NR
		Coastal (Agadir)	Barley	$<10 - 25 \times 10^{-3}$	NR
Kashparov et al. (2005)	Study where ¹²⁵ I was added to various soils, vegetables grown and CR calculated. ¹²⁵ I added as KI at 5 mg ¹²⁵ I m ⁻² . Podzoluvisol: 0.4 mg ¹²⁷ I kg ⁻¹ , 0.8 % ‘humus’, pH 6.3. Greyzem 1.0 mg ¹²⁷ I kg ⁻¹ , 1.1 % ‘humus’, pH 7.9.	Podzoluvisol	Radish	NR	0.012 – 0.047
			Beans	NR	0.0033 – 0.0037
		Greyzem	Radish	NR	0.0028 – 0.014
			Beans	NR	$4 \times 10^{-4} - 7 \times 10^{-4}$
Rui et al. (2009)	Study of effect of N fertiliser application on iodine content in China (control plot).	No details	Corn grain	26.5	NR
Sheppard et al. (1993)	Field lysimeter experiment. Soil 18.4 % SOM, pH 7.5, I_s unknown. Iodine (species not specified) added as ‘potassium salt’ at 4 and 10 g I m ⁻² .	‘Typical garden soil’, Canada	Beetroot	0.60 – 2.6	0.024 – 0.19 (all crops)
		Cabbage	0.1 – 2.4		
		Sweetcorn	0.30 – 1.1		
Sheppard et al. (2010)	Comparison of field and garden vegetation iodine concentrations. Soils: $1.7 \% \leq \text{SOM} \leq 8.5 \%$ and $6.3 \leq \text{pH} \leq 7.8$. I_s not stated.	Agricultural soils	Various fruit and vegetables	NR	0.002 – 0.082

Author, date	Experimental details	Soil type	Vegetation type	I _v (mg I kg ⁻¹ dry weight)	CR*
Smith et al. (1999)	Test of whether spraying iodine onto pasture improved animal blood iodine concentrations (control plots).	Various	Pasture	0.26 – 3.04	NR
Whitehead (1984)	Review of values quoted in the literature to date, from studies in the United States, United Kingdom, France, and New Zealand.	Various	Various vegetables and grasses	0.05 – 0.5	NR
Northern Ireland (this study)	Soil and vegetation samples from across eastern NI.	Various	Various including pasture	0.185 – 3.62	0.00953 – 0.277

*CR = I_v / I_s

A significant negative correlation was observed for I_V with distance from the coast ($r = -0.493$, $p = 0.027$). Several processes may be responsible for transferring iodine directly to vegetation in coastal regions. Volatilisation of iodine from some species of seaweed is known to contribute to locally elevated atmospheric iodine concentrations (Chance et al., 2009; Nitschke et al., 2011; Saiz-Lopez et al., 2006) and iodine in rainfall (Gilfedder et al., 2008). Gaseous iodine species including I_2 and various organic molecules are, however, short-lived (hours), as a result of their involvement in reactions including photolysis (Bloss and Ball, 2009; Gilfedder et al., 2007). Only locations relatively close to the coast would therefore be expected to receive significant iodine concentrations by this mechanism (Baker et al., 2000). Sea-spray inputs are likely to be significant only at even shorter distances due to the size of spray particles and their limited aerodynamic range. Uptake of iodine directly through leaves has been shown to occur rapidly, probably as I^- (in wet deposition) and gaseous CH_3I and I_2 (Collins et al., 2004; Shaw et al., 2007; Tschiersch et al., 2009). Landini et al. (2011) investigated uptake of iodine by tomato plants and reported that uptake via leaves, despite being rapid, resulted in lower iodine uptake than when supplied via roots. Marine sources of iodine reaching land may increase solution-iodine concentrations, providing iodine in a form that is phyto-available and rapidly taken up by plants before it can react with and be retained by the soil.

A significant positive correlation between I_S and I_V was observed for all samples: $r = 0.756$, $p < 0.001$, which was weaker when the two coastal soils were removed: $r = 0.625$, $p = 0.006$ (Figure 3.7). Values of I_V for NI05 and NI08 were comparable to those in other vegetation samples of similar type despite the corresponding I_S values being up to a factor of ten greater. Similar observations were made in experiments by Weng et al. (2008a; 2008b). They observed an approximate linear increase in I_V for cucumbers, radishes and aubergines and Chinese cabbage up to $I_S \approx 50 \text{ mg I kg}^{-1}$, beyond which point the rate of increase in I_V dropped. They explained their observations in terms of toxicity to the plants although no mechanism for this was proposed and high levels of seedling death at $I_S > 150 \text{ mg I kg}^{-1}$ suggested that iodine exclusion of to prevent toxicity was not occurring.

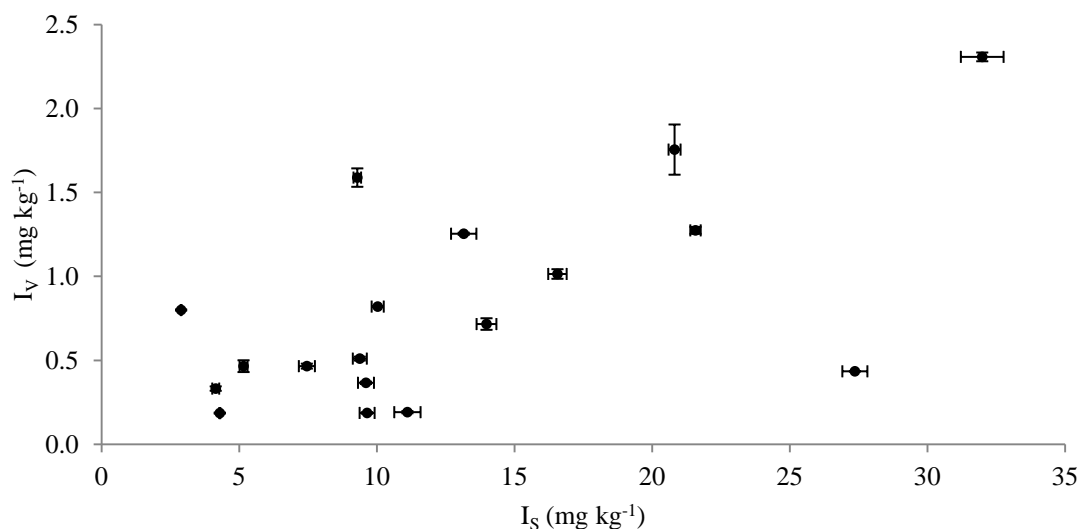


Figure 3.7. Relationship between total iodine in soil (I_S) and total iodine in (unwashed) vegetation (I_V). Error bars show the standard error of triplicate analyses. The two coastal soils (NI05 and NI08) are excluded.

The relationship between soil (I_S) and vegetation (I_V) iodine concentrations can be expressed as a concentration ratio, CR (Eqn. 3.1):

$$CR = \left(\frac{I_V}{I_S} \right) \quad (3.1)$$

The CR values determined in this study range from 0.00953 – 0.277, with a median of 0.0612 (Table 3.3), reflecting variations in iodine input mechanisms and vegetation types. The values are all within the ranges quoted in other studies (Table 3.3) with the exception of NI01 (CR = 0.277). This is higher than the maximum values in Table 3.3, quoted by Sheppard et al. (1993) where highest CR values were 0.15 (beetroot leaf), 0.10 (early cabbage) and 0.19 (bottom of sweetcorn plant). The difference in CR values from the study by Sheppard et al. (1993) and others in Table 3.3 is likely to be the relatively high rate of iodine addition, resulting in a large concentration of available iodine. Therefore NI01 is likely to have either a high proportion of available soil iodine, or readily phyto-available atmospheric inputs, despite having the lowest I_S concentration of all the NI sites. The importance of both soil type and vegetation species on determining CR was observed by Kashparov et al. (2005) and Sheppard et al. (2010).

When the two coastal soils were excluded, there was a significant linear positive correlation between I_V and SOC: $r = 0.580$, $p = 0.012$, although Figure 3.8A shows that the relationship may not be simply linear. For the same soils there was a significant negative correlation between pH and I_V : $r = -0.544$, $p = 0.020$ (Figure 3.8B). These observations mimic those observed in the soil, and given that I_V and I_S are positively correlated, the increase in I_V values may simply be a reflection of greater I_S concentrations.

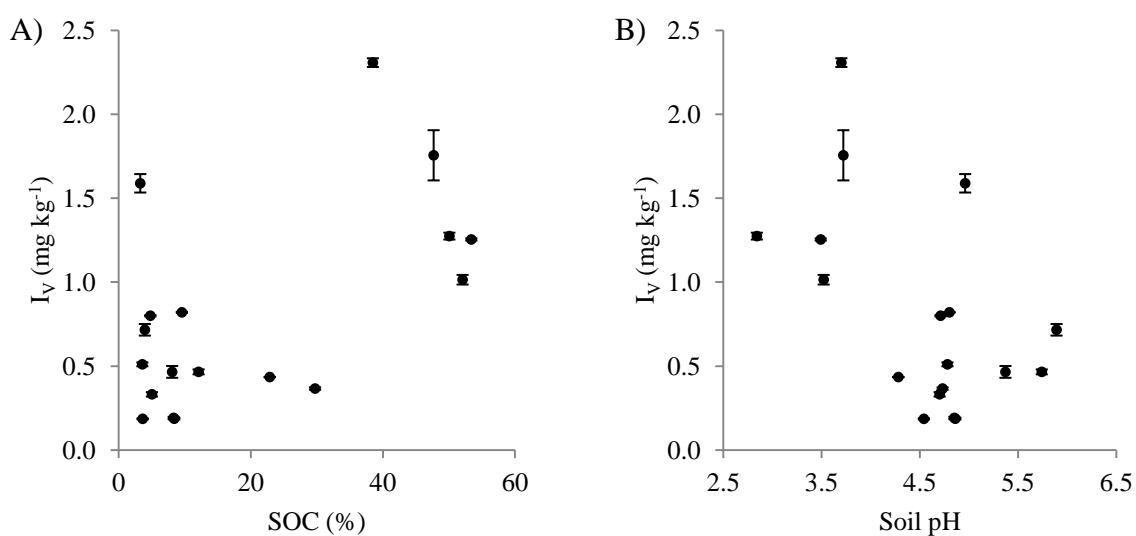


Figure 3.8. Relationship of vegetation iodine concentration (I_V) with A) soil organic carbon (SOC) and B) soil pH. The two coastal soils (NI05 and NI08) are excluded.

Both Fe and Mn oxides were significantly negatively correlated with I_V (Fe: $r = -0.770$, $p = 0.000$; Mn: $r = -0.657$, $p = 0.003$; coastal soils excluded) but no significant correlation with Al was observed. Higher Fe and Mn oxides therefore appear to fix iodine within the soil, making it less phyto-available. This contrasts with sorption linked to greater SOC and lower pH, which resulted in an increase in both I_S and I_V . Sorption of iodine to Al oxide was shown by Muramatsu et al. (1990) to be less important than sorption to Fe oxide, which may explain the disparity between effects of different metal oxides on I_V .

3.3.3 Total iodine in rainfall

Measured iodine concentrations in rainfall samples (I_R) are presented in Table 3.4. They range between $0.778 - 6.36 \mu\text{g I L}^{-1}$ (median $2.25 \mu\text{g I L}^{-1}$) with no apparent dependence on season (Table 3.4). There was no significant difference between values measured in the presence or absence of 0.1 % TMAH ($p = 1.00$), and values for both are presented, so the mean of the two values have been used for discussion. Concentrations were similar to those reported for Western Europe: Aldahan (2009) reported $2.37 - 2.77 \mu\text{g I L}^{-1}$ over low-altitude sites in Sweden and Denmark and $1.05 \mu\text{g I L}^{-1}$ at higher altitudes. Over the North Sea, Campos et al. (1996) measured $0.86 \pm 0.95 \mu\text{g I L}^{-1}$. Neal et al. (2007) determined a value of $1.55 \mu\text{g I L}^{-1}$ in rainfall over Wales and a concentration of $1.27 \mu\text{g I L}^{-1}$ was reported for Wallingford, England (Truesdale and Jones, 1996).

Table 3.4. Rainfall volumes and iodine concentrations (I_R) in samples collected in Hillsborough, NI. All were collected over a period of seven days. I_R was measured in the presence/absence of 0.1 % TMAH matrix and the mean of the two values calculated. NR = volume not recorded, or insufficient sample to analyse.

Collection start date	Volume collected (ml)	I_R ($\mu\text{g I L}^{-1}$)		
		0 % TMAH	0.1 % TMAH	Mean
18/01/2012	346	0.944	0.901	0.923
25/01/2012	424	2.12	2.08	2.10
01/02/2012	138	1.28	1.23	1.26
08/02/2012	525	0.980	0.936	0.958
15/02/2012	215	0.808	0.748	0.778
22/02/2012	163	1.00	0.950	0.973
29/02/2012	135	2.13	2.11	2.12
07/03/2012	NR			
14/03/2012	87	6.27	6.46	6.36
21/03/2012	NR			
28/03/2012	NR			
04/04/2012	161	2.70	2.24	2.47
11/04/2012	359	1.71	1.42	1.57
18/04/2012	425	2.74	2.24	2.49
25/04/2012	180	5.59	4.70	5.15
02/05/2012	150	4.87	4.03	4.45
09/05/2012	235	2.34	1.98	2.16
16/05/2012	153	2.88	2.41	2.64
23/05/2012	NR	2.69	2.56	2.62
30/05/2012	NR	2.87	2.72	2.80
06/06/2012	NR	2.86	2.70	2.78
13/06/2012	NR	2.41	2.28	2.35
20/06/2012	NR	1.08	1.09	1.08

Truesdale and Jones (1996) suggested that as rainwater ‘washes’ iodine from the atmosphere, there should be an inverse relationship between rainfall amount and I_R . A weak correlation was observed for these samples: $r = -0.447$, $p = 0.095$ (Figure 3.9).

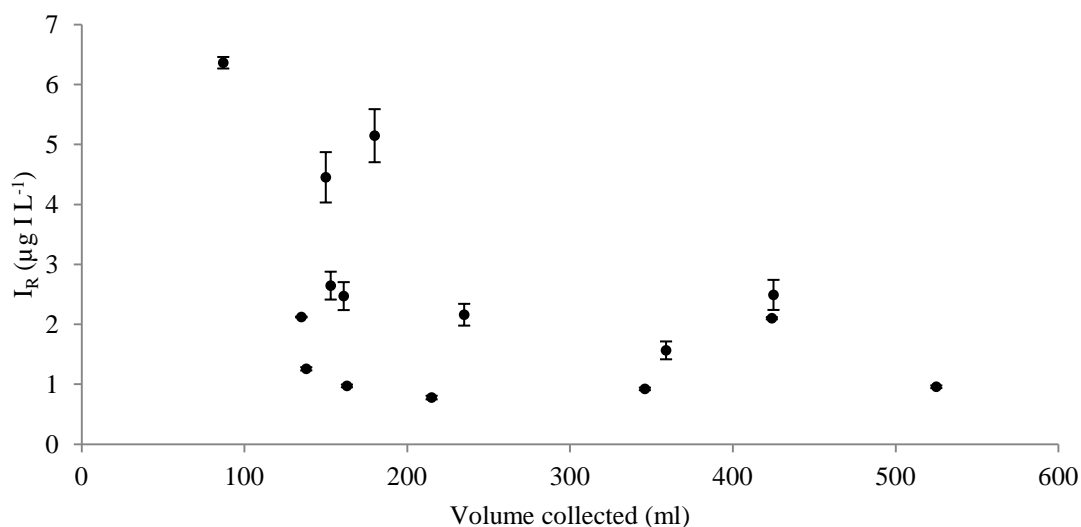


Figure 3.9. Relationship between rainfall volume and iodine concentration in rain (I_R).

A significant linear correlation between total annual rainfall and I_S was observed ($r = 0.671$, $p = 0.002$) when coastal samples were excluded (Figure 3.10), in agreement with the observations of other studies (Aldahan et al., 2009; Schnell and Aumann, 1999; Truesdale and Jones, 1996). No significant relationship between total annual rainfall and I_V was observed.

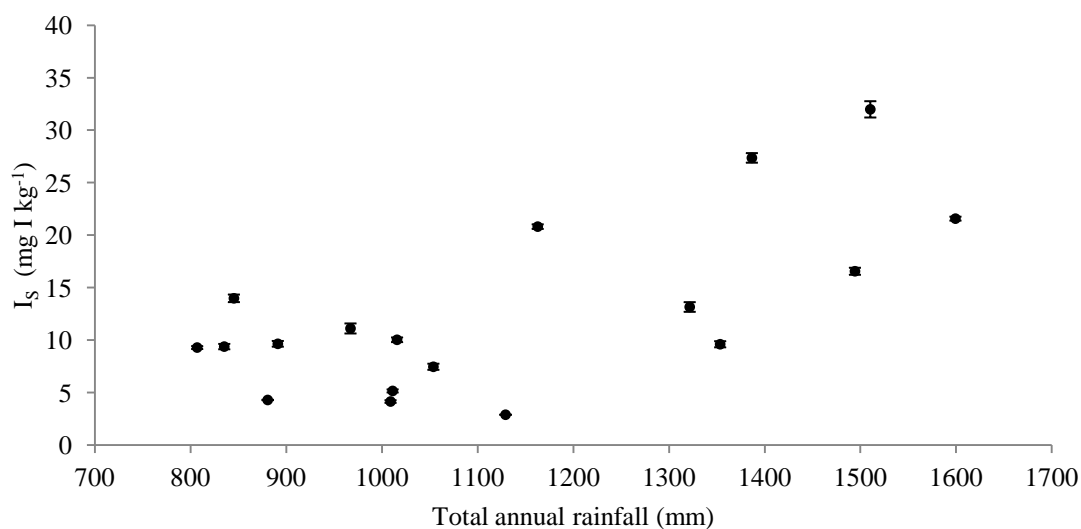


Figure 3.10. Relationship between total annual rainfall and soil iodine (I_S) concentration. Error bars show standard error of three replicates. The two coastal soils (NI05 and NI08) are excluded.

As rainfall is the main input of iodine to soils it is important to consider concentrations of I_S in the context of I_R and average rainfall volumes. Iodine input from rainfall (I_{in} , $\text{g I ha}^{-1} \text{ yr}^{-1}$, Table 3.5) during a given year is:

$$I_{\text{in}} = \frac{I_{\text{R}} \times V_{\text{R}}}{1,000,000} \quad (3.2)$$

where I_{R} = iodine concentration in rain ($\mu\text{g I L}^{-1}$) and V_{R} = volume of rain ($\text{L ha}^{-1} \text{yr}^{-1}$), calculated from total annual rainfall (Table 3.1). The total weight of iodine in each hectare of soil ($I_{\text{tot}} \text{ g I ha}^{-1}$) was calculated (Eqn. 3.3, Table 3.5):

$$I_{\text{tot}} = I_{\text{S}} \times (W_{\text{S}} \div 1000) \quad (3.3)$$

where W_{S} = weight of soil in top 20 cm (kg ha^{-1} , assumed to be $2,500,000 \text{ kg ha}^{-1}$). The removal of iodine by off-take of vegetation ($I_{\text{off}}, \text{ g I ha}^{-1} \text{yr}^{-1}$) was calculated on the basis that 10 t of vegetation was produced each year (Eqn. 3.4, Table 3.5). This yield is representative of the best yields from Rothamsted Park Grass (Rothamsted Research, 2006) and therefore will represent an over-estimate for most of the sites, particularly those on mountain tops which support only heather or moss, but is reasonable for grazed and improved grassland locations.

$$I_{\text{off}} = I_{\text{V}} \times 10 \quad (3.4)$$

The number of years (Yr) for current topsoil I_{S} to be achieved can then be calculated assuming that there are no losses to leaching, volatilisation, or runoff, and that there is full retention of incoming rainfall iodine (Eqn. 3.5, Table 3.5).

$$\text{Yr} = I_{\text{tot}} / I_{\text{in}} \quad (3.5)$$

Results (Table 3.5) demonstrate that for the vast majority of sampling locations the measured I_{S} concentrations can be accumulated after durations between 300 and 2400 yr. These timescales are in good agreement with those of Schnell and Aumann (1999) who calculated durations between 700 and 2,100 yr in a similar study of German soils. Where longer timescales are calculated, additional significant inputs of iodine from marine sources is likely to be the main reason (e.g. samples NI05 and

NI08). In all cases, except for sample NI05, rainfall supplies more iodine than is estimated to be removed from the system by vegetation off-take.

It is unlikely that in any soil system 100 % of iodine in rainfall is retained, however these timescales suggest that with just 10 % retention, rainfall provides sufficient iodine to influence I_S within relatively short timescales e.g. within the 10,000 – 20,000 yr since the last major glaciations of this region (Goldschmidt, 1958). This mass balance approach also demonstrates that an insignificant amount of soil iodine is removed by vegetation off-take in any year (Table 3.5).

Table 3.5. Iodine mass balance calculations: annual input from rainfall (I_{in}); the amount of soil iodine per hectare (I_{tot}); estimated annual iodine off-take by vegetation (I_{off}); the number of years to reach current values of I_S (Yr), assuming full retention of incoming rainfall iodine; and I_{off} as a percentage of I_{tot} .

Site	I_{in} (g I ha ⁻¹ yr ⁻¹)	I_{tot} (g I ha ⁻¹)	I_{off} (g I ha ⁻¹ yr ⁻¹)	Yr (yr)	I_{off} as percentage of I_{tot} (x 10 ⁻² %)
NI01	25.4	7,220	7.99	284	0.111
NI02	19.8	10,700	1.85	542	1.73
NI03	26.2	52,000	17.5	1,990	3.37
NI04	18.2	23,2000	15.9	1,280	6.84
NI05	18.2	685,000	36.2	37,700	0.528
NI06	18.8	23,400	5.10	1,250	2.17
NI07	19.0	35,000	7.16	1,840	2.05
NI08	25.8	318,000	12.1	12,300	0.381
NI09	34.0	80,000	23.1	2,350	2.88
NI10	33.6	41,400	10.1	1,230	2.45
NI11	22.9	25,000	8.20	1,100	3.27
NI12	22.7	10,400	3.31	456	3.20
NI13	23.7	18,600	4.65	786	2.49
NI14	22.8	12,900	4.65	567	3.61
NI15	31.2	68,400	4.34	2,190	0.635
NI16	36.0	53,900	12.7	1,500	2.36
NI17	29.7	32,900	12.5	1,100	3.81
NI18	20.1	24,100	1.86	1,200	0.772
NI19	21.8	27,800	1.91	1,280	0.687
NI20	30.5	24,000	3.66	788	1.52

3.3.4 Site-specific inputs of iodine

The major regional inputs of iodine from rainfall and marine sources can be reasonably easily established and quantified, particularly with a large dataset such as that accumulated by the Tellus Survey. Unique site inputs may also be important but are less readily quantified. Such inputs may originate from anthropogenic or natural sources, including the historical use of seaweed as a fertiliser (Cornish Seaweed Resources, 2010; Fuge and Johnson, 1986; Moreda-Pineiro et al., 2011; Romaris-Hortas et al., 2011); inundation by seawater in coastal areas; or the use of iodine supplements. Site specific factors that may have affected iodine concentrations are given in Table 3.6.

Table 3.6. Site-specific iodine inputs recorded during sampling.

Type of source	Specific source	Location observed
Anthropogenic	Iodophore disinfectants used for teat cleaning.	NI05, NI19. (Definitely not used at NI07, NI08, NI11, NI12)
	Iodine supplement in cattle feed when IDD's observed.	NI07
	Iodine-containing supplement bucket observed at or near sampling site.	NI15, NI20
	Farmyard manure fertiliser.	NI18 (approximately 1 year before sampling)
	Seaweed possibly used as fertiliser 30 – 50 years ago.	NI08
Natural	Deposition through cloud.	NI03, NI09
	Sea flooding, until sea wall built ~1990.	NI04
	Waste from seaweed-eating geese, encouraged as part of stewardship scheme.	NI04

3.4 CONCLUSIONS

Soil iodine concentrations varied widely but were within a similar range to that expected for coastal regions. Concentrations as a balance of input and retention was evident, with two coastally located soils containing significantly more iodine than the majority, and a greater range of iodine concentrations near the coast. SOC was the

most important factor for determining iodine retention, and metal oxides did not have a significant effect. Lower soil pH was associated with higher I_s , which may be due to pH influence on soil chemistry, or a result of the association between high SOC and low pH values. Site specific iodine inputs were too diverse and unquantifiable to include in discussions of individual sites.

Concentrations of iodine in vegetation varied considerably less than I_s concentrations, although there was a significant positive correlation between I_s and I_v for all samples. This correlation is likely to explain the relationships of I_v with SOC and soil pH. Although Fe and Mn oxides did not significantly affect retention of iodine by soils, they were associated with lower I_v . This suggests that unlike sorption to organic matter, sorption to metal oxides results in a non phyto-available form of iodine. There was a significant negative correlation between I_v and coastal proximity, which may also be reliant on I_s concentrations or may reflect aerial uptake of the greater atmospheric iodine concentrations closer to the coast. Annual off-take of iodine by vegetation was estimated to typically represent less than 0.07 % of soil iodine.

In agreement with the balance of modern literature, rainfall iodine concentrations and volumes have been used to confirm that rainfall provides sufficient iodine to account for the build-up in soil observed since the last glaciation, in conjunction with marine input where relevant. Rainfall was also estimated to provide more iodine than is removed annually by vegetation off-take. The dynamics of recently-added iodine, simulating the behaviour within soil of that originating from rain, are explored in Chapter 4. Subsequent uptake by plants and its dependence on soil properties is investigated in Chapter 6.

4 IODINE DYNAMICS IN NORTHERN IRELAND SOILS

4.1 INTRODUCTION

Total iodine concentration in soils (I_s) collected from NI varied from 2.89 mg I kg⁻¹ to 274 mg I kg⁻¹; variations in input alone were not sufficient to explain the differences observed (Chapter 3). Thus, the effect of soil characteristics on iodine retention may explain these differences (Fuge, 1996; Fuge and Johnson, 1986; Whitehead, 1984). The importance of pH and concentrations of organic matter and metal oxides in determining iodine sorption to soil have been established in the literature (Chapter 3), however experiments to determine their importance often rely on isolation or removal of individual soil components. For example Whitehead (1973a; 1974a; 1974b) investigated the effect of chalk, organic matter and metal oxides in isolation from, or added to, soils. Fox et al. (2009) and Allard et al. (2009) reported iodine transformations controlled by synthetic manganese oxides. While these results give important information about parts of the retention process, natural soils clearly contain different proportions of these components, which may interact with one another and do not necessarily influence iodine in isolation in the same way. Iodine dynamics in whole soils have been observed (Muramatsu et al., 1990; Sheppard and Thibault, 1992) and reports often qualitatively link sorption and desorption rates to soil properties (Sheppard et al., 1996; Whitehead, 1978). Only a small number of studies have examined iodine transformations and sorption in terms of soil properties (Dai et al., 2009; Shetaya et al., 2012).

It is important when investigating iodine dynamics to consider both inputs and soil properties. For example, both iodide and iodate have been measured in rainfall and therefore both must be included in any experiments relating to iodine input from rain (Aldahan et al., 2009; Dai et al., 2009; Dai et al., 2004; Lucia and Campos, 1997; Truesdale and Jones, 1996). Whitehead (1973a) showed a reduction in sorption of iodide onto dry soil, and Ashworth and Shaw (2006a) confirmed the importance of redox conditions on iodine sorption. This is likely to be relevant in NI due to the prevalence of gley soils. Ashworth and Shaw (2006b) noted that traditional batch sorption techniques may not accurately reflect sorption to soils under natural conditions, due to the effect on redox conditions of increased solution:soil ratio. The batch technique was, however, used in this work as it allowed solution to be removed

from the system with minimal change to soil:solution ratios. Furthermore, since dynamics were followed for only 24 hr, the system was unlikely to have turned anoxic (Ashworth and Shaw, 2006b).

Information about iodine species in solution is essential as these are likely to be the forms that are most readily available to plants (Dai et al., 2006). This was also recognised by Hong et al. (2012), who linked soil iodine dynamics with availability to pak choi, however they only used three soils so were unable to quantify availability in terms of soil properties. This chapter investigates transformations in solution and sorption of iodine to twenty soils after addition of $500 \mu\text{g } ^{129}\text{I kg}^{-1}$ as iodide or iodate. Changes in iodine fractionation over a 24 hour period were modelled and model parameters related to soil properties. The same soils were then used to relate phyto-availability to iodine dynamics, again as a function of soil properties (Chapter 6).

4.1.1 Aims

The aims of the work presented in this chapter were:

- to measure and model the dynamics of iodine immediately following addition to soil, as a simulation of iodine deposition from rainfall;
- to determine how soil properties affect rates and dynamics of iodine transformations in soil;
- to determine whether instantaneous sorption of iodine to soil solid phase is due to interaction with metal oxides or organic matter.

4.2 MATERIALS AND METHODS

Twenty soil samples from NI were used, after preparation as described in Section 2.2.1. All soils were used while still moist from collection in the field and sieved to < 4 mm. Soils NI10 and NI16 were too high in organic matter/fibrous material to sieve and so were broken up and homogenised as much as possible before use. For each soil in triplicate, 20 ml of 0.0125 M KNO_3 was added to 4.00 g dry weight of soil, with the exceptions of soils with particularly high organic matter content, where the following (equivalent) dry weights were used: 2.0 g for soils NI03, NI09 and NI20, 1.34 g for NI19, 1.0 g for NI10 and 0.67 g for NI16. Soils were spiked with $500 \mu\text{g } ^{129}\text{I kg}^{-1}$ either as iodide ($^{129}\text{I}^-$) or iodate ($^{129}\text{IO}_3^-$). Samples were shaken end-over-end for 24 hr at room temperature and supernatant was sampled 1, 3, 7 and 24 hr after spiking,

following centrifugation at 3000 rpm for 15 mins. Soil and solution were thoroughly mixed and returned to the shaker immediately after sampling the supernatant.

Supernatant samples were analysed for DOC, total iodine, iodide and iodate according to methods described in Chapter 2. Limits of detection (LODs) were: 4 $\mu\text{g L}^{-1}$ for DOC; 1.26 $\mu\text{g }^{127}\text{I L}^{-1}$ ($\sim 0.008 \text{ mg }^{127}\text{I kg}^{-1}$) for total ^{127}I ; 0.34 $\mu\text{g }^{129}\text{I L}^{-1}$ ($\sim 0.002 \text{ mg }^{129}\text{I kg}^{-1}$) for total ^{129}I ; 0.25 $\mu\text{g I L}^{-1}$ for iodine speciation (I^- and IO_3^-) for both isotopes, which was equivalent to 0.001 - 0.002 mg I kg^{-1} , depending on the sample. All concentrations were measured as concentration in solution ($\mu\text{g L}^{-1}$), but due to differences in soil:solution ratio, are presented as concentrations in solid soil ($\mu\text{g kg}^{-1}$) to allow direct comparison of soils. All results are quoted as measured, regardless of whether they were below LOD. Organic iodine concentration (OrgI) was calculated indirectly according to Eqn. 4.1, for both Org^{129}I and Org^{127}I .

$$\text{Org}^{129}\text{I}_L = {}^{129}\text{I}_L - \left({}^{129}\text{I}_L^- + {}^{129}\text{IO}_3^- \right) \quad (4.1)$$

Where $\text{Org}^{129}\text{I}_L$ = organic spike iodine in solution ($\mu\text{g I L}^{-1}$), ${}^{129}\text{I}_L$ = total spike iodine in solution ($\mu\text{g I L}^{-1}$), ${}^{129}\text{I}_L^-$ = spike iodide in solution ($\mu\text{g I L}^{-1}$), ${}^{129}\text{IO}_3^-$ = spike iodate in solution ($\mu\text{g I L}^{-1}$). $\text{Org}^{129}\text{I}_L$ was calculated for each sample, before conversion to concentration in solid ($\mu\text{g I kg}^{-1}$).

4.3 RESULTS AND DISCUSSION

Results of analyses for DOC, total iodine content and inorganic iodine speciation in solution are presented in Appendix 2 as gravimetric concentrations per mass of soil solid phase ($\mu\text{g kg}^{-1}$). For all soils, and both added species (500 $\mu\text{g I kg}^{-1}$ as ${}^{129}\text{IO}_3^-$ and ${}^{129}\text{I}$), the total concentration of spiked iodine remaining in solution (${}^{129}\text{I}_L$) was progressively and substantially reduced within 24 hr of contact (Figure 4.1 and Figure 4.2). The overall rate of sorption was soil dependent but much of the variability seen between soils was actually due to differences in a very rapid initial adsorption reaction. Soils in Figure 4.1 and Figure 4.2 are classified by properties identified in Chapter 3: ‘coastal’ soils, NI05 and NI08, were sampled from coastally exposed locations and contained extremely large concentrations of native iodine; ‘organic’ soils had SOC contents > 38 %; ‘mineral’ soils had a mixed mineral composition and

moderate-to-low iodine concentrations. When iodate was added, there was no consistent difference in sorption rate according to soil classification. By contrast, when iodide was added, faster initial sorption was apparent after 1 hr and 3 hr in the coastal soils followed by the organic soils, with the mineral soils showing the slowest rate of sorption. The rate of sorption was also species-dependent: iodate showed the fastest initial adsorption, within 1 – 3 hr, but from 7 hr onwards, iodide showed a greater rate of time-dependent adsorption. Transformation between inorganic and organic species (including DOC-bonded iodine) shows that reducing $^{129}\text{I}_L$ concentrations do not necessarily involve adsorption by the soil solid phase of the originally added species. Furthermore, reactions of iodide and iodate with soil are likely to follow different pathways due to the different chemical properties of each species, such as oxidation state and differences in affinity for soil adsorption surfaces. This, and the effect of soil properties on reaction mechanisms, is explored further in Section 4.5.

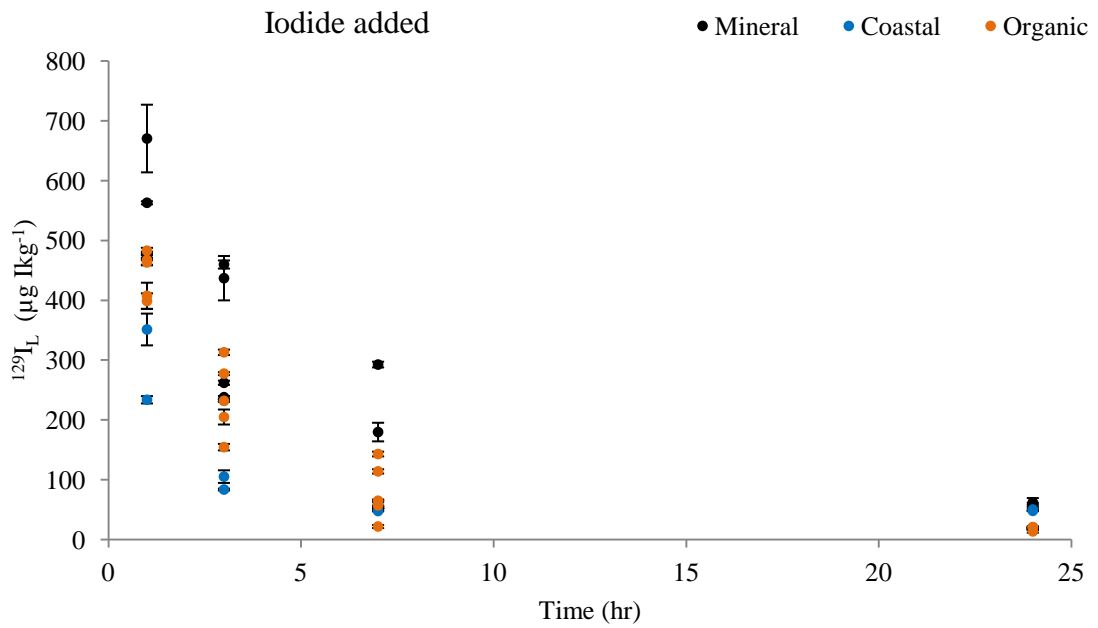


Figure 4.1. Change in the concentration of spike iodine in solution ($^{129}\text{I}_L$) with time, following addition equivalent to $500 \mu\text{g } ^{129}\text{I kg}^{-1}$ as iodide. Data points represent individual soils; error bars show standard error of triplicate measurements for each soil.

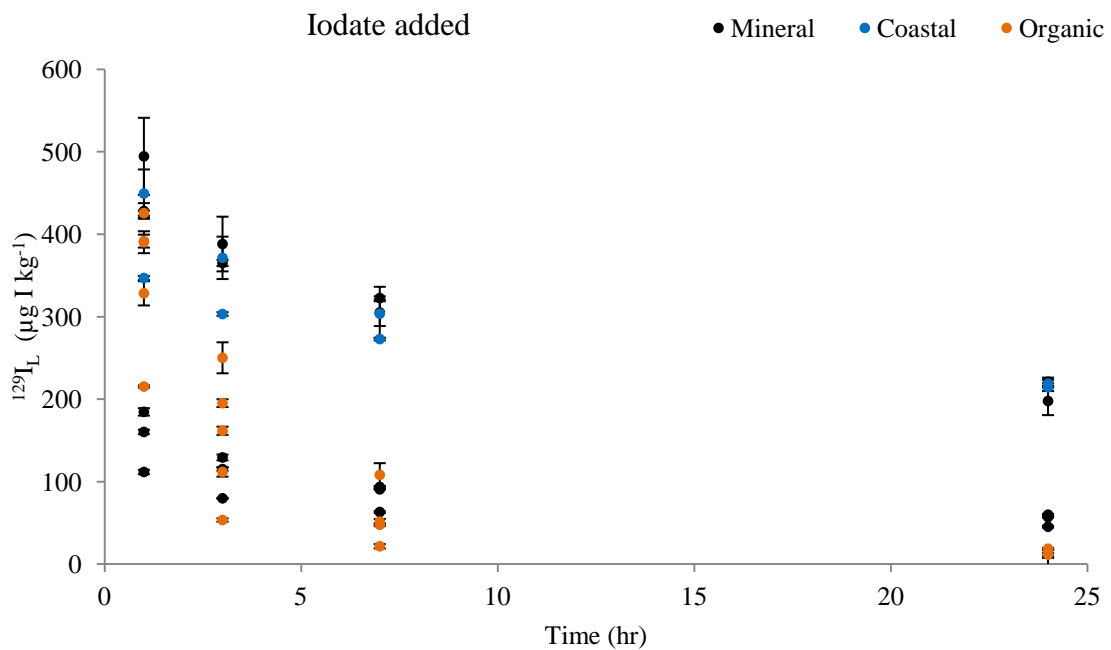


Figure 4.2. Change in the concentration of spike iodine in solution ($^{129}\text{I}_L$) with time, following addition equivalent to $500 \mu\text{g } ^{129}\text{I kg}^{-1}$ as iodate. Data points represent individual soils; error bars show standard error of triplicate measurements for each soil.

4.3.1 Organic iodine in solution

Organic iodine was the dominant species in solution (OrgI_L) for native iodine. Over all soils and all time points the median value for $\text{Org}^{127}\text{I}_L$ as a percentage of $^{127}\text{I}_L$ was 93 %. This was supported by the significant positive correlation between $^{127}\text{I}_L$ and DOC for non-coastal soils at all time points, when samples spiked with ^{129}I as iodide and iodate were considered together ($r = 0.912$, $p < 0.001$, Figure 4.3). In the coastal soils, the correlation was very weak ($r = 0.209$, $p = 0.154$, Figure 4.3) but $\text{Org}^{127}\text{I}_L$ still contributed the majority of $^{127}\text{I}_L$ (median 97.0 %). In most soils, the median ratio $\text{Org}^{127}\text{I}_L/\text{DOC}$ (for all incubation times) was 0.000125 (range 0.000 – 0.00422), while in the coastal soils the median value was 25 times higher, at median $\text{Org}^{127}\text{I}_L/\text{DOC} = 0.00307$ (range 0.00199 – 0.0136). Organic matter in solution in the coastal soils was, as for all soils, iodine-enriched compared to organic matter in the solid phase: $\text{Org}^{127}\text{I}_L$ (mg I kg^{-1})/DOC (mg kg^{-1}) was c. 10 – 1000 times greater than I_S (mg I kg^{-1})/SOC (mg kg^{-1}). The $\text{Org}^{127}\text{I}_L/\text{DOC}$ ratio increased with time for the coastal soils, suggesting release of iodine from the solid phase. This was not observed for most of the other soils. The near-constant input of iodine to the coastal soils is likely to result in initial binding to the most thermodynamically stable binding sites, with subsequent binding to more labile sites. Thus, as soil particles were broken down due to shaking in this experiment, the more loosely-bound iodine was released, resulting in increasing $\text{Org}^{127}\text{I}_L/\text{DOC}$ ratio with time and overall iodine-enriched DOC compared to the other soils.

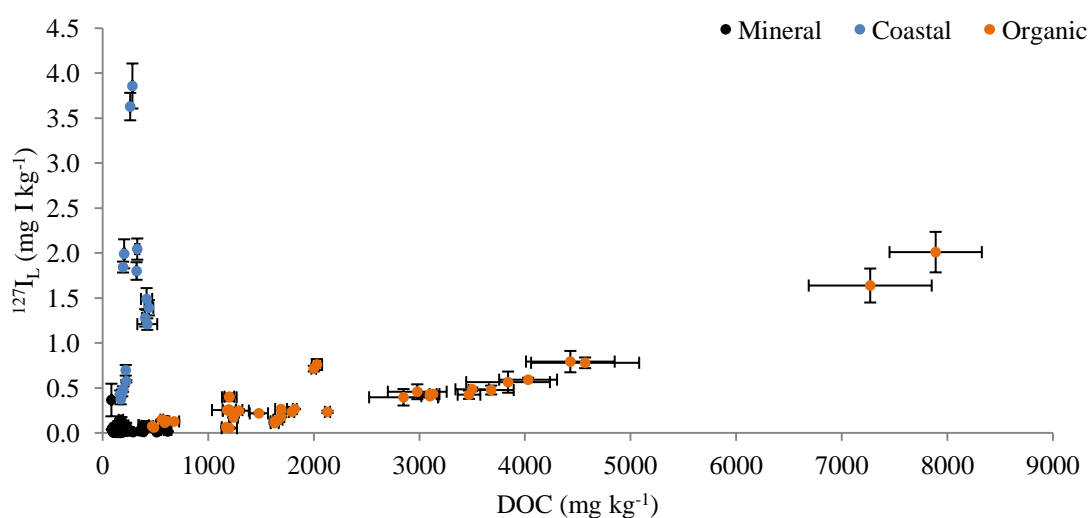


Figure 4.3. Relationship between DOC and native iodine in solution ($^{127}\text{I}_L$), following addition of $500 \mu\text{g } ^{129}\text{I kg}^{-1}$ as iodide and iodate. Data points represent individual soils and species incubated for 1, 3, 7 or 24 hr; error bars show standard error of triplicate measurements for each sample.

Transformation of spiked iodide and iodate to Org¹²⁹I_L was rapid: after just 1 hr Org¹²⁹I_L was observed in almost all samples (Figure 4.4 E and F). Differences in reaction mechanisms of the two species resulted in different Org¹²⁹I_L profiles through time, however. When iodide was added there was no consistent trend in concentration of Org¹²⁹I_L and after 24 hr Org¹²⁹I_L represented a median of 100 % of ¹²⁹I_L. Values above 100 % were obtained when ¹²⁹I_L was measured as negative but inorganic species were detectable, resulting in ¹²⁹I_L < ¹²⁹I⁻_L + ¹²⁹IO₃⁻_L. When iodate was added, two processes were more evident: initial, rapid transformation of iodate to Org¹²⁹I was followed by slower assimilation of Org¹²⁹I onto the solid soil phase, resulting in an overall decrease in concentration of Org¹²⁹I through time. After 24 hr Org¹²⁹I_L comprised a median 42.5 % of ¹²⁹I_L, the remainder being iodate. Therefore, despite initially faster sorption from solution, the subsequent rate of reaction of iodate was slower than for added iodide.

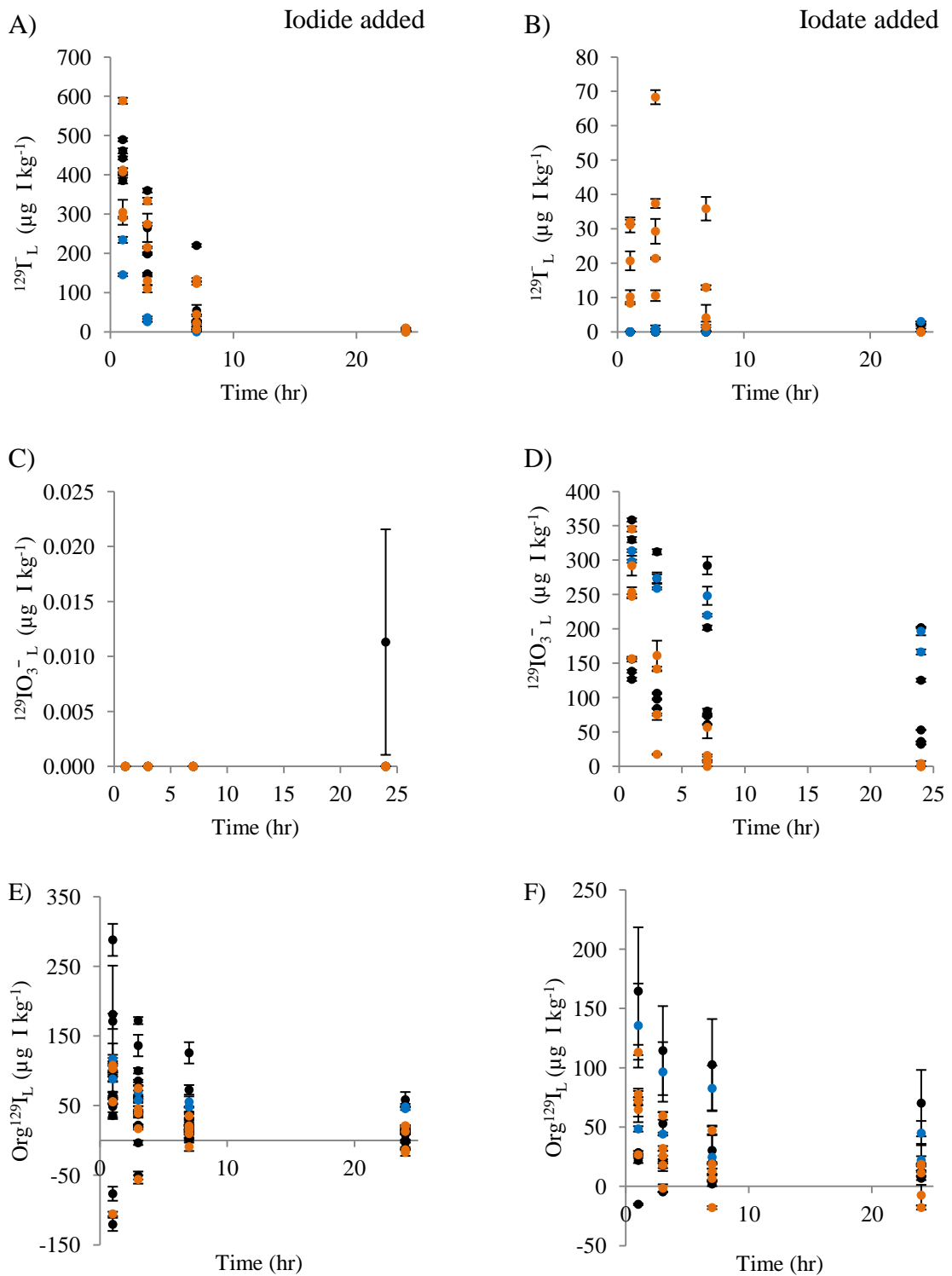


Figure 4.4. Change in the concentration of ^{129}I species in solution with time, following addition of $500 \mu\text{g } ^{129}\text{I kg}^{-1}$ as iodide (left-hand column) or iodate (right-hand column). Species measured include iodide ($^{129}\text{I}^-$; A and B), iodate ($^{129}\text{IO}_3^-$; C and D) and organic iodine (Org^{129}I ; E and F). Soils are classified as 'coastal' (blue circles), 'organic' (orange circles) and 'mineral' (black circles). Data points represent individual soils; error bars show standard error of triplicate measurements for each soil. Notice that Y-axis scales are unique to each graph.

Twenty four hours after the addition of $^{129}\text{I}^-$, the proportion of $^{129}\text{I}_L$ present as $\text{Org}^{129}\text{I}_L$ was similar to that seen for native iodine; this was not achieved within the same timeframe when $^{129}\text{IO}_3^-$ was added. However, the correlation between DOC and $^{129}\text{I}_L$ after 24 hr, compared to the same correlation for $^{127}\text{I}_L$, indicated that further transformations would occur in both sets of samples at longer incubation times. With the exception of soil NI20 (in box on Figure 4.5), there was a significant positive correlation at 24 hr between $^{129}\text{I}_L$ and DOC for the ‘mineral’ and ‘coastal’ soils combined: for iodide added $r = 0.375$ ($p = 0.014$); for iodate added $r = 0.381$ ($p = 0.013$). In the organic soils, however, there was a negative correlation with DOC: for iodide added $r = -0.566$ ($p = 0.028$); for iodate added $r = -0.224$ ($p = 0.423$). This reflects an important aspect of solubility and iodine speciation in organic soils: although peat soils would be expected to generate a large DOC concentration, which may react rapidly with incoming iodine, there is also rapid sorption of iodine from solution onto solid phase organic sites which limits solubility despite high DOC concentrations.

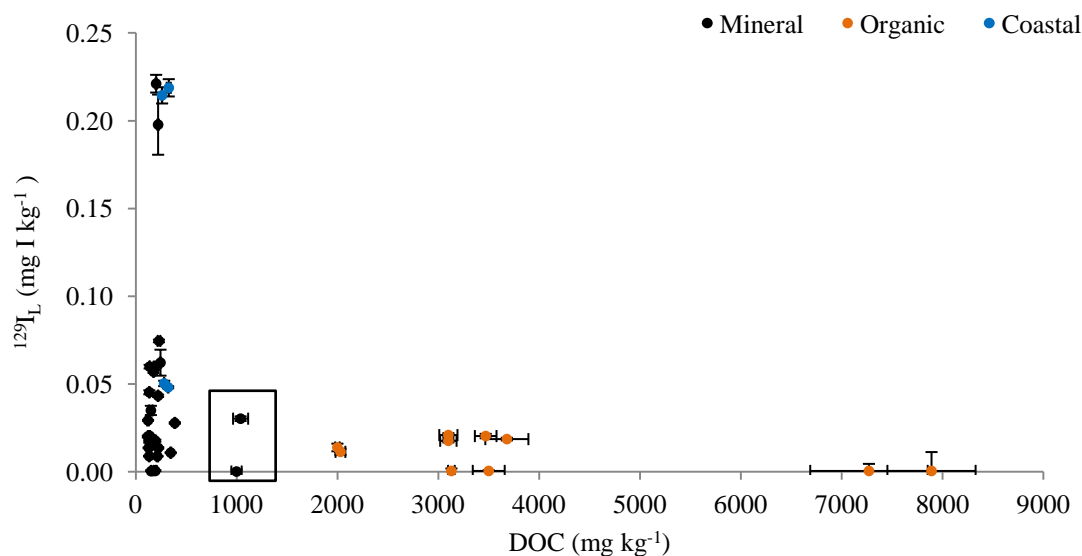
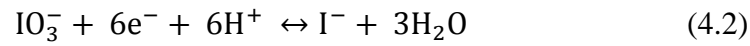


Figure 4.5. Relationship between DOC and spike iodine in solution ($^{129}\text{I}_L$), following addition of $500 \mu\text{g } ^{129}\text{I kg}^{-1}$ as iodide and iodate. Data points represent individual soils and species added after 24 hr incubation; error bars show standard error of triplicate measurements for each sample. Box encloses samples from soil NI20.

4.3.2 Transformation between inorganic species

When $^{129}\text{IO}_3^-$ was added, production of $^{129}\text{I}^-$ in solution was observed for organic soils only (Figure 4.4B). This peaked at 3 – 7 hr after addition, after which time $^{129}\text{I}^-$ became wholly sorbed to the soil solid phase or transformed to $^{129}\text{OrgI}_L$ by 24 hr. In

contrast, when $^{129}\text{I}^-$ was added, no $^{129}\text{IO}_3^-$ was detected (Figure 4.4C). No $^{127}\text{IO}_3^-$ was observed in any samples, confirming that iodide was more stable than iodate under the experimental conditions. The reaction describing redox coupling of iodide and iodate (Eqn. 4.2) proposed by Francois (1987) provides an explanation for this and why reduction of iodate to iodide was only observed in organic soils.



In order to reduce iodate to iodide, electron and proton donors are required (Eqn. 4.2). Humic acids can behave as an electron acceptor, or as electron shuttles to allow redox reactions to take place (Bradley et al., 1998), but also as an electron donor (Schlegel et al., 2006; Xu et al., 2012; Yamaguchi et al., 2010). Reduction of iodate to iodide has been seen under reducing conditions, but there is no clear evidence of the reverse reaction in soils (Kodama et al., 2006). The organic soils also had low pH values ($2.8 \leq \text{pH} \leq 3.7$), which would enhance the reduction reaction by providing protons. Oxidation of iodide to iodate by the reverse reaction in Eqn. 4.2 would be much less favourable.

4.4 MODELLING IODINE DYNAMICS

Results of the experiment were used to create and parameterise a predictive model, to aid understanding of mechanisms occurring and to link the kinetics of iodine transformations to soil properties. Initially each soil was fitted to the same model structure individually; then rate parameters were correlated to soil properties. A final ‘array’ model was produced, in which rate parameters were described in terms of soil properties to enable prediction of iodine dynamics from accessible soil characteristics. Throughout this chapter, “fitted” parameters refer to values determined by fitting individual soils models; “regressed” parameters are those calculated using equations from regression between soil properties and fitted parameters; and “optimised” parameters are determined by the final ‘array’ model, using information from all soils.

4.4.1 Model structure and fitting

Of the model structures tested, the one that gave the best fit to measured results for ^{129}I is shown in Figure 4.6. All the rate constants (k) and partition coefficients (kd) were fitted to the available data within the model. Partition coefficients were applied only

at $t = 0$ while rate constants were applied dynamically. Initially the model was set up for each soil individually, with iodate-added and iodide-added scenarios fitted concurrently to produce a set of rate parameters for each soil. Once the model structure had been developed, it was set up to include all soils, with parameters described in terms of soil properties (Section 4.5).

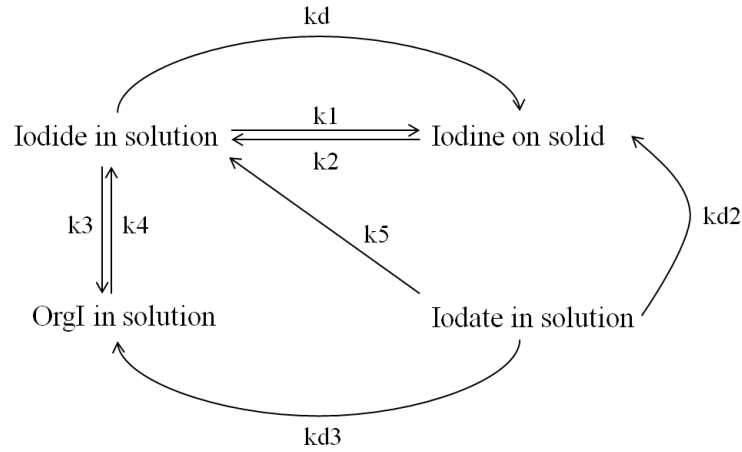


Figure 4.6. Conceptual model describing iodine dynamics in soil.

A full description of the model is presented in Appendix 3. Two variations of the model were trialled: Model A allowed all parameters to be fitted independently, while Model B constrained k_4 and k_2 according to measured equilibrium concentrations of ^{127}I , as described by Eqns. 4.3 and 4.4.

$$k_2 = \frac{k_1 \times {}^{127}\text{I}_L^-}{{}^{127}\text{I}_{\text{solid}} \times (m/v)} \quad (4.3)$$

$$k_4 = \frac{k_3 \times {}^{127}\text{I}_L^-}{\text{Org}^{127}\text{I}_L} \quad (4.4)$$

Where ${}^{127}\text{I}_L^-$ = native iodide in solution ($\mu\text{g I L}^{-1}$), ${}^{127}\text{I}_{\text{solid}}$ = native iodine on solid ($\mu\text{g I kg}^{-1}$), m = mass of soil in system (kg), v = volume of liquid in system (L), $\text{Org}^{127}\text{I}_L$ = native OrgI in solution ($\mu\text{g I L}^{-1}$) and $k_1 - k_4$ are rate parameters (hr^{-1}).

Modelled concentrations for ^{129}I species in solution were fitted against directly measured concentrations of iodide in solution (${}^{129}\text{I}_L^-$), iodate in solution (${}^{129}\text{IO}_3^-$) and

total iodine in solution ($^{129}\text{I}_\text{L}$). Marquardt fitting was used, changing parameter values to minimise the residual sum of squares (RSS) when comparing measured vs modelled results. Parameter values were fitted for each soil up to five times, or until the RSS did not change between fittings, whichever came first. Usually this resulted in three attempts at optimisation per soil.

4.4.2 Model development

The first phase of model development was to fit iodide-added results only, without the $^{129}\text{IO}_3^-_\text{L}$ term. Results from iodate-added experiments were then included and used to fit parameters (k5, kd2 and kd3) associated with $^{129}\text{IO}_3^-_\text{L}$ transformations. For both added iodide and added iodate, instantaneous partitioning to solid (kd and kd2 respectively) was required to make the model fit the data. No iodide to iodate term was included because $^{129}\text{IO}_3^-_\text{L}$ was never observed in soils spiked with ^{129}I .

Each data point was weighted, initially using the standard error associated with the measurement, however this resulted in over-fitting of the very smallest values. Therefore a single weight was calculated for all the data points associated with each soil: any values where at least two of the three replicates were measured to be <LOD were set equal to $\frac{1}{2}$ LOD, with weight = $\frac{1}{2}$ LOD. For the remaining values, the coefficient of variation was calculated for each value (standard error divided by the mean of the 3 replicates, for each of four time points for each soil, per added species), then the mean coefficient of variation for the soil (mean of 4 times and 5 species per soil: $\text{Org}^{127}\text{I}_\text{L}$, $^{127}\text{I}^-_\text{L}$, $\text{Org}^{129}\text{I}_\text{L}$, $^{129}\text{I}^-_\text{L}$ and $^{129}\text{IO}_3^-_\text{L}$) was used as the weight for all (non-LOD) data points for that soil.

4.4.3 Results of modelling

The fitted parameters and associated RSS values are presented in Table 4.1 (Model A) and Table 4.2 (Model B). Comparisons of all measured and modelled concentrations for individually fitted soils are shown in Figure 4.7 (Model A) and Figure 4.8 (Model B). Examples of fitted model results for NI01, NI03 and NI05 are shown in Figure 4.9 – Figure 4.11. These have been chosen as representative of their class (mineral, organic and coastal, respectively). Overall, both models provided a good description of the data (Model A: $r = 0.991$, $p < 0.001$; Model B: $r = 0.986$, $p < 0.001$). However, $^{129}\text{I}^-_\text{L}$ production in $^{129}\text{IO}_3^-$ -spiked soils was over-estimated in all cases, including

organic soils where a clear measured peak in $^{129}\text{I}^-_{\text{L}}$ was observed. Model A gave the lowest RSS for 17 of the 20 soils, although sometimes only marginally, but this would be expected due to greater freedom in the model since k_2 and k_4 were not constrained. The soils for which the model fitted worst (highest RSS) were NI07, 11 and 13, but these were soils for which some measured values were unrealistic (clearly in error), with $^{129}\text{I}_{\text{L}} < (^{129}\text{I}^-_{\text{L}} + ^{129}\text{IO}_3^-_{\text{L}})$. No soil class gave a noticeably better or worse fit than the other with Model A and B.

The reason for the overestimation of iodide from added iodate is not clear. From the model structure (Figure 4.6) it may be expected to be caused by high values of k_4/k_3 , however this is not borne out by observed results. For example, NI08 and NI09 have the lowest two values of k_4/k_3 but soil NI08 gave the smallest overestimate of $^{129}\text{I}^-_{\text{L}}$, whereas for NI09 the overestimate was large. Overestimation also does not seem to be solely due to the k_5 rate constant: although NI08 produced a low value of k_5 and low level of I^- overestimation, NI07 gave a high value of k_5 and low I^- overestimation.

Table 4.1. Fitted parameters for **Model A**. RSS is residual sum of squares from best model fit. S. D. is the standard deviation of the associated parameter value.

Soil	RSS (x 10 ³)	k1		k2		k3		k4		k5		kd		kd2		kd3	
		Mean	S. D.	Mean	S. D.	Mean	S. D.	Mean	S. D.	Mean	S. D.	Mean	S. D.	Mean	S. D.	Mean	S. D.
NI01	115	0.330	0.0228	0.0000	0.0050	0.0154	0.0103	0.0000	0.0428	0.0610	0.0131	0.0000	0.228	18.3	1.50	0.107	0.0876
NI02	115	0.420	0.0255	0.0000	0.0052	0.0210	0.0098	0.0040	0.0346	0.0399	0.0085	0.0000	0.212	27.7	1.99	0.0000	0.0886
NI03	115	0.414	0.0854	0.0000	0.0102	0.0355	0.0269	0.0136	0.0831	0.289	0.0449	9.79	2.41	28.9	3.05	0.0000	0.0747
NI04	130	0.176	0.0361	0.0000	0.0006	0.0889	0.0441	0.0725	0.0618	0.0326	0.0123	0.0001	0.499	3.14	0.612	0.366	0.165
NI05	32.1	0.760	0.142	0.0063	0.0115	0.149	0.0266	0.0601	0.0265	0.0170	0.0032	0.0000	0.829	3.54	0.231	0.392	0.0591
NI06	184	0.328	0.0328	0.0000	0.0074	0.0444	0.0191	0.0626	0.0696	0.0299	0.0109	0.0000	0.303	22.0	2.37	0.122	0.153
NI07	275	0.110	0.0104	0.0001	0.0039	0.504	0.436	2.09	1.96	0.0154	0.0026	0.0000	0.156	3.21	0.182	0.155	0.0475
NI08	53.1	1.28	0.249	0.0596	0.0182	0.317	0.0578	0.447	0.126	0.0074	0.0011	0.0001	1.24	5.37	0.153	0.162	0.0318
NI09	10.1	0.779	0.157	0.0000	0.0018	0.0600	0.0271	0.0000	0.641	0.410	0.0817	6.79	3.56	37.5	5.36	0.0000	0.0782
NI10	26.2	0.275	0.0654	0.0000	0.0059	0.0000	0.0025	0.0000	0.257	0.366	0.0836	63.2	7.72	188	26.8	0.0339	0.121
NI11	409	0.462	0.0416	0.0000	0.0052	0.0001	0.0144	0.0000	0.0907	0.0407	0.0271	0.0000	0.381	41.2	8.08	0.212	0.264
NI12	127	0.423	0.0394	0.0001	0.0055	0.381	0.338	1.65	1.69	0.0320	0.0183	0.0000	0.328	49.8	7.75	0.0026	0.326
NI13	910	0.245	0.0365	0.0000	0.0170	0.0000	0.0171	0.0136	0.105	0.0351	0.0244	0.0000	0.415	20.5	3.98	0.256	0.286
NI14	25.0	0.901	0.135	0.0000	0.0000	257	5230	157	3220	0.0478	0.0101	0.0000	0.0000	23.0	1.60	0.553	0.198
NI15	5.90	1.21	0.0863	0.0084	0.0078	5.26	109	8.88	170	0.0515	0.0101	0.0001	4.54	54.3	3.34	0.0506	0.225
NI16	0.806	0.481	0.105	0.0000	0.0023	0.0998	0.0344	0.0374	0.0698	0.236	0.0313	199	27.6	358	27.8	0.0288	0.0721
NI17	93.5	0.206	0.0339	0.0000	0.0021	0.188	0.271	1.19	1.98	0.435	0.244	44.5	4.45	211	90.6	0.0000	0.453
NI18	20.4	1.05	0.167	0.0000	0.0129	0.0499	0.0130	0.0543	0.0818	0.0349	0.0155	0.0001	0.969	97.3	12.6	0.241	0.268
NI19	23.3	0.682	0.0603	0.0000	0.0064	0.391	1.17	2.70	8.16	0.0585	0.0179	0.0000	0.614	50.1	4.92	0.106	0.256
NI20	49.1	1.17	0.103	0.0000	0.0037	0.847	0.281	1.35	0.469	0.0692	0.0065	4.84	1.75	70.5	2.12	0.527	0.0846

Table 4.2. Fitted parameters for **Model B**. RSS is residual sum of squares from best model fit. S. D. is the standard deviation of the associated parameter value.

Soil	RSS (x 10 ³)	k1		k2		k3		k4		k5		kd		kd2		kd3	
		Mean	S. D.	Mean	S. D.	Mean	S. D.	Mean	S. D.	Mean	S. D.	Mean	S. D.	Mean	S. D.	Mean	S. D.
NI01	119	0.333	0.0196	0.0006	0.0001	0.0157	0.0079	0.0146	0.0082	0.0603	0.0108	0.0000	0.208	18.3	1.37	0.0898	0.0737
NI02	69.4	0.421	0.0215	0.0007	0.0002	0.0217	0.0090	0.0334	0.0162	0.0418	0.0079	0.0000	0.193	27.6	1.98	0.0000	0.0786
NI03	205	0.447	0.0531	0.0002	0.0000	0.0261	0.0154	0.0012	0.0008	0.296	0.0429	9.06	1.79	28.8	2.64	0.0000	0.0039
NI04	143	0.177	0.0327	0.0002	0.0001	0.0474	0.0175	0.0051	0.0023	0.0423	0.0117	0.0000	0.468	3.16	0.576	0.258	0.112
NI05	44.2	0.748	0.0432	0.0001	0.0000	0.106	0.0166	0.0023	0.0006	0.0245	0.0032	0.0000	0.172	3.62	0.236	0.273	0.0410
NI06	182	0.334	0.0265	0.0003	0.0001	0.0483	0.0184	0.0073	0.0038	0.0325	0.0097	0.0000	0.265	21.8	2.16	0.0900	0.127
NI07	872	0.102	0.0099	0.0001	0.0000	0.0172	0.0060	0.0027	0.0014	0.0195	0.0040	0.230	0.211	3.43	0.274	0.0486	0.0483
NI08	102	0.989	0.172	0.0001	0.0000	0.151	0.0129	0.0023	0.0005	0.0092	0.0013	1.04	1.14	5.49	0.149	0.113	0.0205
NI09	10.2	0.778	0.146	0.0002	0.0001	0.0600	0.0249	0.0011	0.0006	0.410	0.0752	6.81	3.30	37.6	4.95	0.0000	0.0627
NI10	26.3	0.276	0.0309	0.0002	0.0001	0.0000	0.0169	0.0000	0.0010	0.364	0.0772	63.4	5.92	192	23.0	0.0418	0.0917
NI11	412	0.464	0.0387	0.0002	0.0001	0.0000	0.0089	0.0000	0.0047	0.0398	0.0180	0.0000	0.356	41.6	6.38	0.207	0.172
NI12	169	0.381	0.0290	0.0005	0.0002	0.0233	0.0092	0.0070	0.0035	0.0421	0.0205	0.0000	0.280	48.7	8.22	0.0000	0.174
NI13	1150	0.237	0.0251	0.0001	0.0000	0.0000	0.0091	0.0000	0.0108	0.0407	0.0172	0.0000	0.356	19.9	3.07	0.189	0.162
NI14	314	0.651	0.274	0.0002	0.0001	0.225	0.0684	0.0366	0.0145	0.0845	0.0522	0.0000	1.74	20.7	5.47	0.0579	0.247
NI15	38.0	0.971	0.190	0.0003	0.0001	0.0658	0.0172	0.0086	0.0035	0.0520	0.0210	0.0001	1.27	51.7	7.68	0.0083	0.148
NI16	0.867	0.504	0.0712	0.0007	0.0002	0.0805	0.0211	0.0028	0.0010	0.237	0.0293	195	22.0	352	23.8	0.0002	0.0500
NI17	104	0.191	0.0227	0.0003	0.0001	0.0242	0.0161	0.0016	0.0011	0.390	0.117	47.5	3.80	222	36.2	0.0000	0.132
NI18	23.4	1.06	0.0988	0.0006	0.0002	0.0332	0.0070	0.0032	0.0018	0.0475	0.0154	0.0001	0.623	92.1	10.3	0.175	0.125
NI19	27.2	0.659	0.0466	0.0004	0.0001	0.0514	0.0149	0.0084	0.0035	0.0858	0.0230	0.0000	0.357	47.5	6.79	0.0000	0.0929
NI20	38.8	1.43	0.516	0.0003	0.0001	0.183	0.0364	0.0083	0.0028	0.119	0.0215	0.0000	5.97	61.5	4.97	0.0718	0.0684

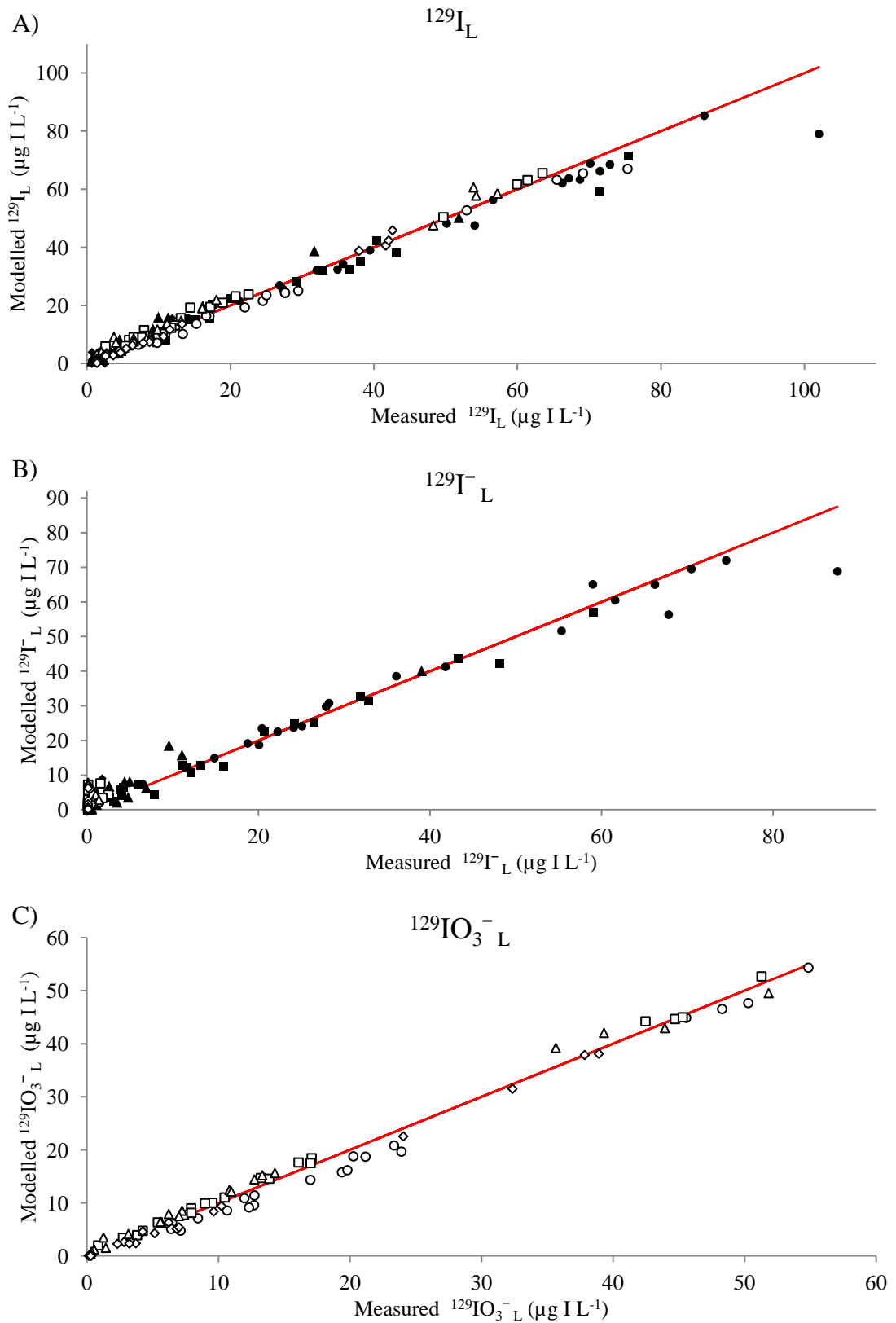


Figure 4.7. Comparison of measured and modelled concentrations of iodine species for **Model A**. Solid and open symbols denote iodide- and iodate-spiked soils respectively. Data includes measurements made after 1 hr (\circ, \bullet), 3 hr (\square, \blacksquare), 7 hr ($\triangle, \blacktriangle$) and 24 hr (\diamond, \blacklozenge). The solid line represents a 1:1 relation.

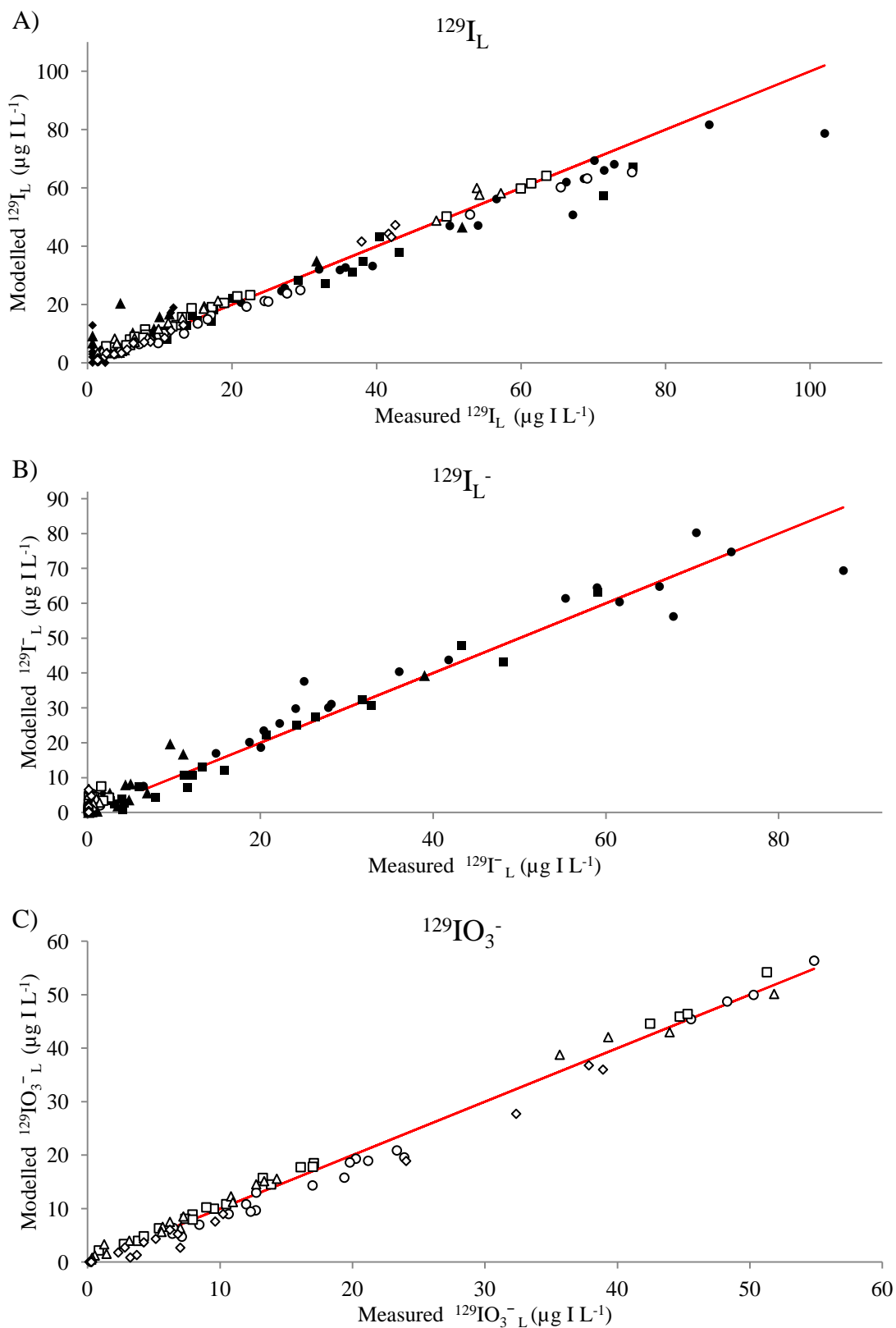


Figure 4.8. Comparison of measured and modelled concentrations of iodine species for **Model B**. Solid and open symbols denote iodide- and iodate-spiked soils respectively. Data includes measurements made after 1 hr (\circ, \bullet), 3 hr (\square, \blacksquare), 7 hr ($\triangle, \blacktriangle$) and 24 hr (\diamond, \blacklozenge). The solid line represents a 1:1 relation.

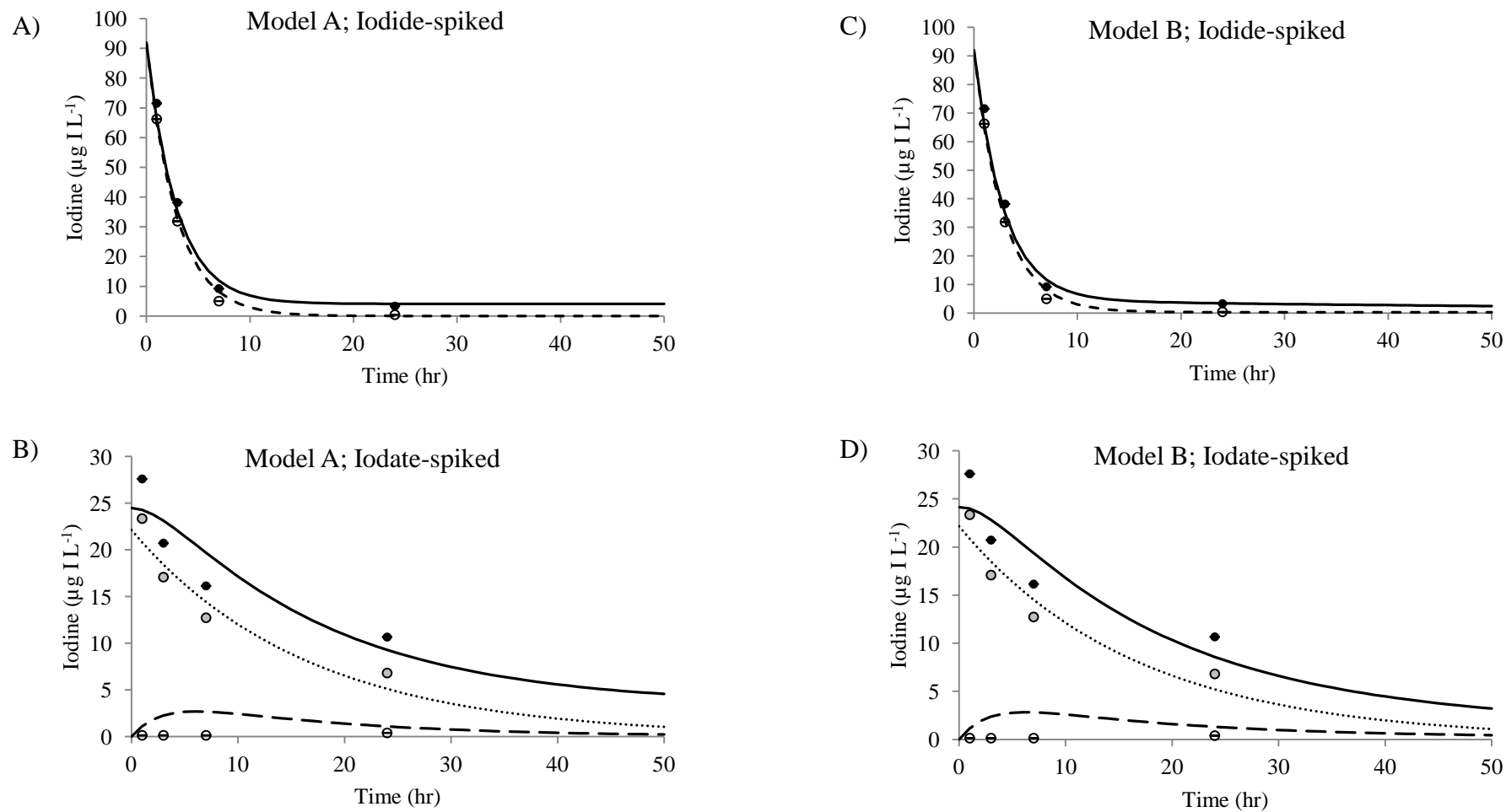


Figure 4.9. Results of modelling data for soil NI01 applying Models A and B to both iodide- and iodate-spiked suspensions, as indicated. The three variables measured and modelled are $^{129}\text{I}_L$ (closed circles; solid line), $^{129}\text{IO}_3^-_L$ (shaded circles; dotted line) and $^{129}\text{I}^-_L$ (open circles; dashed line). Error bars show mean coefficient of variance on measured values.

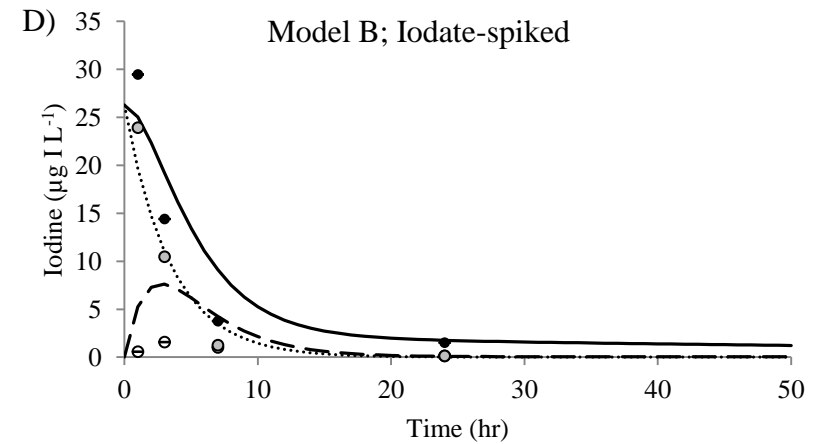
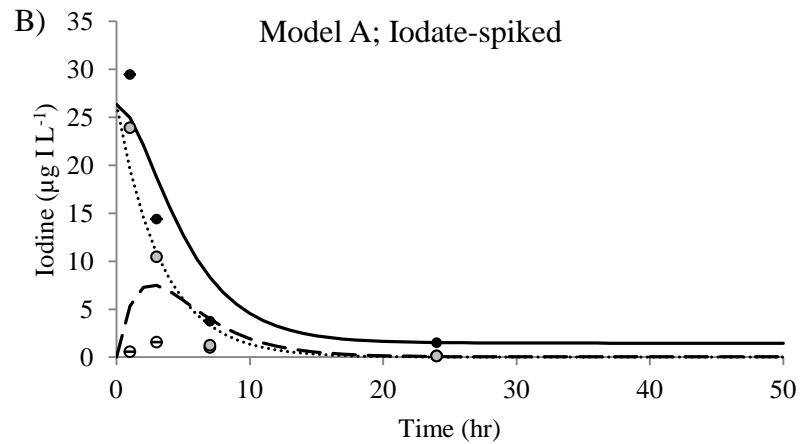
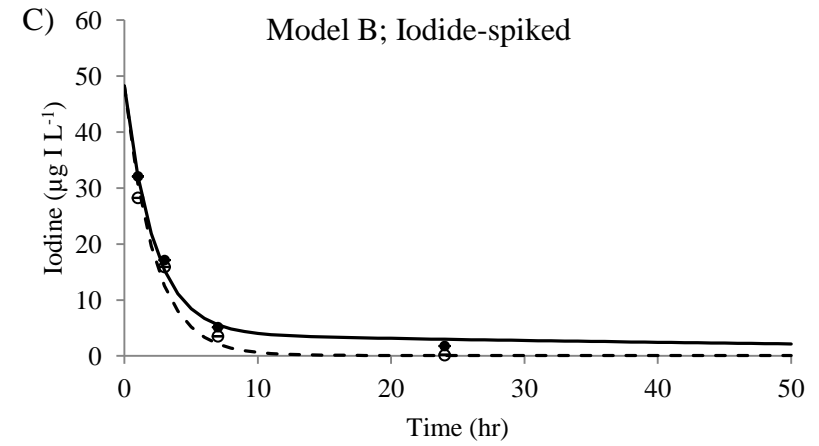
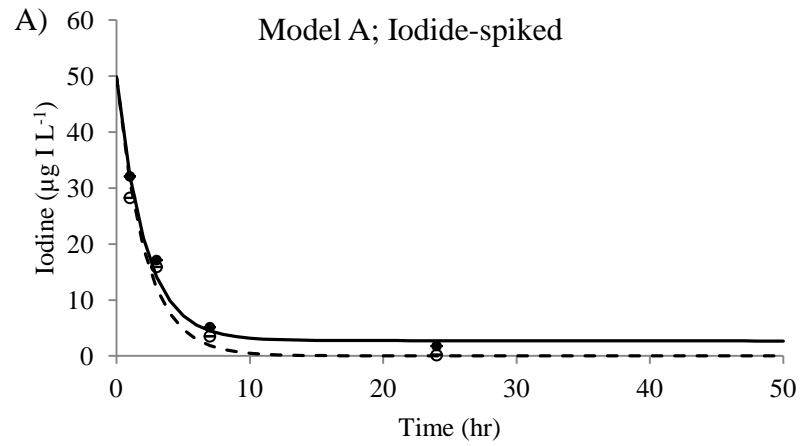


Figure 4.10. Results of modelling data for soil NI03 applying Models A and B to both iodide- and iodate-spiked suspensions, as indicated. The three variables measured and modelled are $^{129}\text{I}^-$ (closed circles; solid line), $^{129}\text{IO}_3^-$ (shaded circles; dotted line) and $^{129}\text{I}^-$ (open circles; dashed line). Error bars show mean coefficient of variance on measured values.

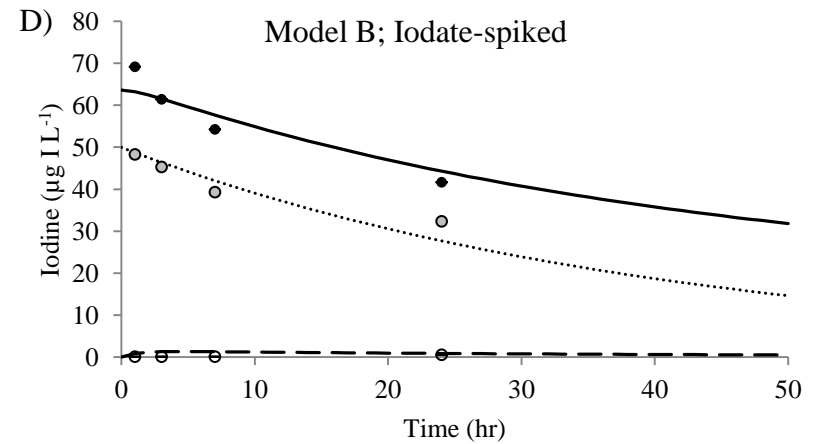
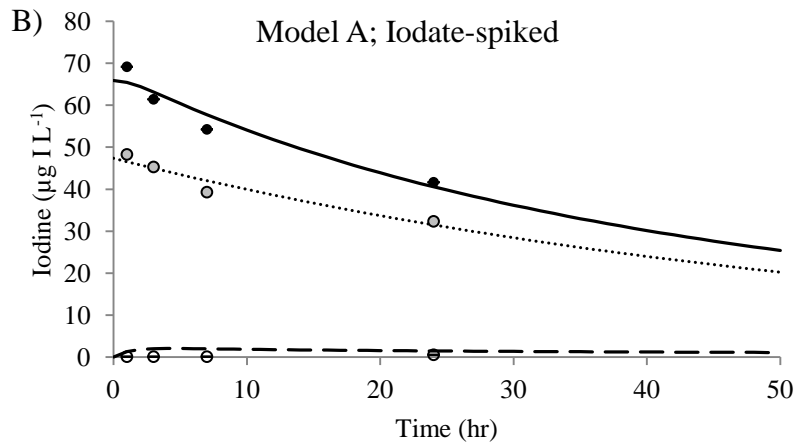
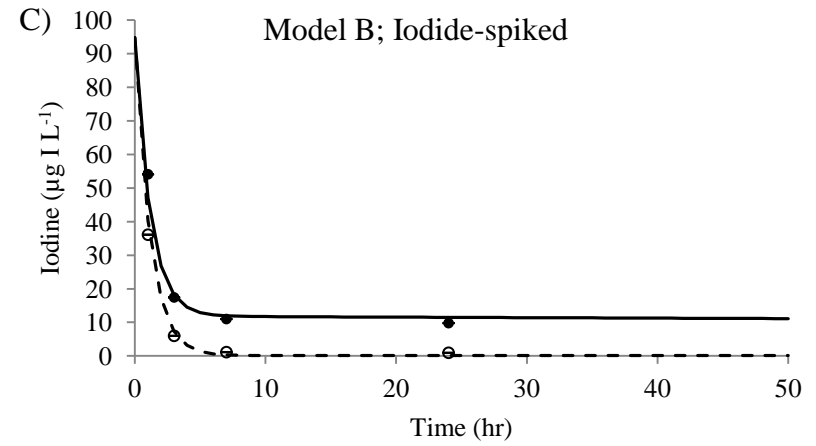
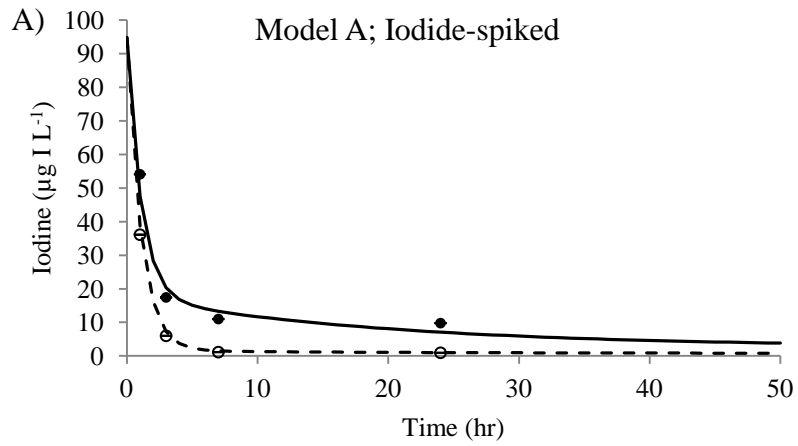


Figure 4.11. Results of modelling data for soil NI05 applying Models A and B to both iodide- and iodate-spiked suspensions, as indicated. The three variables measured and modelled are $^{129}\text{I}^-$ (closed circles; solid line), $^{129}\text{IO}_3^-$ (shaded circles; dotted line) and $^{129}\text{I}^-$ (open circles; dashed line). Error bars show mean coefficient of variance on measured values.

4.5 LINKING MODEL PARAMETERS TO SOIL PROPERTIES

To enable the prediction of iodine dynamics from soil characteristics, rate parameters were related to measured soil properties. For each soil, a stepwise regression was carried out using the soil properties Al, Fe and Mn oxide content, pH, SOC concentration and I_s (Chapter 3) as predictors for rate parameters $k_1 - k_5$ and $k_d - k_{d3}$. Graphs of soil properties plotted against model parameters were scrutinised to identify any non-linear relationships or outliers, as were graphs to identify correlations between parameters. For k_d values, the relationship between $\log(k_d)$ and soil properties was investigated. Many parameters were correlated to I_s , but this was considered likely to be a result, rather than a driver, of iodine dynamics and therefore stepwise regression was repeated without I_s . By combining these regressions and correlations, a descriptive equation for each parameter was derived. To determine the best description of each parameter in terms of soil properties, results were considered in the following order, and the first equation to give $r^2 \geq 0.7$ and $p \leq 0.05$ when all soils were considered together was used.

1. Stepwise regression equation excluding I_s
2. Stepwise regression equation including I_s
3. Correlation with other parameters
4. Mean value from all soils: this approach was used if the uncertainty of the parameter value was large and no other equations gave satisfactory results.

This process revealed that many parameters for Model A were not predictable from soil properties, and therefore only Model B was pursued. Relationships between parameters and properties in Model B are discussed in the following sections.

4.5.1 Parameters related to reaction mechanisms

The main properties shown to influence model parameters were Al, SOC and pH. This section discusses the likely influence of individual properties on rate parameters, based on reported literature. Subsequent sections discuss the derivation of specific equations relating model parameters to soil properties. The role of soil properties in determining I_s was discussed in Chapter 3, therefore discussion here is limited to the effect of soil properties on model rate parameters.

High SOC results in faster sorption of both iodide and iodate to the soil solid phase (Shetaya et al., 2012; Yamaguchi et al., 2010), and therefore may be expected to affect

k_1 , k_d and k_{d2} . The presence of SOC is also likely to be important for reduction of iodate to iodide in solution, thus affecting the value of k_5 (Francois (1987), Eqn. 4.2). The chemical composition of SOC affects the rate at which iodine reacts with it, so there is likely to be a range of reaction rates contributing to any apparent overall rate, dependent on the nature of SOC in individual soils (Warner et al., 2000; Xu et al., 2012). More SOC is likely to increase DOC, and therefore promote formation of OrgI in solution, affecting k_3 and k_{d3} ; formation of OrgI in solution before sorption to solid has been observed previously (Keppler et al., 2003; Shetaya et al., 2012; Xu et al., 2011a; Yamaguchi et al., 2010). There is strong covalent bonding between iodine and organic matter (Shetaya et al., 2012; Xu et al., 2011a; Yamaguchi et al., 2010) so removal of iodine bound to SOC may be expected to be slow, occurring in the model as low k_2 values. Conversely, sorption onto metal oxides is likely to be reversible (Xu et al., 2011a; Yamaguchi et al., 2010), thus forming an equilibrium between iodine in solution and adsorbed forms, if this mechanism applies.

The observed rapid sorption of iodate to soils with low SOC contents is likely to be due to interaction with metal oxides. Most studies report stronger adsorption of iodate than iodide to metal oxides (Kodama et al., 2006; Muramatsu et al., 1990; Shetaya et al., 2012; Xu et al., 2011a) whereas Dai et al. (2009) reported sorption of iodide to metal oxides. Another role that metal oxides are likely to play in soil iodine dynamics is to enhance the reaction between iodine and SOC. Anschutz et al. (2000) showed that manganese oxides can act as catalyst for reduction of iodate to iodide; Gallard et al. (2009) suggested that MnO_2 can polarise I_2 that is bonded to it, creating $\text{I}^{\delta+}$ which can then react with sites on negatively charged humus molecules, resulting in OrgI. Oxidation of iodide to OrgI in the presence of pure MnO_2 , under acidic conditions (pH 5 – 7), was reported by Xu et al. (2011a) and the reaction can progress further, resulting in iodate production from added iodide (Allard et al., 2009; Fox et al., 2009; Gallard et al., 2009). This reaction was not evident in this study, however, suggesting that there was not enough MnO_2 present, or that any iodate produced was transitory in an otherwise reducing environment. The role of Al in iodine dynamics is infrequently mentioned in the literature, although its role in iodine binding has been reported (Whitehead, 1978). Aluminium oxide content was found (empirically) to be important in describing several of the rate parameters for this model. Its function is unclear but is unlikely to involve redox reactions.

The effect of pH on iodine dynamics is complex, affecting the chemistry of both iodine and soil components. Faster sorption of iodine to soils with lower pH values has been shown (Fox et al., 2009; Shetaya et al., 2012; Yoshida et al., 1992). This may be a result of improved sorption to metal oxides (Whitehead, 1973a; Whitehead, 1984; Yoshida et al., 1992). It may alternatively be due to the frequent co-occurrence of low pH and high SOC in soils, such as in peats, and the important role of organic matter in sorbing iodine. Higher pH results in greater negative charge on both oxides and humus, which should limit adsorption of both I⁻ and IO₃⁻; and causes greater competition for adsorption sites from other anions (HCO₃⁻, OH⁻, other weak acids, etc.) (Dai et al., 2009; Hong et al., 2012).

4.5.2 Fate of iodide

Iodide undergoes rapid sorption to solid phases (k_d) and slower, reversible, reactions with iodine on solid phases (k_1/k_2) and OrgI in solution (k_3/k_4). For all soils, the reactions away from iodide were more favourable than production of iodide. Sorption to solid was faster than transformation to OrgI: $k_1 > k_3$ in all cases.

4.5.2.1 Instantaneous partitioning to solid

The best fit for predicting instantaneous partitioning to solid (fitted vs regressed: $r^2 = 0.997$, $p < 0.001$ when all soils were included) was obtained when k_d was described by different equations for organic soils and coastal/mineral soils (Eqns. 4.5 and 4.6).

If SOC < 38 % (coastal and mineral soils):

$$k_d = 10^{-26.17 + (3.8 \times \text{pH})} \quad (4.5)$$

Correlation between fitted and regressed: $r^2 = 0.836$, $p < 0.001$

If SOC > 38 % (organic soils):

$$k_d = 10^{5.12 - (0.95 \times \text{pH}) - (0.194 \times \text{Al})} \quad (4.6)$$

Correlation between fitted and regressed: $r^2 = 0.995$, $p < 0.001$

The linear relationship with pH was stronger when $\log(k_d)$, rather than k_d , was used (Figure 4.12A and B). Separate equations were required for organic and non-organic soils, suggesting a difference in interaction mechanism of iodide with different soil

types. For soils with SOC < 38 %, $k_d \approx 0$ with large uncertainty and some dependence on pH (Eqn. 4.6, Figure 4.12). For organic soils, instantaneous partitioning of iodide to solid was much more important, and was enhanced at lower pH (Eqn. 4.5, Figure 4.12). This supports the role of organic matter in promoting rapid sorption of iodide, rather than rapid sorption to metal oxides. Although the latter mechanism should apply in all soils to some degree it appears that iodide is able to undergo particularly rapid oxidation (possibly to I_2 or HOI) and sorption to humus.

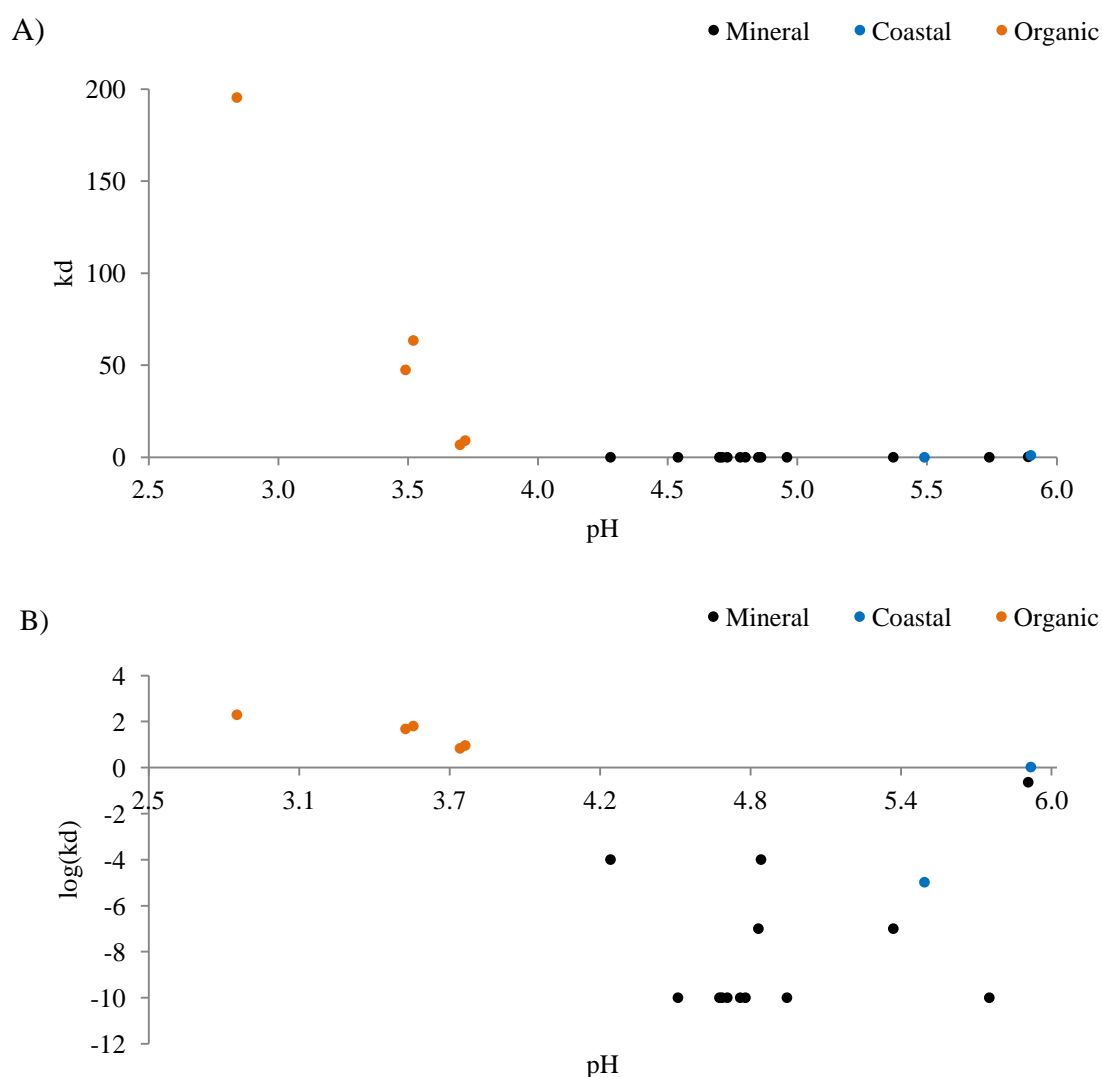


Figure 4.12. Comparison of relationship between A) fitted k_d and pH, and B) fitted $\log(k_d)$ and pH.

4.5.2.2 Equilibrium with iodine on solid

One equation was required to describe k_1 for all soils (Eqn. 4.7), giving a good correlation between fitted and regressed values of k_1 as a function of soil Al oxide content (Al) ($r^2 = 0.782$, $p < 0.001$).

$$k_1 = 0.275 + (0.102 \times \text{Al}) \quad (4.7)$$

k_2 according to Eqn. 4.3

The role of Al in enhancing sorption to solid may be the provision of direct binding sites on Al oxides, or in somehow catalysing the reaction with organic matter. For example, bonding of Al^{3+} and AlOH^{2+} to humus would tend to suppress the negative charge on humic colloids, thus potentially facilitating interaction with I^- and IO_3^- anions. Transfer to solid soil was very favourable compared to remaining as iodide in solution: in all cases $0.001 \leq k_2/k_1 \leq 0.0001$.

4.5.2.3 Equilibrium with OrgI in solution

The rate of iodide transformation to OrgI in solution (OrgI_L) was well described by Eqn. 4.8, with correlation between fitted and regressed: $r^2 = 0.917$, $p = 0.001$.

$$k_3 = 0.0224 + (0.0093 \times \text{Al}) + (0.00033 \times I_S) \quad (4.8)$$

k_4 according to Eqn. 4.4

The role of Al in increasing k_3 is unclear, although as for k_1 , it may enhance the reaction with SOC. There was no correlation between measured Al and SOC contents. It is likely that DOC was important in determining the rate of transformation of iodide to OrgI_L , but since measured DOC changed throughout the experimental equilibration period (Appendix 2), it could not be included in the regression. When I_S was excluded from Eqn. 4.8 the correlation between fitted and regressed k_3 values declined markedly to $r^2 = 0.365$, $p = 0.114$. This suggests that increasing the rate of reaction at higher values of I_S is important. Therefore it is likely that I_S is a driver, rather than a product, of k_3 , enabling maintenance of the I^-/OrgI_L balance as I_S changes.

For all soils, the value of k_4 was not negligible. Generally, $k_3 > k_4$ and $0.02 \leq k_4/k_3 \leq 0.9$, showing that although OrgI_L was the more favourable species, the reverse

transformation was also important. Exceptions to this were NI02 and NI13 where $k_4/k_3 = 1.5$ and 1.2 respectively, although these soils did not have any particularly unusual properties compared to the other soils.

4.5.3 Fate of iodate

Rapid sorption of iodate to solid (k_{d2}), and rapid transformation to OrgI_L (k_{d3}) were required for a good model fit, but subsequent slower reactions with these species were not, which is a contrast to the behaviour of added iodide. Non-instantaneous reduction to iodide in solution occurred (k_5), but the reverse reaction was never observed and therefore was not included in the model.

Information about the rapid reactions of iodate can be obtained from comparison of fitted k_{d2} and k_{d3} values (Figure 4.13). In general, the organic soils tended to have larger k_{d2} and smaller k_{d3} values, indicating preferential sorption to solid soil rather than transformation to OrgI_L . For non-organic soils, there were a range of values for both parameters which is likely to reflect competition between binding to solid soil, whether to metal oxides or SOC, and transformation to OrgI_L . In all cases, $k_{d2} > k_{d3}$, confirming a preference for binding to solid soil overall.

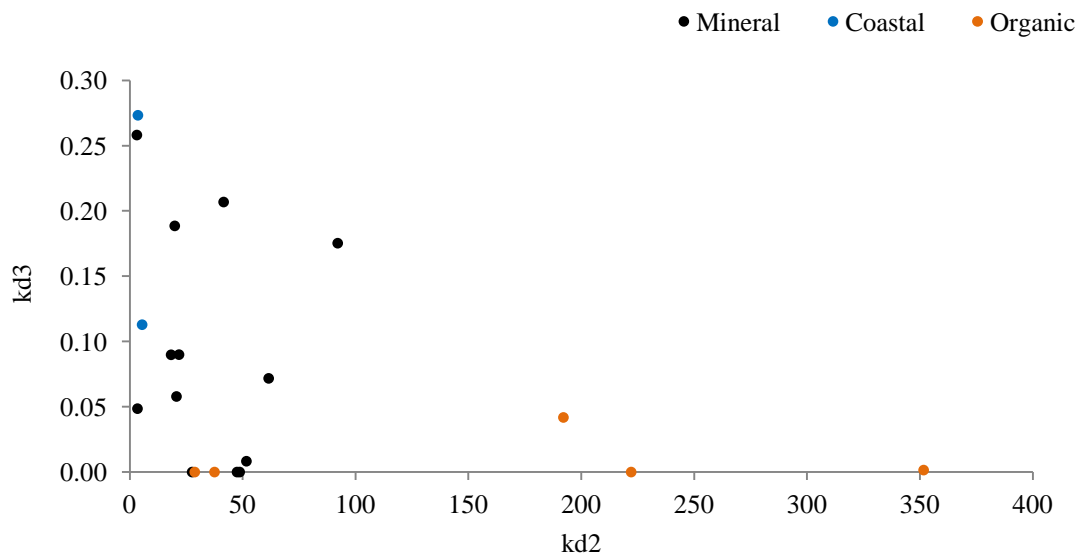


Figure 4.13. Relationship between fitted values of k_{d2} and k_{d3} for Model B.

4.5.3.1 Instantaneous partitioning to the soil solid phase

The best fit for the description of kd_2 (fitted vs regressed, all soils: $r^2 = 0.972$, $p < 0.001$) required separate equations for organic and non-organic soils, and a log relationship between kd_2 and soil properties (Eqn. 4.9 and 4.10).

If $SOC < 38\%$ (coastal and mineral soils):

$$kd_2 = 10^{2.89 + (0.046 \times Fe) - (0.470 \times pH) + (0.042 \times Al)} \quad (4.9)$$

Correlation between fitted and regressed: $r^2 = 0.652$, $p = 0.008$

If $SOC > 38\%$ (organic soils):

$$kd_2 = 10^{4.04 - (0.215 \times Al) - (0.471 \times pH)} \quad (4.10)$$

Correlation between fitted and regressed: $r^2 = 1.000$, $p < 0.001$

The linear relationship between $\log(kd_2)$ and pH was stronger than that for kd_2 and pH (Figure 4.14A and B). Rapid partitioning of iodate to solid was required for all soils ($kd_2 > 0$ in all cases) however the relationship between kd_2 and apparent sorption mechanism depended on soil type (Eqns. 4.9 and 4.10). In non-organic soils, sorption to metal oxides was important, supported by the positive dependence of kd_2 on both Fe and Al in conjunction with a negative trend with pH. In organic soils, the value of kd_2 was also increased at lower pH but unlike the non-organic soils, did not depend on Fe. This may indicate reduction facilitated by organic matter supplying sufficient protons (Eqn. 4.2), rather than a dependence on metal oxides.

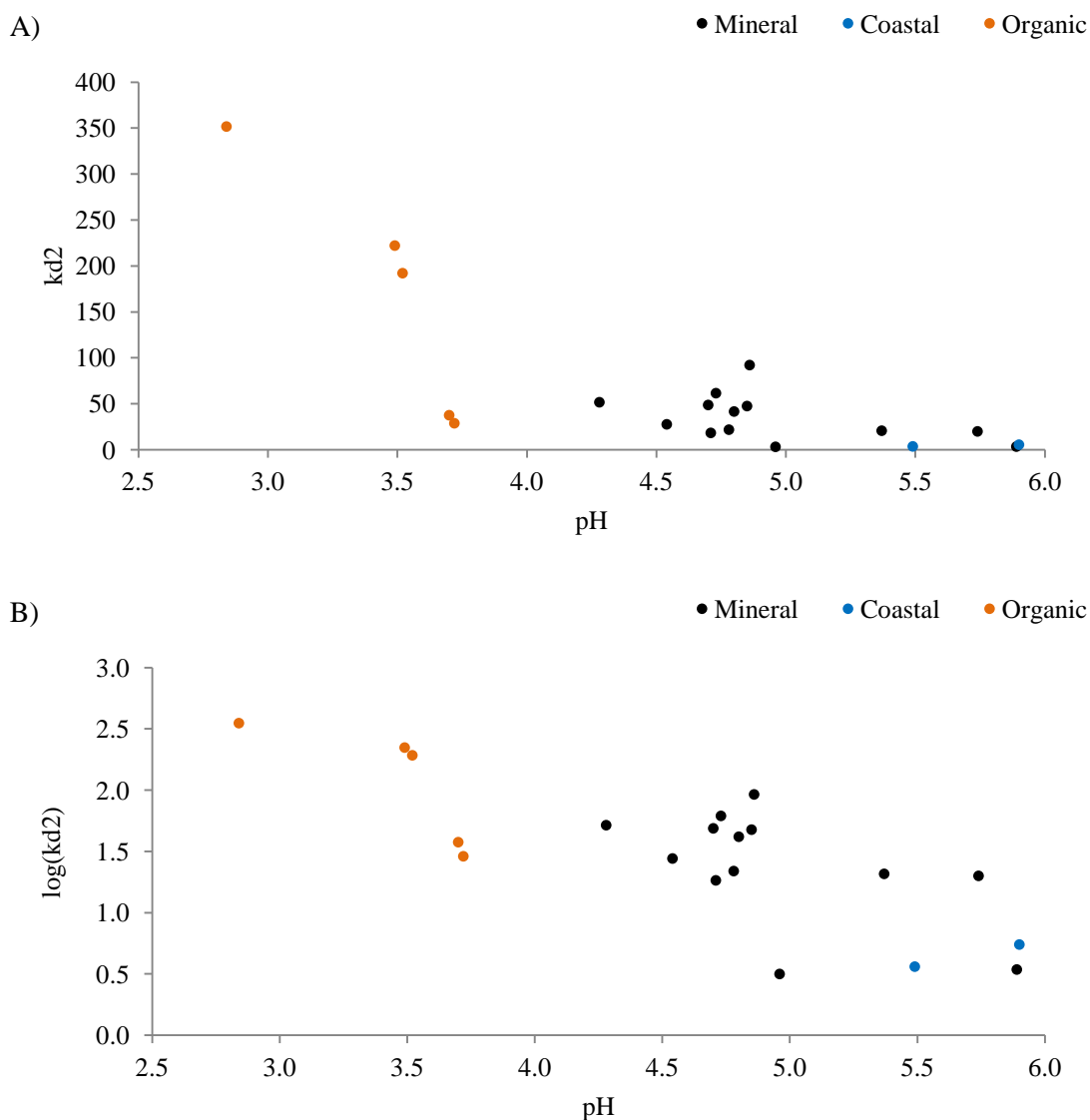


Figure 4.14. Comparison of relationship between A) fitted kd_2 and pH, and B) fitted $\log(kd_2)$ and pH.

4.5.3.2 Instantaneous partitioning to OrgI in solution

The instantaneous partitioning coefficient kd_3 was not well-represented by the equation from stepwise regression using soil properties ($r^2 = 0.547$, $p = 0.012$ for fitted vs regressed), or by correlation with any other model parameters. Also the standard deviation of estimates for this parameter was usually large (std. dev./mean > 0.7 for all but 3 soils), representing significant uncertainty in the fitted values. Nevertheless, inclusion of kd_3 was required for the model to fit the data. Therefore the parameter was set to the mean of values for all soils, according to Eqn. 4.11.

$$kd_3 = 0.0812 \quad (4.11)$$

DOC is likely to influence the value of k_d3 but, as noted for k_3 , the concentration of DOC changed over the duration of the experiment and therefore could not be included in the model. The k_d terms were required to explain changes in speciation observed within 1 hr of spiking. Experimentally revealing the mechanisms controlling sorption within that time span would be difficult to separate from simple physical diffusion to adsorption sites within soil micro-aggregates.

4.5.3.3 Reduction to iodide

Reduction of iodate to iodide was represented by a single (net) rate parameter k_5 (Eqn. 4.12), as no evidence of a reverse reaction was observed.

$$k_5 = 0.0221 + (0.00647 \times \text{SOC}) - (0.0082 \times \text{Al}) \quad (4.12)$$

Correlation between fitted and regressed: $r^2 = 0.929$, $p < 0.001$.

Reduction of iodate to iodide is enhanced by the presence of an electron and proton donor (Section 4.5.1) such as SOC. Plots of soil properties against fitted model parameters showed a significant negative correlation between k_5 and pH ($r^2 = -0.801$, $p < 0.001$), but this is likely to have been covariant with SOC due to the significant negative correlation between SOC and pH in these soils (Chapter 3). The importance of SOC in predicting k_5 was confirmed when the regression was repeated without Al as a predictor. The resulting equation (Eqn. 4.13) gave excellent agreement between fitted and regressed values, which was only slightly improved by the inclusion of Al (Eqn. 4.12).

$$k_5 = -0.001008 + (0.00654 \times \text{SOC}) \quad (4.13)$$

Correlation between fitted and regressed: $r^2 = 0.913$, $p < 0.001$.

The role of Al is therefore apparently minor, and the mechanism reliant upon it is unclear. Its single dominant oxidation state precludes its involvement in redox reactions, unlike Fe and Mn, however the correlation between k_5 and Al was positive for non-organic soils (Figure 4.15). Therefore the negative dependence on Al in Eqn. 4.12 may be a factor of the regression method rather than indicative of a reaction mechanism.

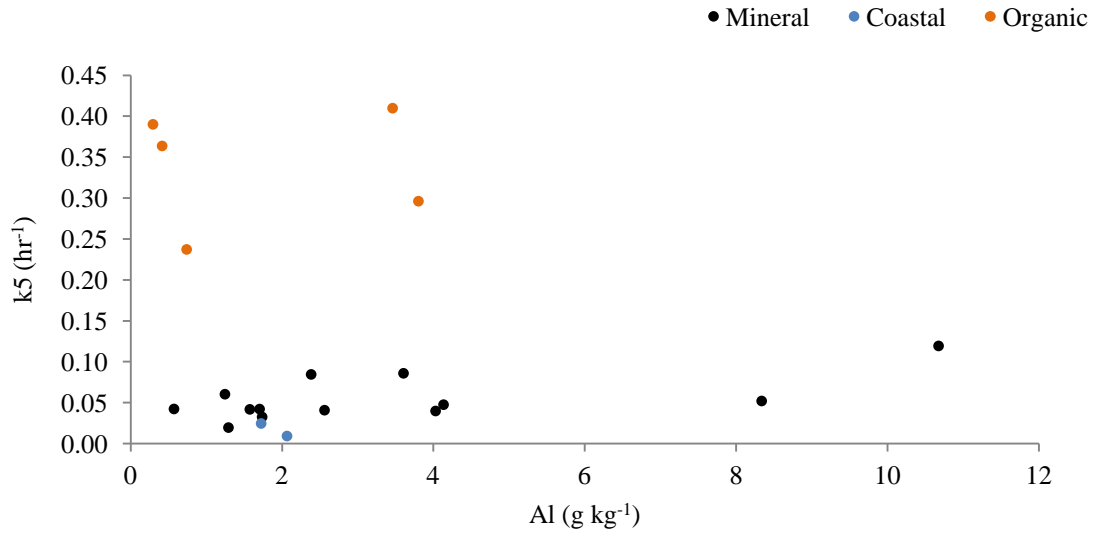


Figure 4.15. Relationship between fitted k5 and Al content of soils.

4.5.4 Model predicting iodine dynamics from soil properties

The equations predicting parameters from soil properties (the ‘regressed’ parameters) were used to produce a single soil iodine dynamics model, the ‘Array model’ (details of the model implementation are presented in Appendix 4). The model uses inputs of soil properties, including $^{127}\text{I}_s$, to predict the dynamics of ^{129}I freshly added as iodide or iodate. The model structure is unchanged from Figure 4.6, with rate parameters k1 – k5 and kd – kd3 described in terms of soil properties according to Eqns. 4.14 – 4.23. These are based on Eqns. 4.5 – 4.12 but allow simultaneous fitting of the regression parameters a – h, w and aa – mm, to give optimised values.

For all soils:

$$k1(i) = a + (b \times \text{Al}(i)) \quad (4.14)$$

$$k2(i) = \frac{k1(i) \times {}^{127}\text{I}_L^-(i)}{{}^{127}\text{I}_{\text{solid}}(i) \times (m(i)/v(i))} \quad (4.15)$$

$$k3(i) = c + (d \times \text{Al}(i)) + (e \times {}^{127}\text{I}_s) \quad (4.16)$$

$$k4(i) = \frac{k3(i) \times {}^{127}\text{I}_L^-(i)}{\text{Org}^{127}\text{I}_L(i)} \quad (4.17)$$

$$k5(i) = f = (g \times \text{SOC}(i)) - (h \times \text{Al}(i)) \quad (4.18)$$

$$kd3(i) = w \quad (4.19)$$

If $SOC(i) < 38$:

$$kd(i) = 10^{aa+(bb \times pH(i))} \quad (4.20)$$

$$kd2(i) = 10^{cc+(dd \times Fe(i)) - (ee \times pH(i)) + (ff \times Al(i))} \quad (4.21)$$

If $SOC(i) > 38$:

$$kd(i) = 10^{gg-(hh \times pH(i)) - (jj \times Al(i))} \quad (4.22)$$

$$kd2(i) = 10^{kk-(ll \times Al(i)) - (mm \times pH(i))} \quad (4.23)$$

Where (i) indicates that the value is calculated for each soil (in the case of parameters $k1 - k5$ and $kd - kd3$) or is an input value for each soil referenced by the model (in the case of soil properties, e.g. $Al(i)$). Regressed and optimised values of parameters $a - h$, w and $aa - mm$ are presented in Table 4.3. Results of the optimised array model are shown in Figure 4.16, and graphs of the time-dependence of iodine speciation in soils NI01, 03 and 05 are shown in Figure 4.17 - Figure 4.19, as examples representative of their class (mineral, organic and coastal, respectively). For all variables and all soils, a correlation of array modelled vs measured concentrations gave $r = 0.925$ ($p < 0.001$), which is very good compared to the correlation obtained from the individually fitted models (Section 4.4.3): $r = 0.986$, $p < 0.001$. Some loss of prediction is to be expected since the array model is a compromise, giving the best fit for all 20 soils. There was very little bias between modelled and measured concentrations in Figure 4.16 across the range of values measured. Iodate concentrations were better modelled compared to iodide and total iodine concentration in solution. The model does seem to fit less well at higher measured concentrations, with $^{129}I_L$ (Figure 4.16A) and $^{129}I_L^-$ (Figure 4.16B) modelled values showing under-prediction above measured $I \approx 40 \mu g I L^{-1}$. Figure 4.17 to Figure 4.19 show that the overestimation of $^{129}I_L^-$ when iodate was added (seen in Section 4.4.3) was still present in the array model, but that the peak of $^{129}I_L^-$ present at 3 – 7 hr in the organic soils was successfully modelled. The good

overall fit obtained justifies the relationships between soil properties and model parameters that were determined earlier in this section.

Table 4.3. Parameters for the array model, predicting iodine dynamics from soil properties. Regressed parameter values were determined in Sections 4.5.2 and 4.5.3; optimised values are the result of the fitted array model.

Parameter	Regressed parameter value	Optimised parameter value	
		Mean	S. D.
a	0.275	0.0693	0.0188
aa	-26.2	-26.2*	
b	0.102	0.135	0.00989
bb	3.80	3.80*	
c	0.0224	0.0285	0.0130
cc	2.89	3.66	0.251
d	0.00930	0.0000	0.00544
dd	0.0460	0.0492	0.00467
e	0.000330	0.000231	0.000112
ee	0.470	0.614	0.0445
f	0.00221	0.00432	0.00805
ff	0.0420	0.0585	0.0147
g	0.00647	0.00668	0.00207
gg	5.12	6.46	5.05
h	0.00820	0.0123	0.00701
hh	0.950	1.31	1.35
jj	0.194	0.209	0.0865
kk	4.04	4.05	3.68
ll	0.215	0.247	0.0654
mm	0.471	0.435	1.01
w	0.0812	0.0953	0.0370

*Parameters aa and bb were not fitted by OpenModel, as changing them had no effect on results.

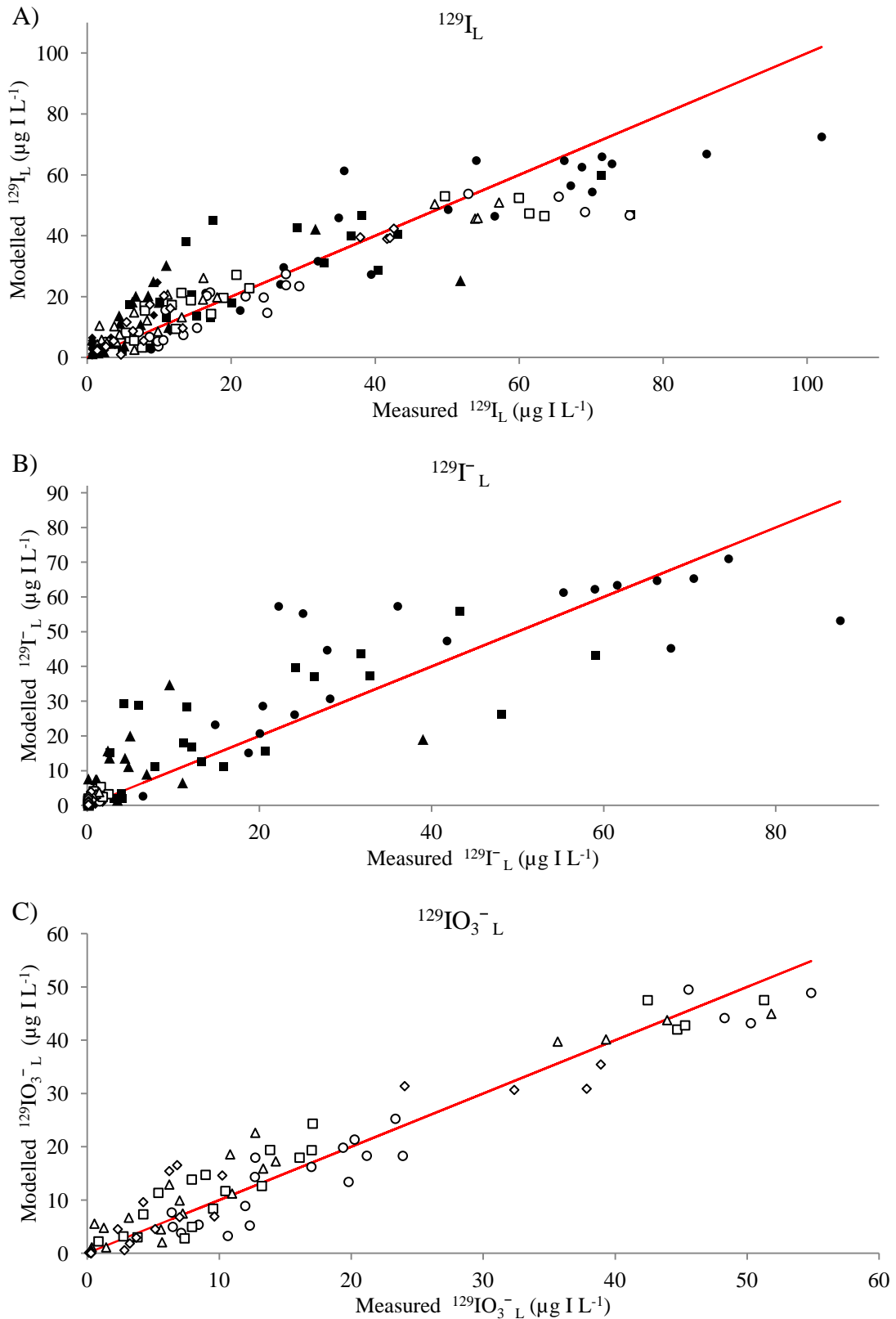


Figure 4.16. Comparison of measured and modelled concentrations of (A) $^{129}\text{I}_L$, (B) $^{129}\text{I}^-_L$ and (C) $^{129}\text{IO}_3^-_L$ for the Array Model using soil properties to predict rate parameters and partition coefficients. Spiked ^{129}I was added as iodide (solid symbols) or iodate (open symbols); equilibration times were 1 hr (circles), 3 hr (squares), 7 hr (triangles) and 24 hr (diamonds). The solid line is the 1:1 relationship.

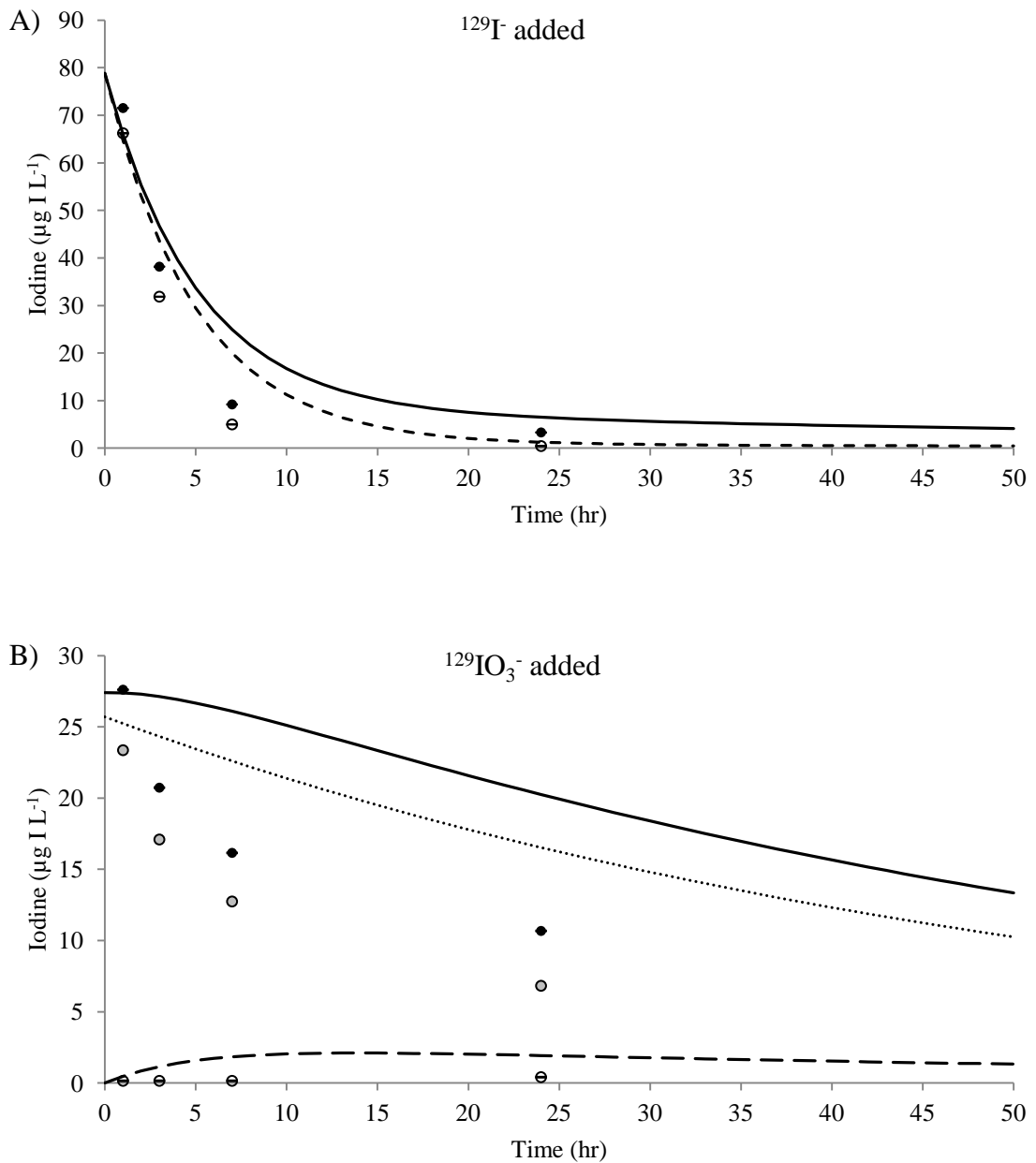


Figure 4.17. Array Model fits for soil NI01, utilising optimised rate parameters and partition coefficients determined by soil properties: A) iodide added, B) iodate added. Data and model fits include: $^{129}\text{I}_L$ (closed circles; solid line), $^{129}\text{IO}_3^-_L$ (shaded circles, dotted line) and $^{129}\text{I}_L$ (open circles, dashed line). Error bars show mean coefficient of variance on measured values. Error bars not visible are within the symbol.

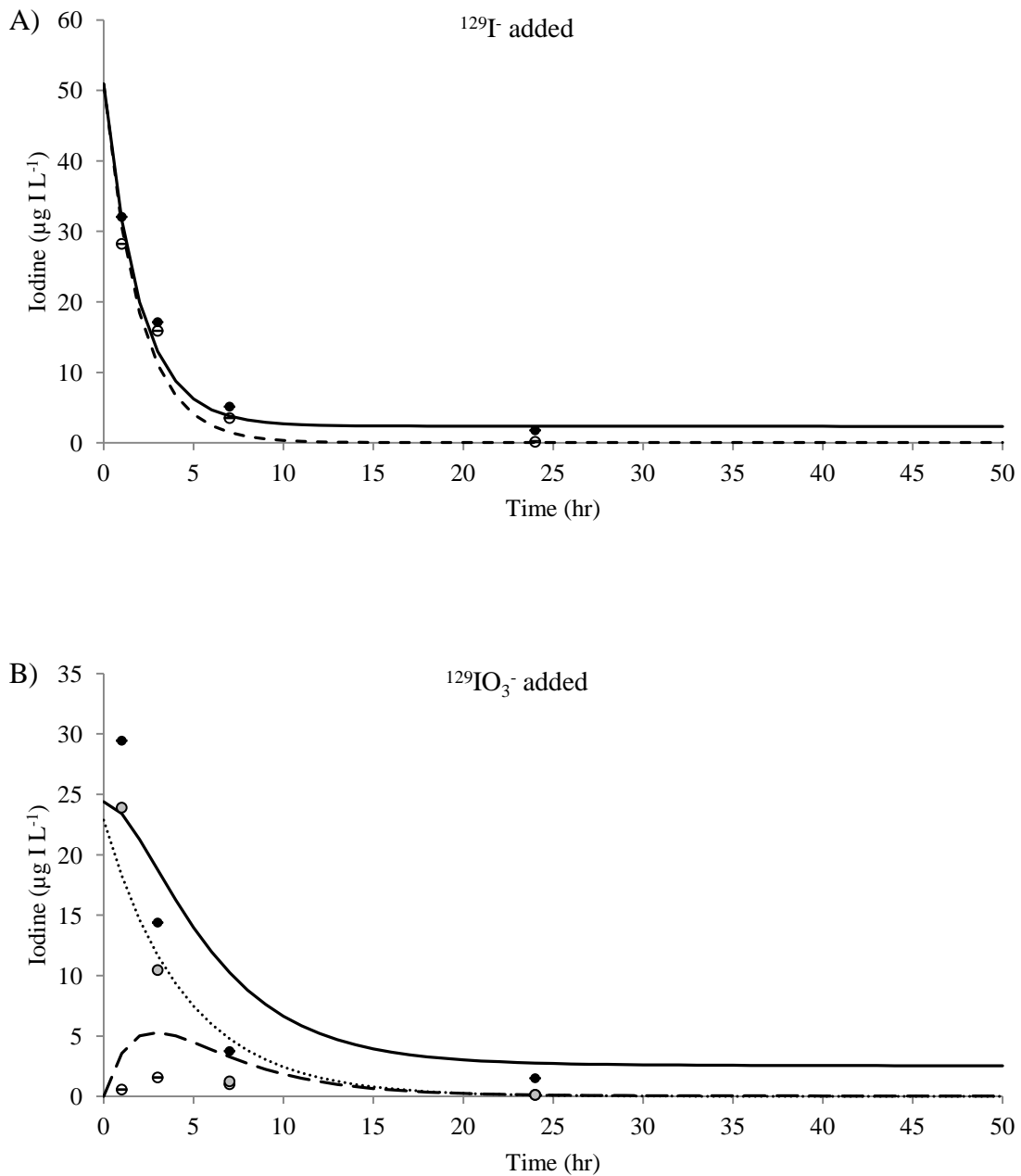


Figure 4.18. Array Model fits for soil NI03, utilising optimised rate parameters and partition coefficients determined by soil properties: A) iodide added, B) iodate added. Data and model fits include: $^{129}\text{I}_L$ (closed circles; solid line), $^{129}\text{IO}_3^-_L$ (shaded circles, dotted line) and $^{129}\text{I}^-_L$ (open circles, dashed line). Error bars show mean coefficient of variance on measured values. Error bars not visible are within the symbol.

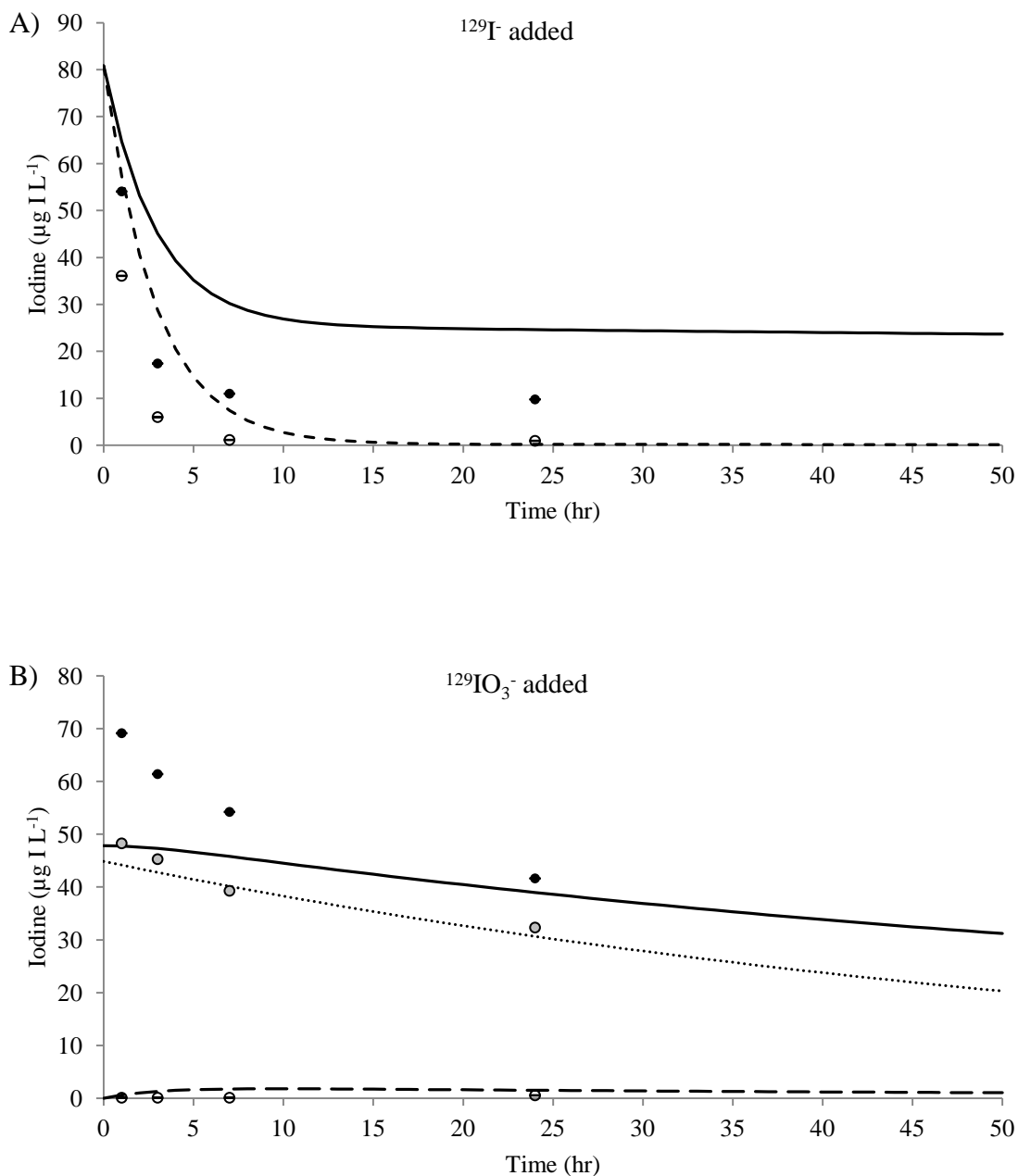


Figure 4.19. Array Model fits for soil NI05, utilising optimised rate parameters and partition coefficients determined by soil properties: A) iodide added, B) iodate added. Data and model fits include: $^{129}\text{I}_L$ (closed circles; solid line), $^{129}\text{IO}_3^-_L$ (shaded circles, dotted line) and $^{129}\text{I}_L$ (open circles, dashed line). Error bars show mean coefficient of variance on measured values. Error bars not visible are within the symbol.

4.6 CONCLUSIONS

Iodine dynamics in a range of 20 soils from NI were quantified by measuring transformations between species in solution and sorption to solid, between 1 and 24 hr after spiking with ^{129}I as iodide and iodate. A predictive model was produced, using rate parameters and partition coefficients related to accessible soil properties. The

relationships between model parameters and soil properties reveal some aspects of underlying reaction mechanisms. However, a full mechanistic understanding of iodine dynamics remains compromised by soil variability, covariance of soil properties and uncertainty over reaction mechanisms.

When iodine was added as iodide or iodate to soil suspensions, it was rapidly sorbed onto the solid phase at a rate dependent on soil properties. The mechanism of sorption appeared to depend on the original species added: in highly organic soils, both species were rapidly sorbed onto SOC, while in soils with lower SOC (< 38 %), sorption to metal oxides was rapid for iodate but not observed for iodide. The equilibria between iodide and both I_{solid} and OrgI were reversible, but the reverse transformations (to iodide) were extremely slow. No production of iodate from iodide addition was observed under any conditions. Iodate reacted more quickly immediately after addition than did iodide. In highly organic soils, sorption of iodate to solid SOC was rapid, followed by production of iodide after 3 – 7 hr. When SOC < 38 %, both I_{solid} and OrgI were produced within 1 hr, but no iodide was observed. From the limited evidence afforded by correlations with soil properties, it was suggested that reduction of iodate to iodide was probably facilitated by donation of protons and electrons by SOC and there was no evidence of a metal oxide-mediated reduction process. Metal oxides did allow rapid sorption of iodate to solid soils with low SOC contents; the rate of this process was inversely proportion to pH and followed a trend consistent with the adsorption envelope of anions on oxides.

The dominant form of iodine in soil solution was OrgI shortly after addition of $^{129}\text{I}^-$ or $^{129}\text{IO}_3^-$, although iodate was more rapidly transformed than iodide. The instantaneous transformation of iodate to OrgI was not explained by soil properties, although it is likely that DOC was involved. Further investigation into the process whereby an anion (I^- , IO_3^-) can become very rapidly, and strongly, bonded to a negatively charged macromolecule such as humic or fulvic acid is necessary and may require monitoring of species in solution over very short time spans.

5 IODINE DYNAMICS IN HUMIC ACID

5.1 INTRODUCTION

Humic acid (HA) is the colloidal fraction of humus. Its large surface area and significant presence in soil organic matter mean that it is highly influential in determining soil iodine dynamics (Allard, 2006; Francois, 1987; Hansen et al., 2011; Xu et al., 2011b; Yamada et al., 2002). Humic acid consists of both aliphatic and aromatic moieties, with relative proportions of the two affected by the degree of humification and the original vegetation source of the soil organic matter. Although the exact composition of HA varies between soils, the functional groups present are similar and therefore understanding iodine dynamics in HA contributes significantly to understanding its dynamics in soil (Saunders et al., 2012; Schlegel et al., 2006; Warner et al., 2000). Several of the NI soils used in the current study have very high SOC contents and therefore reactions between HA and iodine are likely to represent transformation processes in these soils.

X-ray absorption spectroscopy has been used to confirm that iodine binds directly to solid organic matter both in soils and in isolation, mainly through covalent bonding to aromatic structures (Schlegel et al., 2006; Xu et al., 2012; Yamaguchi et al., 2010). In natural waters, iodine is mainly bound to DOC (Gilfedder et al., 2009), which has implications for provision of iodine in drinking water. Radlinger and Heumann (2000) suggested that water processing removes DOC, thus reducing the iodine content of drinking waters, while Andersen et al. (2009) reported that iodine binding to DOC in well-water in China resulted in high iodine concentrations that caused hypothyroidism. It is well-established that in solid-liquid systems, flocculated humic substances cause fixation of iodine to the solid phase (e.g. Shetaya (2012), Shimamoto (2011)), and are the main reservoir for iodine (Bostock et al., 2003; Hansen et al., 2011; Xu et al., 2011b). Chemical mechanisms for the iodination of HA have been sought (Christiansen and Carlsen, 1991; Reiller et al., 2006), however investigations into transformation rates between iodine species in HA suspensions are scarce.

This chapter explores the transformations of iodine added to HA in solution, at three concentrations and as three combinations of species over a period of 73 days. Concentrations of iodide, iodate and OrgI were measured directly by size exclusion

chromatography, rather than one fraction being inferred from concentrations of other species, as is commonly the case in reported literature. Interactions between added species have been elucidated, and transformations have been modelled to support proposed mechanisms. These results have then been related to iodine dynamics in soil.

5.1.1 Aims

The aims of the work presented in this chapter were:

- to measure and model the dynamics of iodine over a period of months following addition to humic acid;
- to determine whether there is a non-labile pool of OrgI unavailable for interaction with added inorganic iodine species;
- to compare the dynamics of iodine interaction with HA with those of the whole soil.

5.2 MATERIALS AND METHODS

The HA was extracted using sodium hydroxide from soil from a coniferous plantation in Leicestershire (Benscliffe Wood, SK519123) as described by Marshall (1992). Humic acid was dissolved in 0.016 M NaOH and adjusted to pH 7.0 to give a final concentration of 7.18 mg HA ml⁻¹. The DOC concentration of this solution was measured according to Section 2.4.3.

Samples were spiked with ¹²⁹I to give final concentrations of 22.1 µg ¹²⁹I L⁻¹, 44.1 µg ¹²⁹I L⁻¹ and 88.2 µg ¹²⁹I L⁻¹, which are referred to as '+20 ppb', '+40 ppb' and '+80 ppb' respectively in this chapter. Iodine-129 was added, in triplicate, as iodide, iodate, or equal amounts of both, to give the final concentrations above (Table 5.1) and samples were stored in polyethylene ICP sample tubes at 10 °C to represent average UK soil temperature. Spiking was carried out at 8 time intervals between 73 days and 1 day before analysis, resulting in incubation times of 1, 3, 6, 13, 24, 38, 55 and 73 days. Precise incubation times were affected by the exact timing of analytical runs, so for each sample were recorded in hours (26, 79, 155, 328, 596, 992, 1404 and 1855 hr). Confusion with the ICP-MS booking timetable resulted in 24 – 73 day incubations of 'a' replicates being incubated for an extra 7 days, which is reflected in

the error bars on relevant Figures. Day 50 ‘a’ replicate samples had too much HA added to them and therefore have been excluded from all calculations and graphs.

Table 5.1. Details of humic acid solutions incubated in triplicate with ^{129}I as iodide, iodate and both inorganic species together.

Solution	Nominal additions	Actual concentration $^{129}\text{I}^-$ added ($\mu\text{g } ^{129}\text{I L}^{-1}$)	Actual concentration $^{129}\text{IO}_3^-$ added ($\mu\text{g } ^{129}\text{I L}^{-1}$)
1	20 ppb iodide	22.1	0
2	40 ppb iodide	44.1	0
3	80 ppb iodide	88.2	0
4	20 ppb iodate	0	22.1
5	40 ppb iodate	0	44.1
6	80 ppb iodate	0	88.2
7	20 ppb mix	11.0	11.0
8	40 ppb mix	22.1	22.1
9	80 ppb mix	44.1	44.1

At the end of the incubation period, all samples were analysed for iodine species by SEC according to Section 2.6.2.2. Limits of detection were $0.047 \mu\text{g } ^{127}\text{I L}^{-1}$ and $0.014 \mu\text{g } ^{129}\text{I L}^{-1}$. Since known concentrations of ^{129}I were added to each sample, a ‘standard addition’ approach was used to quantify mean sensitivity (ICPS ppb $^{-1}$) across all samples in each run, which was then used to quantify concentration of ^{129}I and ^{127}I in each chromatography peak. Therefore standards consisted of identical matrices to samples, removing any analytical uncertainty due to matrix effects. Twelve HA samples spiked with 0.2 ml MQ water were analysed alongside ^{129}I spiked samples to determine the equilibrium speciation of ^{127}I .

5.3 RESULTS AND DISCUSSION

Results of analyses for total iodine and iodine speciation for both isotopes in HA solution are presented in Appendix 5. The DOC concentration of HA solution was determined to be 3.67 mg ml^{-1} . Concentrations of ^{127}I species represented iodine at equilibrium with HA, with median values of $98.0 \mu\text{g I L}^{-1}$ Org ^{127}I and $15.1 \mu\text{g I L}^{-1}$ $^{127}\text{I}^-$; iodate ($^{127}\text{IO}_3^-$) was not detected. Speciation of ^{129}I changed through time, progressing towards the equilibrium position, and transformation between species was comparable to that determined in spiked soils. Thus, for all samples, the concentration of Org ^{129}I increased through time (Figure 5.1 – Figure 5.3). For iodate-spiked and

mixed-spike samples, inorganic iodine was transformed to Org¹²⁹I within 24 hr of contact. Direct comparison to soil cannot be made due to differences in measurement times. However in soils, Org¹²⁹I was observed in solution within 1 hr of adding ¹²⁹IO₃⁻ and the presence of ¹²⁹IO₃⁻ only persisted until 24 hr after spiking at 500 µg I L⁻¹ (Chapter 4). In iodide-spiked HA solutions, Org¹²⁹I was only detected 150 hr (+20 ppb and + 40 ppb) and 24 hr (+80 ppb) after spiking. This rate of transformation was much slower than for iodide added to soils, when Org¹²⁹I was observed 1 hr after spiking. As with the soil samples, production of ¹²⁷IO₃⁻ and increase in ¹²⁹IO₃⁻ concentration were not observed. However, when ¹²⁹IO₃⁻ was added, ¹²⁹I⁻ was produced throughout the observed time period; this was only observed in NI soils with SOC > 38 %. This confirms the ability of HA to reduce iodate to OrgI in the absence of metal oxides.

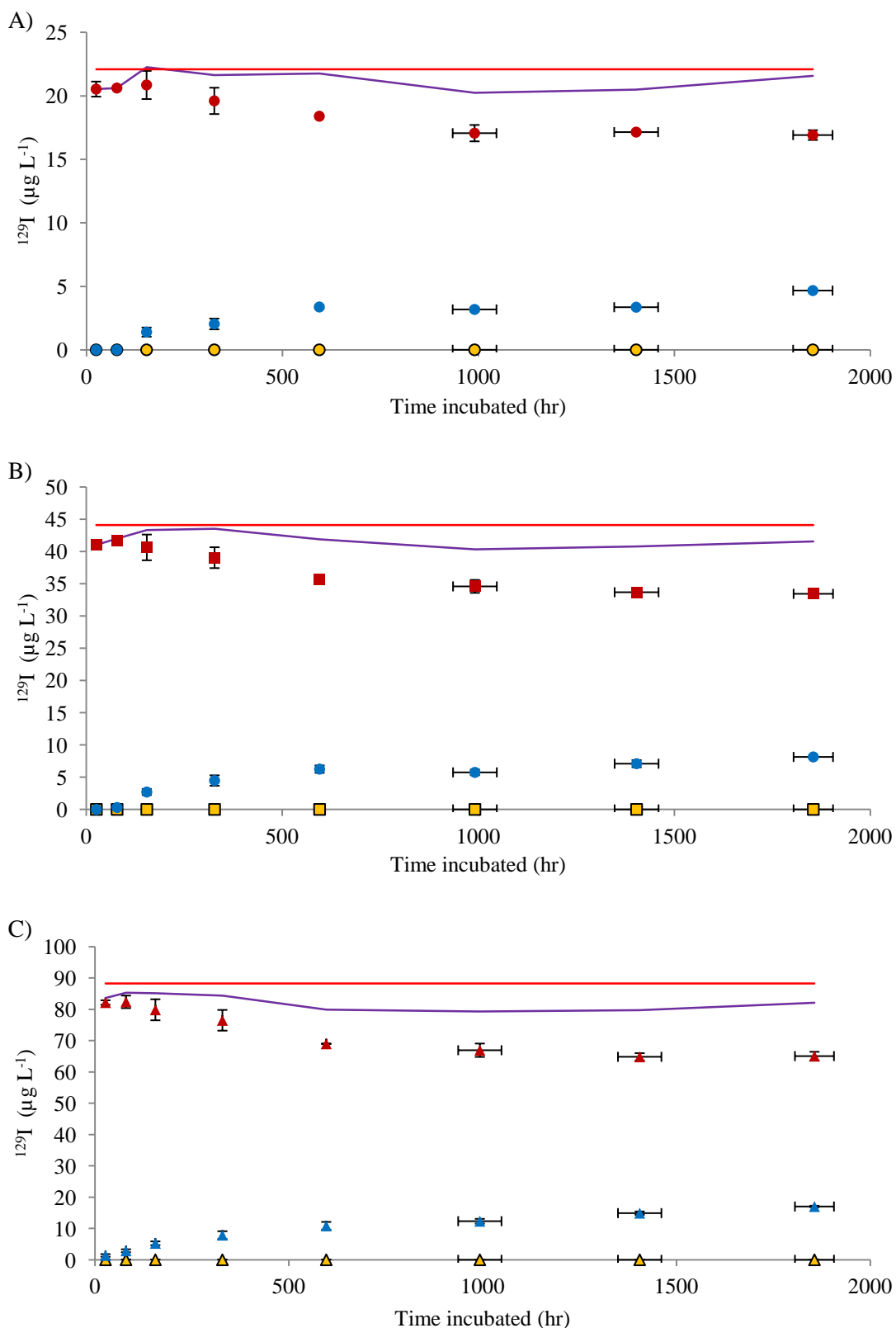


Figure 5.1. Change in ^{129}I concentrations with time following spiking with ^{129}I as **iodide** at a range of concentrations: A) $22.1 \mu\text{g IL}^{-1}$ added, B) $44.1 \mu\text{g IL}^{-1}$ added, C) $88.2 \mu\text{g IL}^{-1}$ added. Species measured included $^{129}\text{I}^-$ (red symbols), $^{129}\text{IO}_3^-$ (yellow symbols) and Org^{129}I (blue symbols); the purple and red lines represent the measured and expected sum of ^{129}I species respectively. Error bars show standard error of triplicate measurements.

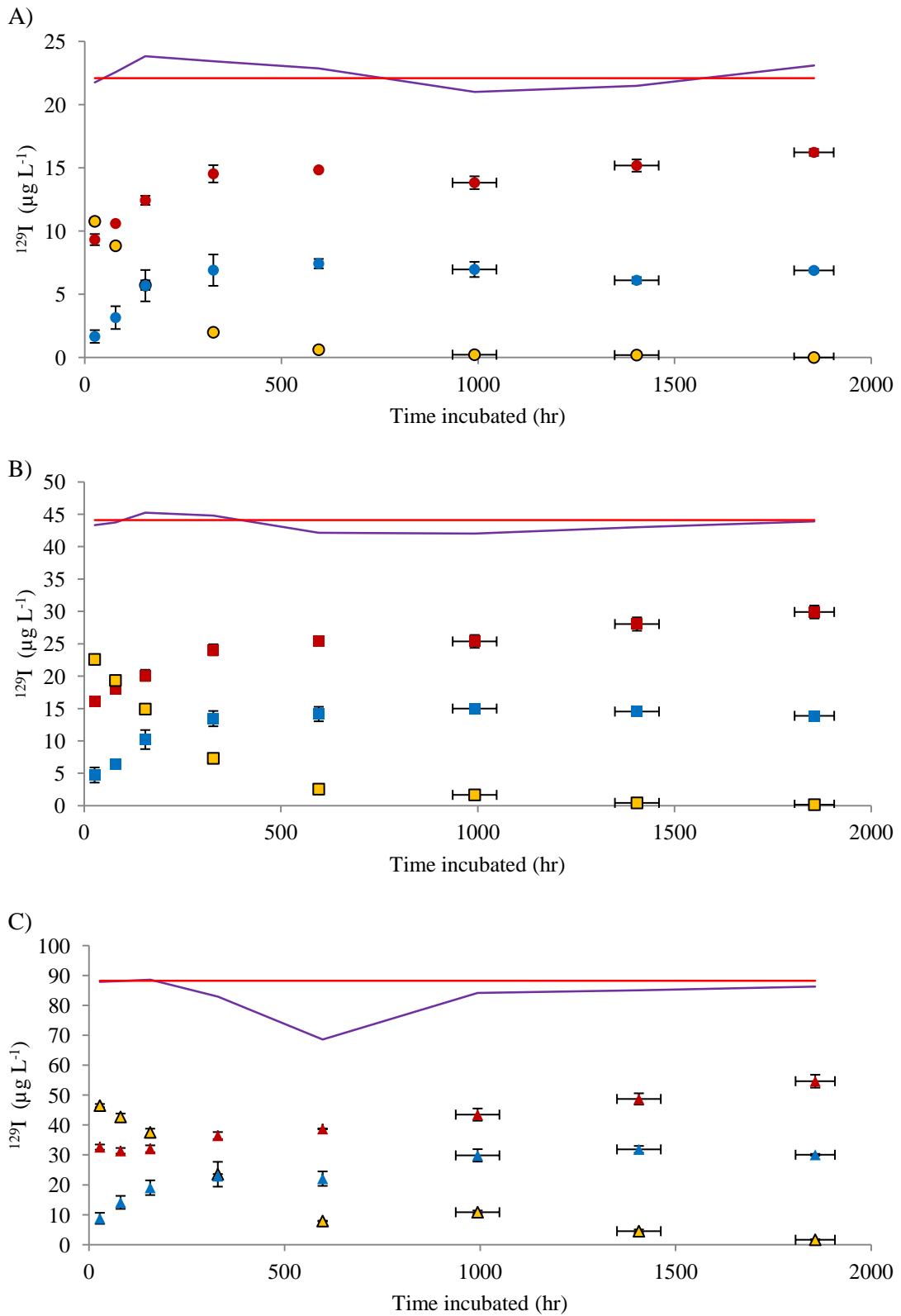


Figure 5.2. Change in ^{129}I concentrations with time following spiking with ^{129}I as **equal concentrations of iodide and iodate** at a range of total concentrations: A) $22.1 \mu\text{g IL}^{-1}$ added, B) $44.1 \mu\text{g IL}^{-1}$ added, C) $88.2 \mu\text{g IL}^{-1}$ added. Species measured included $^{129}\text{I}^-$ (red symbols), $^{129}\text{IO}_3^-$ (yellow symbols) and Org^{129}I (blue symbols); the purple and red lines represent the measured and expected sum of ^{129}I species respectively. Error bars show standard error of triplicate measurements.

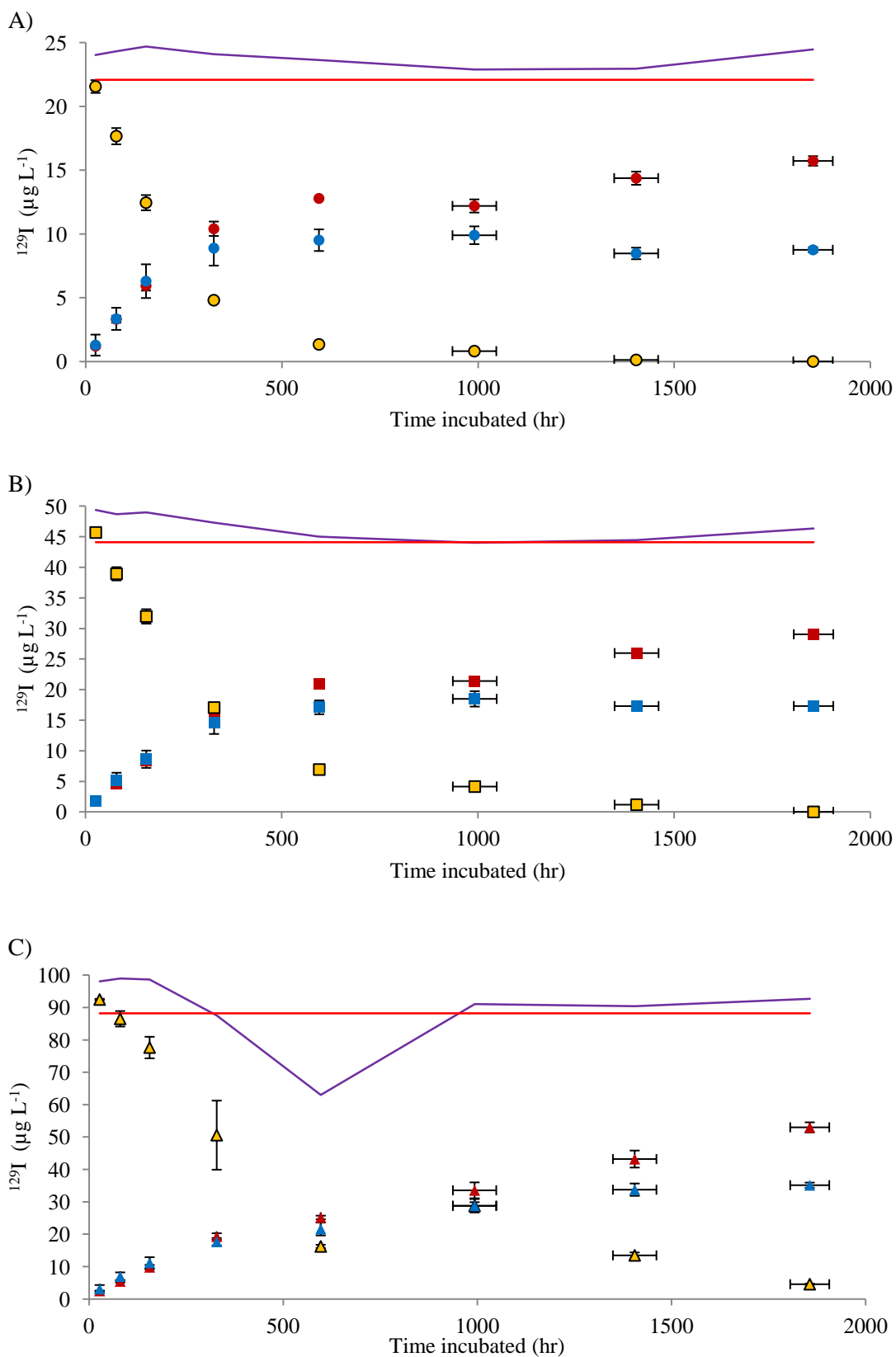
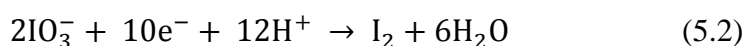


Figure 5.3. Change in ^{129}I concentrations with time following spiking with ^{129}I as iodate at a range of concentrations: A) 22.1 $\mu\text{g I L}^{-1}$ added, B) 44.1 $\mu\text{g I L}^{-1}$ added, C) 88.2 $\mu\text{g I L}^{-1}$ added. Species measured included ^{129}I (red symbols), $^{129}\text{IO}_3^-$ (yellow symbols) and Org ^{129}I (blue symbols); the purple and red lines represent the measured and expected sum of ^{129}I species respectively. Error bars show standard error of triplicate measurements.

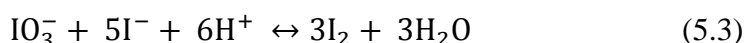
5.3.1 Rates of reaction

The rate of production of Org¹²⁹I varied according to the species added. In all cases, added iodide reacted more slowly than either added iodate or mixture of species. In general, Org¹²⁹I production in the mixed spike system was more rapid than in iodate-spiked solutions, rather than intermediate between iodate- and iodide-spiked samples as may be expected (Figure 5.4). At lower concentrations the difference between iodate- and mixed-spike solutions was less pronounced, but added iodide always reacted much more slowly. Iodate may be able to react with HA more rapidly by polarising its negative charge towards the oxygen atoms, creating I^{δ+} that can approach the negatively charged surface of HA more easily than iodide can. The polarisation of I₂ by metal oxides to enable catalysis of its reaction with organic matter was proposed by Allard et al. (2009), and Goldschmidt (1958) remarked on the polarisable nature of iodide. The presence of oxygen to act as an electron withdrawal sink may therefore enable iodate to behave in the same way.

The reactions of iodide and iodate with organic matter are likely to progress via a reactive species such as I₂ or HOI, the production of which requires oxidation of iodide and reduction of iodine in iodate (Francois, 1987; Shimamoto et al., 2011; Yamaguchi et al., 2010). Humic acid has been reported to both reduce iodate and oxidise iodide (Yamaguchi et al., 2010), however the oxidation of iodide by organic matter is expected to be much slower than the reduction of iodate by the same mechanism (Schlegel et al., 2006). In soils, oxidation of iodide can be catalysed by the presence of some Fe^{III} and Mn^{IV} oxides (Allard et al., 2009; Fox et al., 2009; Gallard et al., 2009), but these are not expected to be present in purified HA suspensions at concentrations great enough to enable the same reaction. The results for the mixed-spike system suggest that a redox couple between iodide and iodate may increase the rate of iodide oxidation, in place of metal oxides. This would occur according to Eqns. 5.1 – 5.3.



which combine to give:



Support for this proposition comes from Figure 5.4, which shows that the rate of Org¹²⁹I production was faster when both species were added than when either iodide or iodate were added individually. The rate of iodide reaction in particular was increased by the presence of added ¹²⁹IO₃⁻. In iodate-spiked systems, some ¹²⁷I was naturally present, with which the redox couple could form. When only ¹²⁹I was added there was no ¹²⁷IO₃⁻ present, however, and oxidation was reliant electron consumption by HA alone. A decrease in concentration of ¹²⁷I through time was observed, further supporting this mechanism. It would be expected from Eqn. 5.3 that when only ¹²⁹IO₃⁻ was added, five times as much ¹²⁷I as ¹²⁹IO₃⁻ would be lost from solution. This was not observed, however, due to the production of ¹²⁹I from ¹²⁹IO₃⁻ which could then become involved in the redox reaction as well; and the concurrent direct reaction of ¹²⁹IO₃⁻ with HA.

Further confirmation that both iodide and iodate participated in a redox reaction is evident from the observation that transformation rates of both ¹²⁹I species were affected by the concentration of the other inorganic species. When only ¹²⁹I was added, its transformation was not concentration dependent (Figure 5.5), suggesting an oxidation mechanism that was independent of the presence of another species. Humic acid was present in excess, so the reaction may have been limited by diffusion or another physical mechanism. Production of ¹²⁹I in the mixed spike system was faster when lower total concentrations of ¹²⁹I were added, however, which is consistent with faster reduction of ¹²⁹IO₃⁻ occurring at higher iodide/iodate ratios (Figure 5.5). Removal of iodate from solution was slightly faster in the mixed spike system than when ¹²⁹IO₃⁻ alone was added (Figure 5.6), and in both cases the transformation was concentration dependent. In all scenarios when iodate was added, transformation of iodate was faster when the ratio of iodide/iodate was greater, i.e. at lower added concentrations and/or when both ¹²⁷I and ¹²⁹I were present.

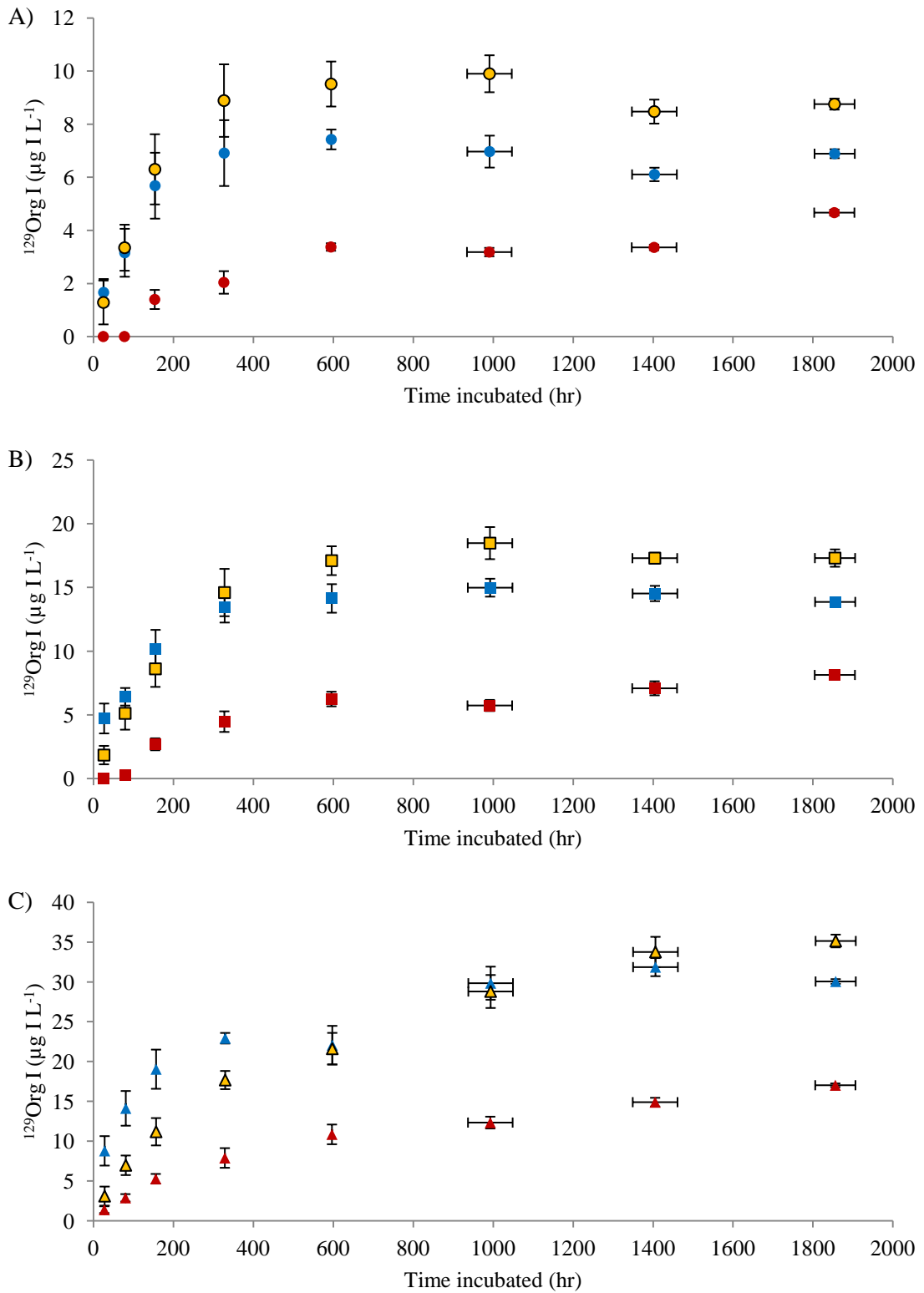


Figure 5.4. Change in concentration of Org^{129}I with time following addition of ^{129}I as iodide (red symbols), iodate (yellow symbols) and a mixed spike (blue symbols). Total concentrations of added ^{129}I include: A) $22.1 \mu\text{g IL}^{-1}$, B) $44.1 \mu\text{g IL}^{-1}$ and C) $88.2 \mu\text{g IL}^{-1}$. Error bars show standard error of triplicate measurements. Note that y axis scales differ.

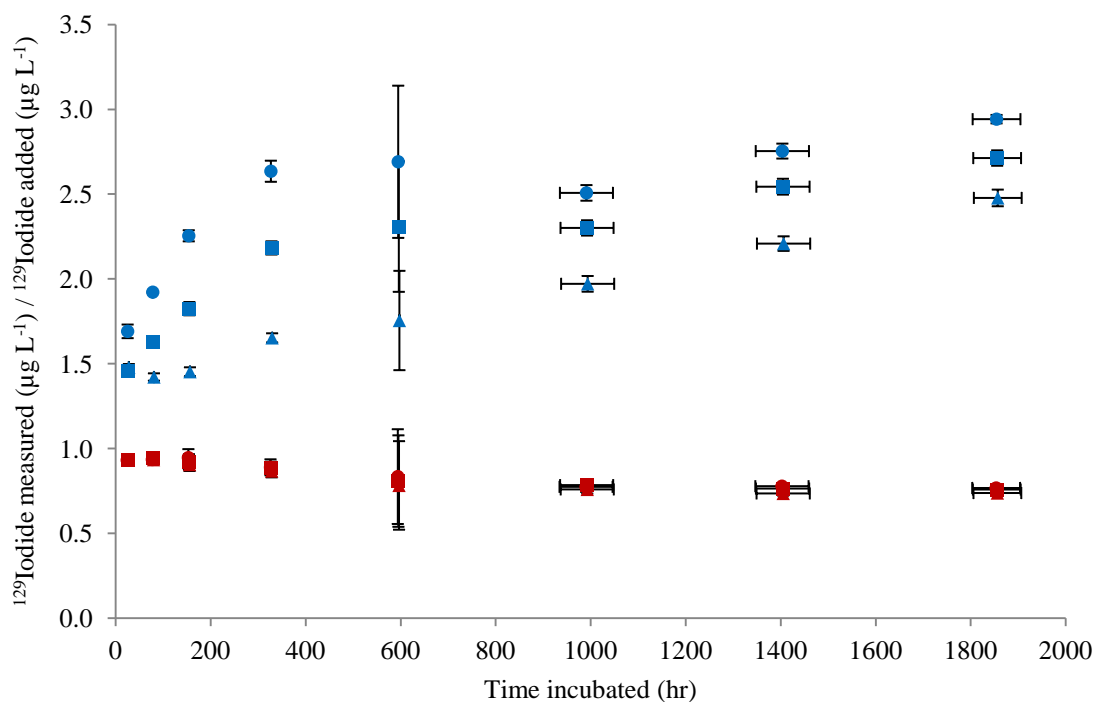


Figure 5.5. Change in the ratio of (measured iodide)/(added iodide) with time, following addition of iodide (red symbols) and mixed iodide/iodate ^{129}I spikes (blue symbols). Total concentrations of ^{129}I added were: $22.1 \mu\text{g I L}^{-1}$ (circles), $44.1 \mu\text{g I L}^{-1}$ (squares) and $88.2 \mu\text{g I L}^{-1}$ (triangles). Error bars show standard error of triplicate measurements.

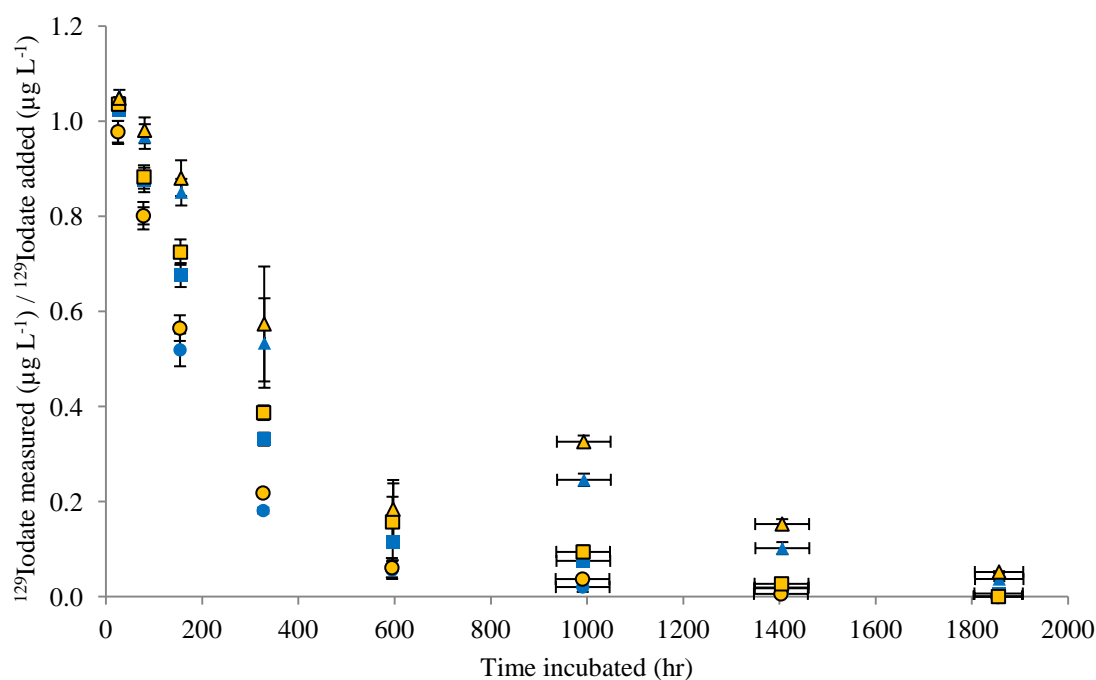


Figure 5.6. Change in ratio of (measured iodate)/(added iodate) with time, following addition of iodate (yellow symbols) and mixed iodide/iodate ^{129}I spikes (blue symbols). Total concentrations of ^{129}I added were: $22.1 \mu\text{g I L}^{-1}$ (circles), $44.1 \mu\text{g I L}^{-1}$ (squares) and $88.2 \mu\text{g I L}^{-1}$ (triangles). Error bars show standard error of triplicate measurements.

5.3.2 Production of Org¹²⁹I

The extent of Org¹²⁹I production from inorganic species can be seen in Figure 5.7, which shows the organic iodine section of SEC-chromatograms (¹²⁹I and ¹²⁷I) of +80 ppb samples after 26 hr incubation. In the mixed spike systems, Org¹²⁹I was clearly visible but when iodate was added, a smaller amount of Org¹²⁹I was evident and when iodide was added, even less was detected. The shape of the Org¹²⁹I chromatogram for the mixed spike system is similar to that of the native iodine (¹²⁷I), with ¹²⁹I present in both the ‘low’ and ‘high’ molecular weight (MW) ranges – i.e. below and above the column exclusion limit. It may be expected that HA with lower MW would react more easily with iodine, due to a greater surface area and therefore greater accessibility to reactive sites. This was reported by Xu et al. (2011a) to be the case 72 hr after iodate was added to HA at pH 3, where lower MW HA (3,000 – 50,000 Da) sorbed more iodine than high MW HA (> 50,000 Da). On the other hand the negative charge density on the lower MW HA fractions is likely to be greater and therefore could exclude or delay I⁻ and IO₃⁻ ions from interaction with HA to a greater degree.

To further investigate the MW range of newly-iodinated HA, the isotopic ratio ¹²⁷I/¹²⁹I was calculated at each measured time point, one day after spiking (Figure 5.8). All values were background corrected, so at elution times when, on average, iodine concentrations were zero, approximately half the integrated counts per second (ICPS) data points were negative. Therefore when only ¹²⁷I was present the isotopic ratio was negative for, on average, half the data points, creating the ‘mirroring’ effect visible in Figure 5.8. There was less mirroring evident when a mixed spike was added, due to greater Org¹²⁹I formation than when iodide or iodate were added alone. The pattern of data for all three scenarios follow the general shape of Org¹²⁷I, indicating that ¹²⁹I was approximately evenly distributed throughout the chromatogram; this can be inferred by knowing that changes in the concentration of ¹²⁷I with elution time cause the observed changes to the ratio. A smaller ratio of ¹²⁷I/¹²⁹I indicates greater relative representation of spiked ¹²⁹I. Hence in the +80 ppb mixed-spike system where the reaction had proceeded furthest, the isotopic ratios in the range 450 – 700 s elution were generally slightly lower and exhibited less spread and mirroring than when iodide or iodate were added alone.

At equilibrium, ^{129}I should be fully mixed with ^{127}I and therefore the pattern of $^{127}\text{I}/^{129}\text{I}$ data should be consistent around a single value (equal to the overall isotopic ratio in the sample, $^{127}\text{I}/^{129}\text{I} = 1.16$) and show no mirroring. After 1855 hr, the three systems showed varying stages towards this end-point (Figure 5.9), with notable changes compared to Figure 5.8. Firstly, many fewer negative points were present than there were after 26 hr incubation, particularly in the iodate and the mixed spike systems, signifying greater incorporation of ^{129}I into HA. Secondly, although the large spread of values in Figure 5.8 was still present in the iodide-added sample, it was less evident in the iodate and mixed spike systems. The data were also generally much more consolidated than after 26 hr contact between iodine and HA: in the +80 ppb iodate and +80 ppb mixed samples, isotopic ratios tended to be more tightly clustered around the overall isotopic ratio, indicated by the bright red line. This clustering was slightly more pronounced at lower MW, possibly supporting the greater accessibility to iodine of smaller organic molecules in the longer term.

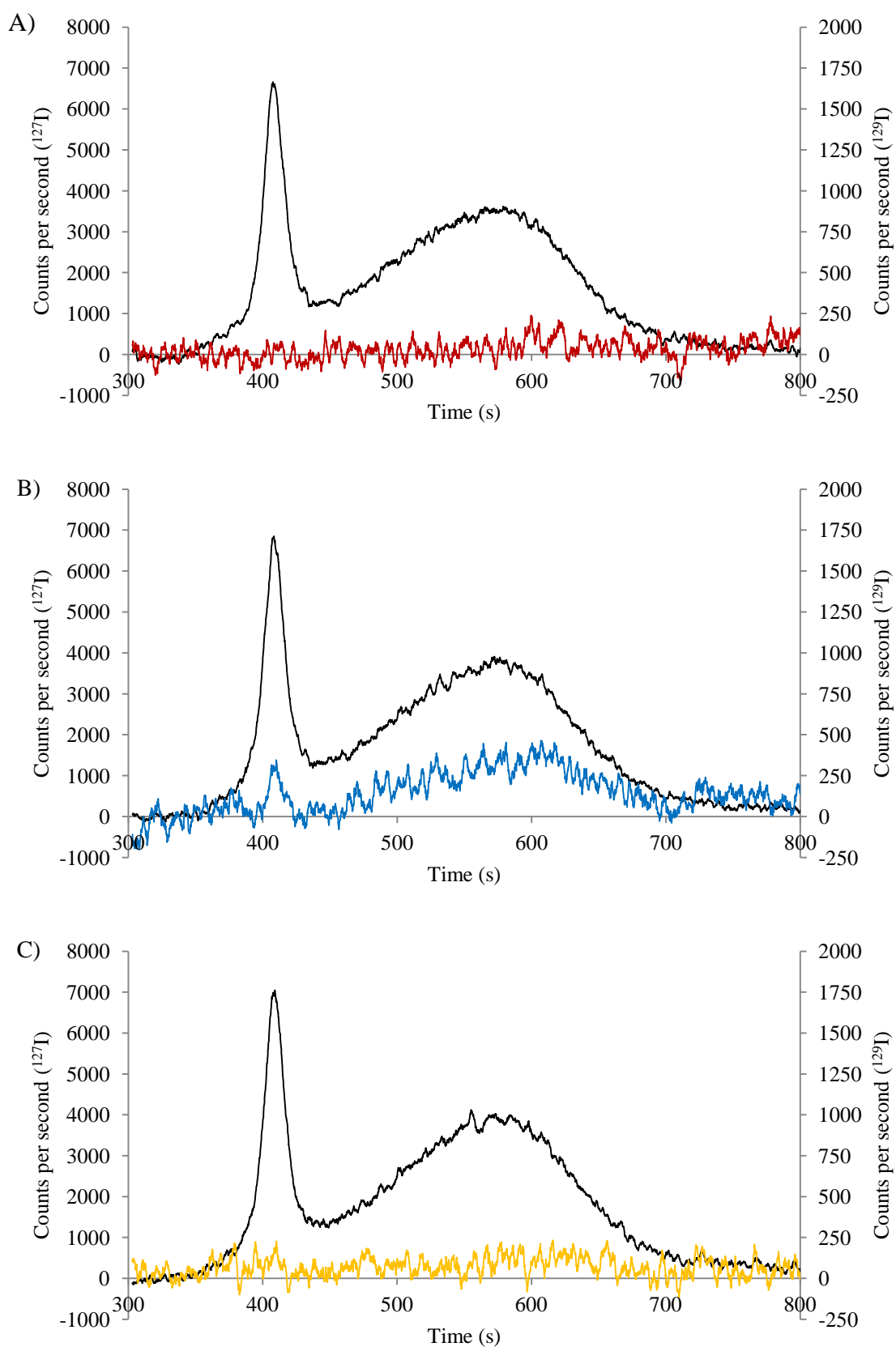


Figure 5.7. Size exclusion chromatograms of humic acid incubated for 26 hr with $88.2 \mu\text{g } ^{129}\text{I L}^{-1}$ as A) iodide, B) a mixed spike of iodide and iodate and C) iodate. Black lines show ^{127}I ; coloured lines show ^{129}I . Both isotopes have been background corrected. Lines are moving averages of detected values, over 20 points.

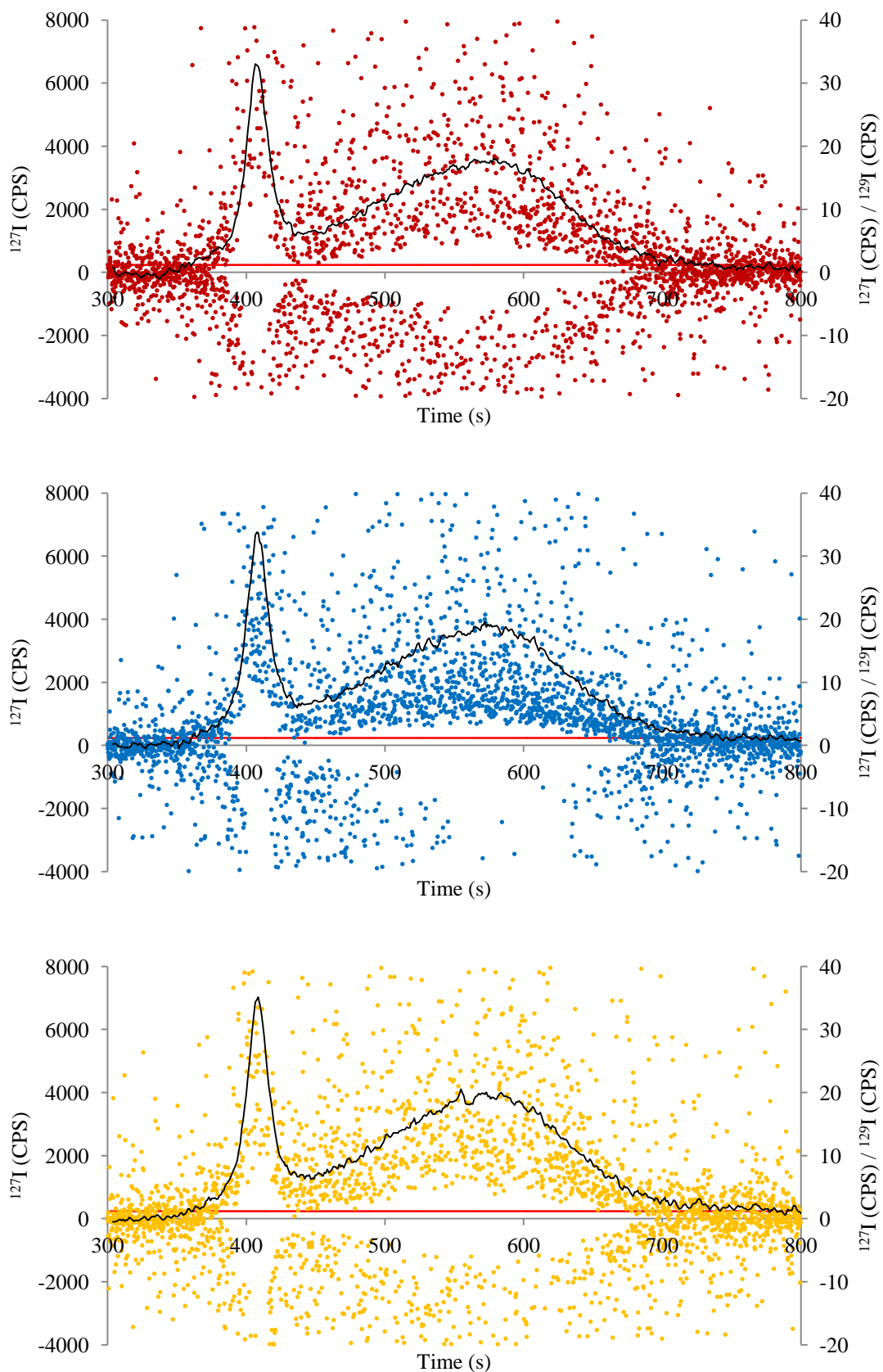


Figure 5.8. Size exclusion chromatograms of humic acid incubated for 26 hr with $88.2 \mu\text{g } ^{129}\text{I L}^{-1}$ as A) iodide, B) a mixed spike of iodide and iodate and C) iodate. Black lines show ^{127}I , coloured dots show ratio of $^{127}\text{I}/^{129}\text{I}$ at each time point. Red line shows overall ratio of $^{127}\text{I}/^{129}\text{I}$ in the sample. Values have been background corrected.

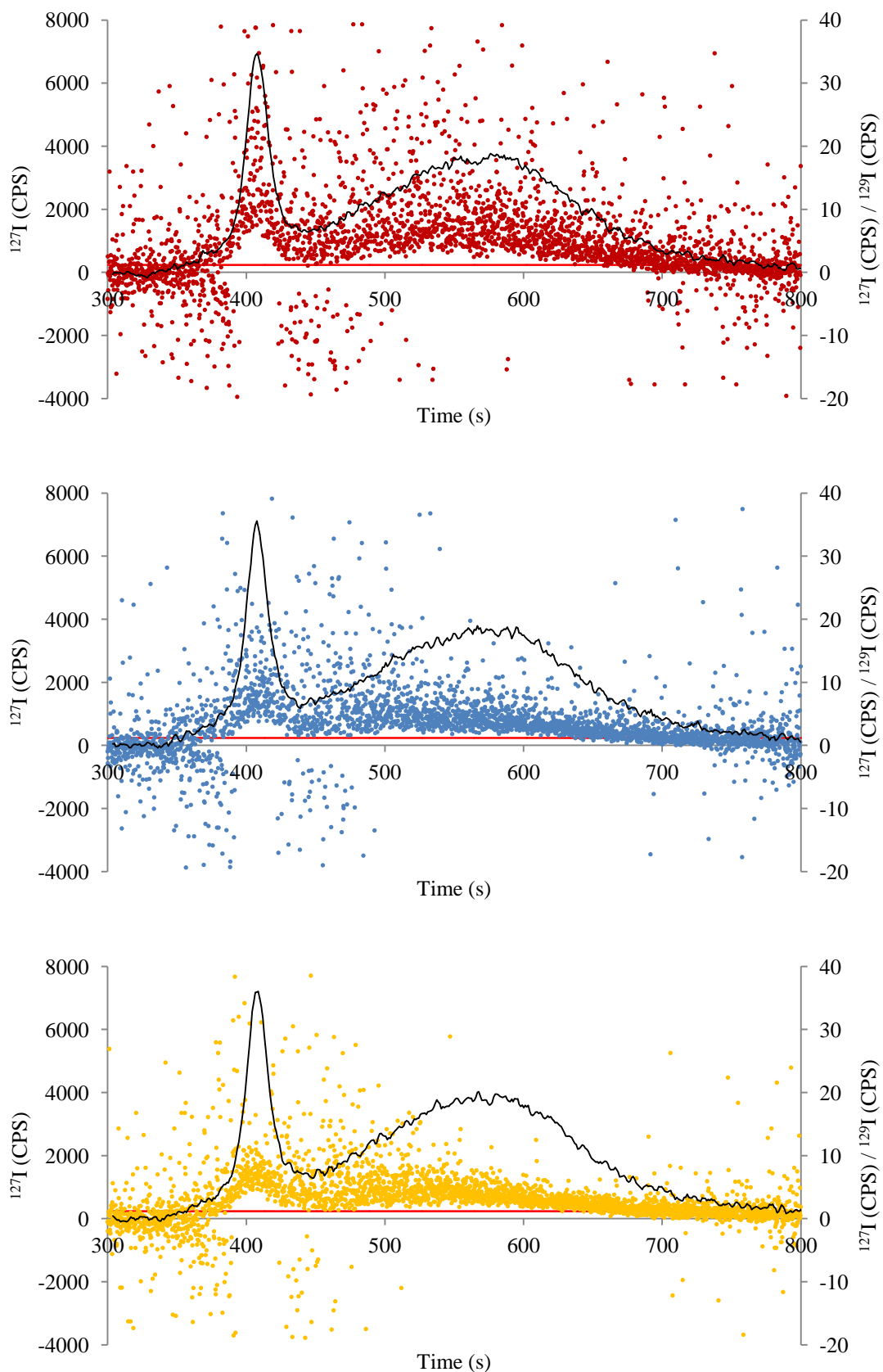


Figure 5.9. Size exclusion chromatograms of humic acid incubated for 1855 hr with $88.2 \mu\text{g } ^{129}\text{I L}^{-1}$ as A) iodide, B) a mixed spike of iodide and iodate, and C) iodate. Black lines show ^{127}I , coloured dots show ratio of $^{127}\text{I}/^{129}\text{I}$ at each time point. Red line shows overall ratio of $^{127}\text{I}/^{129}\text{I}$ in sample. Values have been background corrected.

5.4 MODELLING IODINE DYNAMICS IN HUMIC ACID

Experimental results from all 9 scenarios were used to create and optimise a predictive model of iodine interactions with HA. In contrast to modelling iodine dynamics in soil, all three spiked systems were used together to parameterise a single model.

5.4.1 Model development

The basic model structure based on experimental observations allowed transformation between species as shown in Figure 5.10. As in soil iodine dynamics, there was no evidence of (native) $^{127}\text{IO}_3^-$ production and so it was not included in the model.

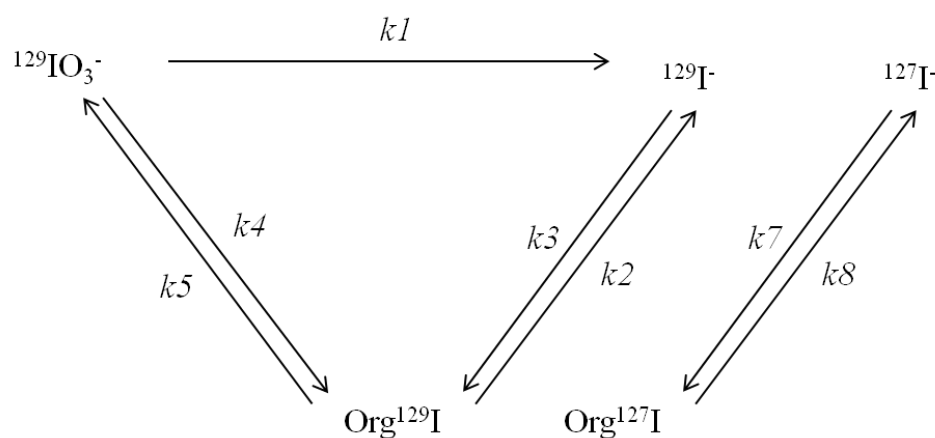


Figure 5.10. Conceptual model describing iodine transformations in the presence of HA. Spike and native iodine allowed independent description of their dynamic behaviour.

Unexpectedly, Org^{127}I concentration apparently increased during the first 200 hr of incubation of HA with $^{129}\text{I}^-$, $^{129}\text{IO}_3^-$ and in the mixed spike system; this was generally accompanied by a loss of native $^{127}\text{I}^-$. This transfer of native $^{127}\text{I}^-$ to humic-bound forms implied some form of interaction between the isotope species, probably linked to redox coupling of iodide and iodate (Section 5.3.1). Therefore variations on parameter values and species used for fitting within this structure were trialled to investigate possible relationships between isotopes as well as transformations of added ^{129}I (Table 5.2). The variations tested allowed fitting to various combinations of: ^{129}I concentrations as iodide, iodate and OrgI; ^{127}I concentrations as iodide and OrgI; and total (sum of isotopes) concentrations of iodide and OrgI. No trial was carried out fitting all three of ^{129}I concentrations, ^{127}I concentrations and total concentrations, as this would be equivalent to fitting results from both isotopes twice. Parameters were either allowed to be fully fitted for all reactions, as shown in Figure 5.10, or the reversible reaction between $^{127}\text{I}^-$ and Org^{127}I was fixed to have the same rate

parameters as the equivalent reaction for ^{129}I , i.e. $k_8 = k_2$ and $k_7 = k_3$. Models were compared on the basis of their overall relative sum of squares, divided by the number of species fitted (RSS per species). This was to account for the additional uncertainty associated with fitting more parameter values.

Table 5.2. Details of HA-iodine dynamics models trialled and comparison of overall relative sum of squares (RSS). Parameters refer to those shown in Figure 5.10; where only $k_1 - k_5$ were used, $k_8 = k_2$ and $k_7 = k_3$. RSS per species was calculated by dividing RSS by the number of fitted species.

Model	Species fitted	Parameters used	RSS ($\times 10^6$)	RSS ($\times 10^6$) per species
1	^{129}I , $^{129}\text{IO}_3^-$, Org^{129}I	$k_1 - k_5$	1.27	0.424
2	^{129}I , $^{129}\text{IO}_3^-$, Org^{129}I , ($^{129}\text{I} + ^{127}\text{I}$), ($\text{Org}^{129}\text{I} + \text{Org}^{127}\text{I}$)	$k_1 - k_5$	5.71	0.952
3	^{129}I , $^{129}\text{IO}_3^-$, Org^{129}I , ($^{129}\text{I} + ^{127}\text{I}$), ($\text{Org}^{129}\text{I} + \text{Org}^{127}\text{I}$)	$k_1 - k_8$	2.34	0.390
4	^{129}I , $^{129}\text{IO}_3^-$, Org^{129}I , ^{127}I , Org^{127}I	$k_1 - k_8$	2.02	0.336

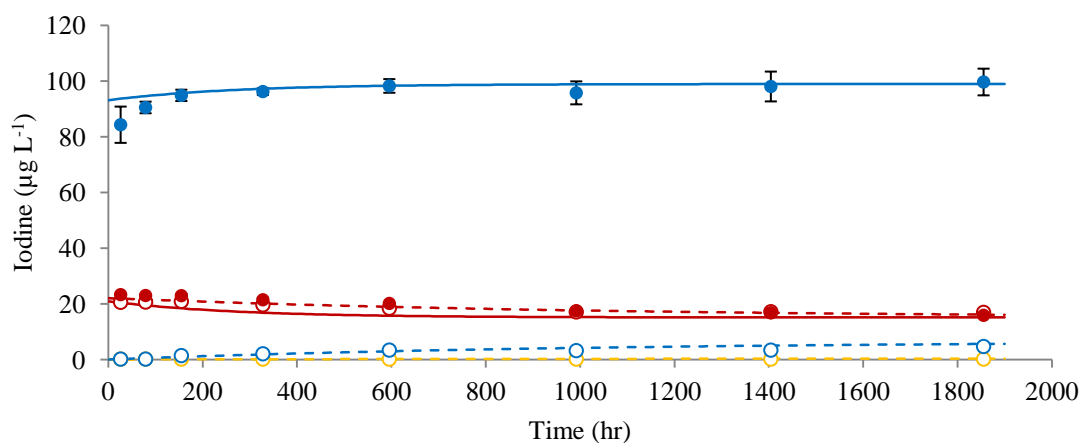
5.4.2 Final model description

Model 4 gave the lowest value of RSS per species (Table 5.2). Details of this model structure are presented in Appendix 6, and values of fitted parameters are in Table 5.3. Simulated and measured speciation dynamics are compared in Figure 5.11 - Figure 5.13 and comparison of all modelled and measured species concentrations are presented in Figure 5.14.

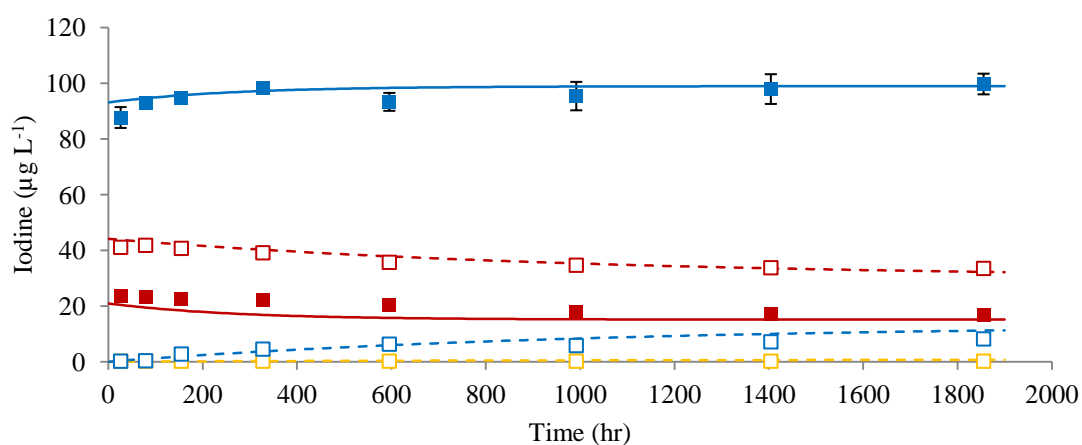
Table 5.3. Optimised parameter values describing HA-iodine dynamics in Model 4.

Parameter	Mean	S. D.
k1	0.00411	0.00010
k2	0.000467	0.00004
k3	0.000316	0.00002
k4	2.62	0.00000
k5	0.157	0.00003
k7	0.00323	0.00081
k8	0.000493	0.00013

+ 20 ppb iodide



+40 ppb iodide



+80 ppb iodide

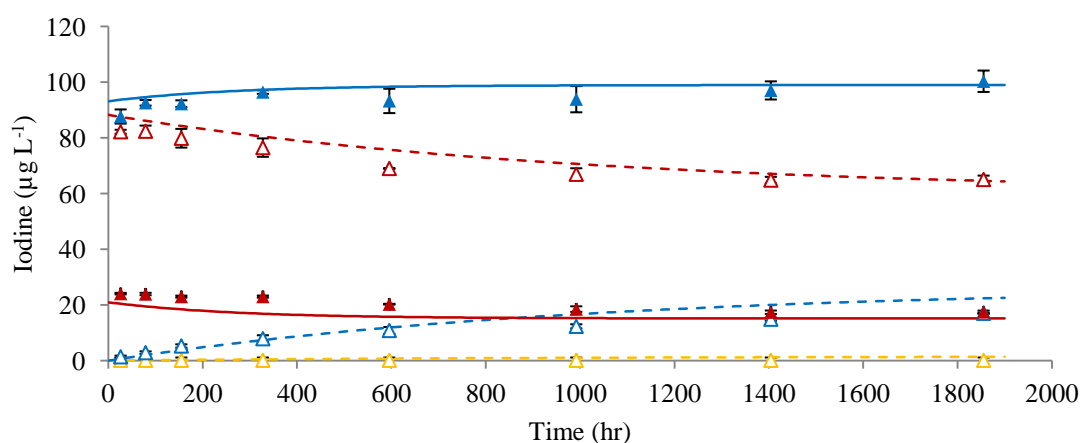


Figure 5.11. Results of Model 4 when $^{129}\text{I}^-$ was added at concentrations of $22.1 \mu\text{g I L}^{-1}$ (20 ppb, circles), $44.1 \mu\text{g I L}^{-1}$ (40 ppb, squares) and $88.2 \mu\text{g I L}^{-1}$ (80 ppb, triangles); see Table 5.1. Measured data and modelled lines are shown for ^{127}I (closed symbols, solid lines) and ^{129}I (open symbols; dashed lines). Species include iodide (red symbols), iodate (yellow symbols) and OrgI (blue symbols). Error bars show coefficient of variance on measured values; where not visible they are within the symbol.

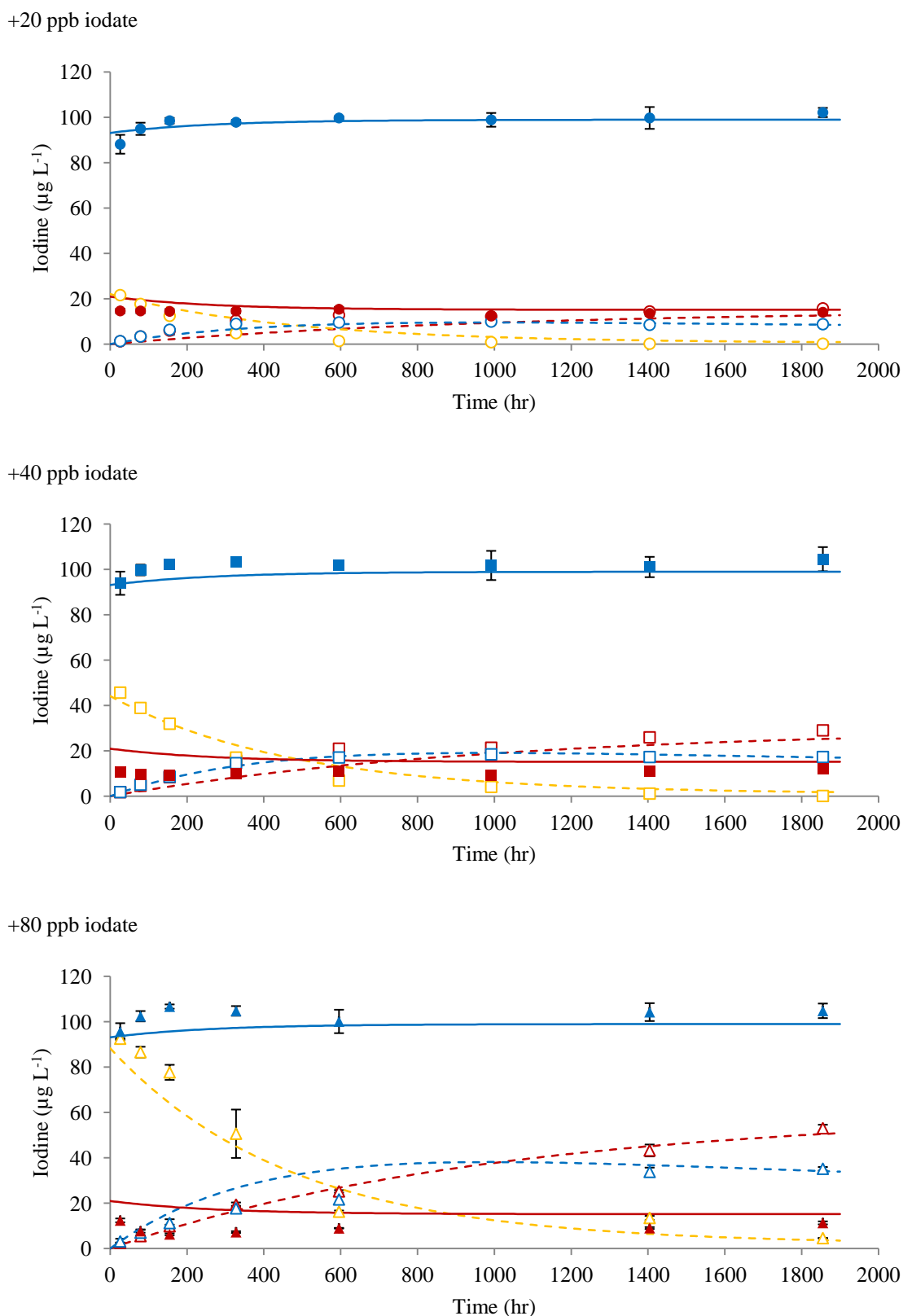
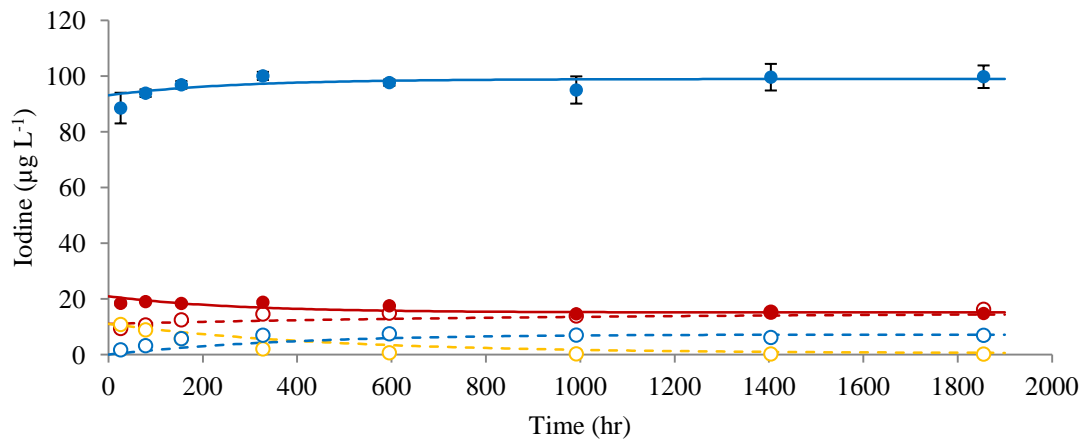
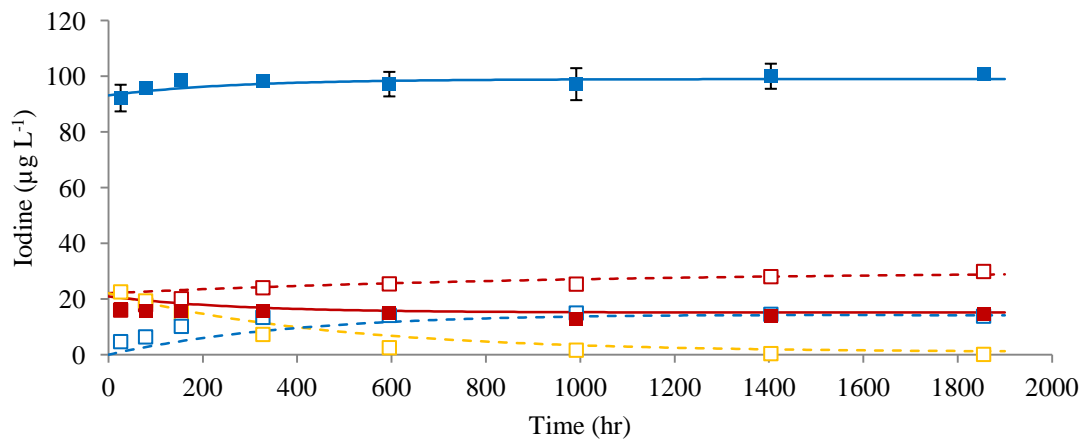


Figure 5.12. Results of Model 4 when $^{129}\text{IO}_3^-$ was added at concentrations of $22.1 \mu\text{g I L}^{-1}$ (20 ppb, circles), $44.1 \mu\text{g I L}^{-1}$ (40 ppb, squares) and $88.2 \mu\text{g I L}^{-1}$ (80 ppb, triangles); see Table 5.1. Measured data and modelled lines are shown for ^{127}I (closed symbols, solid lines) and ^{129}I (open symbols; dashed lines). Species include iodide (red symbols), iodate (yellow symbols) and OrgI (blue symbols). Error bars show coefficient of variance on measured values; where not visible they are within the symbol.

+20 ppb mixed species



+40 ppb mixed species



+80 ppb mixed species

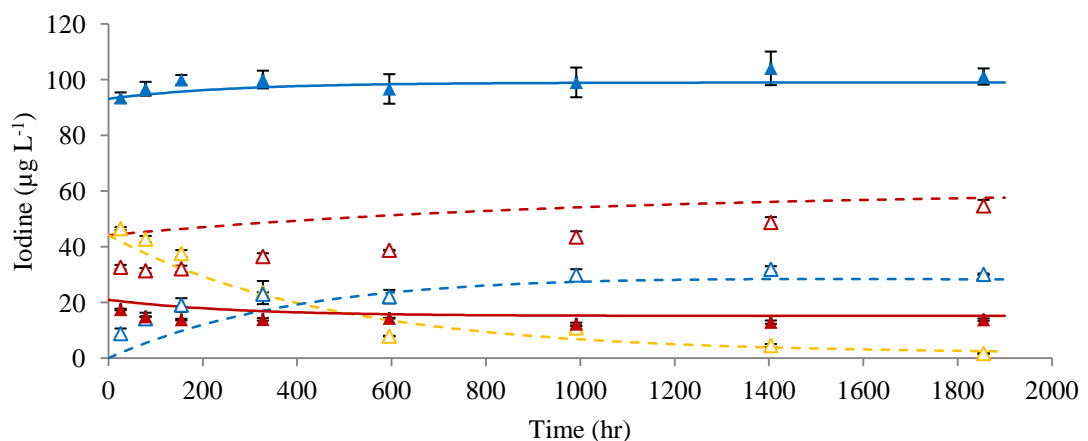
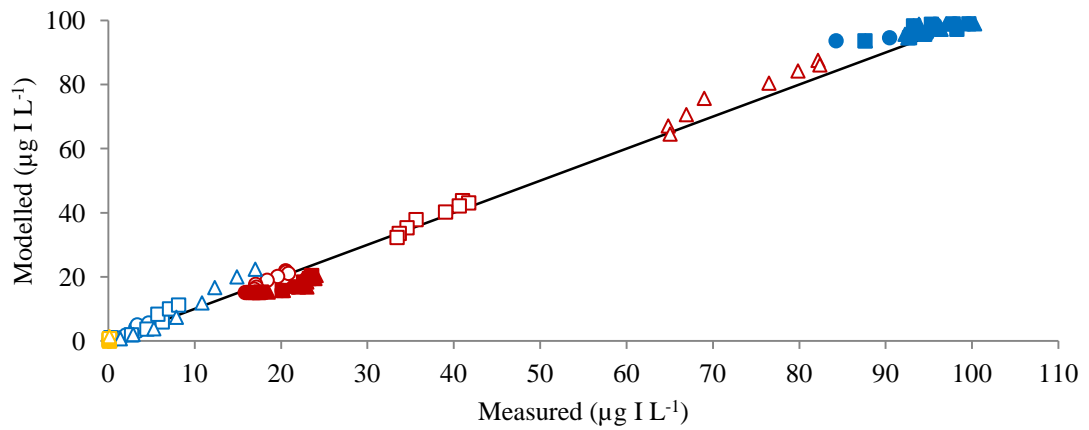
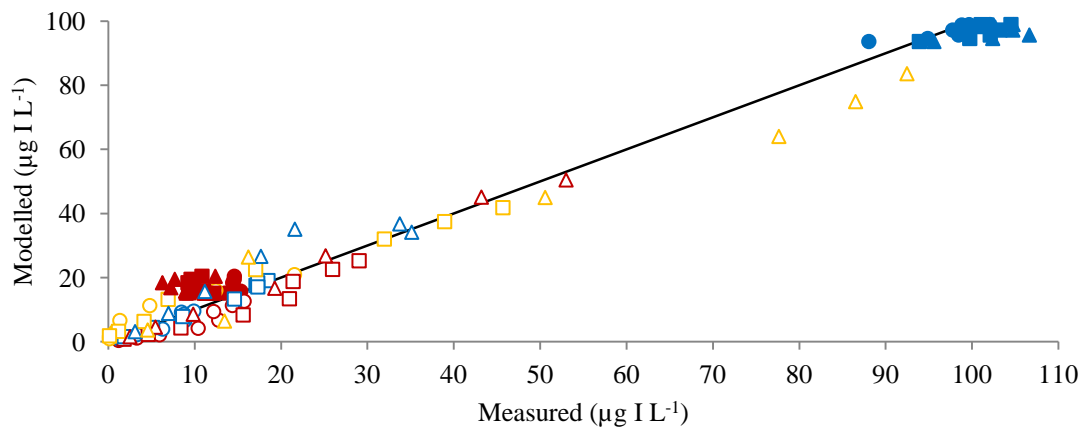


Figure 5.13. Results of Model 4 when equal concentrations of $^{129}\text{I}^-$ and $^{129}\text{IO}_3^-$ were added at total concentrations of $22.1 \mu\text{g IL}^{-1}$ (20 ppb, circles), $44.1 \mu\text{g IL}^{-1}$ (40 ppb, squares) and $88.2 \mu\text{g IL}^{-1}$ (80 ppb, triangles); see Table 5.1. Measured data and modelled lines are shown for ^{127}I (closed symbols, solid lines) and ^{129}I (open symbols; dashed lines). Species include iodide (red symbols), iodate (yellow symbols) and OrgI (blue symbols). Error bars show coefficient of variance on measured values; where not visible they are within the symbol.

Iodide added



Iodate added



Mixed species added

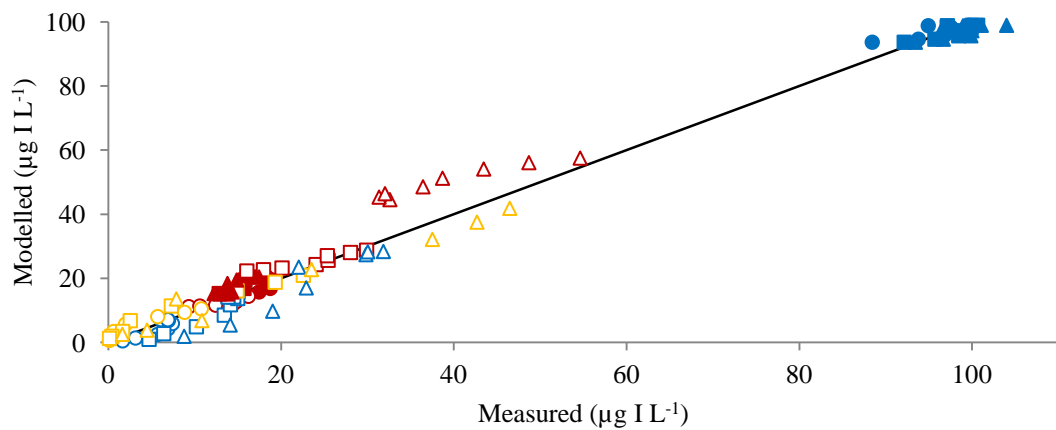


Figure 5.14. Comparison of modelled and measured concentrations of iodine when ^{129}I was added at total concentrations of $22.1 \mu\text{g I L}^{-1}$ (circles), $44.1 \mu\text{g I L}^{-1}$ (squares) and $88.2 \mu\text{g I L}^{-1}$ (triangles) as iodide, iodate and a mixed spike; see Table 5.1. Isotopes are ^{127}I (closed symbols) and ^{129}I (open symbols) measured as the species: iodide (red symbols), iodate (yellow symbols) and OrgI (blue symbols).

5.4.3 Results of modelling

Overall the model fit was very good (for all data: $r = 0.994$, $p < 0.001$), thus supporting the model structure. The best overall fit was obtained when iodide was added, and in general the worst fitting species was Org^{127}I (Figure 5.14). The increase in Org^{127}I observed at early times in all scenarios may indicate oxidation of $^{127}\text{I}^-$, although this was only reflected in $^{127}\text{I}^-$ concentrations when ≥ 40 ppb $^{129}\text{IO}_3^-$ was added and as a consequence was not well modelled. The model did not allow any direct influence of ^{129}I on ^{127}I such as would occur if a redox couple between the two isotopes existed. This may well be the reason for the poorer fit, as ^{129}I concentrations were generally better modelled than ^{127}I concentrations, despite separate fitting of the five observed isotope-specific species ($^{127}\text{I}^-$, Org^{127}I , $^{129}\text{I}^-$, $^{129}\text{IO}_3^-$ and Org^{129}I) with independent rate parameters for the two isotopes.

5.4.3.1 Unavailable iodine

The best fit was obtained when ^{127}I and ^{129}I were allowed different rate parameters to describe the equilibrium between iodide and OrgI. This suggests that different fractions of the two isotopes were involved in transformation between species and, specifically, that there is a ‘fixed’ or ‘non-labile’ fraction of Org^{127}I that is unavailable for interaction with added ^{129}I species. The final ratios of I/OrgI for the two isotopes were calculated using modelled values for long contact times. There was negligible change in modelled concentrations between 5,000 hr and 6,000 hr for all species, so it was assumed that 6,000 hr after spiking represented a pseudo-steady state. At this time, the species ratios were significantly different: $^{129}\text{I}/\text{Org}^{129}\text{I} = 0.24$ and $^{127}\text{I}/\text{Org}^{127}\text{I} = 0.17$. Therefore although equilibrium had apparently been reached, a greater proportion of ^{127}I than ^{129}I existed as OrgI, confirming the presence of a recalcitrant pool of ^{127}I . Keppler et al. (2003) and Xu et al. (2011b) suggested that HA traps iodine as it forms, then as humification continues, fewer iodine-binding sites remain available. Steric hindrance by aliphatic chains may also make some aromatic binding sites less accessible to spiked iodine, while ‘fixing’ native iodine (Xu et al., 2012). Schwehr et al. (2009) also observed that recently added iodide was less strongly sorbed than naturally present iodine, and that greater added concentrations resulted in a smaller bound proportion. This was attributed to a limited number of immediately available binding sites, and progressively stronger binding of iodine through time. It is likely that some of the native iodine in this experiment was bound

to HA during its formation and subsequent changes in HA structure have rendered some of that iodine unavailable for (isotopic) mixing. In the natural environment, chemical changes in the soil may initiate changes in the supramolecular structures within HA, potentially releasing iodine binding sites for incoming iodine to access (Sutton and Sposito, 2005).

5.4.3.2 Comparison to soil dynamics

Transformations between species in HA solutions were similar to those occurring in soil during the first 24 hr after spiking: OrgI was the dominant form, iodide was naturally present, no $^{129}\text{IO}_3^-$ was produced and no $^{127}\text{IO}_3^-$ was observed. Iodide was produced from added iodate in all cases, as observed in highly organic soils. The successful model structures for dynamics of iodine in HA and soil were similar, confirming the role of organic matter, specifically HA, in soil iodine dynamics. Despite these similarities, there were also some significant differences, which provide additional insights into the mechanisms operating under the two sets of conditions. While iodate reacted relatively quickly with both HA and soil, transformation of iodide to OrgI occurred much more slowly in HA solution than it did in soils. Also, the observed instantaneous sorption of both inorganic species to the soil solid phase was not reflected by a similar instantaneous transformation to OrgI in HA solution. It is likely that metal oxides, not present in HA, enhanced the transformations in soil.

Modelling iodine dynamics in HA solution showed that recalcitrant ^{127}I was present in HA, and is therefore likely to be the location of ‘trapped’ iodine in soils, with concentration dependent on the amount of SOC. This highlights the importance of using iodine speciation rather than total concentration to assess likely phyto-available iodine: in highly organic soils with high iodine concentrations, a large proportion is likely to be bound to HA and therefore not available for uptake to plants.

5.5 CONCLUSIONS

Iodine dynamics in humic acid solution were measured over 1855 hr (73 days) and modelled to longer timescales. This has allowed information to be gained about the similarities and differences between reactions of inorganic iodine with HA and with soil; and about interactions between species. In HA solution, the rate of ^{129}I transformation was enhanced by the presence of $^{129}\text{IO}_3^-$, suggesting a redox couple

forming between the two iodine species. This was supported by the fact that reduction of $^{129}\text{IO}_3^-$ to Org^{129}I was faster than the transformation of $^{129}\text{I}^-$ to Org^{129}I when species were spiked individually; the former reaction being enhanced by the presence of $^{127}\text{I}^-$. The model did not directly allow redox coupling between iodide and iodate of the two isotopes, although the two isotopes were described by independent rate parameters. The result of this was that the small changes in concentration of Org^{127}I and $^{127}\text{I}^-$ at early times were not well represented. Despite this, the dynamics of ^{129}I and ^{127}I were well-modelled overall, and the best agreement was obtained when iodide was added alone. Results of the model showed that some native iodine was unavailable for mixing with spiked iodine. This has implications for biofortification strategies as HA is the main pool of iodine in most soils and therefore a considerable proportion of native iodine may not be phyto-available. The best method for determining the role of soil components, including HA, in controlling the availability of iodine in soil is therefore likely to be direct measurement of uptake to plants, as described in the next chapter.

6 POT TRIAL TO MEASURE UPTAKE OF IODINE FROM NORTHERN IRELAND SOILS BY RYEGRASS

6.1 INTRODUCTION

Understanding phyto-availability of iodine in soils is vital for planning biofortification, whether the intention is to add iodine to a productive area or optimise iodine availability in productive areas. Research into iodine mobility in, and uptake from, soil has been carried out in the context of radio-iodine repositories (Xu et al., 2011a) and aerial deposition of radioactive isotopes (Hansen et al., 2011; Kashparov et al., 2005), as well as to improve understanding of how to enhance the iodine content of foodstuffs (Hong et al., 2012; Sheppard et al., 2010; Weng et al., 2009).

Iodine is not essential to plant growth (Dai et al., 2006; Whitehead, 1973c). Purely passive uptake in the transpiration stream would result in iodine uptake being directly proportional to uptake of soil solution (Dai et al., 2006). There is evidence that this does not occur, however: Whitehead (1973c) concluded that more iodine was taken up by ryegrass, timothy and clover grown hydroponically than would be expected from a purely passive uptake, and Weng et al. (2008b) found that iodine concentration in a range of vegetables increased linearly up to soil iodine concentrations of 55 mg I kg⁻¹, at which point the rate of uptake decreased. Plant species also affects iodine uptake: Whitehead (1973c) reported different iodine concentrations in the shoots of four plant types grown in hydroponic solution at four iodine concentrations (0.2 x 10⁻⁷ M, 1.0 x 10⁻⁷ M, 5.0 x 10⁻⁷ M, and 1.0 x 10⁻⁶ M), with the most marked difference at higher solution iodine concentrations. Hong et al. (2009) concluded that plants take up only a tiny portion of soil iodine, with significant differences between uptake by celery, radish, pak choi and pepper grown in iodine-spiked soil in a pot experiment. Kashparov et al. (2005) compared uptake from four types of ¹²⁵I-contaminated soil and concluded that both plant species and soil type affect iodine phyto-availability. Although comparison of both soil type and plant species would give the most comprehensive information about iodine dynamics and uptake, the size of experiment required to produce meaningful results would be very large. Therefore investigations often focus on one plant type to assess the influence of soil properties. Ryegrass has been used as an example crop to investigate iodine dynamics previously (Ashworth and Shaw, 2006a; Whitehead, 1973c; Whitehead, 1975), and is particularly important

due to its use as a fodder crop for sheep and cattle, therefore providing the link between soil and the human diets as well as being directly involved in animal health (Barry et al., 1983; Hauschild and Aumann, 1989; Smith et al., 2006).

In the 1920s, the addition of iodine to soil or directly to plants was investigated as a method of improving iodine content of plants as food (Hercus and Roberts, 1927; Orr et al., 1928), and this method is still being investigated with a range of crops, with varying success (Dai et al., 2006; Hong et al., 2009; Landini et al., 2011; Smith et al., 1999; Smoleń et al., 2011). A practice that seems particularly effective for increasing iodine intake by humans, crops and animals is to add iodine via irrigation water (Cao et al., 1994; Fordyce, 2003; Fordyce et al., 2003; Ren et al., 2008). It is now widely accepted that understanding the dynamic equilibrium between phyto-available and phyto-unavailable iodine forms is essential for optimum iodine management (Dai et al., 2006; Fordyce et al., 2003; Hong et al., 2009; Johnson, 2003b), and therefore investigation into soil iodine speciation dynamics and subsequent uptake is becoming increasingly prevalent (Sheppard and Evenden, 1988; Shetaya et al., 2012; Whitehead, 1975; Xu et al., 2011a; Xu et al., 2011b). Results are frequently inconclusive, often based on studies that use too few soil types to be able to quantify soil effects (Hong et al., 2012; Kashparov et al., 2005).

In this experiment, perennial ryegrass was grown from seed under controlled conditions for 15 weeks. It was grown on nineteen soils from across eastern NI, which were spiked with $^{129}\text{IO}_3^-$ immediately prior to seeding. Growing conditions used were intended to be representative of NI in the summer; soil moisture content was maintained at just below field capacity with almost-daily watering. Total iodine concentrations measured in soil and vegetation from NI, and subsequent experiments into iodine dynamics, have provided information about how soil properties affect retention and transformations of iodine in soil (Chapters 3 – 5). By linking iodine uptake to soil properties, this chapter quantifies the effect of soil chemistry on the availability of iodine to plants.

6.1.1 Aims

The aims of the work presented in this chapter were:

- to grow ryegrass as a typical component of animal pasture in NI and monitor how iodine uptake changes with grass yield and soil properties;
- to monitor the uptake of spiked iodine (^{129}I) and iodine in irrigation water (^{127}I), as a simulation of iodine deposition from rainfall;
- to see how proportions of spiked and native iodine in grass changed with time, as time-dependent sorption of ^{129}I -spike to solid soil progressed;
- to quantify the uptake of iodine using soil properties by developing a predictive model.

6.2 MATERIALS AND METHODS

6.2.1 Pot trial structure

Twenty soils were sampled from across eastern NI and processed as described in Section 2.2. Of these, nineteen (excluding NI16, which had a very high organic matter content) were suitable for a pot trial. For each soil the following process was carried out: a volume of moist soil equivalent to three pots full was mixed, using a domestic food mixer, with KNO_3 and $^{129}\text{IO}_3^-$ in solution at rates equivalent to $0.78 \text{ kg N ha}^{-1}$ and 64.1 g I ha^{-1} . The amounts of fertiliser and iodine spike were determined on the basis of the surface area of the pots used (8 cm x 8 cm, black plastic). The exact weight of moist soil depended on soil density; it was c. 900 g for most soils. The soil was then split equally between three replicate pots with filter papers in the base, onto each of which 1 g of perennial ryegrass (*Lolium perenne* L.) seeds were sprinkled.

6.2.1.1 Growing conditions and maintenance

Grass was grown for 15 weeks after set-up under conditions representing those in June in NI: sunrise started at 04.45, with full light intensity 2 hr later; sunset started at 19.45, with full darkness 2 hr later; average temperatures were 17°C in the daytime and 9°C at night; average daytime light level was c. $250 \mu\text{mol s}^{-1} \text{ m}^{-2}$. Temperatures were calculated as averages for June across NI and sunrise and sunset times for mid-June in Belfast were used. Soil was fertilised with KNO_3 in water at a rate equivalent to 50 kg N ha^{-1} on days 31, 45, 67 and 90 after setting up the potted soils. Soil moisture content was maintained by adding deionised water to the soil surface,

avoiding grass leaves where possible, every 1 – 3 days, minimising drainage from the pot. The deionised water was found to contain $0.8 \mu\text{g I L}^{-1}$. For 12 days during cut 4 growing time, the volume of water added to each pot was recorded, to give an estimated daily water input per pot.

6.2.1.2 Grass harvesting

Using clean stainless steel scissors, grass was cut to approximately 1 cm length on days 29 (28 days of growth), 44 (15 days of growth), 67 (23 days of growth) and 104 (37 days of growth), and transferred to brown paper bags. Samples were dried immediately at $30 \text{ }^\circ\text{C}$ for 3 days before being chopped into small pieces using scissors and stored in zip-lock plastic bags. Yields of dry material were recorded for each sample.

6.2.2 Grass and soil analysis

After the final harvest, deionised water was added to all pots to make soils wet but not draining and this was maintained for 3 days. A portion of the soil was then centrifuged at 10,000 rpm for 20 mins using a Beckman Avanti centrifuge and custom-made centrifuge tubes with a separate section to collect filtered drainage solution (Di Bonito, 2005) to separate soil solution from solid soil. Soil solution was filtered to $\leq 0.45 \mu\text{m}$ using Millex syringe filters and refrigerated at $4 \text{ }^\circ\text{C}$ until analysis two days later. Remaining soil and grass roots/shoots were left in the pot to air dry under growing conditions. Vegetation was then separated from soil by hand and soil was broken down as much as possible. The soil was extracted to determine total iodine content using TMAH according to Section 2.4.5 with one amendment: 20 ml rather than 5 ml water was added before centrifuging. The moisture content of air dried soil was measured and total iodine concentrations were corrected to an oven dry basis ($105 \text{ }^\circ\text{C}$ for 3 days).

All chopped grass samples were extracted in TMAH to determine total iodine concentration according to Section 2.4.5 with the following amendments: 20 ml rather than 5 ml water was added after heating and samples were filtered to $0.22 \mu\text{m}$ directly into ICP tubes for analysis, rather than being centrifuged. Where samples size was too small to allow 0.25 g samples, 0.1 g was weighed, and TMAH and water volumes adjusted appropriately to give the same solid:liquid ratio. Samples were not milled as

there was insufficient material in some cases. Extraction efficiency of chopped grass compared to milled grass was confirmed using test samples before analysis.

6.2.2.1 Total iodine analysis

Total iodine concentrations (^{127}I and ^{129}I) in soil and grass extracts, and soil solution, were measured according to Section 2.6.2.1. Some ^{127}I concentrations measured in soil TMAH extracts caused the ICP-MS detector to trip to analogue mode, so the internal detector cross-calibration was implemented and samples quantified against high concentration standards. The accuracy of these values may be slightly lower than for pulse-counted values, but it was considered unwise to dilute the solutions, due to the very low ^{129}I concentrations present. Limits of detection were $0.047 \mu\text{g I L}^{-1}$ for ^{127}I and $0.014 \mu\text{g I L}^{-1}$ for ^{129}I .

6.2.2.2 Iodine speciation

Iodine speciation in soil solution (iodide, iodate and OrgI for both ^{127}I and ^{129}I) was measured by SEC – ICP-MS according to Section 2.6.2.2. Limits of detection were $0.25 \mu\text{g I L}^{-1}$ for both isotopes.

6.2.2.3 Dissolved organic carbon (DOC)

DOC in soil solution was measured according to Section 2.4.3.

6.3 RESULTS AND DISCUSSION

6.3.1 Total iodine in soil and grass

All ^{127}I concentration values were above the LOD. Concentrations of ^{129}I were generally above LOD, with the exception of grass cuts 2 – 4 from NI13 and NI20, cuts 2 and 3 from NI14, and cut 4 from the NI07 soil. These values are discussed as measured throughout the chapter. There was generally good agreement between post-harvest and previously measured (Section 3.3) concentrations of ^{127}I in soil ($^{127}\text{I}_\text{S}$), and between added and measured concentrations of ^{129}I in soil ($^{129}\text{I}_\text{S}$) (Table 6.1). In Chapter 3, I_V (mg I kg^{-1}) represented iodine content of the vegetation growing at each site. In this chapter, iodine content in ryegrass I_G (mg I kg^{-1}) is used as vegetation did not vary between soils. Concentrations of $^{127}\text{I}_\text{G}$ (excluding NI05 and NI08) ranged between 0.0741 and $0.774 \text{ mg I kg}^{-1}$ (median $0.189 \text{ mg I kg}^{-1}$; Figure 6.1 and Table 6.2) which represented $4.66 \times 10^{-4} \%$ - 2.51% (median 0.347%) of the ^{127}I content of

the soil ($^{127}\text{I}_\text{S}$), based on concentrations and masses of grass and soil. Concentrations of ^{127}I in NI05 and NI08 grass were higher than those in other samples (1.22 – 4.23 mg I kg⁻¹ and 0.274 – 2.90 mg I kg⁻¹ respectively) but were within the same range of uptake as a proportion of soil iodine content. Concentrations of $^{129}\text{I}_\text{G}$ were 0.00 – 1.20 x 10⁻² mg I kg⁻¹ (median 1.57 x 10⁻³ mg I kg⁻¹), with exceptions NI10: 1.52 x 10⁻³ – 1.73 x 10⁻² mg I kg⁻¹ and NI17: 1.13 x 10⁻³ – 2.40 x 10⁻² mg I kg⁻¹ (Figure 6.2 and Table 6.2). As a percentage of $^{129}\text{I}_\text{S}$, uptake was very low in all cases, at 0.0003 % - 4.53 % (median 0.276 %). None of the measured $^{127}\text{I}_\text{G}$ concentrations were large enough to reduce the post-harvest $^{127}\text{I}_\text{S}$ concentrations compared to measurements made before the start of the experiment (Table 6.1). Post harvest recovery of ^{129}I from the soil ranged from 77 % (NI10) to 100 % (NI08), excluding one soil (NI04, 51%) where analytical error was suspected. The median value for % recovery of ^{129}I in the soil was 88 %. This confirms that there is strong retention of both iodide and iodate by soil with limited uptake by grass or loss by leaching or volatilization.

Table 6.1. Total soil iodine content: mean and standard error of three replicates.

Soil	¹²⁷ I _s post-harvest (mg I kg ⁻¹)		¹²⁷ I _s (Chapter 3) (mg I kg ⁻¹)		¹²⁹ I _s post-harvest (mg I kg ⁻¹)		Added ¹²⁹ I (mg I kg ⁻¹)
	Mean	S. E.	Mean	S. E.	Mean	S. E.	Mean
NI01	2.69	0.0573	2.89	0.0153	0.137	0.00372	0.153
NI02	4.49	0.0494	4.29	0.0204	0.117	0.00622	0.135
NI03	26.8	2.33	20.8	0.218	0.457	0.0355	0.518
NI04	9.32	0.358	9.29	0.138	0.120	0.0145	0.236
NI05	297	2.78	274	14.9	0.111	0.00254	0.119
NI06	9.79	0.411	9.38	0.254	0.110	0.00381	0.126
NI07	14.7	0.475	14.0	0.360	0.0974	0.00462	0.120
NI08	141	5.76	127	2.63	0.144	0.00764	0.144
NI09	38.8	1.80	32.0	0.776	0.524	0.0329	0.620
NI10	18.6	0.865	16.6	0.335	0.868	0.0362	1.13
NI11	11.4	0.482	10.0	0.220	0.190	0.0176	0.208
NI12	4.09	0.0982	4.15	0.127	0.139	0.00408	0.157
NI13	8.24	0.187	7.46	0.292	0.172	0.00389	0.203
NI14	5.58	0.294	5.16	0.145	0.162	0.0106	0.181
NI15	31.6	0.704	27.4	0.455	0.262	0.00880	0.290
NI17	15.6	0.571	13.2	0.460	0.701	0.0328	0.862
NI18	10.8	0.183	9.64	0.272	0.190	0.00236	0.211
NI19	12.5	0.395	11.1	0.478	0.183	0.00322	0.208
NI20	12.2	0.696	9.60	0.290	0.423	0.0347	0.469

Table 6.2. Total ^{127}I and ^{129}I measured in grass harvested during experiment. Mean and standard error of three replicates. Values below LOD are underlined.

Soil	$^{127}\text{I}_G$ ($\mu\text{g I kg}^{-1}$)								$^{129}\text{I}_G$ ($\mu\text{g I kg}^{-1}$)							
	Cut 1		Cut 2		Cut 3		Cut 4		Cut 1		Cut 2		Cut 3		Cut 4	
	Mean	S. E.	Mean	S. E.	Mean	S. E.	Mean	S. E.	Mean	S. E.	Mean	S. E.	Mean	S. E.	Mean	S. E.
NI01	198	26.0	120	7.00	187	7.29	345	7.26	3.16	0.282	1.49	0.0501	1.25	0.268	1.26	0.207
NI02	161	10.8	128	6.44	195	3.57	359	12.0	3.55	0.445	1.93	0.193	1.56	0.114	1.84	0.328
NI03	154	9.34	137	15.4	336	86.9	424	29.2	1.03	0.431	0.721	0.0508	1.89	1.20	1.26	0.166
NI04	193	15.2	133	8.81	199	3.12	471	31.3	2.00	0.161	1.07	0.0736	0.701	0.108	2.95	0.692
NI05	3120	574	1390	167	1600	94.6	1680	146	7.02	0.977	3.33	0.581	3.22	0.517	2.76	0.437
NI06	182	13.6	175	19.2	255	16.2	452	44.0	4.17	0.552	2.35	0.177	1.87	0.267	2.53	0.347
NI07	140	4.05	106	9.60	167	7.19	291	18.4	1.44	0.257	0.827	0.223	0.568	0.222	<u>0.285</u>	0.110
NI08	913	479	347	37.9	543	75.9	1680	615	2.71	0.505	1.63	0.183	1.53	0.172	5.86	2.98
NI09	230	88.3	202	90.7	291	14.6	528	53.5	0.672	0.206	0.695	0.465	0.852	0.585	2.02	0.293
NI10	204	30.7	163	29.7	288	15.0	627	78.9	4.00	1.50	2.16	0.383	4.33	1.03	12.9	2.23
NI11	203	17.9	124	11.1	158	4.47	306	22.5	3.29	0.359	1.79	0.407	1.53	0.0814	1.23	0.299
NI12	174	26.0	125	9.14	206	19.9	381	46.0	2.95	0.557	2.52	0.794	1.69	0.472	1.77	0.159
NI13	136	15.3	92.7	11.6	153	10.3	297	37.1	1.17	0.229	<u>0.457</u>	0.0945	<u>0.215</u>	0.102	<u>0.432</u>	0.258
NI14	146	19.7	123	2.14	178	10.1	346	31.0	1.38	0.331	<u>0.471</u>	0.0812	<u>0.460</u>	0.0959	0.695	0.367
NI15	212	26.8	191	37.2	227	49.4	329	60.1	1.95	0.264	1.25	0.238	0.722	0.214	1.67	0.640
NI17	169	75.6	121	11.7	307	23.6	592	90.5	4.76	2.27	1.66	0.243	8.27	4.29	15.1	4.26
NI18	193	40.3	149	25.6	204	5.84	384	16.3	2.03	0.531	1.02	0.232	0.621	0.193	0.952	0.138
NI19	173	22.1	118	11.1	195	9.26	406	37.7	2.70	0.691	1.29	0.337	1.55	0.0798	1.35	0.160
NI20	176	9.96	118	3.60	195	7.03	327	11.0	1.27	0.154	<u>0.215</u>	0.0389	<u>0.285</u>	0.110	<u>0.401</u>	0.114

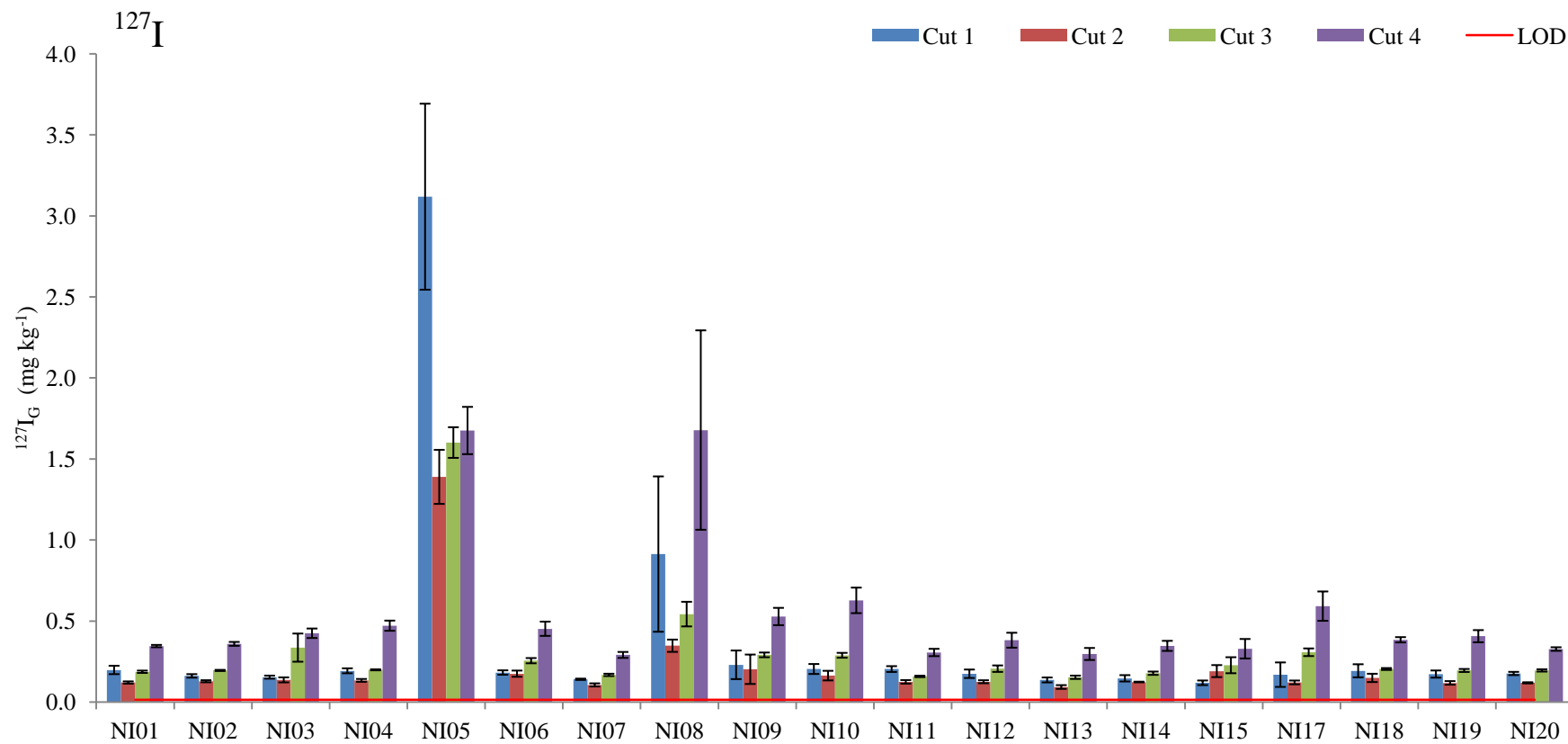


Figure 6.1. Concentrations of $^{127}\text{I}_G$ for each ryegrass cut; the LOD ($0.0139 \text{ mg I kg}^{-1}$) is shown by a red line. Error bars represent the standard error of triplicate pots for each soil.

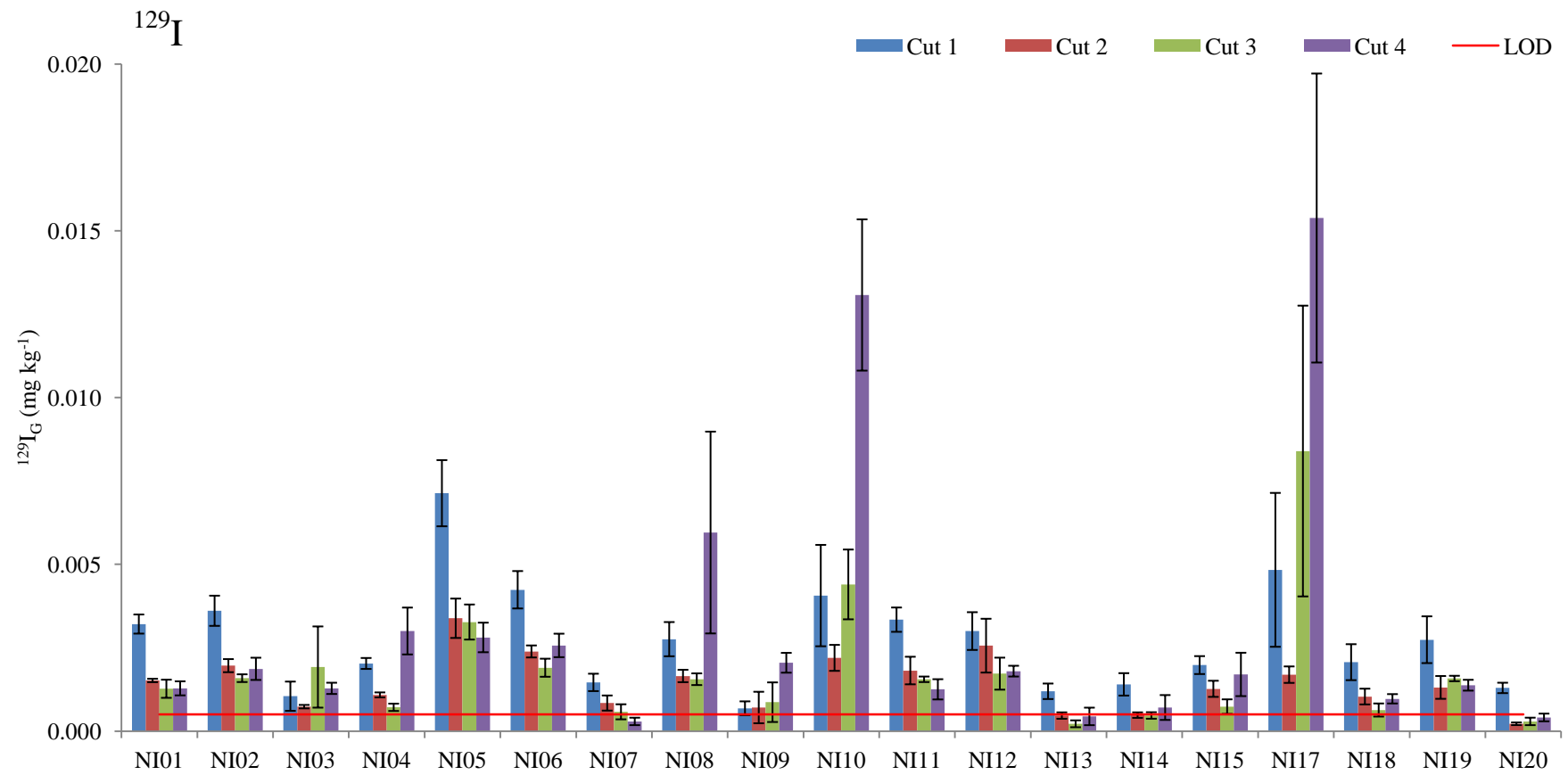


Figure 6.2. Concentrations of $^{129}\text{I}_G$ for each ryegrass cut; the LOD ($0.0005 \text{ mg I kg}^{-1}$) is shown by a red line. Error bars represent the standard error of triplicate pots for each soil.

Although off-take of iodine by grass did not reduce $^{127}\text{I}_\text{S}$ values, there was a significant positive correlation between $^{127}\text{I}_\text{G}$ and $^{127}\text{I}_\text{S}$ (Pearson correlation coefficient $r = 0.818$, $p < 0.001$), confirming the importance of soil in supplying iodine to vegetation (Figure 6.3). This correlation was dominated by soils NI05 and NI08 (which had $\text{I}_\text{S} > 100 \text{ mg I kg}^{-1}$), but, although it was much weaker, the same trend was apparent when these were excluded ($r = 0.158$; $p = 0.024$). In addition to the correlation between $^{127}\text{I}_\text{G}$ and $^{127}\text{I}_\text{S}$, $^{127}\text{I}_\text{G}$ reflected the length of time for which grass was grown: cut 4 had the longest growth time and greatest concentrations of $^{127}\text{I}_\text{G}$, while the shortest growth time (cut 2) resulted in the smallest value of $^{127}\text{I}_\text{G}$ (Figure 6.1 and Figure 6.3). This is discussed further in Section 6.3.8.

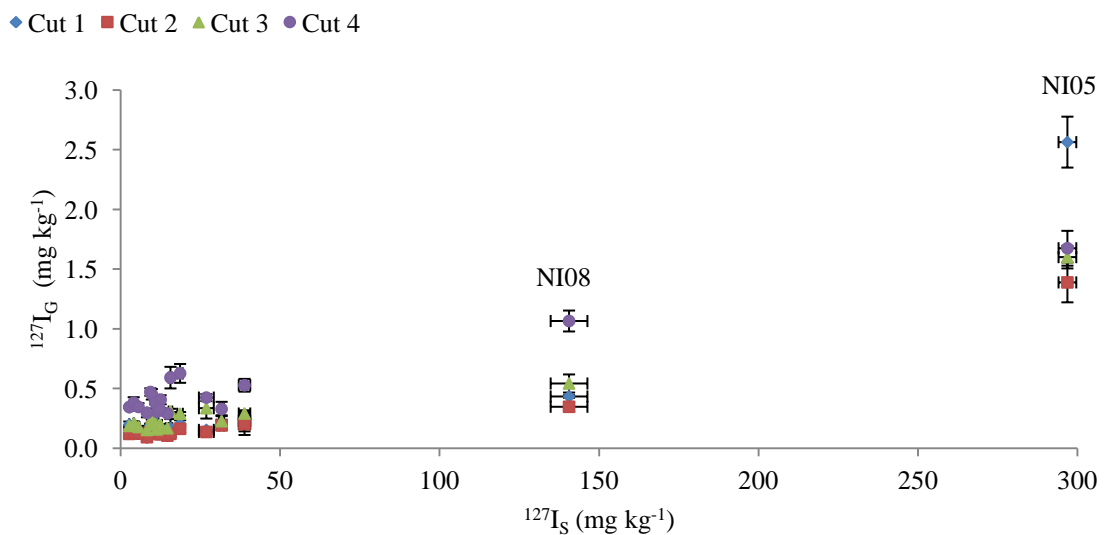


Figure 6.3. Relationship between ^{127}I iodine in grass ($^{127}\text{I}_\text{G}$) and in soil ($^{127}\text{I}_\text{S}$). Error bars show standard error of three replicates for each soil and each cut.

For ^{129}I , the correlation was very much less clear (Figure 6.4) and changed depending on whether soils NI10 and NI17 (with SOC $> 50\%$) were included: for all samples $r = 0.350$, $p < 0.001$; with NI10 and NI17 excluded $r = -0.284$, $p < 0.001$. Although the same ^{129}I spike was added to all soils, those with larger SOC contents had a greater gravimetric concentration of ^{129}I due to their lower dry bulk densities. Soils with large SOC contents may also be expected to sorb the ^{129}I more quickly. Thus, the overall trend in uptake with ^{129}I concentration is likely to be complicated by these two contradictory factors.

The dependence of vegetation iodine on soil iodine has been discussed previously (Chapter 3). Results from this experiment show that although a positive correlation existed between ^{127}I concentrations in soil and grass, the relationship for freshly-added iodine (^{129}I) was more complicated, and appeared to be more dependent on soil properties influencing sorption and phyto-availability. This relationship is further investigated in Section 6.4.

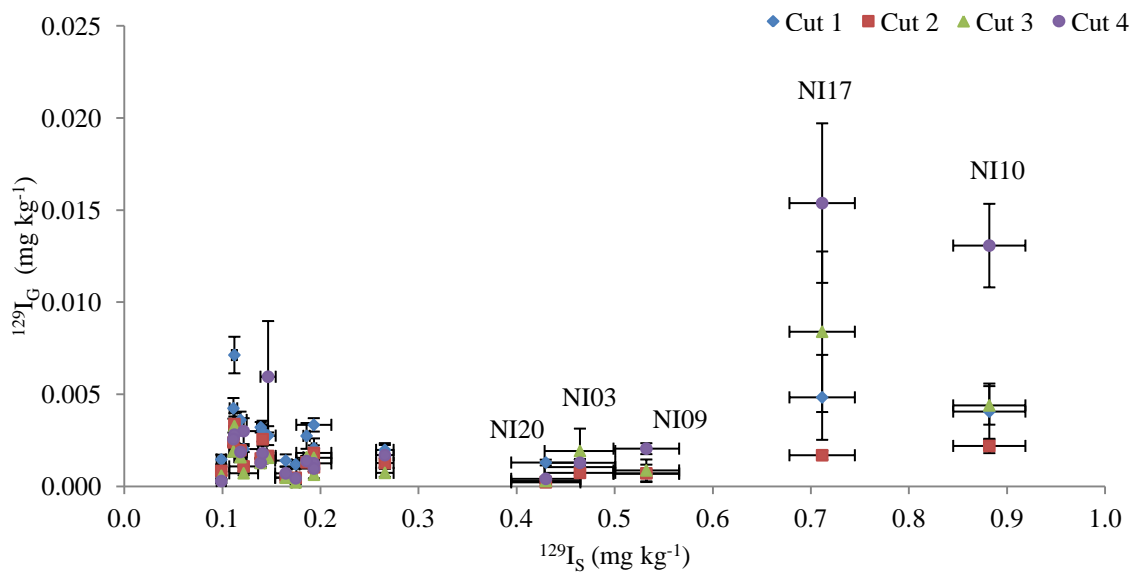


Figure 6.4. Relationship between ^{129}I in grass ($^{129}\text{I}_G$) and soil ($^{129}\text{I}_S$). Error bars show standard error of three replicates for each soil and each cut.

6.3.2 Effect of yield on iodine concentration

Grass yields varied more between soils than they did between cuts of the same soil (Figure 6.5). The median yield across all soils and grass harvests was 0.593 g, within a range of 0.257 – 1.36 g per pot, except NI10 (0.140 – 0.231 g) and NI17 (0.133 – 0.273 g). Soils NI10 and NI17 did not support healthy grass growth in the field (Appendix 1) so it is not surprising that yields from these soils were lower than for most soils. There was a significant negative correlation between grass yield and iodine concentration for both isotopes, although for ^{127}I this relied upon excluding NI05 and NI08. For yield vs $^{129}\text{I}_G$, with all samples, $r = -0.360$ ($p < 0.001$); for yield vs $^{127}\text{I}_G$, with all samples, $r = -0.079$ ($p = 0.236$); for yield vs $^{127}\text{I}_G$, with NI05 and NI08 excluded, $r = -0.268$ ($p < 0.001$).

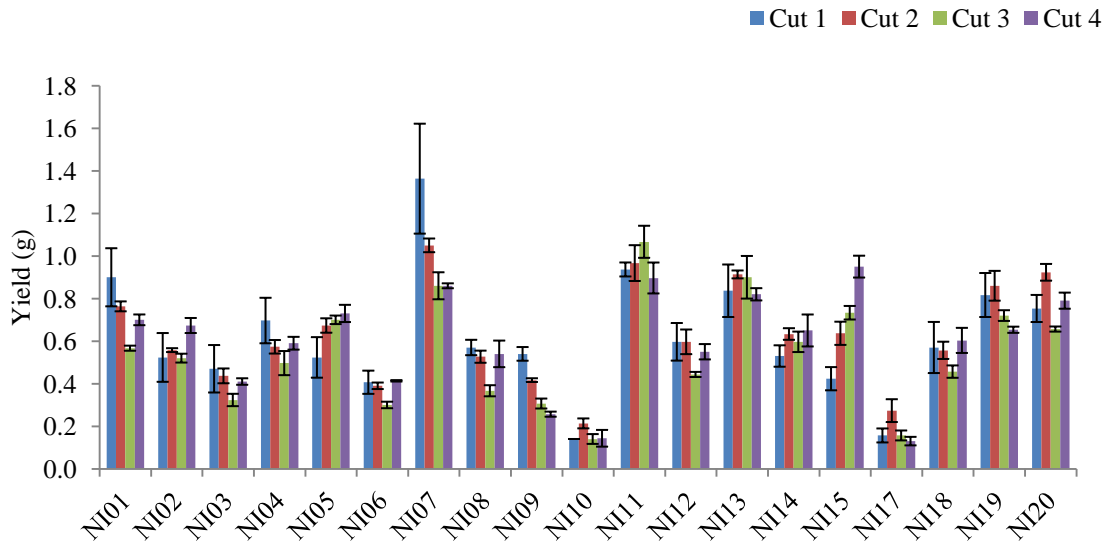


Figure 6.5. Grass yield for each soil and each cut. Error bars show standard error of triplicate pots.

The cuts were timed to allow sufficient grass yield (for analysis) on all soils, rather than being at constant intervals, but there was no correlation between yield and growth time (t_G) ($r = -0.010$, $p = 0.878$), due to the variation in yield between soils. The influence of t_G on iodine concentration in grass was evident for $^{127}\text{I}_G$ (Figure 6.1), where for each soil, $^{127}\text{I}_G$ followed the pattern cut 2 < cut 3 \approx cut 1 < cut 4, reflecting the number of days growth for each cut. A similar effect was not observed for $^{129}\text{I}_G$, however, possibly highlighting the importance of continuing soil sorption during the course of the pot trial in determining availability of this isotope.

To account for the variation in t_G and clarify the role of yield in determining $^{127}\text{I}_G$ and $^{129}\text{I}_G$, growth rate (GR) was calculated:

$$\text{GR} = \left(\frac{Y}{t_G} \right) \quad (6.1)$$

Where GR = growth rate (g day^{-1}); Y = yield (g); and t_G = growth time (days). This was calculated for each soil, for each cut, in triplicate, and a linear correlation calculated with the corresponding values of $^{127}\text{I}_G$ and $^{129}\text{I}_G$. Figure 6.6 shows GR vs $^{127}\text{I}_G$, $r = -0.184$, $p = 0.005$; Figure 6.7 shows GR vs $^{129}\text{I}_G$, $r = -0.346$, $p < 0.001$, although the correlation appears less linear when $\text{GR} < 0.01$. This confirms that the apparent negative correlation between yield and grass iodine concentration is a result of growth rate, rather than just yield. Immediately available iodine is in soil solution

and is replenished from iodine sorbed to the solid phase (Dai et al., 2009; Landini et al., 2011; Shetaya et al., 2012) (Chapter 4). Therefore the rates of plant growth, and removal of iodine from the soil solution, may exceed the rate at which it can be replenished, resulting in lower overall concentration at greater growth rates. If replenishment of the phyto-available pool was independent of soil type, a single trend would be expected in Figure 6.6 and Figure 6.7. This was not observed, and confirms the dependence on soil properties of desorption of iodine into solution.

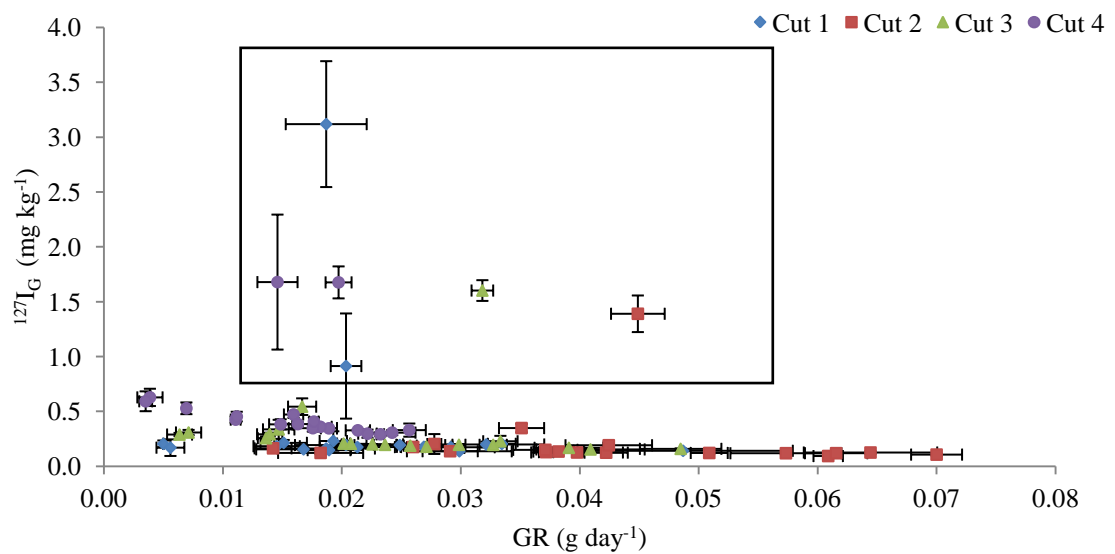


Figure 6.6. Relationship between ^{127}I in grass ($^{127}\text{I}_G$) and growth rate (GR). Samples in box are from NI05 (cuts 1 – 4) and NI08 (cuts 1 and 4). Error bars show standard error of triplicate measurements.

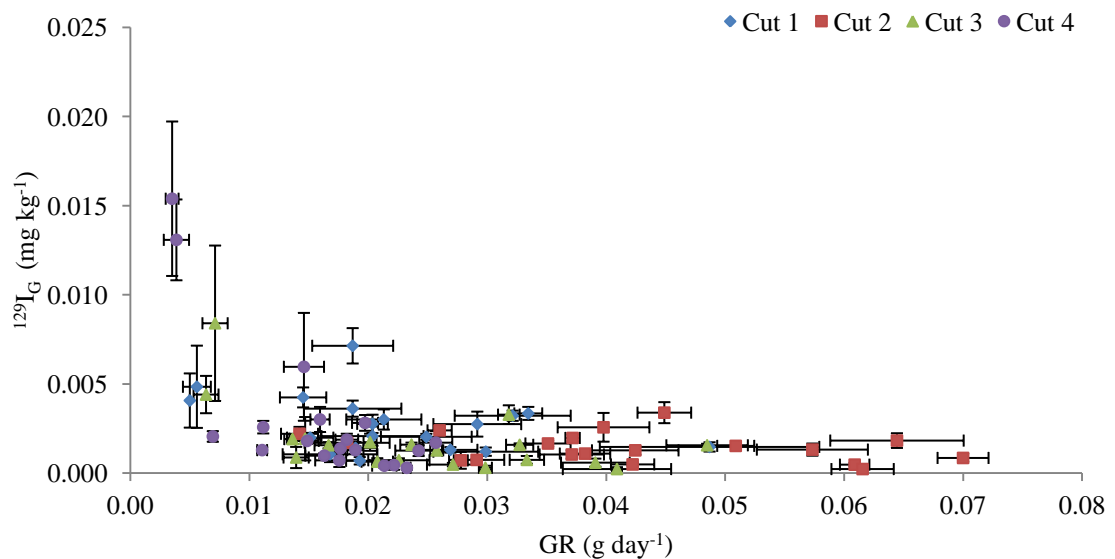


Figure 6.7. Relationship between ^{129}I in grass ($^{129}\text{I}_G$) and growth rate (GR). Error bars show standard error of triplicate measurements.

6.3.3 Spike / non-spike ratios in grass and soil

To further understand the influence of soil on iodine uptake, it is useful to consider the ratio of $^{129}\text{I}_G$ to $^{127}\text{I}_G$ as an index of relative availability. This is particularly important in this experiment because all soils contained different gravimetric concentrations of both ^{127}I and ^{129}I . Therefore the ‘grass/soil ratio’ was expressed as an index ($I_{G/S}$; Eqn. 6.2):

$$I_{G/S} = \left(\frac{\frac{^{129}\text{I}_G}{^{127}\text{I}_G}}{\frac{^{129}\text{I}_S}{^{127}\text{I}_S}} \right) \quad (6.2)$$

where $I_{G/S}$ is the ratio of ^{129}I to ^{127}I in the grass divided by the equivalent ratio in the soil, and I_G and I_S represent iodine concentrations (mg I kg^{-1}) in grass and soil respectively (Figure 6.8). It was expected that the ^{129}I would be initially more available than the ^{127}I , resulting in values of $I_{G/S} > 1$ which subsequently decreased towards 1 with progressive mixing between the two isotopes. Most soils did show a relative reduction in ^{129}I availability over the four harvests, indicating that throughout the experiment there was progressive mixing between ^{129}I and ^{127}I in the soil. In soils 13, 14, 18 and 20, the initial decrease in ^{129}I phyto-availability slowed markedly towards the end of the experiment. In their study of uptake of freshly added ^{125}I in field trials, Kashparov et al. (2005) noticed a rapid decrease in phyto-availability of iodine to various plants up to 30 – 50 days, with little further change. This is a similar time period to cut 2 – 3 in this experiment, but although the apparent fixation was described by Kashparov et al. (2005) using an exponential equation, the link to soil properties was not explored. Soils 13, 14, 18 and 20 contained relatively high concentrations of aluminium and iron oxides compared to most other soils (Section 3.3); these constituents certainly adsorb iodate in soils (Shetaya et al., 2012) but according to Whitehead (1975), did not significantly affect uptake of added iodate by ryegrass. For three soils (9, 10 and 17), there was an approximately constant value of $I_{G/S}$, observed across all 4 cuts. These soils all had SOC contents $> 38\%$ which may have caused faster sorption of iodate (Shetaya et al., 2012) resulting in a pseudo-steady state even before cut 1. Adding organic matter to soil has been shown to

reduce uptake of recently added iodine (as KI, KIO₃ and I₂) by ryegrass from sandy loam (Whitehead, 1975).

While the changes in value of $I_{G/S}$ with time broadly support the gradual transformation of ¹²⁹I into phyto-unavailable forms, absolute values give additional information about the source of phyto-available iodine. In soils 05 and 08, $I_{G/S} > 1$ for all cuts, as expected, so ¹²⁹I was more phyto-available than ¹²⁷I. However, in soils 06, 07, 08, 15 and 19, the first one or two cuts had $I_{G/S} > 1$ but values fell below 1.0 thereafter (Figure 6.8) and for most soils $I_{G/S}$ was < 1 even for cut 1. From this information alone it would have to be concluded that, for most soils, the added ¹²⁹I was apparently less phyto-available than ¹²⁷I, which is clearly contrary to expectations. This anomaly can only be accounted for by including the (deionised) irrigation water as an additional source of ¹²⁷I. Since this was added every one to three days directly to the phyto-available pool, it would have been more continuously available than ¹²⁹I, which was progressively transformed to unavailable forms following addition at the start of the experiment. The contribution of irrigation water is investigated in the following section; modelling uptake of the two isotopes is pursued further in Section 6.4.

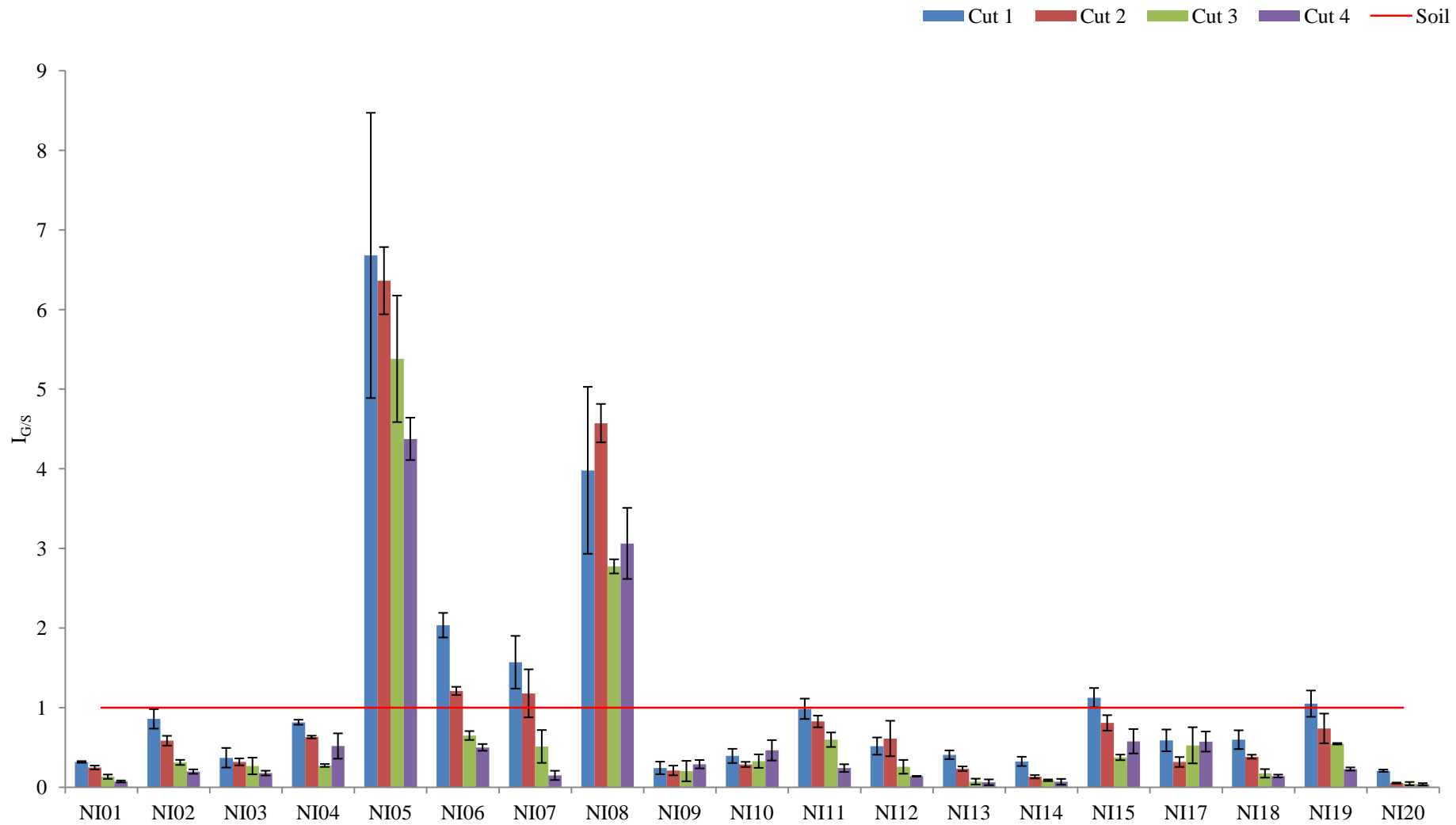


Figure 6.8. Grass/soil ratio for each cut: $I_{G/S} = (^{129}I_G / ^{127}I_G) / (^{129}I_S / ^{127}I_S)$. Error bars represent standard error of three replicates for each cut and soil.

6.3.4 Contribution of irrigation water to phyto-available iodine

It is possible to estimate the proportion of iodine in grass originating from irrigation water by assuming initially perfect mixing between added ^{129}I -labelled iodate ($^{129}\text{I}_\text{S}$) and native soil iodine ($^{127}\text{I}_\text{S}$), i.e. ignoring any time-dependent changes in phyto-availability of added ^{129}I . The added ^{129}I is then simply a label for the soil iodine and permits discrimination between ^{127}I in the irrigation water and soil-derived iodine (also ^{127}I). Considering the preceding discussion of ^{129}I dynamics observed, this criterion was not fully met in practice, and immediate perfect mixing of the added ^{129}I almost certainly did not occur. Nevertheless, it is useful to follow the calculation of plant iodine derived from irrigation water through the four cuts of grass; as the ^{129}I assimilates more fully with the native soil iodine so the validity of the calculation increases. Thus it can be assumed that:

$$\frac{^{127}\text{I}_{\text{G(S)}}}{^{127}\text{I}_{\text{S}}} = \frac{^{129}\text{I}_{\text{G(S)}}}{^{129}\text{I}_{\text{S}}} \quad (6.3)$$

By mass balance,

$$^{127}\text{I}_{\text{G(T)}} = ^{127}\text{I}_{\text{G(S)}} + ^{127}\text{I}_{\text{G(Ir)}} \quad (6.4)$$

where I_G and I_S indicate iodine measured in grass and soil respectively (mg I kg^{-1}), with the source in brackets (T = total, S = soil, Ir = irrigation). Then by rearranging Eqn. 6.3 to define $^{127}\text{I}_{\text{G(S)}}$ and substituting into Eqn. 6.4 after rearrangement, the concentration of iodine in irrigation water can be calculated from Eqn. 6.5. In Eqn. 6.5 the result of non-perfect mixing occurring, against the assumption made, is that $^{127}\text{I}_{\text{G(Ir)}}$ would be underestimated.

$$^{127}\text{I}_{\text{G(Ir)}} = ^{127}\text{I}_{\text{G(T)}} - \left(^{127}\text{I}_{\text{S}} \times \frac{^{129}\text{I}_{\text{G(S)}}}{^{129}\text{I}_{\text{S}}} \right) \quad (6.5)$$

Having obtained $^{127}\text{I}_{\text{G(Ir)}}$ (mg I kg^{-1}), this was converted to a percentage of total iodine in grass (mg I kg^{-1}), $\text{I}_{\text{G(Ir,E)}}$ (estimated percentage of iodine in grass from irrigation water) (Table 6.3) and expressed as a mean value (across all soils) for each cut (Figure 6.9). Some values of $^{127}\text{I}_{\text{G(Ir)}}$ and $\text{I}_{\text{G(Ir,E)}}$ were negative. This occurred when $\text{I}_{\text{G/S}} > 1.0$, indicating greater availability of ^{129}I over ^{127}I , which then resulted in a gross overestimation of ^{127}I uptake from soil sources. These values are specified as ‘neg’ in Table 6.3; their actual value is meaningless as the premise of complete mixing of added ^{129}I with soil iodine is clearly invalid in such cases.

Table 6.3. Estimated contribution of grass iodine from irrigation water, as a concentration ($^{127}\text{I}_{\text{G(Ir)}}$, mg I kg⁻¹), and as a percentage of total iodine in grass ($\text{I}_{\text{G(Ir,E)}}$, %). ‘Neg’ indicates that a negative value was calculated and so the calculation of $\text{I}_{\text{G(Ir,E)}}$ is invalid.

Soil	Cut 1				Cut 2				Cut 3				Cut 4			
	$^{127}\text{I}_{\text{G(Ir)}}$ (mg I kg ⁻¹)		$\text{I}_{\text{G(Ir,E)}}$ (% of total I)		$^{127}\text{I}_{\text{G(Ir)}}$ (mg I kg ⁻¹)		$\text{I}_{\text{G(Ir,E)}}$ (% of total I)		$^{127}\text{I}_{\text{G(Ir)}}$ (mg I kg ⁻¹)		$\text{I}_{\text{G(Ir,E)}}$ (% of total I)		$^{127}\text{I}_{\text{G(Ir)}}$ (mg I kg ⁻¹)		$\text{I}_{\text{G(Ir,E)}}$ (% of total I)	
	Mean	S. E.	Mean	S. E.	Mean	S. E.	Mean	S. E.	Mean	S. E.	Mean	S. E.	Mean	S. E.	Mean	S. E.
NI01	0.136	0.0196	67	1	0.091	0.0082	74	2	0.162	0.00696	86	3	0.32	0.00688	92	1
NI02	0.0254	0.0214	14	12	0.0538	0.00916	41	6	0.134	0.00871	68	3	0.288	0.0103	80	3
NI03	0.0946	0.014	63	12	0.0945	0.0169	68	4	0.228	0.0216	73	11	0.35	0.0318	82	3
NI04	0.0357	0.00686	18	3	0.0497	0.00563	37	2	0.144	0.00491	72	2	0.228	0.0728	48	16
NI05	neg	2.91	neg	178	neg	1.28	neg	42	neg	1.24	neg	79	neg	0.952	neg	27
NI06	neg	0.0355	neg	15	neg	0.00599	neg	5	0.0882	0.0108	35	6	0.227	0.0309	50	4
NI07	neg	0.0473	neg	33	neg	0.0295	neg	30	0.0788	0.0315	49	21	0.25	0.0319	85	6
NI08	neg	0.0317	neg	104	neg	0.13	neg	24	neg	0.0977	neg	9	neg	2.2	neg	44
NI09	0.179	0.0767	76	8	0.15	0.0554	79	6	0.229	0.0319	80	13	0.377	0.0559	71	5
NI10	0.118	0.00173	60	9	0.117	0.0232	70	3	0.196	0.0335	66	9	0.353	0.111	53	13
NI11	0.00767	0.0241	2	13	0.0209	0.00811	17	7	0.0643	0.0158	40	9	0.23	0.00567	76	5
NI12	0.0876	0.0306	48	11	0.0511	0.0281	38	22	0.156	0.0316	74	9	0.329	0.0411	86	0
NI13	0.0798	0.00857	59	6	0.0708	0.00754	76	3	0.142	0.0129	93	4	0.276	0.0252	94	4
NI14	0.0972	0.0083	67	6	0.107	0.00413	87	2	0.162	0.00834	91	1	0.323	0.0333	93	4
NI15	neg	0.024	neg	12	0.0387	0.0252	19	10	0.139	0.0218	62	4	0.124	0.0373	42	15
NI17	0.064	0.0271	40	14	0.0836	0.0148	67	6	0.136	0.0595	47	23	0.243	0.0706	42	12
NI18	0.0787	0.0267	40	12	0.0916	0.015	61	3	0.168	0.00612	82	5	0.33	0.00805	86	2
NI19	neg	0.0328	neg	16	0.0298	0.0194	26	19	0.0885	0.00522	45	1	0.314	0.0308	77	2
NI20	0.14	0.00923	79	1	0.112	0.00362	95	1	0.187	0.0106	95	2	0.315	0.0147	96	1

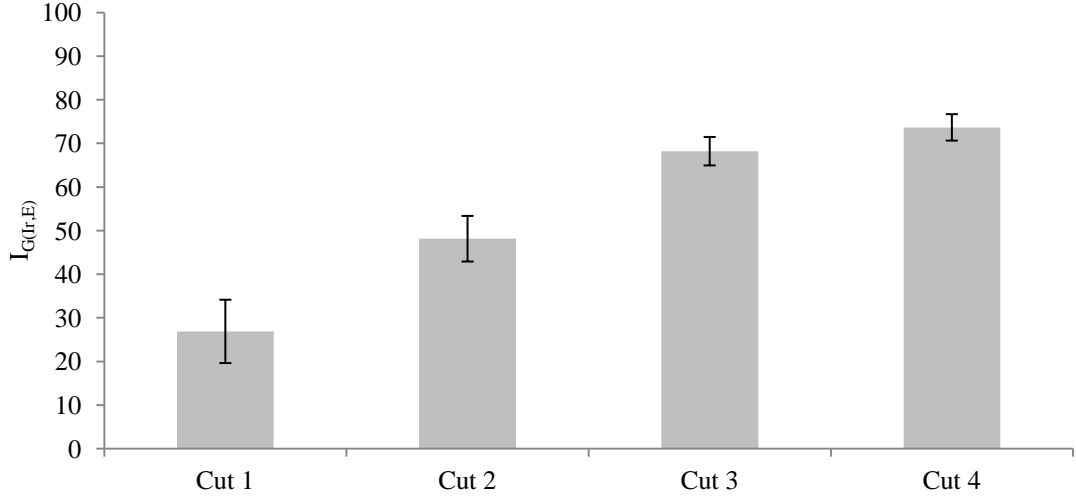


Figure 6.9. Estimated percentage of iodine in grass originating from irrigation water ($I_{G(Ir,E)}$). Mean $I_{G(Ir,E)}$ values for each cut from three replicates of 17 soils (standard deviation shown by error bars): NI01 – NI20 excluding NI05 and NI08 (all values negative) and NI16 (not included in experiment).

The assumption of Eqn. 6.3 could not have been valid in the earlier harvests, because ^{129}I became less phyto-available with time, and in soils where $I_{G/S}$ continued to decrease through all cuts, the assumption was still unlikely to have been true by the end of the experiment. In other soils (especially those with large SOC contents) $I_{G/S}$ values indicated that mixing had reached an approximate steady state by the later harvests. Even if all soils had reached perfect mixing there would still be variation in the contribution from irrigation due to variation in the ratio of $^{127}\text{I}/^{129}\text{I}$ between soils. Despite these caveats, the average value of $I_{G(Ir,E)}$ seemed to move towards an asymptote, with standard deviation decreasing through time (Figure 6.9). The mean value of $I_{G(Ir,E)}$ from cut 4 (74 %, ± 3 % standard deviation) therefore represents the best estimate of the average contribution from irrigation water, across all soil types. Cut 4 values for $I_{G(Ir,E)}$ ranged from 42 % (± 13 %; NI17) to 96 % (± 1 %; NI20).

It is also useful to compare $I_{G(Ir,E)}$, the estimated contribution of irrigation water to total uptake ($^{129+127}\text{I}_G$), with the potential provision of iodine from irrigation water, to confirm that $I_{G(Ir,E)}$ values are realistic. Therefore Eqn. 6.6 was calculated for each soil and each cut:

$$I_{G(Ir,A)} = 100 \times \left(\frac{{}^{127}\text{I}_{\text{Ir}} \times V_{\text{Ir}} \times t_{\text{G}}}{{}^{129+127}\text{I}_G \times Y} \right) \quad (6.6)$$

where $I_{G(Ir,A)}$ is the total amount of iodine provided by irrigation water during the experiment, expressed as a percentage of the iodine uptake in grass; $^{127}I_{Ir}$ is the concentration of ^{127}I in irrigation water ($\mu\text{g I L}^{-1}$); V_{Ir} is the mean volume of irrigation water provided (L day^{-1}); t_G is growth time (days); $^{129+127}I_G$ is total concentration of iodine in grass ($\mu\text{g I g}^{-1}$); and Y is yield of grass (g). The proportion of iodine provided by irrigation water ($I_{G(Ir,A)}$) is expressed as a percentage of the total iodine taken up by grass, rather than a percentage of the ^{127}I taken up. This is to compare the relative contributions from irrigation water and soil, irrespective of isotope. Since the vast majority of iodine in grass was ^{129}I , there was no significant difference between $I_{G(Ir,A)}$ expressed as a percentage of $^{127}I_G$ or as a percentage of $^{127+129}I_G$; (ANOVA, $p = 0.991$).

A comparison of $I_{G(Ir,A)}$ and $I_{G(Ir,E)}$ was made for each soil, using cut 4 only (Figure 6.10). The final harvest was used because the ^{129}I spike would be closest to being fully equilibrated with soil iodine and so $I_{G(Ir,E)}$ would provide the best estimate of irrigation contribution to I_G . For all soils $I_{G(Ir,A)} > I_{G(Ir,E)}$ (ANOVA, $p < 0.001$). The calculation method for $I_{G(Ir,E)}$ means that the value is an underestimate when the two isotopes are not perfectly mixed, which is likely to have still been the case at cut 4. Additionally, there may have been variation in $^{127}I_{Ir}$ which would have an effect on calculated values of $I_{G(Ir,A)}$, although this was accounted for to some extent in the value of $^{127}I_{Ir}$ used, which was the mean of several measurements on two occasions (mean $^{127}I_{Ir} = 0.76 \mu\text{g I L}^{-1}$, standard error $0.14 \mu\text{g I L}^{-1}$ from eight samples taken on two occasions). Overall, however, this comparison shows that irrigation water provided more than enough ^{127}I to account for iodine off-take by grass.

‘Passive uptake’ has been suggested as the most likely transport mechanism for uptake of iodine by plants (Dai et al., 2006). In this experiment, irrigation water was added to compensate for evapotranspiration from the pots and to maintain a constant moisture content. Values of $I_{G(Ir,A)}$ were all, with the exception of the coastal soils, well above 100 %, therefore either passive uptake did occur but there were large losses to evaporation, or iodine was excluded by plants. NI10 and NI17 had particularly high values of $I_{G(Ir,A)}$, but in these cases this is likely to be due to (abiotic) evaporation, as they did not support healthy grass growth and the soil was very exposed. Therefore

the results obtained cannot be used to determine whether or not iodine is taken up passively as a component of water.

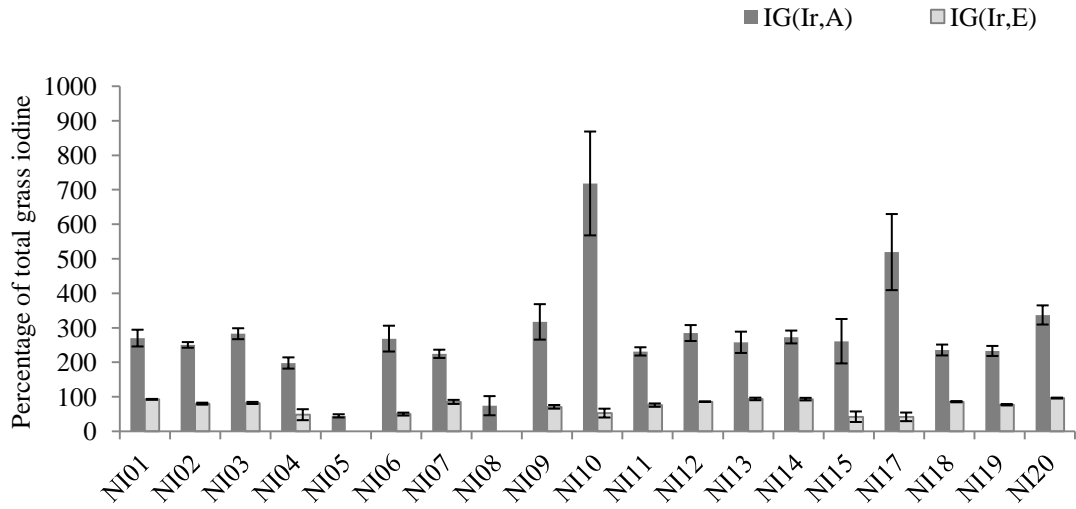


Figure 6.10. Comparison of the actual iodine provision from irrigation water ($I_{G(Ir,A)}$) and estimated irrigation contribution to total iodine in grass ($I_{G(Ir,E)}$), both expressed as a percentage of the total iodine uptake. Error bars show triplicate values for each soil, for cut 4 only. Negative values have been omitted for clarity.

Further confirmation of the role of irrigation water in providing phyto-available iodine can be found by considering values of concentration ratios (CR) for both isotopes, calculated from Eqn. 6.7.

$${}^{127}\text{CR} = \left(\frac{{}^{127}\text{I}_G}{{}^{127}\text{I}_S} \right) \quad (6.7)$$

where ${}^{127}\text{I-CR}$ is concentration ratio of ${}^{127}\text{I}$ (dimensionless) and ${}^{127}\text{I}_G$ and ${}^{127}\text{I}_S$ are concentrations of ${}^{127}\text{I}$ in grass and soil respectively (mg I kg^{-1}). Eqn. 6.7 was also used to calculate ${}^{129}\text{I-CR}$ using equivalent concentrations of ${}^{129}\text{I}$. Concentration ratios were calculated for all soils, for each cut and both isotopes (Table 6.4 and Table 6.5). The median value of ${}^{127}\text{I-CR}$ was 1.66×10^{-2} , with a range of 2.46×10^{-3} (NI08 cut 2; S.E. = 2.23×10^{-4}) to 9.39×10^{-2} (NI12 cut 4; S.E. = 1.38×10^{-2}), while values of ${}^{129}\text{I-CR}$ were similar: median of 8.13×10^{-3} , ranging between 5.03×10^{-4} (NI20 cut 2; S.E. = 5.71×10^{-5}) and 6.32×10^{-2} (NI05 cut 1; S.E. = 7.74×10^{-3}). Iodine-129 was added to the phyto-available pool so should have been more available than ${}^{127}\text{I}$ (${}^{129}\text{I-CR} > {}^{127}\text{I-CR}$). In fact values of ${}^{129}\text{I-CR}$ overall were similar to those of ${}^{127}\text{I-CR}$, and for most soils ${}^{129}\text{I-CR} < {}^{127}\text{I-CR}$ because irrigation water provided additional phyto-available ${}^{127}\text{I}$ (Figure 6.11).

Table 6.4. Concentration ratios for pot experiment (^{127}I -CR cuts 1 – 4) and field samples (^{127}I). Standard error represents variation in three replicates.

Soil	Field ^{127}I -CR ($\times 10^{-2}$)		^{127}I -CR cut 1 ($\times 10^{-2}$)		^{127}I -CR cut 2 ($\times 10^{-2}$)		^{127}I -CR cut 3 ($\times 10^{-2}$)		^{127}I -CR cut 4 ($\times 10^{-2}$)	
	Mean	S. E.	Mean	S. E.	Mean	S. E.	Mean	S. E.	Mean	S. E.
NI01	27.7	0.00591	7.35	0.970	4.46	0.178	6.94	0.279	12.8	0.178
NI02	4.32	0.00674	3.60	0.279	2.86	0.175	4.34	0.0650	8.00	0.315
NI03	8.43	3.26	0.586	0.0846	0.519	0.0770	1.33	0.458	1.59	0.0405
NI04	17.1	0.755	2.08	0.190	1.44	0.152	2.14	0.106	5.09	0.532
NI05	1.32	298.6	1.05	0.198	0.469	0.0583	0.540	0.0340	0.564	0.0440
NI06	5.44	0.293	1.87	0.193	1.81	0.265	2.62	0.209	4.67	0.627
NI07	5.12	1.24	0.960	0.0442	0.722	0.0637	1.15	0.0613	1.99	0.160
NI08	0.953	3.99	0.627	0.306	0.246	0.0223	0.389	0.0614	1.17	0.382
NI09	7.21	2.02	0.617	0.268	0.546	0.271	0.750	0.00900	1.38	0.211
NI10	6.12	0.959	1.11	0.206	0.885	0.174	1.56	0.0828	3.39	0.443
NI11	8.17	0.0672	1.80	0.189	1.10	0.136	1.40	0.0865	2.69	0.157
NI12	7.99	0.168	4.30	0.747	3.06	0.231	5.06	0.623	9.39	1.38
NI13	6.24	0.429	1.66	0.217	1.13	0.167	1.86	0.170	3.62	0.534
NI14	9.01	0.509	2.64	0.383	2.23	0.157	3.22	0.362	6.29	0.894
NI15	1.59	0.0567	0.377	0.0516	0.603	0.116	0.713	0.142	1.04	0.200
NI17	9.53	0.295	1.06	0.444	0.783	0.0992	1.98	0.193	3.83	0.615
NI18	1.93	0.135	1.79	0.410	1.38	0.265	1.88	0.0255	3.55	0.112
NI19	1.72	0.313	1.38	0.168	0.950	0.120	1.56	0.123	3.27	0.408
NI20	3.81	0.205	1.46	0.146	0.983	0.0867	1.62	0.139	2.71	0.232

Table 6.5. Spike concentration ratios for pot experiment (^{129}I -CR cuts 1 – 4). Standard error represents variation in three replicates.

Soil	^{129}I -CR cut 1 ($\times 10^{-2}$)		^{129}I -CR cut 2 ($\times 10^{-2}$)		^{129}I -CR cut 3 ($\times 10^{-2}$)		^{129}I -CR cut 4 ($\times 10^{-2}$)	
	Mean	S. E.	Mean	S. E.	Mean	S. E.	Mean	S. E.
NI01	2.31	0.235	1.09	0.0655	0.923	0.218	0.928	0.175
NI02	3.02	0.242	1.66	0.138	1.35	0.129	1.57	0.236
NI03	0.236	0.113	0.160	0.0189	0.449	0.301	0.280	0.0440
NI04	1.69	0.130	0.904	0.0696	0.581	0.0190	2.65	0.790
NI05	6.32	0.774	3.00	0.491	2.89	0.408	2.49	0.343
NI06	3.84	0.613	2.16	0.228	1.72	0.282	2.33	0.376
NI07	1.49	0.300	0.853	0.224	0.608	0.259	0.283	0.105
NI08	1.86	0.249	1.12	0.0733	1.07	0.142	3.91	1.80
NI09	0.134	0.0474	0.144	0.103	0.154	0.0988	0.390	0.0639
NI10	0.471	0.192	0.252	0.0498	0.496	0.112	1.51	0.317
NI11	1.73	0.0671	0.916	0.142	0.817	0.0842	0.652	0.161
NI12	2.12	0.360	1.79	0.527	1.21	0.309	1.28	0.156
NI13	0.686	0.140	0.268	0.0601	0.125	0.0585	0.258	0.156
NI14	0.878	0.260	0.287	0.0307	0.283	0.0566	0.404	0.192
NI15	0.741	0.0777	0.484	0.108	0.276	0.0819	0.657	0.269
NI17	0.663	0.314	0.238	0.0325	1.13	0.561	2.23	0.742
NI18	1.06	0.267	0.533	0.116	0.329	0.106	0.501	0.0747
NI19	1.47	0.372	0.709	0.191	0.850	0.0591	0.743	0.0979
NI20	0.300	0.0178	0.0503	0.00571	0.0675	0.0253	0.0955	0.0262

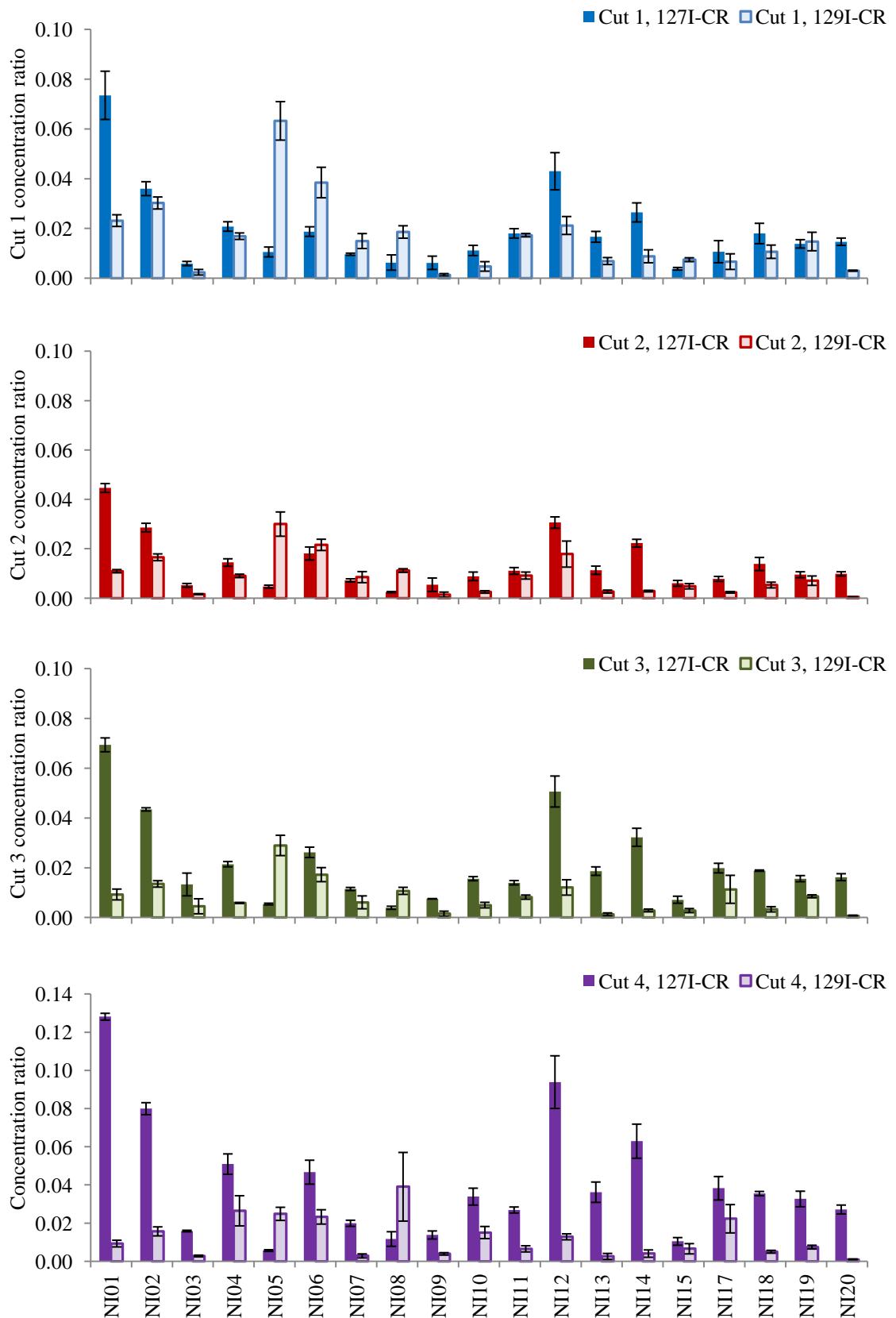


Figure 6.11. Comparison of $^{127}\text{I-CR}$ and $^{129}\text{I-CR}$ for each soil, for each of four cuts. Error bars show standard error of triplicate pots. Note y-axis scales.

6.3.5 Comparison of concentration ratios measured in the field and pot trial

Concentration ratios for field samples ($^{127}\text{I-CR}_F$) were discussed in Chapter 3, but to highlight the importance of iodine input from irrigation water, they are compared here to values from pot trial samples ($^{127}\text{I-CR}_p$). In general $^{127}\text{I-CR}_F$ values (median = 6.01×10^{-2}) were larger than $^{127}\text{I-CR}_p$ values (median = 1.66×10^{-2}), and for most individual soils, $^{127}\text{I-CR}_F$ was larger than $^{127}\text{I-CR}_p$ for the four cuts (Figure 6.12). This is consistent with greater input of ^{127}I from wet and dry deposition in the field: in the pot experiment, irrigation water provided $\sim 0.2 \mu\text{g I L}^{-1}$ iodine, while rain falling in Northern Ireland has been shown to contain $1 - 6 \mu\text{g I L}^{-1}$ iodine (Section 3.3.3). Additionally, some field samples had been subject to iodine deposition from sea-spray and dry deposition, which were not present in the pot experiment.

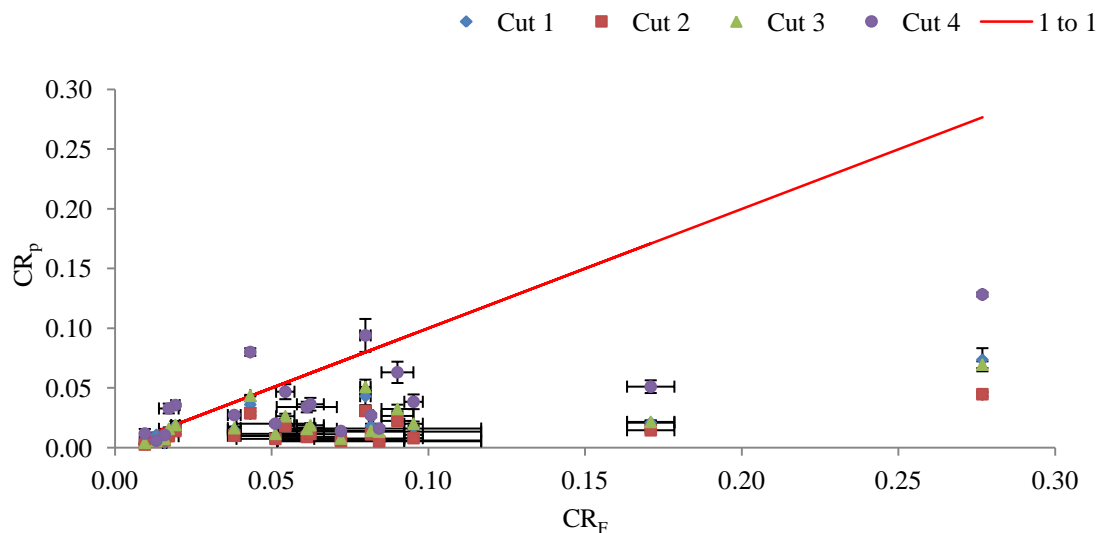


Figure 6.12. Relationship between concentration ratios of ^{127}I in pot and field samples. Error bars show standard error of three pots (pot samples) and triplicate measurements (field samples).

As well as being affected by variable inputs from atmosphere and irrigation, values of CR can be affected by soil characteristics, vegetation type and biomass production. For comparison, CRs from published studies are shown in Table 6.6. The values are of a similar range to those calculated for NI01 – NI20 field samples (see Section 3.3.2), with the exception of those from the study of Dai et al. (2006), when iodate was added. The iodine concentration in irrigation water was not provided for any of the experiments listed in Table 6.6 but results from the current trial show that this is an important parameter to be considered for similar studies in the future.

Table 6.6: Concentration ratios (CR = I_V / I_S) from published studies of iodine uptake from soil in pot experiments grown indoors.

CR	Soil type or texture	Vegetation type	Experimental details	Author, date
0.05 - 5	Sandy loam	Ryegrass	Greenhouse pot experiment. Soil 0.89 % SOC, pH 6.2, 2.2 mg I kg ⁻¹ total. ~20 mg I kg ⁻¹ freshly added ¹²⁷ I as KI, KIO ₃ , I ₂ .	Whitehead (1975)
¹²⁵ I not detected in grass	Sandy loam	Ryegrass	Column experiment (controlled environment). Soil 4.7 % LOI, pH 4.3. Fluctuating water table delivering 20 Bq mL ⁻¹ ¹²⁵ I.	Ashworth and Shaw (2006a)
1.0 – 1.6	Inceptisol	Pak choi	Greenhouse pot experiment Soil 40.9 g kg ⁻¹ organic matter, pH = 5.9, 2.0 mg I kg ⁻¹ total. 10 – 50 mg I kg ⁻¹ added iodine as KI and seaweed. CR estimated from Fig. 3.	Hong et al. (2009)
0.39 – 1.15 (I) 0.39 – 23.2 (IO ₃ ⁻)	Udic luvisol	Spinach	Greenhouse pot experiment. Soil 13.9 g kg ⁻¹ organic matter, pH 7.85, 1.55 mg I kg ⁻¹ total. KI or KIO ₃ added at 0.0 – 2.0 mg I kg ⁻¹ . Values calculated from values in text, assuming vegetation moisture content of 90 %.	Dai et al. (2006)
~0.8 to ~ 1.4 (seaweed I) ~1.1 to ~1.6 (I)	Soil type not stated	Cabbage	Greenhouse pot experiment. Soil details unknown except background 2.02 mg I kg ⁻¹ . KI and seaweed fertiliser added to give 0, 10, 25, 050, 100, 150 mg I kg ⁻¹ in soil. CRs calculated from Fig. 3.	Weng et al. (2008a)

6.3.6 Spike / non-spike ratios in soil solution

Iodine in soil pore solution is more phyto-available than that associated with the solid phase, as illustrated by the apparent availability of iodine in irrigation water compared to native soil-derived ^{127}I . After the end of the pot experiment, deionised water was added to the potted soils until they were wet but not draining (close to field capacity), and allowed to equilibrate with the soil for three days. Soil pore solution was then extracted by centrifugation, and analysed by SEC-ICP-MS described in Section 2.6.2.2. To investigate how well the spike ^{129}I and native ^{127}I had mixed, concentrations of ^{127}I and ^{129}I in the soil solution ($^{127}\text{I}_L$ and $^{129}\text{I}_L$, $\mu\text{g I L}^{-1}$) and dissolved organic carbon (DOC, mg I L^{-1}) were measured (Table 6.7).

Table 6.7. Total concentrations in soil solution of ^{129}I ($^{129}\text{I}_L$), ^{127}I ($^{127}\text{I}_L$), and dissolved organic carbon (DOC). Mean and standard error of three replicates, except for soils NI05 and NI15 ($n = 2$).

Soil	$^{127}\text{I}_L$ ($\mu\text{g I L}^{-1}$)		$^{129}\text{I}_L$ ($\mu\text{g I L}^{-1}$)		DOC (mg I L^{-1})	
	Mean	S. E.	Mean	S. E.	Mean	S. E.
NI01	11.1	5.38	0.672	0.269	106	18.1
NI02	3.40	0.872	0.188	0.0341	56.7	11.5
NI03	4.32	1.74	0.167	0.0223	92.0	17.0
NI04	16.2	3.96	0.429	0.0788	58.5	11.8
NI05	1210	0.994	2.07	0.0560	93.2	6.33
NI06	5.06	1.13	0.173	0.0156	34.4	6.08
NI07	134	34.9	1.88	0.507	241	50.6
NI08	156	15.7	0.646	0.0559	38.2	2.42
NI09	5.83	1.06	0.231	0.0315	97.6	15.1
NI10	3.98	0.700	0.446	0.0539	124	14.0
NI11	37.9	2.70	1.13	0.0158	181	9.23
NI12	2.56	0.574	0.160	0.0375	49.9	11.8
NI13	9.68	1.79	0.315	0.0548	107	19.1
NI14	3.31	0.488	0.0913	0.0359	46.5	7.60
NI15	48.9	20.5	0.692	0.252	268	8.17
NI17	3.34	1.72	0.614	0.321	128	34.9
NI18	1.38	0.452	0.0701	0.00550	36.6	10.1
NI19	7.60	2.35	0.250	0.0553	46.4	5.65
NI20	21.9	3.73	1.35	0.242	296	37.8

To investigate partitioning of isotopes between soil solution and solid, the ‘liquid/soil ratio’ ($I_{L/S}$) was calculated as follows:

$$I_{L/S} = \left(\frac{\frac{^{129}\text{I}_L}{^{127}\text{I}_L}}{\frac{^{129}\text{I}_S}{^{127}\text{I}_S}} \right) \quad (6.8)$$

Where $I_{L/S}$ is the dimensionless ratio of ^{129}I to ^{127}I in soil solution divided by the equivalent ratio in the whole soil; $^{129}\text{I}_L$ and $^{127}\text{I}_L$ are ^{129}I and ^{127}I concentrations in soil solution respectively ($\mu\text{g I L}^{-1}$) and $^{129}\text{I}_S$ and $^{127}\text{I}_S$ are total concentrations of ^{129}I and ^{127}I in soil measured from TMAH extraction (mg I kg^{-1}). Values of $I_{L/S}$ were determined for each sample, then mean values for each soil were calculated (Figure 6.13). For all soils, the greatest uncertainty was due to variations in $^{129}\text{I}_L$ and $^{127}\text{I}_L$, rather than $^{129}\text{I}_S$ and $^{127}\text{I}_S$. As for $I_{G/S}$, if ^{129}I and ^{127}I were fully mixed within the soil, then values of $I_{L/S}$ should be 1.0. In all but one soil (NI14, Figure 6.13) this was not the case and ^{129}I was over-represented in solution, indicating that some soil ^{127}I was in a pool not fully accessed by ^{129}I during the 104 days of the experiment.

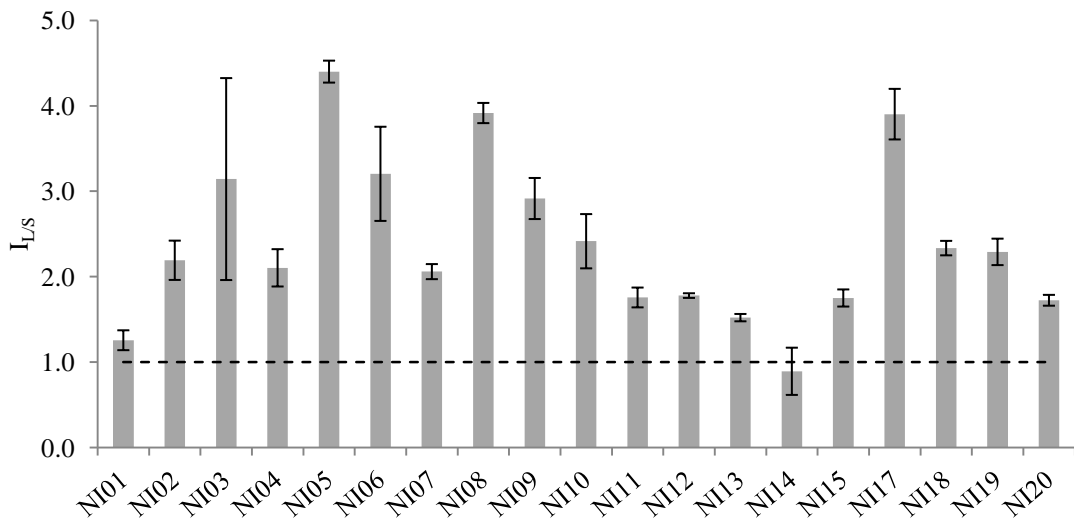


Figure 6.13. Solution/soil ratio ($I_{L/S}$) for each soil. Error bars show standard error of three replicates. Dashed line is at $I_{L/S} = 1$.

Higher $I_{L/S}$ values indicate less mixing between spike and native iodine within the solid phase of the soil. The soils with highest $I_{L/S}$ values were soils 05, 08 and 17. In the case of NI05 and NI08, values of $^{127}\text{I}_L$, $^{129}\text{I}_L$ and $^{127}\text{I}_G$ were also high compared to

other soils. Together with high $I_{L/S}$ values this suggests comparatively greater retention in solution and slower mixing of spike ^{129}I with native soil iodine. In high SOC soils, there are likely to be competing processes occurring regarding mixing of the two isotopes: humus would be expected to reduce the solution:soil ratio of ^{129}I , but conversely native iodine (^{127}I) is also likely to be tightly bound, potentially within hydrophobic moieties (Sheppard and Thibault, 1992; Sutton and Sposito, 2005) and therefore non-labile. The fixation of ^{127}I in the solid phase could delay full mixing and increase $I_{L/S}$. Furthermore, pore solutions in high SOC soils are likely to contain more DOC, in which case ^{129}I may be rapidly assimilated by this and retained in solution to maintain a high $^{129}\text{I}_L/^{127}\text{I}_L$ against more complete mixing with the solid phase iodine pool. The relative extent of these two factors may explain the variability in $I_{L/S}$ in soils 03, 09, 10 and 17, and their relatively high values compared to soils with lower SOC.

Since iodine in pore solution is more available than iodine held on solid phases, a correlation between $^{129}\text{I}_G / ^{127}\text{I}_G$ and $^{129}\text{I}_L / ^{127}\text{I}_L$ would be expected. This was the case when values for cut 4 from all soils were considered ($r = 0.724$, $p < 0.001$), but the relationship was dominated by NI10 and NI17 (Figure 6.14). Values from the 4th harvest were chosen because the concentrations in pore solution were measured at the end of the experiment and therefore most closely represented the isotopic ratios for the final cut. When NI10 and NI17 were excluded from the correlation, the relationship was no longer present: $r = 0.019$, $p = 0.896$. In almost all cases, $^{129}\text{I}_L / ^{127}\text{I}_L > ^{129}\text{I}_G / ^{127}\text{I}_G$, so ^{127}I was over-represented in the grass compared to soil solution. This may appear to be an unusual result because it suggests that ^{129}I in solution was less available to plant roots than ^{127}I in solution. However, there is likely to be a difference in solution speciation between the two isotopes. It is likely that most of the ^{129}I in solution is organically bound to fulvic acid (see following Section 6.3.7), and therefore less available than the mainly inorganic ^{127}I repeatedly added in irrigation water on a daily basis. Again, this result confirms the importance of uptake of ^{127}I in irrigation water. In the case of NI05 and NI08, iodine contribution from irrigation water to grass has been shown to be unimportant, and for those soils, $^{129}\text{I}_L / ^{127}\text{I}_L \approx ^{129}\text{I}_G / ^{127}\text{I}_G$.

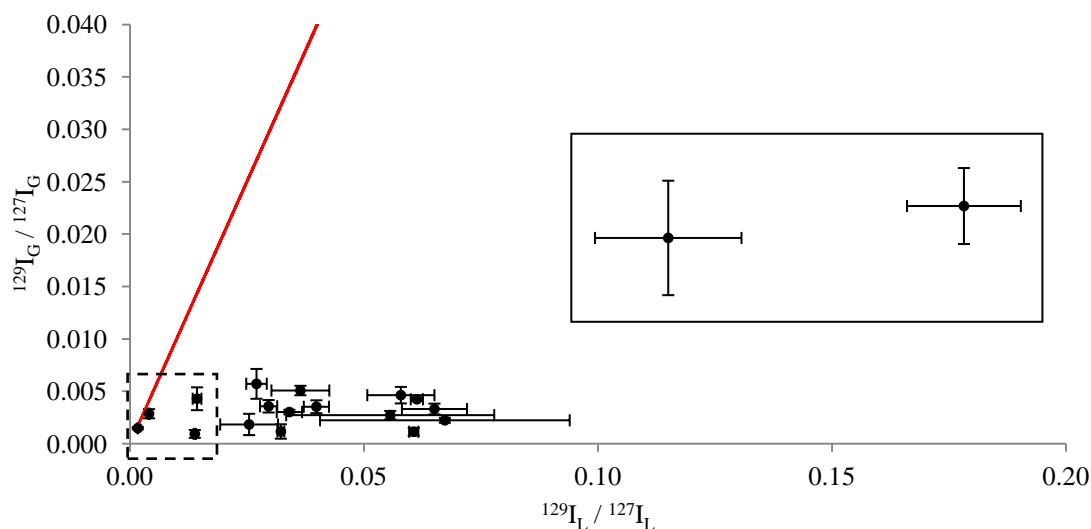


Figure 6.14. Relationship between $^{129}\text{I}_G / ^{127}\text{I}_G$ and $^{129}\text{I}_L / ^{127}\text{I}_L$ for cut 4 values. The box includes values for NI10 and NI17; the dashed box includes values from NI05 and NI08; red line is the 1:1 trend.

6.3.7 Iodine speciation in soil solution

Speciation of the soil solution by SEC-ICP-MS was undertaken on the samples described in the previous section. Individual species were quantified against iodide and iodate standards. The sum of species in each sample was then compared to total iodine in the samples, measured separately by ICP-MS (Table 6.8). Figure 6.15 shows chromatograms from soils 13, 17 and 20, which are representative of ^{127}I chromatography from most of the soil solution samples. Low concentrations in most samples made peak integration very difficult and so conclusions about iodine speciation in solution can only be very general. The uncertainty in species measured by SEC is highlighted by the summation of measured species being outside the range 70 – 130 % of total iodine concentration in solution in most cases. Where peaks were observed, typically >80 % of ^{127}I was in the double-peaked organic component (Org-I), with 0 – 20 % iodide, and iodate not detected. Retention times (RT) of peaks observed were: Org-I 1 (RT \approx 6 - 7 min), Org-I 2 (RT \approx 9 – 13 min), iodate (RT \approx 15 min) and iodide (RT \approx 23 min). Identification of iodide and iodate were confirmed by comparison of RTs with standards, and the early-RT peaks were determined as organic by comparison with humic acid. An unknown peak ('U1') was also observed in some cases, at RT \approx 18 – 19 min (e.g. NI13a, Figure 6.15). Its elution time between iodate and iodide indicates low molecular weight, probably below the molecular weight cut-off of the column but with some chemical separation from other species. No further action was taken to try to identify this species.

Table 6.8. Speciation of soil solution. Individual species are presented as a percentage of sum of species. Sum of species quantified is quoted as percentage of measured total iodine concentration. Replicates a and b for each soil. Values where none of that isotope was measured by SEC are indicated by - .

Soil	¹²⁷ I (%)												¹²⁹ I (%)												
	Org-I 1		Org-I 2		Iodate		U1		Iodide		Sum (% of measured total)		Org-I 1		Org-I 2		Iodate		U1		Iodide		Sum (% of measured total)		
	a	b	a	b	a	b	a	b	a	b	a	b	a	b	a	b	a	b	a	b	a	b	a	b	a
NI01	-	12	-	83	-	0	-	5	-	0	0	189	-	0	-	46	-	54	-	0	-	0	0	187	
NI02	0	0	100	0	0	0	0	100	0	0	27	33	0	-	100	-	0	-	0	-	0	-	481	0	
NI03	0	0	100	83	0	0	0	0	0	17	0	174	0	-	100	-	0	-	0	-	0	-	538	0	
NI04	0	0	87	91	0	0	0	0	13	9	34	114	0	0	100	100	0	0	0	0	0	0	113	148	
NI05	1	1	94	92	0	0	0	0	5	7	72	85	0	0	86	100	0	0	0	0	14	0	102	49	
NI06	0	-	0	-	0	-	59	-	41	-	0	0	0	-	0	-	0	-	59	-	41	-	453	0	
NI07	4	2	96	97	0	0	0	1	0	0	42	130	0	0	100	100	0	0	0	0	0	0	74	178	
NI08	2	0	88	82	0	0	0	0	10	18	69	90	0	-	0	-	47	-	0	-	53	-	134	0	
NI09	0	0	100	0	0	0	0	100	0	0	30	0	-	0	-	0	-	0	-	100	-	0	0	247	
NI10	-	0	-	88	-	0	-	0	-	12	0	291	-	0	-	69	-	0	-	0	-	31	0	409	
NI11	0	7	100	88	0	0	0	5	0	0	56	97	0	-	100	-	0	-	0	-	0	-	111	0	
NI12	0	0	100	59	0	15	0	26	0	0	27	195	-	-	-	-	-	-	-	-	-	-	0	0	
NI13	10	9	72	73	0	0	18	18	0	0	59	102	0	0	100	100	0	0	0	0	0	0	0	147	
NI14	0	0	100	- ²	0	-1	0	104	0	-1	65	45	-	0	-	44	-	25	-	0	-	31	0	715	
NI15	3	4	98	96	0	0	0	0	0	0	35	111	0	-	70	-	30	-	0	-	0	-	223	0	
NI17	9	-	92	-	0	-	0	-	-1	-	167	0	0	-	0	-	0	-	0	-	100	-	88	0	
NI18	-	-	-	-	-	-	-	-	-	-	0	0	-	-	-	-	-	-	-	-	-	-	0	0	
NI19	0	0	46	85	0	0	54	15	0	0	64	130	-	0	-	100	-	0	-	0	-	0	0	310	
NI20	0	8	92	85	0	3	8	3	0	0	54	124	0	-	72	-	0	-	0	-	28	-	81	0	

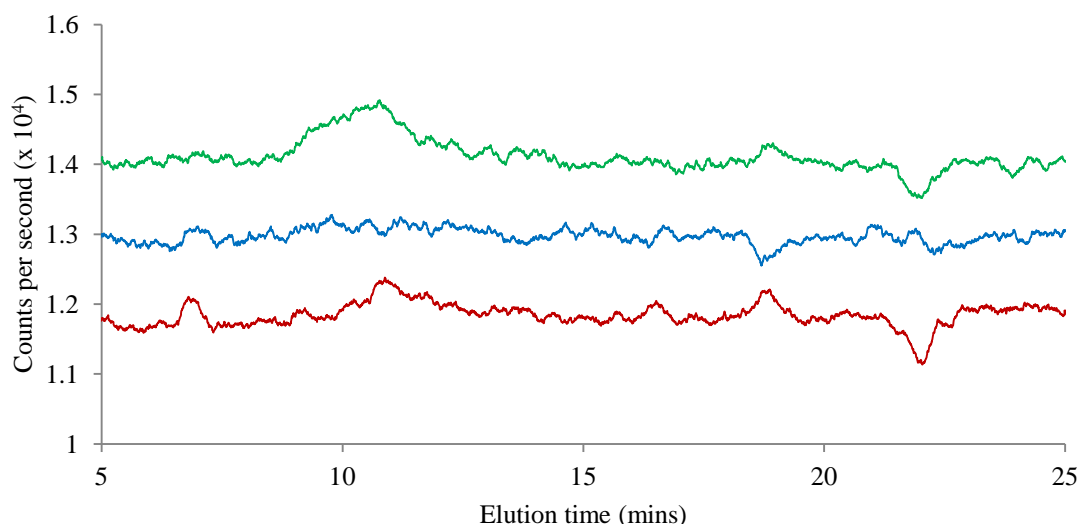


Figure 6.15. Examples of typical size exclusion chromatograms for ^{127}I . Chromatograms are offset by 0.1×10^4 counts per second to allow clear comparison. Red – NI13a; blue – NI17a; green – NI20a.

Interpretation of ^{129}I chromatograms was even more difficult due to the extremely small peaks (e.g. Figure 6.16), leading to great uncertainty in peak identification and quantification. As for the ^{127}I results, the majority of ‘sum of species as % of total’ values were outside the range 70 – 130 % (Table 6.8), but of the peaks observed, organic iodine was the dominant form of ^{129}I . No further interpretation of speciation of ^{129}I was possible.

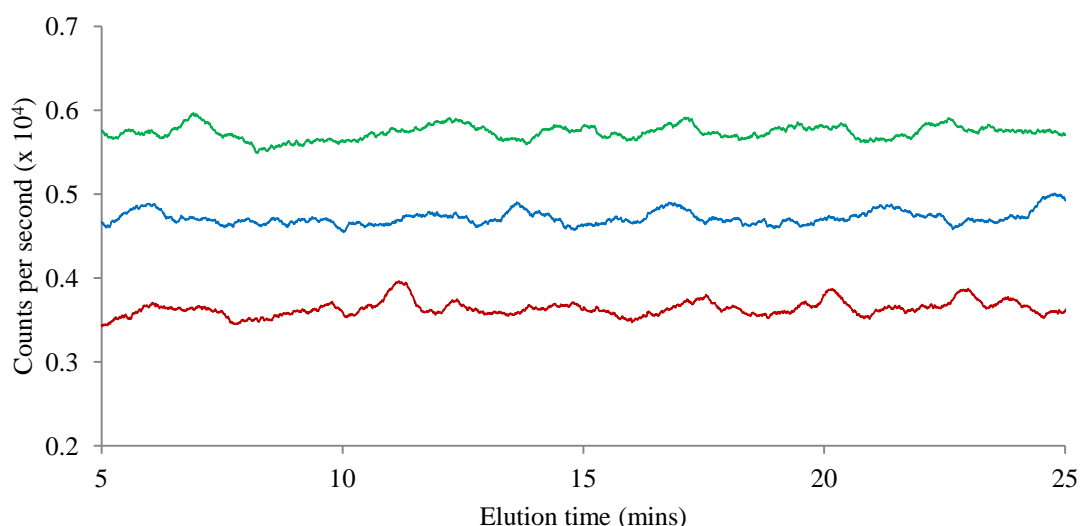


Figure 6.16. Examples of typical size exclusion chromatograms for ^{129}I . Chromatograms are offset by 0.1×10^4 counts per second to allow clear comparison. Red – NI02a; blue – NI04a; green – NI05a.

There was a significant positive correlation between DOC and $^{127}\text{I}_L$ when NI05 and NI08 were excluded: $r = 0.631$, $p < 0.001$ (Figure 6.17), and between DOC and $^{129}\text{I}_L$ when all samples were included ($r = 0.694$, $p < 0.001$). This supports the classification of peaks OrgI 1 and OrgI 2 (which comprised the majority of iodine species observed) as organic species, and is consistent with previous reports of iodine bound to soluble organic molecules (Gilfedder et al., 2009; Keppler et al., 2003). The complexity of humic substances in soil and the range of potential iodine-binding sites have been reported (Hansen et al., 2011; Kodama et al., 2006; Sutton and Sposito, 2005). Organically bound iodine has been shown, by different analysis techniques, to be the dominant form of iodine in (top)soil solutions (Hansen et al., 2011; Shimamoto et al., 2011). The duration of this pot experiment was longer than that required to transform inorganic iodine to organic species in humic acid (Chapter 4), supporting transformation of the added $^{129}\text{IO}_3^-$ to organic forms in solution, such as those identified by Xu et al. (2011a).

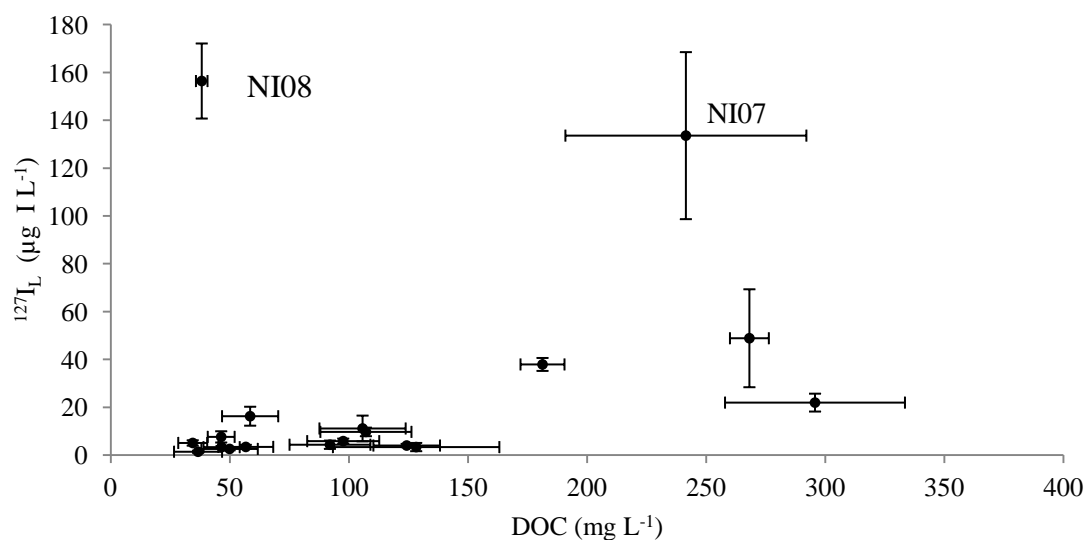


Figure 6.17. Relationship between $^{127}\text{I}_L$ and DOC in soil solution (NI05 not shown: DOC = 93.2 mg I L⁻¹, $^{127}\text{I} = 1210 \mu\text{g I L}^{-1}$).

In a small number of soil solutions, with larger concentrations of iodine, chromatograms were much clearer. Considerable detail in the ^{127}I organic peaks was seen in soils 05, 08 and 07: all had 4 clear peaks within the ‘Org-2’ peak (Figure 6.18) which was reproduced by replicates. Although soils 05 and 08 have repeatedly shown different trends compared to the other soils, in this case the difference seems to be linked to high values of $^{127}\text{I}_L$: only soils 05, 07 and 08 showed the detail clearly, and

these contained the three highest $^{127}\text{I}_L$ concentrations (NI07 $^{127}\text{I}_L = 134 \mu\text{g I L}^{-1}$; Figure 6.17). Some additional detail within the organic iodine peak was also observed in chromatographs NI11 and NI15 (Figure 6.19), which contained the next greatest $^{127}\text{I}_L$ concentrations (37.9 and 48.9 $\mu\text{g I L}^{-1}$ respectively). In order to identify whether the unusual speciation was caused by rhizosphere processes within the pot, solution was extracted from samples of these soils that had not been used in the pot experiment, and re-analysed by SEC. The separate organic iodine peaks were again present in soils NI05 and NI08, although not evident in NI07 (Figure 6.20). These results therefore support the hypothesis that the complex organic iodine speciation seen was pedogenic, rather than phytogenic, in origin and not dependent on the presence of plant roots. The identification of these peaks was not pursued, due to time limitations, however methods that could be used might include (molecular) mass spectrometry (e.g. Moulin et al. (2001)), or X-ray absorption spectroscopy (e.g. Kodama et al. (2006), Shimamoto et al. (2010) and Yamaguchi et al. (2010)). It is possible that the additional peaks were due to iodination of specific classes of aromatic compounds, which have been shown by electrospray ionisation mass spectrometry to form complexes with iodine (Moulin et al., 2001). The nature of the SEC column used means that the fractionation of iodinated species may have occurred according to size or to adsorption behaviour (Chapter 4); further work to confirm their identity would be valuable.

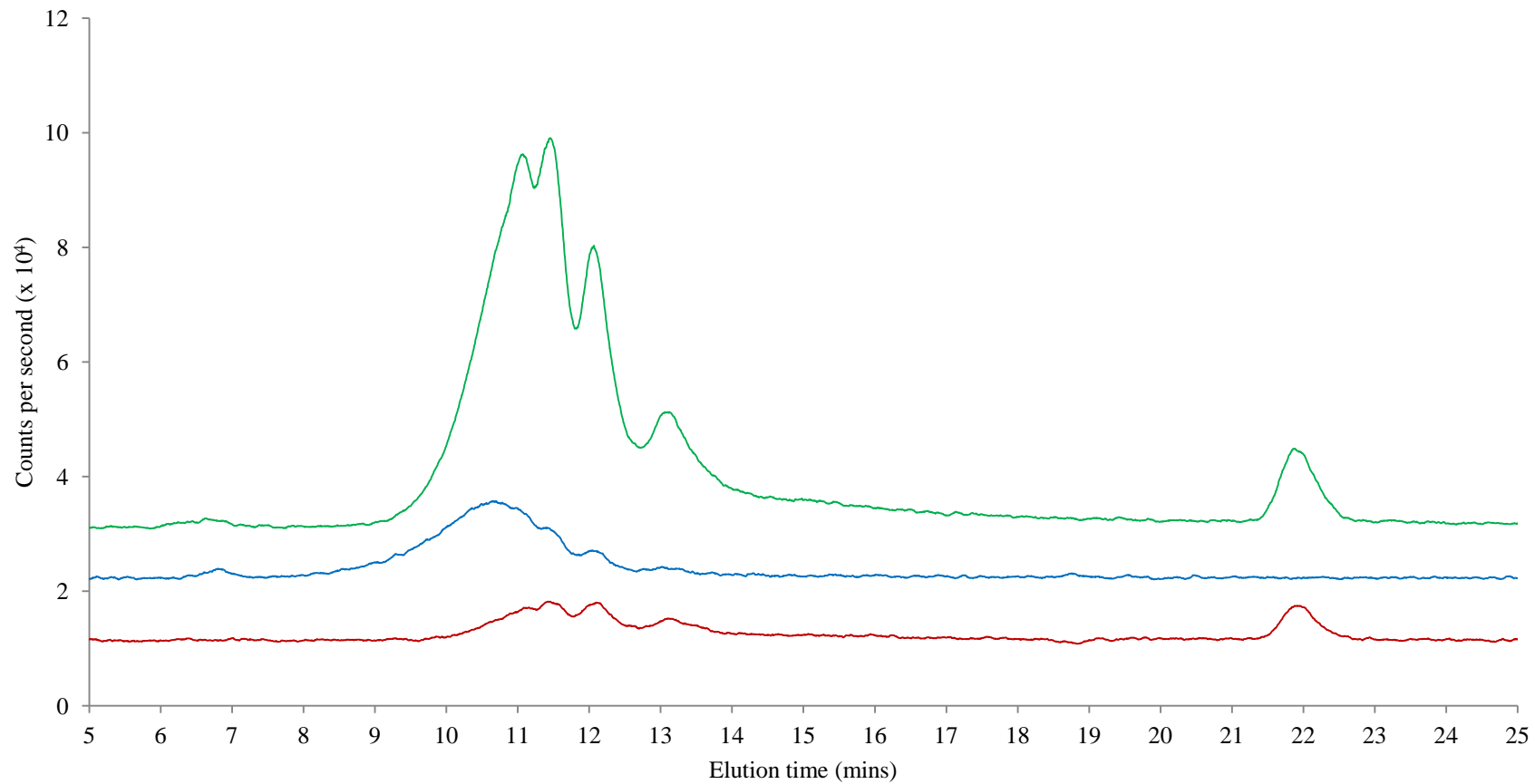


Figure 6.18. Size exclusion chromatograms of ¹²⁷I in soil solution with four clear organic peaks. Chromatograms are offset by 1×10^4 counts per second to allow clear comparison. Red – NI08a; blue – NI07a; green – NI05a.

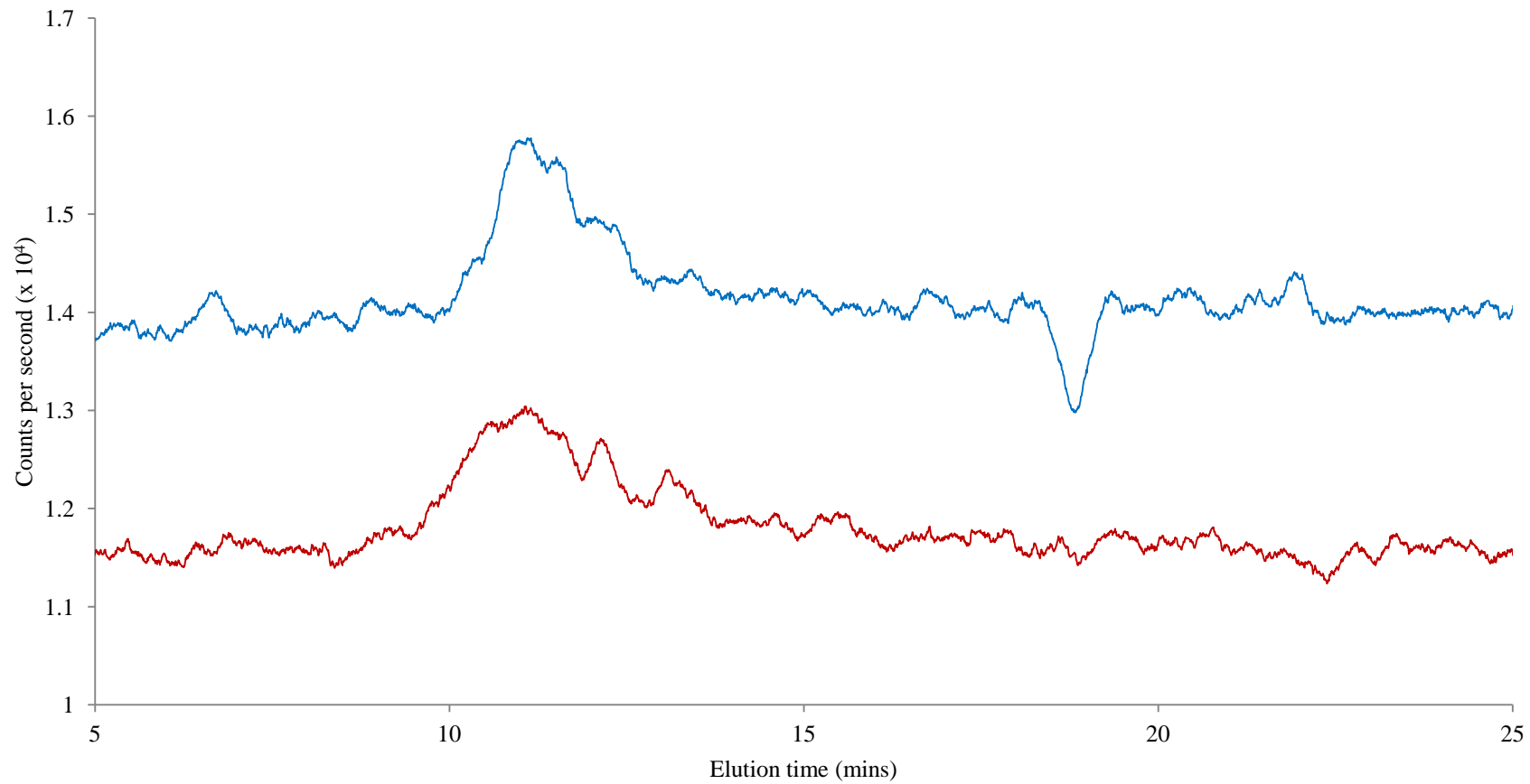


Figure 6.19. Size exclusion chromatograms of ^{127}I in soil solution where separation within organic peak is suggested. Chromatograms are offset by 0.2×10^4 counts per second to allow clear comparison. Red – NI11a; blue – NI15a.

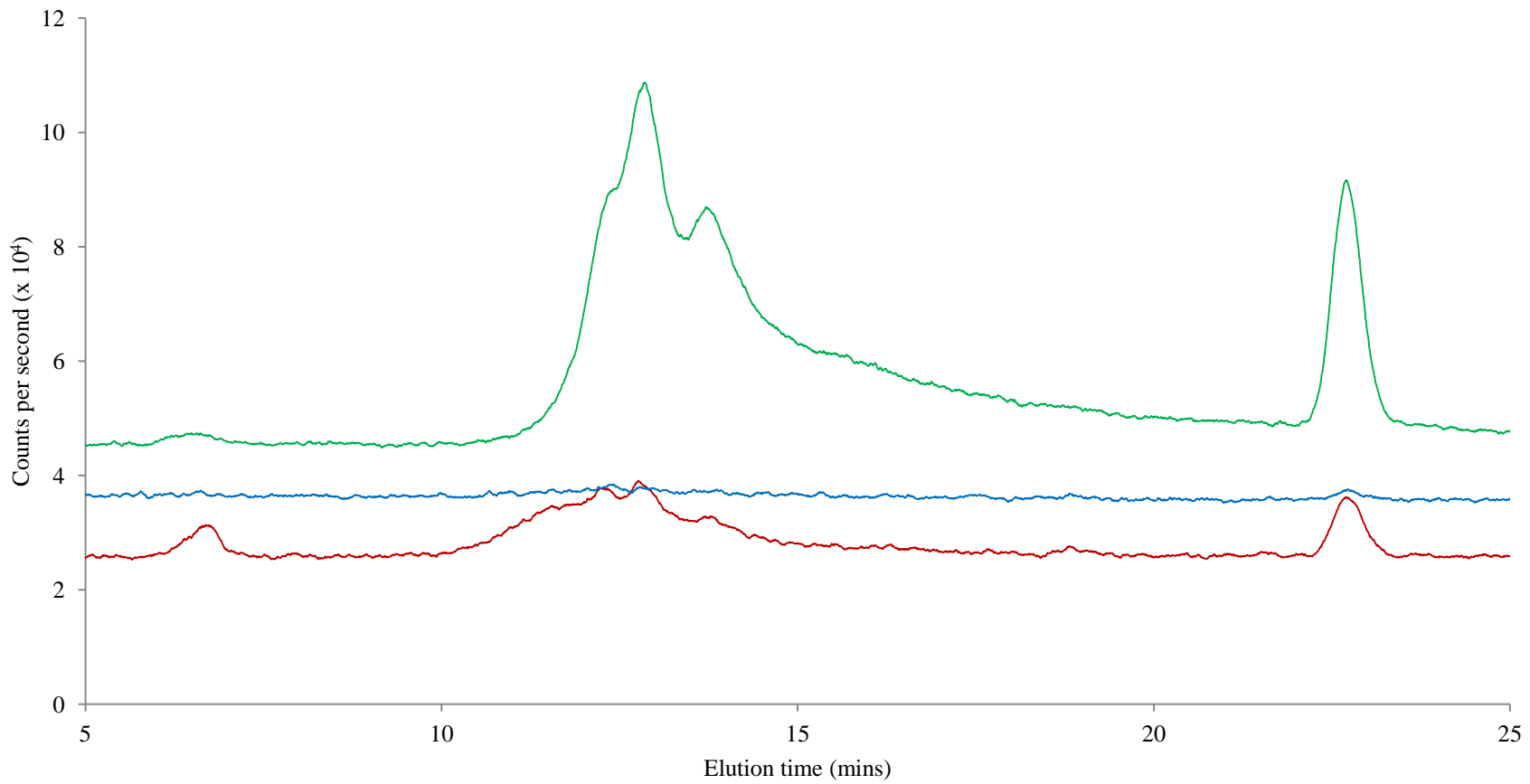


Figure 6.20. Size exclusion chromatograms of ^{127}I in soil solution from soil not used in pot experiment: four clear organic peaks less clear. Chromatograms are offset by 1×10^4 counts per second to allow clear comparison. Red – NI08a; blue – NI07a; green – NI05a.

6.3.8 Phyto-availability of solution iodine

Only cut 4 values have been considered in this section, as soil solution was collected after the end of the pot trial, so the final cut would be most likely to reflect the measured conditions. A correlation between I_L and I_G was expected for both isotopes, based on the phyto-availability of iodine in soil solution. However, there was no correlation between $^{129}I_L$ and $^{129}I_G$, and the correlation between $^{127}I_L$ and $^{127}I_G$ was dominated by soils 05 and 08 (all soils: $r = 0.729$, $p < 0.001$; NI05 and NI08 excluded: $r = -0.432$, $p = 0.083$). This is contrary to the results of Dai et al. (2006) who used ICP-MS to determine iodine in soil solution extracted using rhizon samplers. They reported that uptake by spinach was correlated with soil solution concentrations in the range $8.90 - 819 \mu\text{g I L}^{-1}$. The relatively poor correlation between I_G and I_L in the current study may be due to the timing of extraction of soil solution. Dai et al. (2006) extracted soil solution during growth of the plant, which may be more representative of the growing conditions. Solution from soils NI01 – NI20 was extracted following the last harvest and therefore concentrations measured may not reflect those present in the rhizosphere of actively growing grass. To address this problem, a comparison between $I_{G/S}$ and $I_{L/S}$ was made, since isotope ratios would not be affected by the extraction method in the same way as concentrations. There was a significant positive correlation between $I_{G/S}$ and $I_{L/S}$ for cut 4 data: $r = 0.585$, $p < 0.001$ (Figure 6.21), which was dominated by, but not dependent on, NI05 and NI08 (with NI05 and NI08 excluded $r = 0.400$, $p = 0.004$). This confirms that for all soils, composition of soil solution was important in determining the proportion of each isotope taken up. In all soils except NI05 and NI08, $I_{G/S} < I_{L/S}$, which can be explained by irrigation iodine input ensuring that $I_{G/S} < 1$, while incomplete mixing between isotopes ensured $I_{L/S} > 1$. For NI05 and NI08 the reduced role of irrigation water and apparently large available iodine pools meant that $I_{G/S}$ and $I_{L/S}$ values were similar.

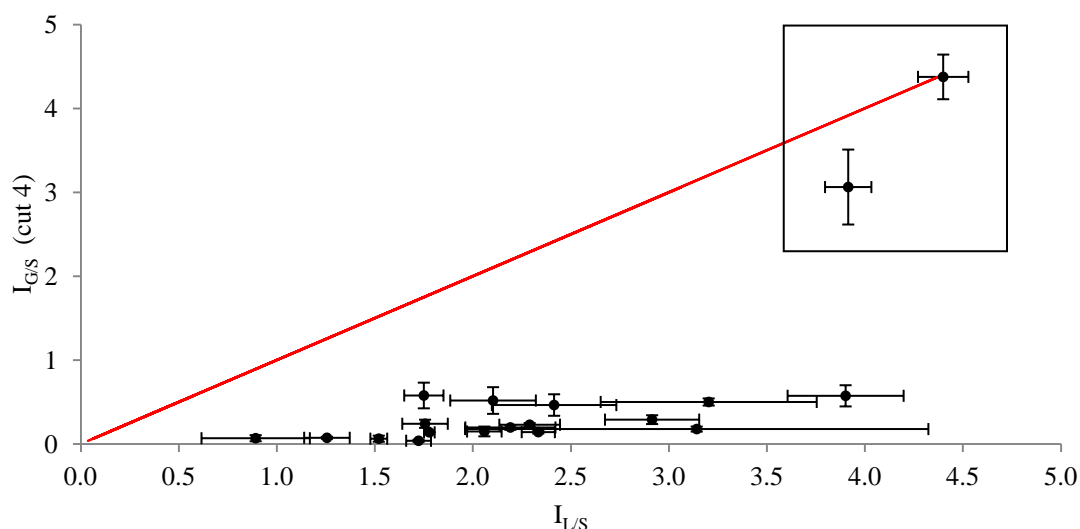


Figure 6.21. Relationship between grass/soil ratio for cut 4 ($I_{G/S}$) and liquid/soil ratio ($I_{L/S}$). Red line is 1:1 line. Solid box includes NI05 and NI08.

There was no correlation between $^{129}\text{I}_G$ or $^{127}\text{I}_G$ and concentration of DOC or individual iodine species in solution. As with interpretation using other solution concentrations, this may be linked to the mismatch between concentrations in solution extracted and those in soil while grass was growing. There is some evidence that different iodine species may be preferentially taken up by plants from hydroponic solution (Whitehead, 1973c; Zhu et al., 2003) and soil (Dai et al., 2006; Smith et al., 1999), although conflicting results have been reported. Hong et al. (2009) investigated uptake of organic iodine (as seaweed) and iodide from soil, but concluded that vegetable type had more effect than iodine species. In both soil and hydroponic solution, transformations between iodine species are likely to occur, so that the species taken up by plants do not necessarily reflect species added. Further experimental investigation into the relationship between iodine speciation in soil solution and uptake by plants is required to clarify the relative availability of species.

6.4 MODELLING UPTAKE FROM SOIL TO GRASS

Results of the experiment were used to create and parameterise a predictive model, to investigate linking uptake of iodine from soil to measurable soil properties. Initially each soil was fitted to the same model structure individually; then rate parameters were correlated to soil properties. These regressions did not satisfactorily describe the uptake parameters, therefore development of a final, optimised model, describing uptake in terms of soil properties, was not possible. Throughout this section, “fitted”

parameters refer to values determined by fitting individual models, and “regressed” parameters are those calculated using equations from regression between soil properties and fitted parameters.

6.4.1 Preliminary model structure and fitting

The soil dynamics ‘array’ model from Chapter 4 was used as the basis for the plant uptake model, with the additions of ^{127}I and ^{129}I uptake from the soil, and incoming ^{127}I in irrigation water, according to Figure 6.22. In the soil dynamics model, concentrations of $^{127}\text{I}_\text{L}$ and $^{129}\text{I}_\text{L}$ were predicted for iodide-added and iodate-added scenarios, but in grass uptake modelling, only concentrations from the iodate-added scenario were used, to match the pot experiment conditions. The model was applied to a period of 2500 hr after spiking, to include the final grass harvest at 2448 hr.

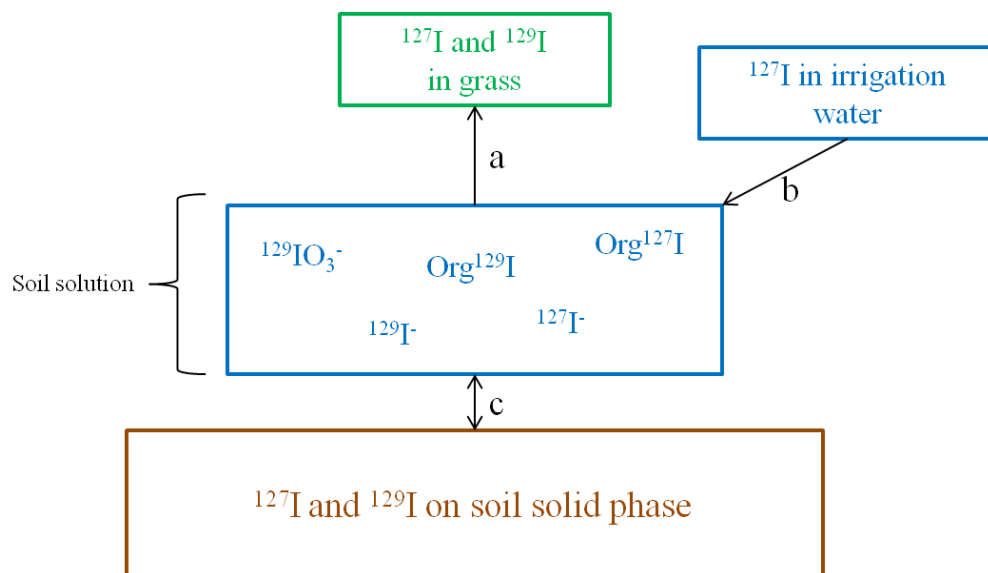


Figure 6.22. Conceptual model of iodine dynamics in a soil-grass system. $^{127}\text{IO}_3^-$ is not represented in solution as it was never observed. $^{129}\text{IO}_3^-$ in solution is included as it was the form in which ^{129}I was added for the pot trial. The values of the coefficients a, b, and c depended on the isotope and were varied as part of method development, as described in the main text.

In Figure 6.22, the coefficients ‘a’, ‘b’, and ‘c’ are used to represent uptake by grass, input from irrigation water and transfers of iodine between pools in soil solution and solid phase respectively. The definitions of a and c were different for the two isotopes and were varied during model development. Incoming ^{127}I in irrigation water (arrow ‘b’ on Figure 6.22) was calculated per hour according to Eqn. 6.9,

$${}^{127}\text{I}_{\text{Ir},t} = \frac{V_{\text{Ir}} \times {}^{127}\text{I}_{\text{Ir}}}{24} \quad (6.9)$$

where ${}^{127}\text{I}_{\text{Ir},t}$ is addition of ${}^{127}\text{I}$ in irrigation water through time ($\mu\text{g I hr}^{-1}$); V_{Ir} is the mean volume of irrigation water provided (L day^{-1}); ${}^{127}\text{I}_{\text{Ir}}$ is the concentration of ${}^{127}\text{I}$ in irrigation water ($\mu\text{g I L}^{-1}$). The value of ${}^{127}\text{I}_{\text{Ir}}$ did not vary between soils, but each soil had a unique value of V_{Ir} , calculated on the basis of water added during the final growth period (cut 4; Section 6.2.1.1). It was assumed that the addition of irrigation water was equal to evapotranspiration from the pot, thus constant soil moisture content was maintained. In the experiment, pots were watered enough to wet the soil but not allow drainage. Therefore there was no leaching term included in the model, but differences in evapotranspiration rates from each soil were accounted for.

Parameter values were fitted to reduce the RSS (residual sum of squares) when comparing measured and modelled values of iodine (${}^{127}\text{I}$ and ${}^{129}\text{I}$) in grass as cumulative values ${}^{127}\text{I}_{\text{G,C}}$ and ${}^{129}\text{I}_{\text{G,C}}$ (μg), rather than concentrations. These are distinct from ${}^{127}\text{I}_{\text{G}}$ and ${}^{129}\text{I}_{\text{G}}$, the concentration of ${}^{127}\text{I}$ and ${}^{129}\text{I}$ in grass ($\mu\text{g I kg}^{-1}$). Simulated uptake of iodine was driven by the total concentrations of iodine in solution (${}^{127}\text{I}_{\text{L}}$ and ${}^{129}\text{I}_{\text{L}}$), thus not assuming a preference for any one species over another. When the model was initially set up, a simple rate coefficient ‘kp’ was used to determine the rate of uptake of both ${}^{127}\text{I}$ and ${}^{129}\text{I}$ to grass. In this case arrow ‘a’ in Figure 6.22 was described in the model by Eqns. 6.10 and 6.11,

$$d({}^{129}\text{I}_{\text{G,C}})/dt = kp \times {}^{129}\text{I}_{\text{L}} \quad (6.10)$$

$$d({}^{127}\text{I}_{\text{G,C}})/dt = kp \times {}^{127}\text{I}_{\text{L}} \quad (6.11)$$

where ${}^{129}\text{I}_{\text{G,C}}$ and ${}^{127}\text{I}_{\text{G,C}}$ are weights (μg) of ${}^{129}\text{I}$ and ${}^{127}\text{I}$ in grass at time t (hr) respectively; kp is the rate coefficient governing uptake of iodine (hr^{-1}), fitted by the model; and ${}^{129}\text{I}_{\text{L}}$ and ${}^{127}\text{I}_{\text{L}}$ are total concentrations of ${}^{129}\text{I}$ and ${}^{127}\text{I}$ in soil solution ($\mu\text{g I L}^{-1}$).

The transfer of ^{129}I between soil solution and solid phase (arrow 'c' on Figure 6.22) was described by dynamics equations determined in Chapter 4. Transfer of ^{127}I between these two pools could have been controlled by the same equations, however this has not been fully investigated and the role of the recalcitrant pool would need accounting for. Therefore solid/liquid partitioning of ^{127}I in this model was simplified to be controlled by a single equilibrium, with rate coefficients k_6 and k_7 defining exchange between the two pools according to Eqns. 6.12 – 6.14:



where

$$\frac{d(^{127}\text{I}_{\text{solid}})}{dt} = (k_7 \times ^{127}\text{I}_{\text{L}}) - (k_6 \times ^{127}\text{I}_{\text{solid}}) \quad (6.13)$$

and

$$\frac{d(^{127}\text{I}_{\text{L}})}{dt} = (k_6 \times ^{127}\text{I}_{\text{solid}}) - (k_7 \times ^{127}\text{I}_{\text{L}}) - (k_p \times ^{127}\text{I}_{\text{L}}) \quad (6.14)$$

where $^{127}\text{I}_{\text{solid}}$ is the concentration of ^{127}I on the soil solid phase ($\mu\text{g I kg}^{-1}$); and parameters k_p (hr^{-1} , uptake to grass), k_6 (hr^{-1} , desorption from solid) and k_7 (hr^{-1} , sorption to solid) were fitted by the model, to optimise values of $^{127}\text{I}_{\text{G,C}}$. The native iodine in soil solution, i.e. ^{127}I not originating from irrigation water, was accounted for in the initial set-up of the model: $^{127}\text{I}_{\text{L}}$ had a soil-dependent non-zero value at $t = 0$ (see Chapter 4 for details). Therefore uptake of native iodine to plant was also included. This set-up results in a build-up of ^{127}I from irrigation water onto the soil solid phase, as no leaching term is included. Although this does not fully represent the field situation, where some loss of iodine to leaching is likely, it does represent the pot experiment from which the data were derived. Another difference between the pot experiment and a field situation is that transfer of iodine from plant to soil may also be expected in a field situation, where vegetation dies and falls back onto the soil surface. This was not the case in this experiment, however, where grass was harvested and removed from the pot. Therefore no plant-to-soil transfer term was included.

6.4.2 Model development

Model development was carried out using data from NI01, modifying the rate coefficients as necessary and fitting parameter values to measured values of $^{127}\text{I}_{\text{G,C}}$ and $^{129}\text{I}_{\text{G,C}}$ at four time points equating to the four grass harvests (672, 1032, 1560 and 2448 hr). Using Eqns. 6.10 and 6.11 to describe uptake resulted in linear increases in $^{127}\text{I}_{\text{G,C}}$ and $^{129}\text{I}_{\text{G,C}}$ with time, which did not match the measured trend in the data. Therefore modifications to Eqns. 6.10 and 6.11 were trialled, in each case replacing ‘kp’ with an alternative rate coefficient (Table 6.9). To account for the apparent decrease in uptake rate of ^{127}I , the rate coefficient in Eqn. 6.11 was first modified to vary with the reciprocal of time, t , to give uptake dependent on $\text{kp}/(t+1)$, where kp was a fitted parameter (Model B). The term was required to be ‘ $t+1$ ’ because if it was just ‘ t ’, it would not be possible to calculate the rate coefficient at $t = 0$. This was successful in fitting to measured $^{127}\text{I}_{\text{G,C}}$ values, so the same modification was made to Eqn. 6.10 for ^{129}I (Model C). Uptake of ^{129}I was not successfully modelled using this rate coefficient, so separate fitted rate parameters kp_S (rate parameter for ‘spiked’ iodine) and kp_N (rate parameter for ‘native’ iodine) were allowed for the two isotopes: the uptake rate coefficient in Eqn. 6.10 became $\text{kp}_\text{S} / (t+1)$ and in Eqn. 6.11 became $\text{kp}_\text{N} / (t+1)$ (Model D). Although a good fit was still obtained for ^{127}I uptake, uptake of ^{129}I was underestimated at longer times, so the dependence on time was removed and therefore the rate coefficient in Eqn. 6.10 became equal to the fitted parameter kp_S . Iodine input from irrigation water and partitioning between solid and solution remained as described in Section 6.4.1. These trials, and the resulting RSS values from fitting parameters k_6 and k_7 concurrently with kp , or kp_S and kp_N , are described in Table 6.9.

Table 6.9. Summary of fitting results for NI01 plant uptake, as the rate coefficient describing uptake varied, sometimes including reciprocal dependence on time, t . The ‘rate coefficients’ listed were substituted for kp in Eqns. 6.10 (^{129}I) and 6.11 (^{127}I) as shown for each model. ‘ kp_S ’ and ‘ kp_N ’ are fitted parameters for ^{129}I and ^{127}I respectively, which form part of the rate coefficient for each isotope.

Model	Rate coefficient (^{129}I)	Rate coefficient (^{127}I)	Total RSS (x 1000)	RSS (^{129}I) (x 1000)	RSS (^{127}I) (x 1000)
A	kp	kp	19.8	0.00379	19.8
B	kp	kp / (t+1)	1.58	1.27	3.12
C	kp / (t+1)	kp / (t+1)	190	190	0.001
D	$\text{kp}_\text{S} / (t+1)$	$\text{kp}_\text{N} / (t+1)$	0.0964	0.0492	0.0472
E	kp_S	$\text{kp}_\text{N} / (t+1)$	0.0509	0.00361	0.0472

6.4.3 Final grass uptake model

RSS values show that the best fit was obtained from Model E (from this point onwards the ‘grass uptake model’), when both isotopes were allowed individual rate parameters, and the uptake rate coefficient was time dependent for ^{127}I but not ^{129}I . The grass uptake model was set up and run for all soils individually; a full model description is presented in Appendix 7 and the conceptual model is shown in Figure 6.23.

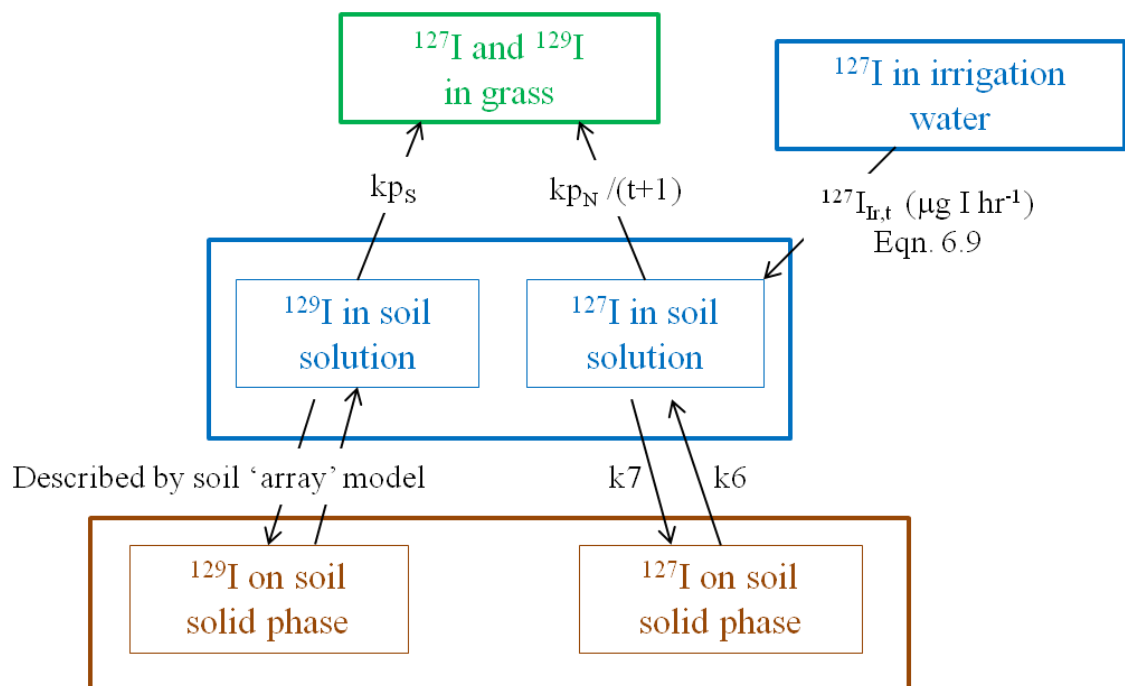


Figure 6.23. Conceptual model of iodine dynamics in a soil-grass system, showing optimised rate parameters.

There was large uncertainty associated with the fitted parameters values in most cases (Table 6.10), which reflected the relatively large standard errors of measured $^{129}\text{I}_{\text{G,C}}$ and $^{127}\text{I}_{\text{G,C}}$ values (example soils in Figure 6.24 and Figure 6.25). Uncertainty in measured $^{129}\text{I}_{\text{G,C}}$ and $^{127}\text{I}_{\text{G,C}}$ values increased with time because they were cumulative, therefore uncertainty in earlier measurements also affected later values. In some soils such as NI03, measured $^{127}\text{I}_{\text{G,C}}$ values did not follow a smooth trend (Figure 6.24D), so the modelled values were a compromise across the modelled timescale. However, the overall fit when all soils were considered was very good: $^{127}\text{I}_{\text{G,C}} - r = 0.948$, $p < 0.001$; $^{129}\text{I}_{\text{G,C}} - r = 0.973$, $p < 0.001$ (Figure 6.26).

Table 6.10. Parameter values for the plant uptake model, individually fitted to all soils used in the pot experiment. Mean and standard deviation values calculated by OpenModel. RSS is the residual sum of squares when $^{127}\text{I}_{\text{G,C}}$ and $^{129}\text{I}_{\text{G,C}}$ were fitted.

Soil	k6 (x1000)		k7 (x1000)		kp _N (x1000)		kp _S (x1000)		RSS (x1000)
	Mean	S.D.	Mean	S.D.	Mean	S.D.	Mean	S.D.	
NI01	2.46	37.1	50.7	19.3	4.13	60.0	0.161	0.0527	0.0509
NI02	0.108	1.30	0.393	0.713	1.46	16.0	0.175	0.108	0.480
NI03	0.342	22.6	0.000	20.8	0.129	8.31	0.0214	0.336	8.01
NI04	0.101	0.641	0.000	0.452	0.971	5.17	0.0129	0.0127	2.90
NI05	0.155	5.38	0.000	2.32	0.109	3.46	0.0274	0.290	1490
NI06	0.767	0.895	0.000	0.821	0.123	0.127	0.108	0.118	4.46
NI07	0.107	2.41	3.65	11.1	2.48	46.5	0.0155	0.0129	0.851
NI08	0.101	1.22	0.000	0.555	0.988	10.6	0.0143	0.0712	88.4
NI09	0.652	58.9	2.89	49.4	0.287	25.1	0.0140	0.133	0.713
NI10	0.386	7.84	0.000	7.55	0.0989	1.97	0.0978	0.270	0.683
NI11	1.06	21.4	0.508	21.4	0.160	3.22	0.0610	0.0424	0.988
NI12	0.0831	0.933	0.000	0.438	1.59	15.0	0.139	0.198	3.27
NI13	0.0873	5.32	0.000	4.84	1.90	110	0.00960	0.0171	0.791
NI14	0.0974	1.04	0.000	0.728	1.14	11.2	0.0644	0.0498	0.201
NI15	0.347	0.966	0.000	0.811	0.226	0.470	0.127	0.287	10.9
NI17	0.224	1.79	0.000	1.39	0.210	1.60	0.0356	0.0615	0.247
NI18	0.404	3.33	0.000	3.23	0.153	1.23	0.0465	0.183	2.53
NI19	0.0926	1.11	1.12	0.824	2.14	22.9	0.220	0.175	13.9
NI20	0.0658	0.854	0.102	0.274	1.10	12.7	0.0441	0.0901	1.92

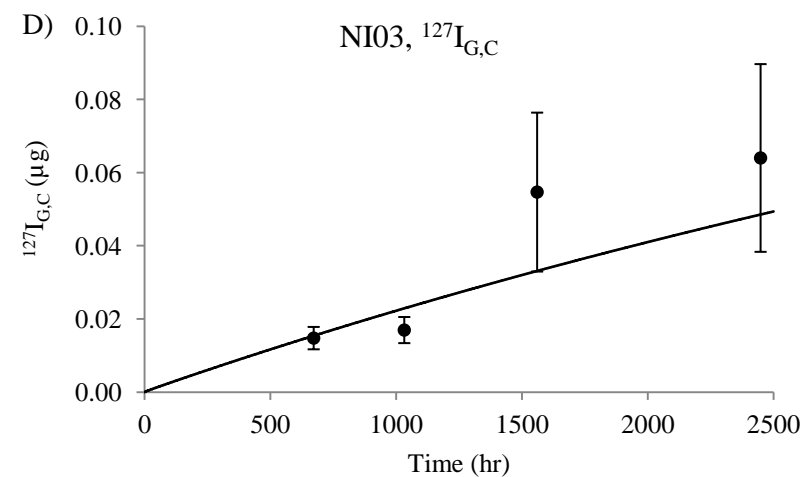
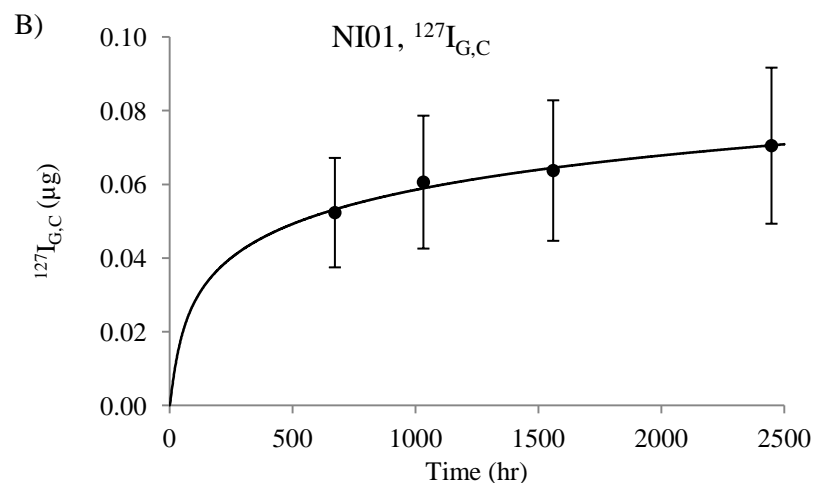
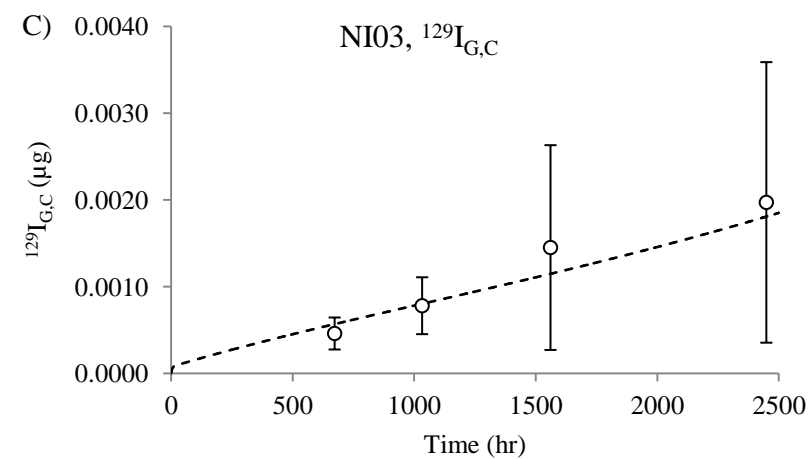
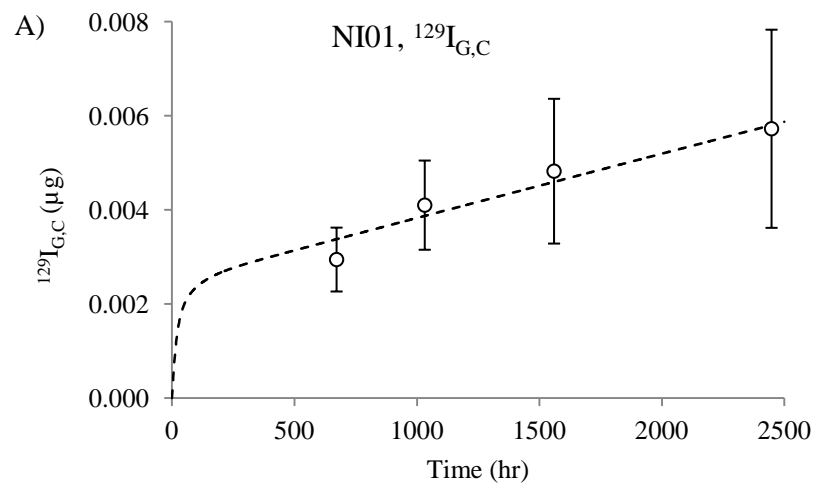


Figure 6.24. Change in the cumulative amount of iodine in grass with time, for Iodine-129 ($^{129}\text{I}_{\text{G,C}}$; A and C) and Iodine-127 ($^{127}\text{I}_{\text{G,C}}$; B and D), following ryegrass cultivation on soil spiked with $64.1 \text{ g } ^{129}\text{I ha}^{-1}$ as iodate. Results for NI01 (A and B), a mineral soil; and NI03 (C and D), an example of a soil with a relatively poor fit to the model. Error bars show standard error of triplicate measurements for each harvest. Notice that Y-axis scales are unique to each graph.

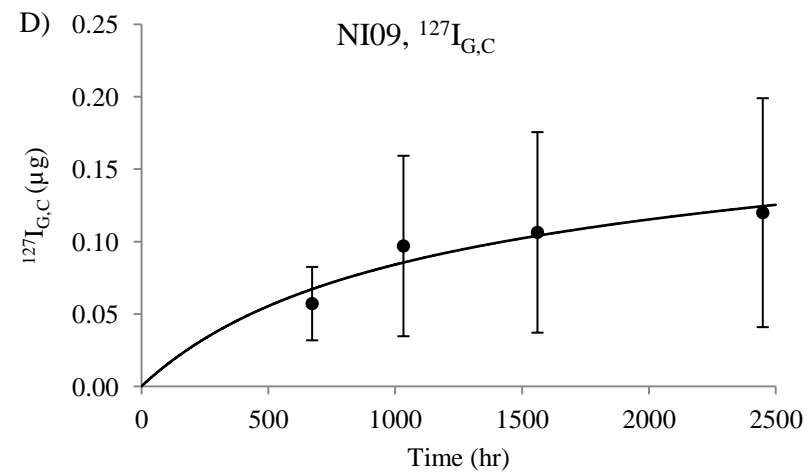
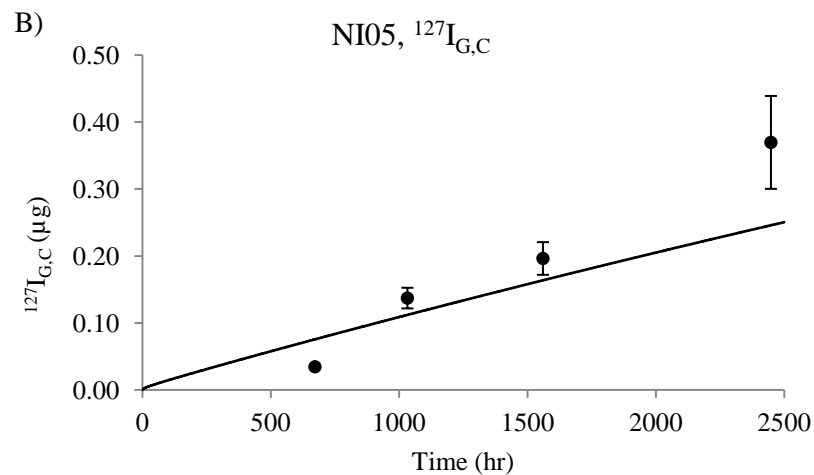
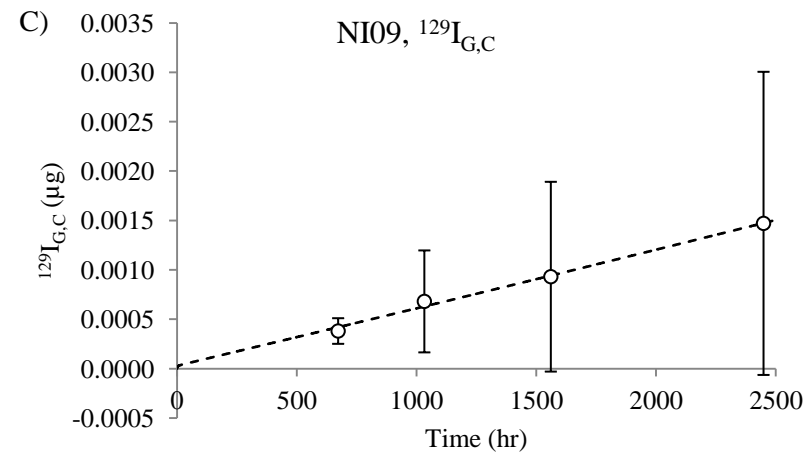
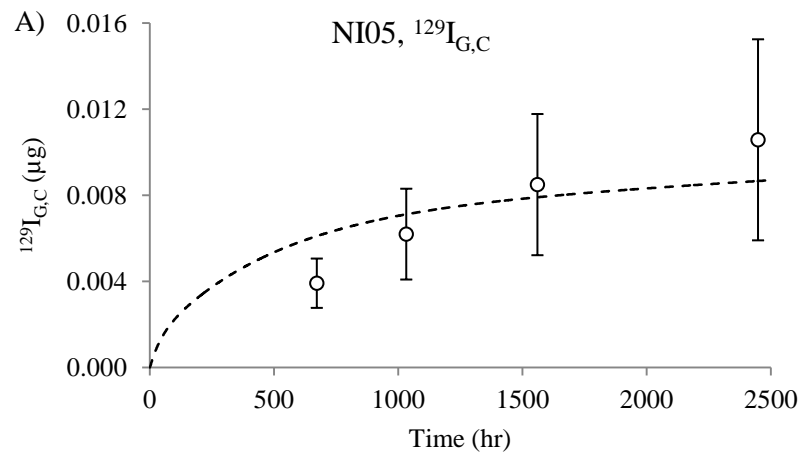


Figure 6.25. Change in the cumulative amount of iodine in grass with time, for Iodine-129 ($^{129}\text{I}_{\text{G,C}}$; A and C) and Iodine-127 ($^{127}\text{I}_{\text{G,C}}$; B and D), following ryegrass cultivation on soil spiked with $64.1 \text{ g } ^{129}\text{I ha}^{-1}$ as iodate. Results for NI05 (A and B), a coastal soil; and NI09 (C and D), an organic soil. Error bars show standard error of triplicate measurements for each harvest. Notice that Y-axis scales are unique to each graph.

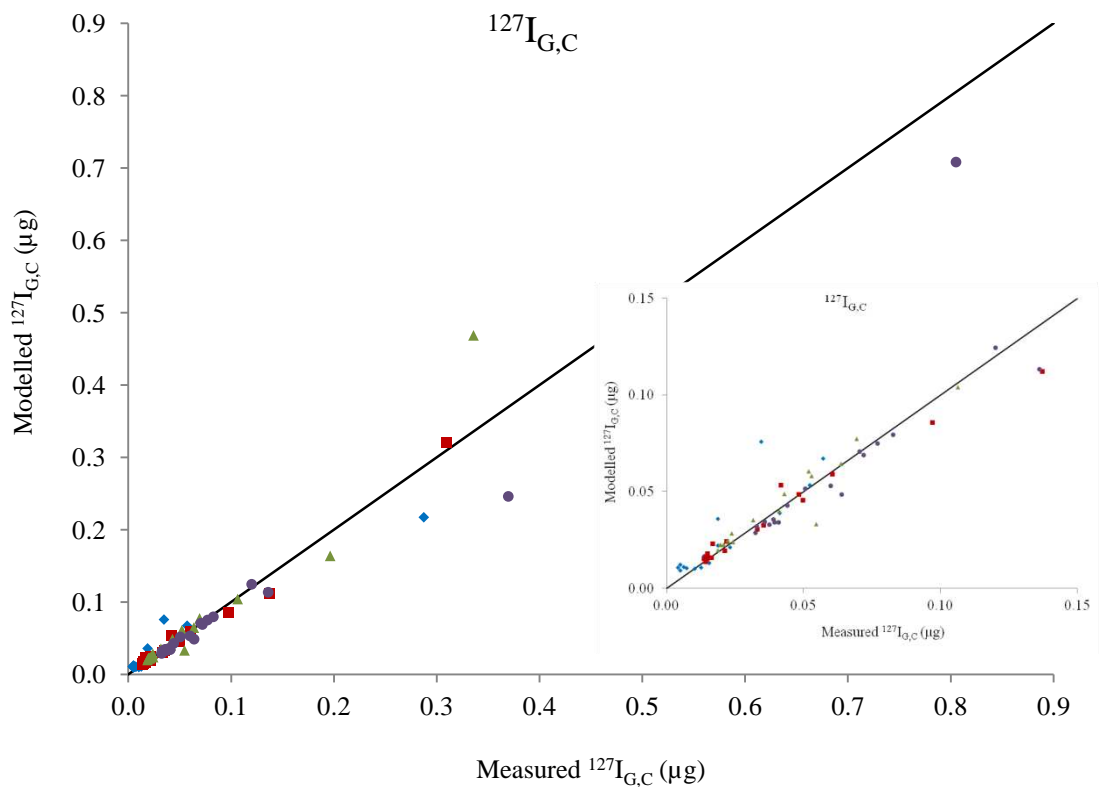
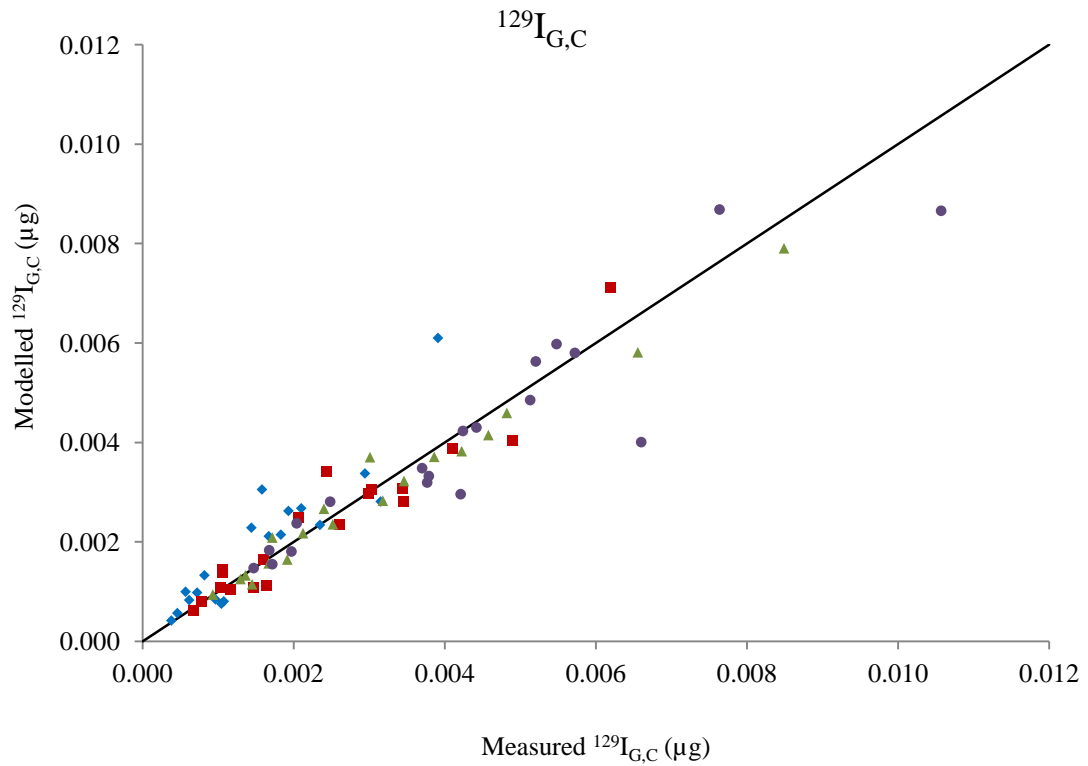


Figure 6.26. Comparison of modelled and measured weights of ^{127}I and ^{129}I in grass ($^{127}\text{I}_{\text{G,C}}$ and $^{129}\text{I}_{\text{G,C}}$ respectively) as labelled, at the four harvest times: cut 1 (672 hr; blue diamonds), cut 2 (1032 hr; red squares), cut 3 (1560 hr; green triangles), cut 4 (2448 hr; purple circles). Inset shows detail of graph close to the origin.

6.4.4 Discussion of fitted results

For a good model fit, the rate coefficients for the two isotopes had to be ascribed different values, suggesting a difference in availability. This is likely to be due to the origin of the two isotopes. Iodine-127 was added every hour in the model and therefore, assuming passive uptake, its uptake relied mainly on the rate of grass growth rather than concentration in solution as determined by sorption to solid phase. As discussed in Section 6.3.4, passive uptake cannot be ruled out by the experimental results obtained. By ascribing reciprocal time-dependence to the uptake rate coefficient for ^{127}I (and assuming passive uptake), then after 2000 hr, the rate of uptake in the model was 1/2000 of what it was at $t = 0$. This initially seems too great a reduction, but may not be unrealistic: initially after germination, the grass was growing strongly, producing new roots and fresh shoots. As time passed and grass matured, growth rate was likely to reduce. By the end of the experiment, the grass looked very unhealthy in many pots and in some cases was pot-bound. Therefore a much slower growth-rate, leading to reduced transpiration and hence passive uptake of ^{127}I , may be realistic. This may not be the case in the field, where growth is unlikely to be restricted by space and soil chemistry as it was in some pots. Therefore under field conditions, the rate coefficient for ^{127}I uptake may be dependent solely on $^{127}\text{I}_L$, as seen for ^{129}I in the experiment. An alternative way to represent the growth-rate effect would be to directly base uptake on growth rate calculated from yield and growth times (g day^{-1}). However, since cut 1 included the time taken to germinate as well as grow, the growth rate calculated would be falsely low for this cut, so an estimation of the actual growth-rate would have to be made.

The rate of ^{129}I uptake was directly dependent on the concentration in solution, with no requirement for the rate coefficient to be dependent on time. Sorption of ^{129}I onto the soil solid phase after spiking (determined by experiment in Chapter 4 to be much more rapid than the time taken for grass ^{129}I to germinate) caused a decrease in $^{129}\text{I}_L$ through time, decreasing the amount of ^{129}I taken up at later times. In many cases (e.g. NI01, Figure 6.24A and NI05, Figure 6.25A), the model predicted that the rate of ^{129}I uptake was very rapid initially, overestimating $^{129}\text{I}_{G,C}$ for cuts 1 and 2, but becoming more constant at 500 – 1000 hr after commencement of the experiment. In the organic soils, e.g. NI03 (Figure 6.24) and NI09 (Figure 6.25), this did not occur. This is likely to have been caused by the difference in sorption behaviour onto the soils: in highly

organic soils, sorption was almost instantaneous and therefore $^{129}\text{I}_L$ concentrations were low from the beginning of the experiment and did not result in fast uptake at early times. Contrastingly, in the majority of soils ^{129}I in solution was maintained for longer and since uptake was directly proportional to $^{129}\text{I}_L$, an early peak in modelled $^{129}\text{I}_{G,C}$ values was observed. This was not reflected in the measured values due to the time delay between spiking and initial grass growth, caused by germination. This could have been prevented by starting grass growth before spiking, however this would have had important repercussions for distribution of the spike through the soil: by spiking first, the soil could be thoroughly mixed to more evenly distribute ^{129}I . Despite this weakness in predictions at early times, prediction of the measured data at later times was generally good.

It was expected that the equilibrium between solid and solution phase for ^{127}I would be controlled by $k_6 < k_7$. In most cases, however, $k_6 > k_7$ (Table 6.10), promoting release of ^{127}I from the solid phase, rather than sorption onto it. Experimental results throughout this thesis have shown that this unlikely to be due to actual release from the solid phase, and therefore is probably a factor of the model as a whole. It is likely that since incoming ^{127}I in irrigation water maintained the $^{127}\text{I}_L$ pool, the k_6/k_7 ratio was affected. Further investigation into ^{127}I soil dynamics, accounting for the recalcitrant portion of ^{127}I that has been inferred, would allow a more comprehensive description of solid-solution dynamics, thereby potentially clarifying the situation.

To try to link uptake to soil properties, a stepwise regression was carried out for each soil using measured properties Al, Fe and Mn oxide content, pH, SOC concentration and I_S as predictors for rate parameters kp_S and kp_N . The resulting predictive equations were poor for all soils in all classes (Eqns. 6.15 and 6.16, Figure 6.27).

$$kp_S = 0.0432 + (0.110 \times \text{Mn}) \quad (6.15)$$

Correlation of fitted vs regressed kp_S : $r = 0.551$, $p = 0.015$ (Figure 6.27A)

$$kp_N = 1.708 - (0.030 \times \text{SOC}) - (0.0054 \times I_S) \quad (6.16)$$

Correlation of fitted vs regressed kp_S : $r = 0.491$, $p = 0.033$ (Figure 6.27B)

The poor prediction from soil properties is likely to be, at least in part, due to the large error associated with both measured $^{127}\text{I}_{\text{G,C}}$ and $^{129}\text{I}_{\text{G,C}}$, and fitted parameter values. This may originate from the k_6/k_7 control on ^{127}I dynamics, or may suggest that further development of the uptake mechanism in the model is required. However, prediction of uptake to grass based on soil properties was not pursued further in this work, due to the poor regression results.

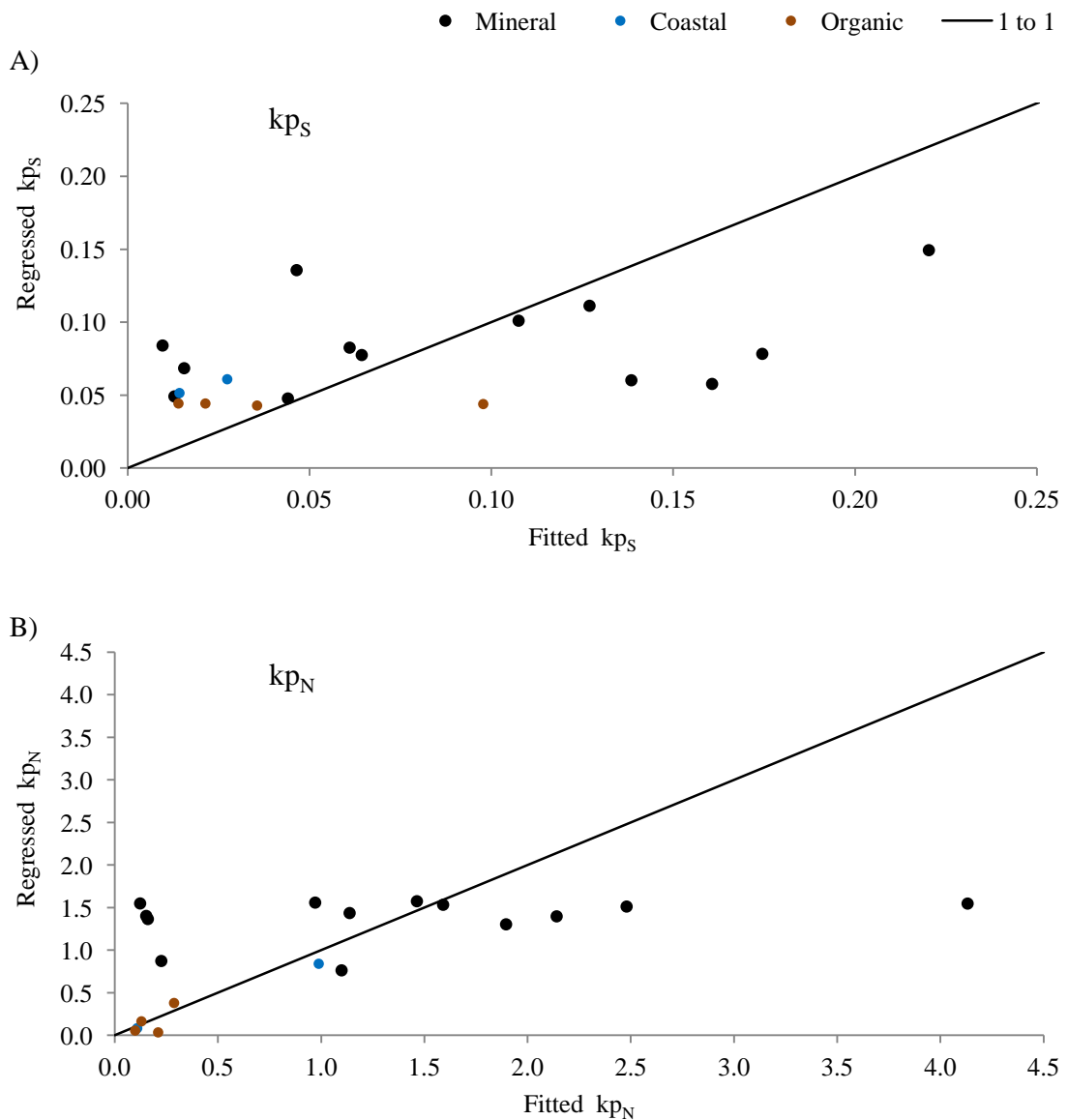


Figure 6.27. Comparison of regressed (based on soil properties) and fitted (from plant uptake model) values of A) k_{pS} and B) k_{pN} .

6.5 CONCLUSIONS

The isotopic composition of iodine taken up by grass grown on soil spiked with $^{129}\text{IO}_3^-$ showed that the main process governing the dynamics of plant uptake is frequent replenishment of a transient phyto-available pool of iodine. Rapid assimilation of the ^{129}I spike into the soil solid phase, and relatively low availability of native iodine, meant that in most cases the majority of phyto-available iodine was provided by background concentrations of iodine in irrigation water (c. $0.8 \mu\text{g I L}^{-1}$). The rate of iodine sorption onto soil depended on soil properties and was most significantly affected by organic matter content. Rapid fixation of ^{129}I onto soil was evident from recovery of ^{129}I in TMAH extractions of the potted soil at the end of the experiment, and the very small proportion of soil iodine taken up by grass (typically 0.000341 % - 4.53 % of added soil ^{129}I and 0.000466 % - 2.51 % of soil ^{127}I). The isotopic ratio in grass ($^{129}\text{I}/^{127}\text{I}$) to that in soil (the 'grass/soil ratio', $I_{G/S}$) confirmed that ^{129}I became progressively less phyto-available with time.

In most cases, ^{127}I was over-represented in grass compared to soil solution, and replenishment to the phyto-available pool in solution was slower than uptake: a significant negative correlation was observed between growth rate and grass iodine concentration for both isotopes, for all soils. Near-constant provision of iodine (^{127}I) in irrigation water superseded the rate of replenishment from within the soils, resulting in an estimated contribution to grass iodine from irrigation water of 74 % (excluding coastal soils). The measured concentration of ^{127}I in irrigation water confirmed that this was the major source of ^{127}I in the grass in most cases. However in the coastal soils, replenishment of phyto-available iodine from the soil was much greater so the ratio of isotopes in grass was similar to that in pore-water; irrigations sources were comparatively minor.

The apparent difference in required rate coefficients for the two isotopes is likely to result from a combination of the model structure and experimental factors. If ^{127}I and ^{129}I were present in the soil solution at the same concentrations and as the same species, there would be no reason for grass to differentiate between them in uptake. However, the concentration of $^{129}\text{I}_L$ was controlled by sorption to the solid phase, while ^{127}I was continually added throughout the experiment. Therefore the reduced uptake due to less vigorous growth at later times was apparent for ^{127}I , but sorption to

the solid phase reduced $^{129}\text{I}_L$ before growth rate affected uptake of ^{129}I . Furthermore, speciation of the two isotopes is likely to have been different during the lifetime of the grass: by the time the grass had germinated, $^{129}\text{I}_L$ would have been mainly organic (see results in Chapter 4), while ^{127}I was being added as mainly inorganic species, due to the low DOC content of the deionised water. The larger physical size of OrgI is likely to preclude its uptake by plants, while iodide and iodate would be more readily taken up as part of the transpiration stream, thus increasing k_{pN} relative to k_{pS} .

It was not possible to model uptake to grass in terms of soil properties, due to the large uncertainty associated with fitted parameters. Further development of the model is necessary to confirm the processes controlling ^{127}I partitioning between solid and solution phase, and to elucidate the controls on uptake from soil for both isotopes. These requirements aside, the model showed that uptake rates for both isotopes varied between soils and therefore are likely to be reliant to some extent on soil properties.

At the end of the ^{129}I -spiked pot experiment (102 days), the dominant form of both ^{127}I and ^{129}I in soil solution was organic. Very low concentrations of both ^{127}I and ^{129}I in the majority of soil pore-waters made integration of chromatograms difficult, and as a result, little emphasis could be placed on the relative importance of individual species in solution, except to confirm the dominance of Org-I. This was supported by a significant positive correlation of both isotopes with DOC in soil pore-water. In soils with high pore-water iodine concentrations, speciation of soil solution by SEC identified four peaks within the ^{127}I organic fraction. The identities of these species were not pursued, but were confirmed to be pedogenic, not phytogenic, in origin and may indicate capacity for rapid iodination of aromatic moieties within soluble humus compounds.

For all but one soil, mixing of spiked and native iodine was incomplete by the end of the experiment, as shown by $I_{L/S} > 1$, where $I_{L/S}$ is the 'liquid/soil ratio'; the isotopic ratio in soil pore-water ($^{129}\text{I}/^{127}\text{I}$) to that in soil. This suggests the presence of a pool of native iodine in the solid phase that was unavailable for mixing in the timescale studied, as identified in humic acid in Chapter 5. Indeed, in the high-SOC soils, there was incomplete isotopic mixing despite extremely rapid sorption of spiked iodine onto SOC. In the coastal soils, slower mixing of the two isotopes resulted in high

liquid/soil concentration ratios. Slow mixing and the consequent persistence of the spike in soil solution implies a large labile pool within the soil in coastal samples subject to high levels of iodine input, which was indicated in Chapter 4.

This chapter has elucidated some information about the availability of iodine freshly-added to soil, both in terms of its availability over months after one addition (^{129}I), and for frequent additions such as would occur in rain. Comparing concentration ratio values between field and pot experiments has confirmed the importance of irrigation/rainwater in providing a consistent source of iodine to grass. However, because the grass was grown in pots, there were aspects of the experiment which did not well-represent field conditions: leaching through the soil profile was not accounted for, and growth restriction may have affected uptake of ^{127}I . These factors still need investigating.

7 TOTAL IODINE IN SOILS AND VEGETATION FROM THE ROTHAMSTED PARK GRASS EXPERIMENT

7.1 INTRODUCTION

The Park Grass experiment at Rothamsted Research, Harpenden, Hertfordshire, was initiated in 1856 and is the longest running experiment on permanent grassland in the world (Rothamsted Research, 2006). Throughout the history of the experiment, samples of vegetation and soil have been collected (usually twice a year) and archived (Rothamsted Research, 2006; Silvertown et al., 2006). Primarily set up to investigate the effect of various soil treatments on hay yields, it has since been used to follow changes in many environmental parameters, e.g. invertebrate species (Morris, 1992); soil chemistry (Blake and Goulding, 2002; Goulding et al., 1989; Johnston et al., 1986; Tye et al., 2009); plant species (Dodd et al., 1994; Silvertown et al., 2006) and vegetation yields (Jenkinson et al., 1994). Plots are treated with combinations of N, P, K, Na, Mg and Si plus farmyard (FYM) and pelleted poultry manures according to set regimes (Table 7.1; Silvertown et al. (2006)). In 1903, plots established in 1856 were split so that the effect of liming (4,000 kg ha⁻¹ lime added every four years) could be seen. In 1965 individual plots were further split into four sub plots, each maintained at a different pH: sub-plot “a” pH = 7; sub-plot “b” pH = 6; sub-plot “c” pH = 5; sub-plot “d”, unlimed (Rothamsted Research, 2006). Natural soil pH at the site is c. 5.5 so sub-plot c only achieves the intended nominal pH of 5 when a treatment has an acidifying effect. In addition to treated plots, two control plots are maintained, subjected only to the liming regime described. The experiment provides a unique opportunity to examine the effects of temporal changes in iodine concentration in soil and vegetation, incorporating the influence of annual rainfall and soil chemistry, without the added complexity of variation coastal proximity, underlying geology, etc.

7.2 MATERIALS AND METHODS

Samples of soil and vegetation from a range of years, treatments and control plots were sampled from the archive. Stored soil samples were dried and some appeared to have been finely ground; others were apparently sieved. Further milling to ensure sample consistency was undertaken as necessary (see Section 2.2.1). Vegetation samples had been dried and milled before archiving so needed no further preparation.

Table 7.1. Details of soil treatments. Codes are those defined in Rothamsted Research (2006). Application rates quoted are from Macdonald, A. (pers. comm.) or Warren and Johnston (1963).

Plot	Treatment codes	Treatment description	Elemental composition (per hectare per treatment)
3	None	None	None
9/2	N2 P K Na Mg	Ammonium sulphate Triple superphosphate Potassium sulphate Sodium sulphate Magnesium sulphate	96 kg N & 110 kg S 35 kg P 225 kg K & 99 kg S 15 kg Na & 10 kg S 10 kg Mg & 13 kg S
12	None	None	None
13/1	(FYM/Fishmeal)	35,000 kg ha ⁻¹ (every 4 years) FYM, last applied in 1993. Fishmeal applied 2 years after FYM, until 1995. Applications every 4th year 1907 - 1955, at 753 kg ha ⁻¹ per application; every 4th year 1959 - 1995, at 63 kg N ha ⁻¹ .	240 kg N, 45 kg P, 350 kg P, 25 kg Na, 25 kg Mg, 40 kg S, 135 kg Ca 63 kg N
13/2	FYM/pelleted poultry manure	35,000 kg ha ⁻¹ FYM every 4 years (2005, 2001, 1997 etc). Fishmeal applied 2 years after FYM, until 1999. Applications every 4th year 1907 - 1955, at 753 kg ha ⁻¹ per application; every 4th year 1959 - 1999, at 63 kg N ha ⁻¹ . Pelleted poultry manure every 4 years (2003, 2007, 2011, etc), replacing fishmeal in 2003.	240 kg N, 45 kg P, 350 kg P, 25 kg Na, 25 kg Mg, 40 kg S, 135 kg Ca 63 kg N 65 kg N
14/2	N*2 P K Na Mg	Sodium nitrate Triple superphosphate Potassium sulphate Sodium sulphate Magnesium sulphate	96 kg N & 157 kg Na 35 kg P 225 kg K & 99 kg S 15 kg Na & 10 kg S 10 kg Mg & 13 kg S

Temporal changes were investigated on samples from plot 3 over the period 1870 – 2008. Chemical treatment effects were compared using samples available from 1876

(plots 9, 12, 13 and 14) and 2008 (plots 9/2, 12d, 13/1, 13/2 and 14/2). Sample details are given in Table 7.2.

Table 7.2. Summary of archived soil and vegetation samples used (*). Individual plot treatments details are given in Table 7.1.

Year	Plot	Liming treatment ^s	Soil sample	Vegetation sample
1870	3	U	*	*
1876	3	U	*	*
1876	9, 12, 13, 14	U	*	
1886	3	U	*	*
1904	3	L		*
1904	3	U	*	*
1923	3	L, U	*	*
1939	3	L, U	*	*
1959	3	L	*	*
1959	3	U		*
1971	3	a	*	*
1971	3	d		*
1991	3	a, d	*	*
1998	3	a, d	*	*
2002	3	a, d	*	*
2005	3	a, d	*	*
2008	3	a, b, c, d	*	*
2008	9/2	a, b, c, d	*	*
2008	12	d	*	
2008	13/1	a, b, c, d	*	*
2008	13/2	a, b, c, d	*	*
2008	14/2	a, b, c, d	*	*

^s L = limed, U = unlimed, a = pH 7, b = pH 6, c = nominal pH 5, d = unlimed.

Applied fertilisers were also sampled from the earliest and latest years available. Samples included; chalk (1972, 2000), FYM (1981, 2001), fishmeal (1971, 1995), K₂SO₄ (1990), poultry manure (2003), NaNO₃ (2004), and Ca(H₂PO₄)₂ (1938, 1968).

7.2.1 Sample characterisation

Soil pH was initially measured at Rothamsted at soil:water ratios of 1:5, and from 1959 at 1:2.5. Little difference between measurements using the two methods were

reported (Johnston et al., 1986). Supplementary pH values were obtained from Silvertown et al. (2006).

Soil organic carbon content was determined as the difference between separately measured total carbon content and inorganic carbon content. Total carbon analysis was carried out using a CE Instruments Flash EA1112 Elemental Analyser, set to CNS mode: soils (c. 15 – 20 mg) were weighed, in duplicate, into foil capsules which were then combusted at 900 °C with copper oxide and electrolytic copper. Standard soils with known carbon concentrations were used for calibration. The resulting gas was dried with $\text{Mg}(\text{ClO}_4)_2$ and carbon detected by thermal conductivity detector. Inorganic carbon was measured using a Shimadzu TOC-VCPH with SSM-5000A solids module: soils (c. 100 mg) were weighed, in duplicate, into ceramic crucibles and acidified with 25 % H_3PO_4 before combustion at 200 °C, after which CO_2 was detected as described in Section 2.4.3 (Ming, 2004).

Iodine in soil, organic fertilizer treatments (FYM and fishmeal) and vegetation samples were extracted, using a method adapted from that described in Section 2.2.5. Triplicate soil or organic fertilizer samples (1 g \pm 0.05 g soil, 0.5 g fertilizer) were suspended in 10 % TMAH (20 ml for soil samples, 10 ml for fertilizers) in polypropylene centrifuge tubes, at 70 °C. Suspensions were shaken after 2 hours and centrifuged at 3,000 rpm for 30 min after 4 hours incubation. The supernatant solution was diluted 1 in 10 with MQ water before analysis by ICP-MS (Section 2.6.2.1). Triplicate vegetation samples (0.25 g \pm 0.01 g) were suspended in 5 ml 5 % TMAH in polypropylene centrifuge tubes at 70 °C. Suspensions were shaken after 2 hours, and after 4 hours incubation 20 ml MQ water was added before shaking and centrifugation at 3,000 rpm for 30 min. Inorganic fertilisers (NaNO_3 and K_2SO_4) were dissolved at 200 mg and 400 mg in 100 ml MQ water, in duplicate. Solutions were analysed by ICP-MS (Section 2.6.2.1).

Superphosphate and chalk were dissolved in acid and iodine was quantified using a standard addition method modified from Julshamn et al. (2001). Triplicate samples (0.2 g \pm 0.01 g) were weighed into PFA vessels to which 0, 1, 10, or 15 mg kg^{-1} of ^{127}I or $^{127}\text{IO}_3^-$ was added. To each, 2 ml conc. HNO_3 , 1 ml conc. H_2O_2 and 1 ml conc. HClO_4 was added before heating at 50 °C for 1 hr. A further 2-3 ml MQ water was

then added and samples heated for a further hour at 50 °C until most solid matter had dissolved. Some undissolved impurities remained, which were most prevalent in the chalk sample from 1938. Following quantitative dilution to 50 ml with MQ water, samples were further diluted 9 parts sample to 1 part internal standard mixture (100 µg L⁻¹ of each Te and Re in MQ water) and analysed by ICP-MS in standard mode, with sample introduction by direct aspiration. Direct aspiration was used to reduce retention of iodine in acidic matrix onto sample tubing.

7.3 RESULTS AND DISCUSSION

Soil and vegetation iodine concentrations are given in Table 7.3 and Table 7.4 alongside vegetation yield (Y , t ha⁻¹ cut⁻¹) resulting total soil iodine (I_{tot} , g I ha⁻¹) and annual vegetation iodine off-take (I_{off} , mg I ha⁻¹ yr⁻¹);

$$I_{\text{tot}} = \left(I_{\text{s}} / 10^3 \right) \times W_{\text{s}} \quad (7.1)$$

where I_{tot} = total soil iodine in top 20 cm (g I ha⁻¹), I_{s} = soil iodine concentration (mg I kg⁻¹), and W_{s} = weight of soil in top 20 cm (kg ha⁻¹, assumed to be 2,500,000 kg ha⁻¹) and

$$I_{\text{off}} = I_{\text{v}} \times (Y/1000) \times 2 \quad (7.2)$$

where I_{v} = vegetation iodine concentration (mg I kg⁻¹). I_{off} as a percentage of I_{tot} was calculated using mean values; note that values in Table 7.3 are $\times 10^{-3}$. Prior to 1875, the Park Grass site was grazed by sheep after the first vegetation was cut. A second cut was introduced from 1875 and vegetation removed between September and November (Jenkinson et al., 1994). Therefore to ensure consistency for comparison purposes, only samples from cut 1 have been used. Where annual yield/iodine off-take is calculated, these are estimated as twice the value of the first cut.

Table 7.3. Control plot results: iodine concentration in soil (I_S) and vegetation (I_V) with vegetation yields from cut 1 (Y) and resulting total soil iodine (I_{tot}) and annual vegetation iodine off-take (I_{off}).

Sample	I_S (mg I kg ⁻¹)		I_{tot} (g I ha ⁻¹)		I_V (mg I kg ⁻¹)		Y (dry) (t ha ⁻¹ cut ⁻¹)	I_{off} (mg I ha ⁻¹ yr ⁻¹)		I_{off} as % of I_{tot} (10 ⁻³ %)
	Mean	S. E.	Mean	S. E.	Mean	S. E.		Mean	S. E.	
1870-3-U	5.56	0.052	13,900	130	0.207	0.028	0.61	126	17.3	0.906
1876-3-U	6.44	0.028	16,100	70.7	0.191	0.008	1.34	257	11.2	1.60
1886-3-U	5.64	0.130	14,100	326	0.179	0.013	2.28	409	30.7	2.90
1904-3-U	6.11	0.052	15,300	130	0.145	0.005	2.14	309	11.3	2.02
1923-3-U	5.99	0.009	15,000	23.3	0.190	0.008	1.31	247	10.2	1.65
1939-3-U	6.15	0.061	15,400	152	0.275	0.019	1.12	308	21.6	2.00
1959-3-U	N/A	N/A	N/A	N/A	0.135	0.011	0.52	70.0	5.88	N/A
1971-3-d	N/A	N/A	N/A	N/A	0.198	0.006	1.50	298	9.52	N/A
1991-3-d	7.05	0.007	17,600	172	0.254	0.014	2.74	695	37.1	3.95
1998-3-d	6.60	0.032	16,500	80.0	0.285	0.019	2.12	605	39.7	3.67
2002-3-d	6.64	0.041	16,600	103	0.250	0.013	2.56	640	33.4	3.86
2005-3-d	6.58	0.029	16,400	73.4	0.154	0.013	1.30	200	16.6	1.22
2008-3-d	6.42	0.142	16,100	355	0.217	0.015	1.47	319	22.0	1.98
Mean unlimed	6.29		15,700		0.206		1.62	345		2.34
Median unlimed	6.42		16,100		0.198		1.47	308		2.00
1904-3-L	N/A	N/A	N/A	N/A	0.134	0.009	2.80	375	24.8	N/A
1923-3-L	5.86	0.134	14,700	336	0.153	0.022	1.28	196	28.4	1.33
1939-3-L	5.55	0.065	13,900	164	0.263	0.019	1.21	320	22.9	2.30
1959-3-L	5.48	0.101	13,700	252	0.161	0.016	1.47	236	22.8	1.72
1971-3-a	4.88	0.044	12,200	110	0.191	0.012	1.61	307	18.9	2.52
1991-3-a	5.28	0.047	13,200	119	0.178	0.024	3.48	620	83.2	4.70
1998-3-a	5.11	0.075	12,800	189	0.201	0.005	2.36	475	12.0	3.71
2002-3-a	5.09	0.090	12,700	226	0.166	0.009	2.75	455	24.4	3.58
2005-3-a	4.82	0.023	12,000	56.5	0.163	0.003	1.86	302	5.56	2.52
2008-3-a	5.06	0.031	12,700	76.8	0.206	0.024	2.67	551	64.0	4.34
Mean limed	5.24		13,100		0.182		2.15	384		2.97
Median limed	5.11		12,800		0.172		2.11	348		2.52

Table 7.4. 2008 results: iodine concentration in soil (I_S) and vegetation (I_V) with vegetation yields from cut 1 (Y) and resulting total soil iodine and vegetation iodine off-take (I_{off}).

Sample	I_S (mg I kg ⁻¹)		I_{tot} (g I ha ⁻¹)		I_V (mg I kg ⁻¹)		Y (dry) (t ha ⁻¹ cut ⁻¹)	I_{off} (mg I ha ⁻¹ yr ⁻¹)		I_{off} as % of I_{tot} (10 ⁻³ %)
	Mean	S. E.	Mean	S. E.	Mean	S. E.		Mean	S. E.	
2008-3-a	5.06	0.031	12,700	76.8	0.206	0.024	2.67	551	64.0	4.34
2008-3-b	6.28	0.055	15,700	139	0.177	0.004	2.82	499	11.7	3.18
2008-3-c	6.15	0.094	15,400	236	0.228	0.018	1.10	251	19.5	1.63
2008-3-d	6.42	0.142	16,100	355	0.217	0.015	1.47	319	22.0	1.98
2008-9/2-a	4.55	0.198	11,400	494	0.119	0.017	5.58	662	94.3	5.81
2008-9/2-b	5.21	0.134	13,000	336	0.112	0.007	5.21	582	37.6	4.48
2008-9/2-c	4.71	0.107	11,800	269	0.121	0.011	4.96	601	53.2	5.09
2008-9/2-d	4.90	0.020	12,200	48.8	0.126	0.013	3.26	412	43.4	3.38
2008-13/1-a	4.92	0.158	12,300	395	0.156	0.016	3.84	597	61.1	4.85
2008-13/1-b	5.17	0.106	12,900	264	0.117	0.0025	2.96	347	7.26	2.69
2008-13/1-c	4.39	0.089	11,000	221	0.141	0.014	1.88	266	25.7	2.42
2008-13/1-d	4.70	0.118	11,700	296	0.163	0.015	1.82	296	28.1	2.53
2008-13/2-a	4.54	0.241	11,300	603	0.132	0.013	3.19	423	40.3	3.74
2008-13/2-b	4.76	0.204	11,900	511	0.119	0.009	3.19	381	28.0	3.20
2008-13/2-c	4.30	0.156	10,700	389	0.128	0.011	3.26	416	36.7	3.89
2008-13/2-d	4.64	0.122	11,600	306	0.125	0.020	3.17	397	63.8	3.42
2008-14/2-a	7.16	0.440	17,900	1,100	0.150	0.029	7.24	1,090	210	6.09
2008-14/2-b	7.82	0.402	19,500	1,010	0.158	0.012	5.52	873	65.7	4.48
2008-14/2-c	7.02	0.148	17,500	371	0.152	0.012	5.25	800	63.8	4.57
2008-14/2-d	6.51	0.250	16,300	624	0.197	0.019	5.02	991	97.3	6.08
Mean 2008	5.46		13,600		0.152		3.67	538		3.89
Median 2008	4.99		12,500		0.146		3.23	461		3.82

7.3.1 Soil pH

In samples from unlimed (“U” and “d”) plots, soil pH decreased between 1850 and 2011 ($r = -0.552$, $p = 0.027$) (Figure 7.1) probably as a result of acidification due to atmospheric deposition (Blake and Goulding, 2002). Limed (“L”) plots were broadly maintained at $\text{pH} = 7$ from 1959, similar to the nominal pH of “a” sub-plots. Limed samples from 1984 and 1991 have lower pH, and no explanation for this is apparent.

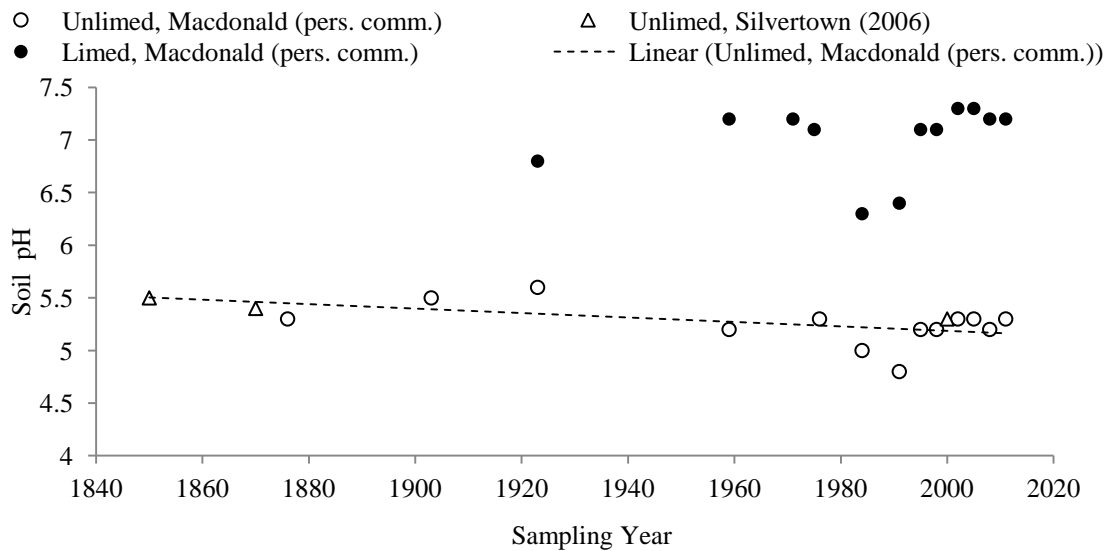



Figure 7.1. Effect of liming as a function of time on soil pH in control plot 3. Data from A. Macdonald (pers. comm.) with additional values from Silvertown (2006).

7.3.2 Soil iodine concentration

Figure 7.2 shows the spatial relationship of plots, allowing comparison of I_s and soil pH values in 1876 with those determined in individual sub-plots in 2008, relative to site location. A significant positive correlation was observed between plot location and I_s for both 1876 ($r = 0.997$, $p < 0.001$) and 2008 ($r = 0.875$, $p = 0.022$) (Figure 7.2). This may be a result of historical land-use or of soil formation, but means that to be evident, any effect of treatment since 1876 would have to be large enough to overcome the pre-existing iodine gradient.

Approximate direction of north 

Plot code: 13/2 13/1 12 9/2 3 14/2
Plot 'location': 1 2 3 7 15 18

1876 I_s (mg I kg⁻¹):	5.3 (0.03)		5.5 (0.05)				5.8 (0.03)						6.4 (0.03)			6.7 (0.03)		
2008 I_s (mg I kg⁻¹):	d	4.6 (0.12) pH 5.2	4.7 (0.12) pH 4.9	5.7 (0.06) pH 5.2			4.9 (0.02) pH 3.7						6.4 (0.14) pH 5.2			6.5 (0.25) pH 6.1		
	c	4.3 (0.16) pH 5.1	4.4 (0.09) pH 4.9				4.7 (0.11) pH 4.8						6.1 (0.09) pH 4.9			7.0 (0.15) pH 6.0		
	b	4.8 (0.20) pH 5.9	5.2 (0.11) pH 5.8				5.2 (0.13) pH 6.3						6.3 (0.06) pH 6.1			7.8 (0.40) pH 6.3		
	a	4.5 (0.24) pH 6.9	4.9 (0.16) pH 6.9				4.5 (0.20) pH 7.1						5.1 (0.03.) pH 7.2			7.2 (0.44) pH 7.0		

Figure 7.2. Schematic diagram showing relative locations of individual plots. Soil iodine concentrations (mg I kg⁻¹ with standard error of three replicates given in brackets) are given for 1876 and 2008 sub plots (a-d). Values in italics are soil pH at the indicated date.

Changes in soil iodine concentration (I_S) over time as a function of liming are shown in Figure 7.3 for historical samples from plot 3. In limed soils, I_S decreased significantly from commencement of liming ($r = -0.797$, $p < 0.001$), while in unlimed soils, I_S increased over the same period ($r = 0.750$, $p < 0.001$). Overall there was a significant negative correlation between I_S and soil pH in the control plots ($r = -0.870$, $p < 0.001$).

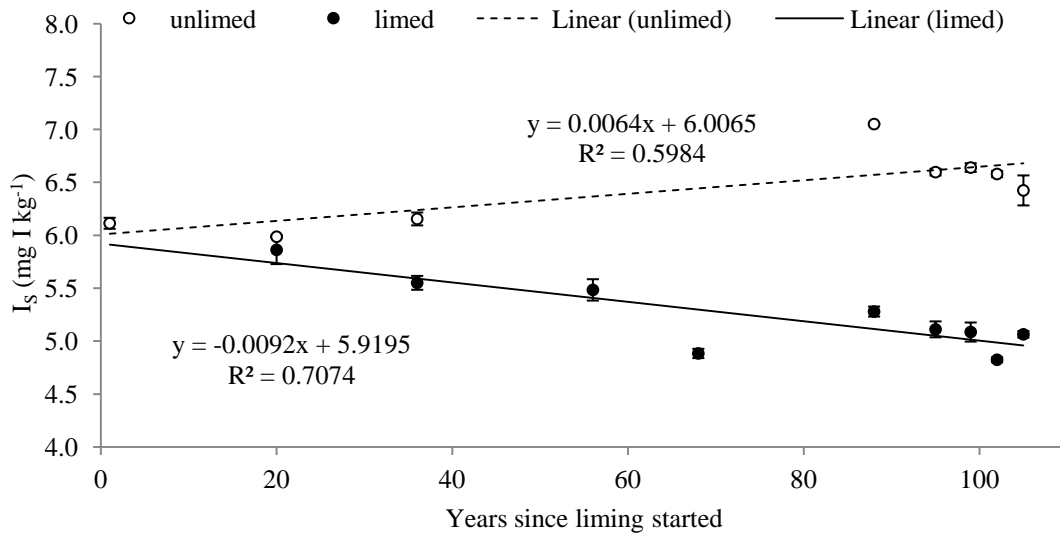


Figure 7.3. Soil iodine concentration (I_S) as a consequence of liming (liming started 1903). Control plot 3 results only. Error bars show standard error of 3 replicate measurements (error bars are within the data point if not shown). Uncertainty due to sampling is unknown.

Given the proximity of the plots, it is reasonable to assume that all receive the same rainfall. Iodine input from rainfall (I_{in} , $g I ha^{-1} yr^{-1}$), during a given year is:

$$I_{in} = \frac{I_R \times V_R}{1,000,000} \quad (7.3)$$

where I_R = iodine concentration in rain ($\mu g I L^{-1}$) and V_R = volume of rain ($L ha^{-1} yr^{-1}$). Mean annual rainfall at Rothamsted is 698 mm (Silvertown et al., 2006) so using a mean I_R value for the UK of $2 \mu g L^{-1}$ (Hou et al., 2009; Johnson, 2003b; Lidiard, 1995; Neal et al., 2007), I_{in} can be estimated as $14.0 g I ha^{-1} yr^{-1}$. This amounts to $\sim 0.1\%$ of I_{tot} in plot 3 in 2008, and suggests that the total amount of iodine added between 1903, when liming began, and 2008 was $1,470 g I ha^{-1}$. This is of a similar order of magnitude to the increase in I_{tot} observed from 1904 to 2008 in the unlimed sub-plots (Table 7.3). Assuming $2,500 t soil ha^{-1}$, the rate of iodine input from rainfall is

0.0056 mg I kg⁻¹ yr⁻¹, which is comparable to the rate of increase in I_S in the unlimed sub-plot (Figure 7.3).

Greater variation in I_S was observed between treated plots than between sub-plots within a treated plot. Unlike in the control plots, no significant correlation was found between soil pH and I_S in the 2008 samples from treated plots ($r = 0.213$, $p = 0.103$). Any effect of treatment was superimposed onto the spatial iodine gradient across the site which was present in 1876 and remained, despite any subsequent treatments, in 2008 (Figure 7.4).

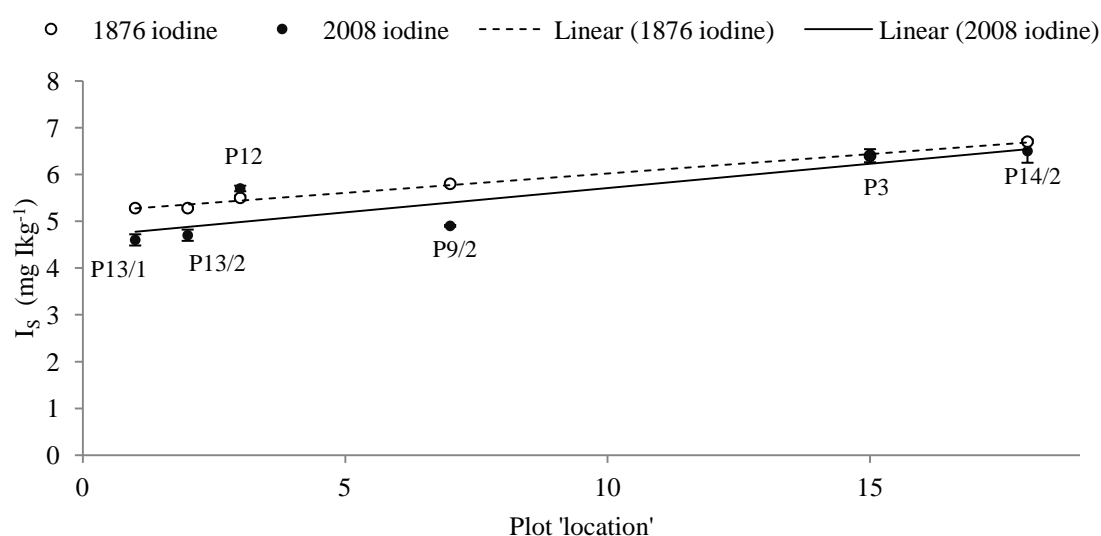


Figure 7.4. Variation in soil iodine concentration across the site in “d” (unlimed) plots, where plot ‘location’ refers to the position of the plot, starting from 1 at the far south-western end (Figure 7.2). ‘P’ numbers are plot names. Error bars are the standard error of three replicates (1876 error bars are within the size of the circles). Lines show significant positive correlations.

Treatments have the potential to increase I_S. Therefore measured iodine concentrations in fertiliser samples (Table 7.5) were used to calculate the mean annual iodine input for each plot where possible (Table 7.6 and Table 7.7). Iodine concentrations for some chemical fertilisers that were unavailable in the archive are unknown therefore absolute amounts of iodine added to selected plots cannot be calculated, however qualitative comparison with rainfall input can still be made. Chalk added 0.3 - 9.5 g I ha⁻¹ yr⁻¹ between 1881 and 2009 (Table 7.6), and other treatments added 2 - 7 g I ha⁻¹ yr⁻¹ (Table 7.7). These were of the same order of magnitude as rainfall inputs and therefore must be considered in an iodine mass-balance in the plots. However rather than adding iodine, treatments appear to reduce

I_s . This effect can be seen in Figure 7.4, where control plots 3 and 12 (subject only to liming) have similar I_s concentrations in 1876 and 2008, but treated plots show a reduction in I_s over the same time. Chemical change as a consequence of the treatments may have reduced the soils' ability to retain incoming iodine.

The measured iodine content of chalk in limed sub-plots (max. $9.50 \text{ g I ha}^{-1} \text{ yr}^{-1}$, Table 7.6) was similar to input from rainfall ($14.0 \text{ g I ha}^{-1} \text{ yr}^{-1}$), and therefore in plot 3 it may be expected to maintain (or slightly increase) I_s of the limed sub-plots. Instead a decrease was observed (Figure 7.3) probably resulting from pH change. Retention is likely to be promoted in unlimed soils, as incoming iodine for example in rainfall, undergoes rapid sorption at low pH, probably to metal oxides (Shetaya et al., 2012; Whitehead, 1984). In limed soil, increases in pH reduce the ability of the soil to retain iodine already present, and I_s decreased through time despite higher iodine inputs. In addition to affecting pH, liming can also affect soil organic matter (SOM) content, as break-down of plant matter occurs at different rates depending on the soil pH (Silvertown et al., 2006). SOM is recognised as an important reservoir of soil iodine so a relationship between the two may be expected (Shetaya et al., 2012; Yamaguchi et al., 2010), however only a weak correlation between SOC (as a measure of SOM) and I_s was observed.

In treated plots 9 and 13 where acidification between 1876 and 2008 due to treatment was greatest and therefore iodine retention may be expected, decreasing I_s was observed. However as no significant correlations were observed between I_s and the measures of soil chemistry available (Olsen P, exchangeable K, Mg and Na) it is difficult to attribute this loss of iodine to any specific factor.

Table 7.5. Total iodine measured in fertiliser samples applied to treated plots, and the number of samples analysed in each case.

Sample	Iodine (mg I kg ⁻¹)		Number of samples
	Mean	S. E.	
Chalk (1972)	9.08	0.487	9
Chalk (2000)	8.69	0.579	9
Fishmeal (1971)	6.39	0.0565	3
Fishmeal (1995)	1.25	0.0259	3
FYM (1981)	1.39	0.0197	3
FYM (2001)	1.98	0.0154	3
Potassium sulphate (1990)	2.25	1.43	4
Poultry manure (2003)	5.85	0.130	3
Sodium nitrate (2004)	3.84	1.50	4
Superphosphate (1938)	5.05	0.384	9
Superphosphate (1968)	11.8	3.07	9

Table 7.6. Iodine contributed by chalk applications, to all plots, between 1881 and 2009. Mean iodine input calculated using mean iodine concentration in chalk (Table 7.5). Some lime was added to plots before liming treatments started, hence sub-plot d ('unlimed') does have some historical lime input.

Plot	Sub-plot	Total chalk input 1881 – 2009 (t ha ⁻¹)	Mean chalk input 1881 – 2009 (t ha ⁻¹ yr ⁻¹)	Mean iodine input 1881 – 2009 (g ha ⁻¹ I yr ⁻¹)
3	a	94.3	0.737	6.55
	b	74.3	0.580	5.15
	c	9.20	0.07	0.639
	d	7.30	0.06	0.507
9/2	a	137	1.07	9.50
	b	105	0.820	7.29
	c	45.4	0.355	3.15
	d	7.30	0.06	0.507
13/1	a	93.9	0.734	6.52
	b	70.8	0.553	4.91
	c	12.3	0.10	0.854
	d	7.30	0.06	0.507
13/2	a	94.4	0.738	6.55
	b	69.4	0.542	4.82
	c	11.4	0.09	0.791
	d	7.30	0.06	0.507
14/2	a	70.7	0.552	4.90
	b	53.0	0.414	3.68
	c	4.00	0.03	0.278
	d	4.00	0.03	0.278

Table 7.7. Iodine contributed by treatments analysed. Iodine content is mean of measured values (Table 7.5). Notes: * Fertilisers unavailable to sample; ^a 4-yearly inputs calculated as mean annual additions; ^b additions between 1870 and 1955; ^c additions from 1959 onwards; ^d additions from 2003 onwards.

Plot	Treatment	Fertiliser added dry weight (kg ha ⁻¹ yr ⁻¹)	Iodine added (g I ha ⁻¹ yr ⁻¹)	Total iodine added 1870 - 2012 (g I ha ⁻¹)	Mean rate of iodine addition 1870 - 2012 (g I ha ⁻¹ yr ⁻¹)
9/2	Ammonium sulphate*	453			
	Magnesium sulphate*	49			
	Potassium sulphate	520	1.17	166	
	Sodium sulphate*	45			
	Superphosphate	132	1.12	158	
	SUM			324	2.28
13/1	FYM	1881 ^a	3.18	451	
	Fishmeal	699 ^{a,b}	6.68	33	
	Fishmeal	744 ^{a,c}	7.10	263	
	SUM			994	7.00
13/2	FYM	1881 ^a	3.18	451	
	Poultry manure	500 ^{a,d}	2.92	263	
	Fishmeal	699 ^{a,b}	6.68	33.4	
	Fishmeal	744 ^{a,c}	7.1	291	
	SUM			1530	1.08
14/2	Magnesium sulphate*	49			
	Potassium sulphate	520	1.17	166	
	Sodium nitrate	581	2.23	317	
	Sodium sulphate*	44			
	Superphosphate	132	1.12	158	
	SUM			641	4.52

The amount of iodine removed from the soil by vegetation cannot be known, as vegetation iodine derives from both aerially deposited iodine and uptake from soil. Estimating iodine removal (I_{off} , g I ha⁻¹ yr⁻¹) suggests that absolute amounts removed are small, with slightly more removed from limed soil (plot 3 unlimed mean I_{off} = 345 mg I ha⁻¹ yr⁻¹, plot 3 limed mean I_{off} = 384 mg I ha⁻¹ yr⁻¹) (Table 7.3). Vegetation off-take represents a tiny proportion of I_{tot} (c. 0.003 %) and is therefore unlikely to cause the differences observed in I_{S} .

7.3.3 Vegetation iodine

Median I_V concentrations were 0.172 mg kg^{-1} (unlimed plot 3 samples, Table 7.3), 0.198 mg kg^{-1} (limed plot 3 samples, Table 7.3) and 0.146 mg kg^{-1} (2008 samples, Table 7.4), and there was a significant difference in I_V between these groups (ANOVA, $p = 0.002$). A significant positive correlation between I_S and I_V was observed for vegetation in control plots ($r = 0.347$, $p = 0.004$), treated plots ($r = 0.361$, $p = 0.005$), and when all plots were considered together ($r = 0.399$, $p < 0.001$; Figure 7.5), in agreement with previous findings (Chapters 3 and 6, Dai et al. (2006), Hong et al. (2012), Weng et al. (2008b)). Uptake was also affected by iodine availability, as shown by the range of I_V concentrations at each I_S concentration. Mean I_V increased with I_S up to soil concentrations of 6.9 mg I kg^{-1} but in plot 14/2 where I_S concentrations were highest, I_V decreased (Figure 7.6). This may indicate low iodine phyto-availability in plot 14/2.

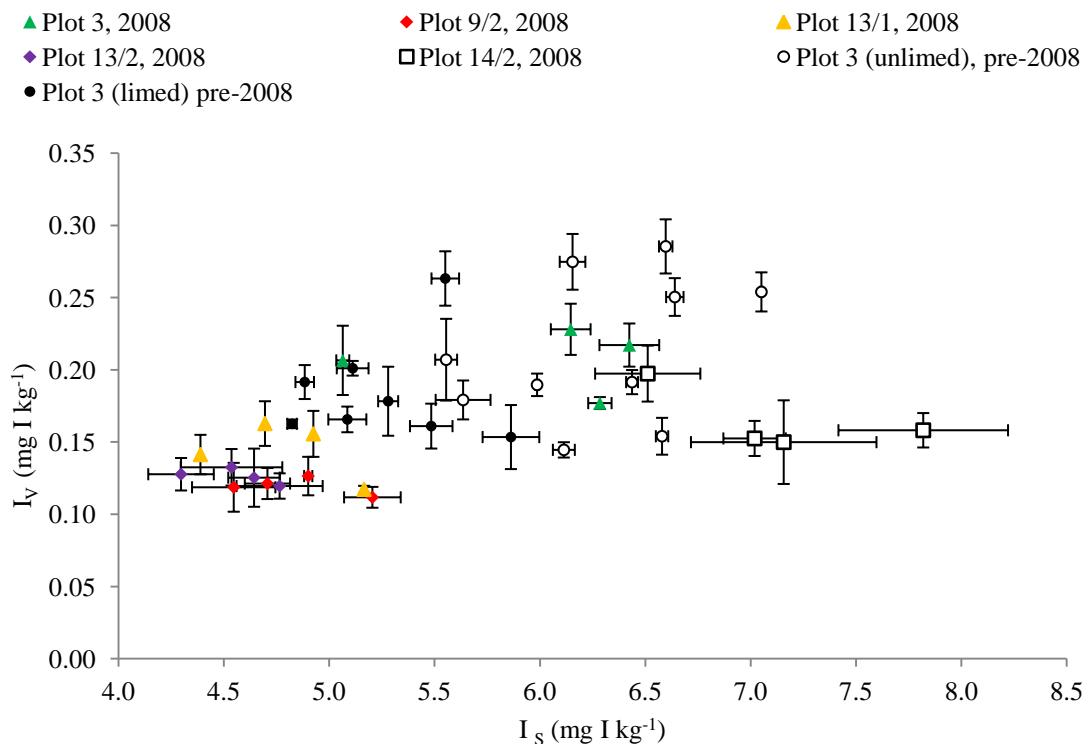


Figure 7.5. Relationship between soil iodine (I_S) and vegetation iodine concentrations (I_V) for all samples. Error bars show standard error of 3 replicate measurements.

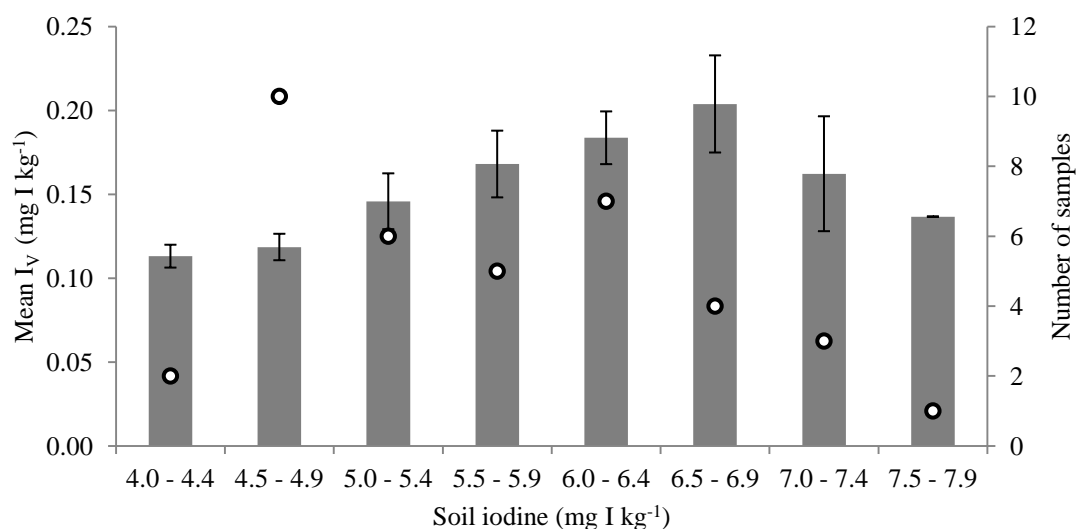


Figure 7.6. Relationship between I_S and I_V for all samples. Each bin is defined by soil iodine concentration, with the number of samples (n) in each bin shown as open circles, quantified on the secondary y axis. Mean vegetation iodine (I_V) is calculated as the mean of n samples, with error bars representing the standard error of the mean.

Yields (Y) from the first cut are presented in Table 7.3 and Table 7.4. There was a highly significant negative correlation between Y and I_V when all samples were included ($r = -0.371$, $p < 0.001$; Figure 7.7). However, a tendency towards a minimum I_V at yields of $3 - 8 \text{ t ha}^{-1}$ was observed, which may suggest a limit dependent on I_S or growing season rainfall (GSR) (Figure 7.7). No correlation between Y and I_V was present when control plots alone were considered ($r = -0.032$, $p = 0.787$), but a significant correlation existed for the 2008 samples ($r = -0.336$, $p = 0.009$). Yield was also negatively correlated with I_V / I_S , although this was strongly affected by plots 9/2 and 14/2 (Figure 7.8). As observed in Chapter 6, a negative correlation between Y and I_V had previously been attributed to slower pasture growth in winter (Smith et al., 1999) and is likely to originate from faster growth resulting in greater yield and therefore removing iodine from the phyto-available pool faster than it can be replenished from the soil solid phase.

A significant positive correlation between Y and I_{off} was observed for all samples, 2008 samples only, limed samples only and unlimed samples only (with $r \geq 0.819$, $p < 0.001$ in all cases), however the correlation between I_V and I_{off} was only significant ($p < 0.7$) for unlimed plot 3 samples ($r = 0.689$, $p < 0.001$) demonstrating that I_{off} was controlled by Y rather than I_V .

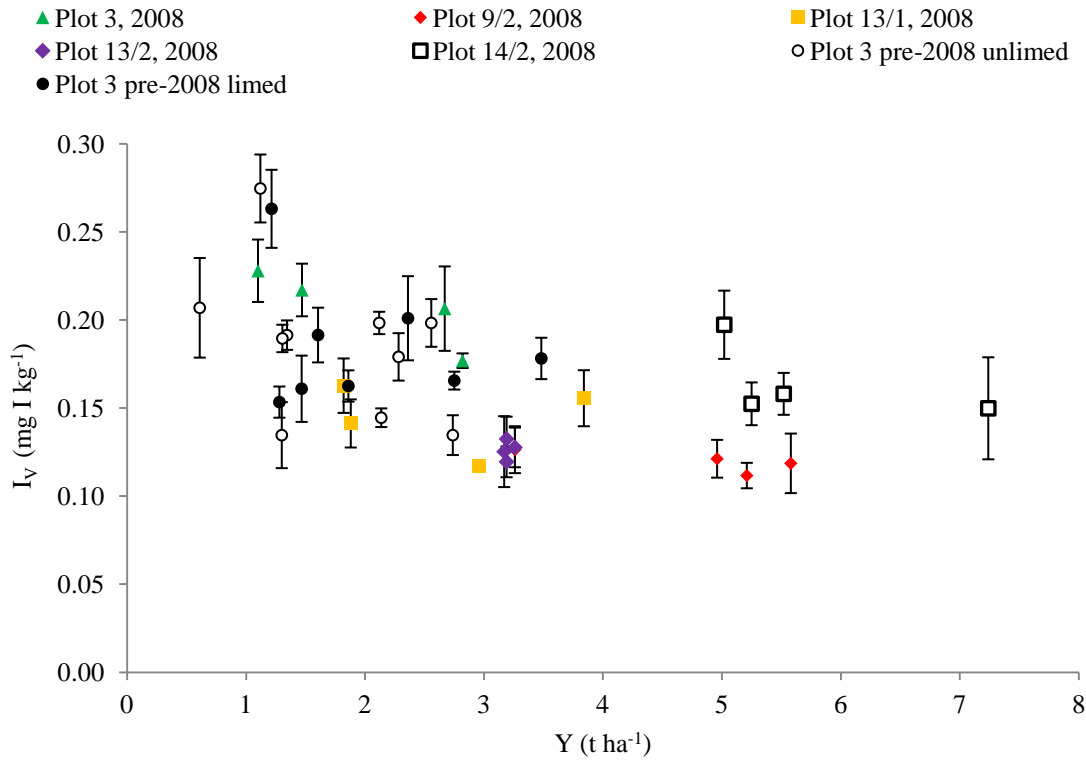


Figure 7.7. Relationship between vegetation iodine concentration (I_V) and vegetation yield (Y). All samples.

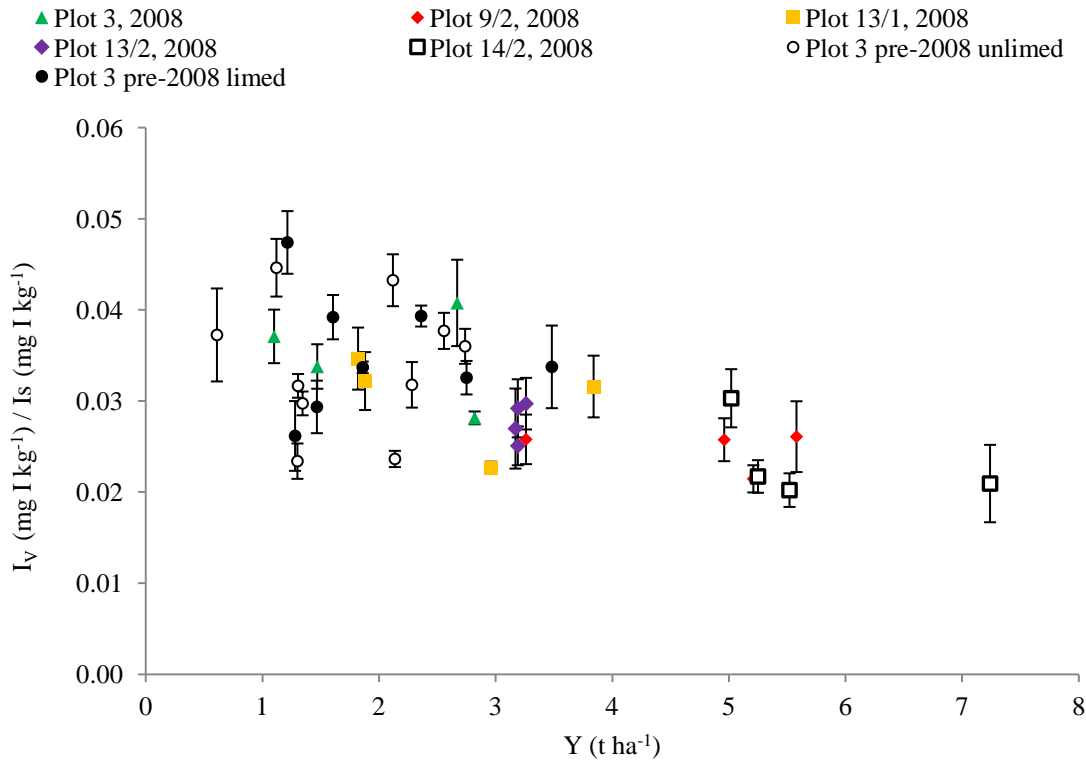


Figure 7.8. Relationship between vegetation yield and vegetation/soil iodine ratio. All samples.

GSR (mm) was nominally defined as the rain that fell between February 1st and the date of the first cut each year. Its effect has only been considered for control plots, as all the 2008 samples, by definition, received the same GSR. The first cut was usually mid- to late-June, and as no cut date was available for 1939 it was set to 20th June. The average input of iodine due to GSR was calculated to be 5,040 mg I ha⁻¹, based on a mean of 0.002 mg I L⁻¹ in rainfall, and a mean GSR of 252 mm in the sampled years. Compared to median I_{off} values of 309 mg I ha⁻¹ yr⁻¹ for plot 3 samples, this demonstrates that rainfall has the potential to influence I_V considerably. GSR and I_V were significantly positively correlated (r = 0.349, p = 0.003) and there was a significant positive correlation between GSR and Y (r = 0.524, p < 0.001) in agreement with published literature (Silvertown et al., 2006; Tilman et al., 1994). The combined effect of GSR on Y (positive correlation), Y on I_V (negative correlation), and GSR on I_V (positive correlation), resulted in an overall significant positive correlation between GSR and I_{off} (r = 0.641, p < 0.001; Figure 7.9), indicating that the provision of iodine from rain exceeded any limitations on availability resulting from increased yield/growth rate. The relative roles of yield dilution and GSR can be illustrated by comparison of I_V under two different GSRs. Regression of Y based on GSR for all control plot samples gives Eqn. 7.4:

$$Y = (0.0085 \times \text{GSR}) - 0.2893 \quad (7.4)$$

If two realistic GSR values of 150 and 250 mm are considered, yields of 0.986 t ha⁻¹ cut⁻¹ (scenario 1) and 0.9857 t ha⁻¹ cut⁻¹ (scenario 2) respectively are calculated. Assuming that I_{off} is 362 mg I ha⁻¹ yr⁻¹ (mean I_{off} from all plot 3 samples), then from Eqn. 7.2, I_V = 0.184 mg I kg⁻¹ (scenario 1) and I_V = 0.0986 mg I kg⁻¹ (scenario 2). The input of iodine from rainfall (I_{in}, g I ha⁻¹ yr⁻¹) is calculated using Eqn. 7.3 as 3 g ha⁻¹ yr⁻¹ and 5 g ha⁻¹ yr⁻¹ for scenarios 1 and 2 respectively. Dividing I_{in} by the annual yield (2Y), rainfall adds 1.52 mg I kg⁻¹ (scenario 1) and 1.35 mg I kg⁻¹ (scenario 2). Therefore while yield dilution results in a difference of 0.0854 mg I kg⁻¹ (I_V = 0.184 mg I kg⁻¹ in scenario 1 minus I_V = 0.0986 mg I kg⁻¹ in scenario 2) input from rainfall causes a difference of 0.17 mg I kg⁻¹, demonstrating that for the control plots additional iodine from rainfall overwhelms any yield dilution effect. The importance of GSR in determining I_{off} is also supported by Figure 7.9, which confirms that there was no appreciable difference in I_{off} between samples from limed and unlimed soil.

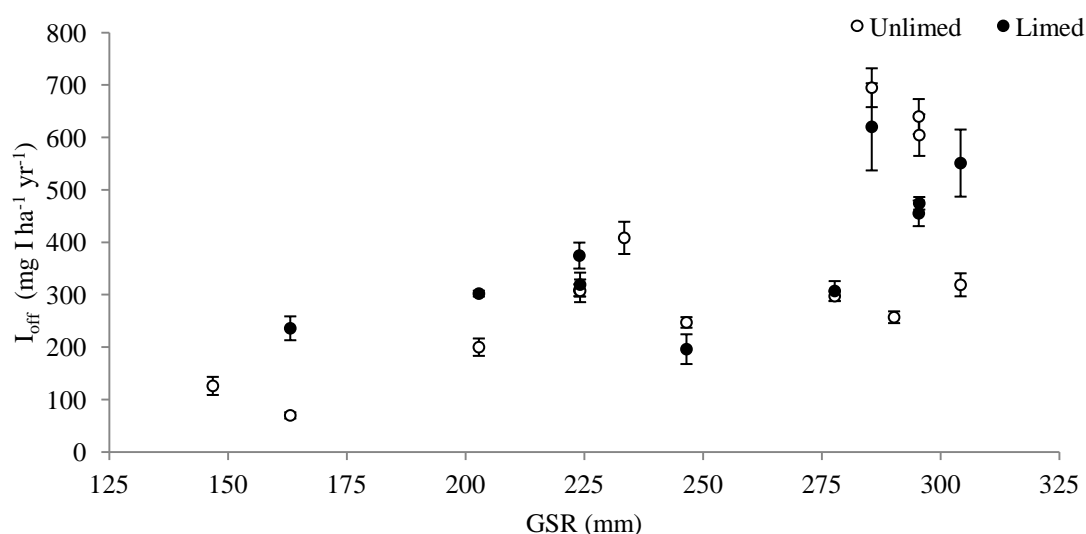


Figure 7.9. Correlation between growing season rainfall (GSR) and annual vegetation iodine off-take (I_{off}) in control plot 3. Error bars show standard error of 3 replicate measurements.

The positive correlation between GSR and I_V may be due to various factors including better root exploration allowing iodine to be removed from larger volumes of soil, and increased uptake directly through leaves (Collins et al., 2004; Smoleń et al., 2011; Tschiersch et al., 2009). Work in Chapter 6 suggested that GSR increases both the concentration of phyto-available iodine in soil solution, and I_S - and therefore the 'stock' of iodine from which the phyto-available pool can be replenished. This is supported by these results for Park Grass. A significant positive correlation between I_S and I_V was observed in the control plots ($r = 0.347$, $p = 0.004$), but this was weaker when limed and unlimed plots were considered separately (limed: $r = 0.018$, $p = 0.929$, unlimed: $r = 0.356$, $p = 0.042$). Both limed and unlimed plots showed significant positive correlations between GSR and I_V , however (limed $r = 0.464$, $p = 0.015$; unlimed $r = 0.588$, $p < 0.001$), showing reliance on frequent, transient iodine input. This was despite apparently reduced retention of iodine in limed soil, confirming that direct contribution of rainfall iodine to vegetation is important, whether through foliar uptake or increasing the phyto-available soil iodine.

No correlation was observed between SOC and I_V . Also no meaningful correlations between I_V and Olsen P or exchangeable cations (used as indicators of soil chemical composition changes resulting from treatments) were observed for the 2008 samples.

A significant negative correlation between soil pH and I_V was observed in the control plots ($r = -0.375$, $p = 0.007$) and resulted in slightly higher I_V concentrations in unlimed samples, although the effect was not significant (ANOVA, $p = 0.038$; Figure 7.10). Lower I_V is likely to be a result of yield dilution since Y was significantly increased under liming (ANOVA, $p = 0.003$; Figure 7.11). In the treated plots, no correlation was observed between soil pH and I_V ($r = 0.027$, $p = 0.835$), although there was a significant correlation between pH and I_{off} ($r = 0.492$, $p < 0.001$) as a result of the correlation between soil pH and Y ($r = 0.485$, $p < 0.001$). The relationship between pH and I_{off} was broadly supported by individual plots (Figure 7.12).

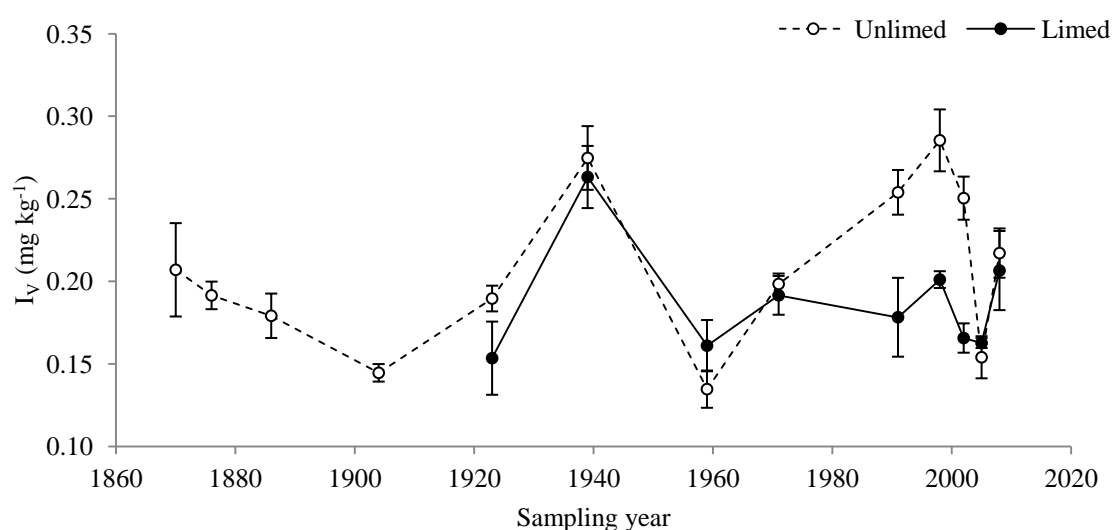


Figure 7.10. Effect of time and liming treatment on vegetation iodine concentration in samples from control plot 3. Error bars show standard error of 3 replicate measurements. Lines are added for clarity but do not represent a temporal trend.

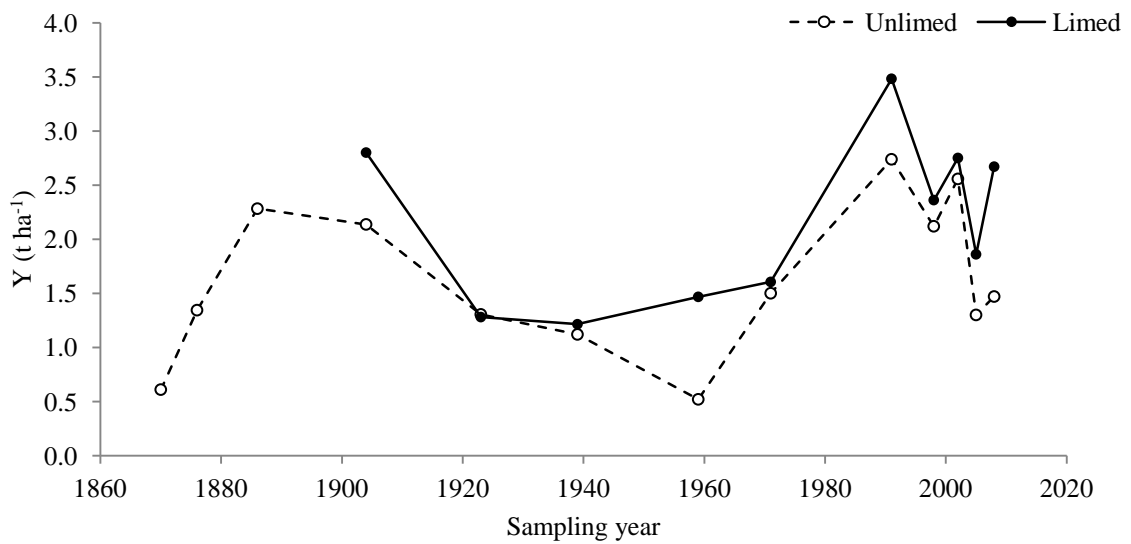


Figure 7.11. Vegetation yield (Y , t ha^{-1}) from cut 1, 1870 to 2008 for limed and unlimed sub-plots of plot 3. Lines are added for clarity but do not represent a temporal trend.

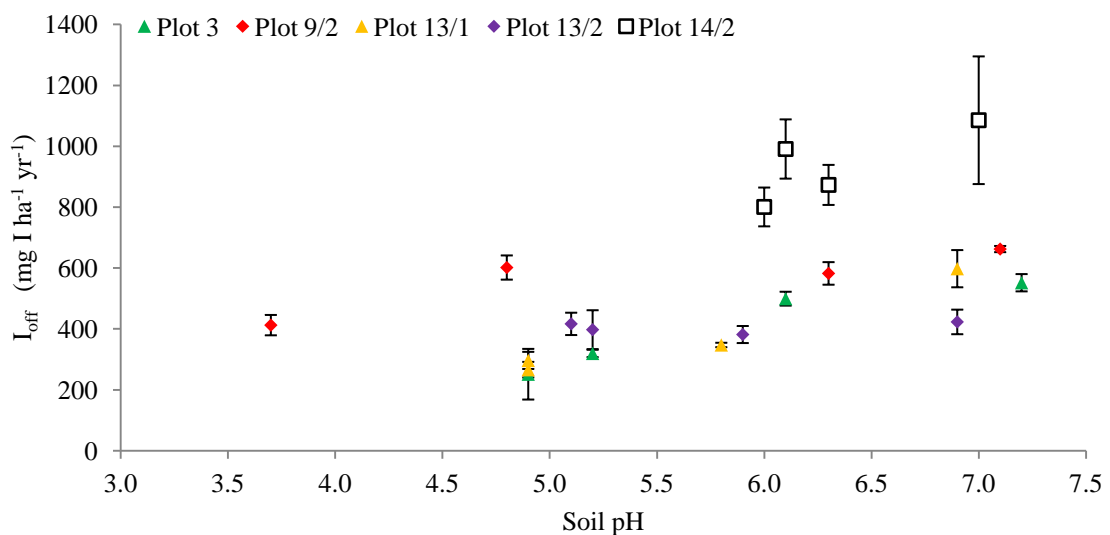


Figure 7.12. Relationship between annual vegetation iodine off-take (I_{off}) and soil pH for 2008 samples.

Since the Park Grass experiment commenced there has been a change in vegetation species growing across the site, with a variety of grasses, legumes and forbs reported on the plots, and even genetic variations of the same species observed on neighbouring plots (Rothamsted Research, 2006; Silvertown et al., 2006; Tilman et al., 1994). Differences in plant species have been shown to affect iodine uptake under normal growing conditions (Sheppard et al., 2010), both through roots (Hong et al., 2009), and via stomata (Collins et al., 2004; Tschiersch et al., 2009). Reasons for uptake differences between species may be because the roots explore different volumes of soil

(Jenkinson et al., 1994), because they may make soil iodine more mobile and therefore more available for uptake (Hong et al., 2009), or water-uptake habits may differ between species, impacting on passive iodine uptake. The effect of soil treatment on plant species diversity in the Park Grass plots has been mainly linked to pH. Addition of $(\text{NH}_4)_2\text{SO}_4$ lowers pH, resulting in fewer plant species; added N allows grasses to dominate; and untreated plots have a more balanced range of species. Unlimed plots typically contain more grasses than other species and produce an overall lower yield than limed plots, and increased yield is correlated with fewer plant species (Rothamsted Research, 2006; Silvertown et al., 2006; Tilman et al., 1994). It is therefore reasonable to assume that the range of plant species present on Park Grass may affect I_v , however it is not possible to disentangle this from direct soil effects in this work.

The various factors that have been discussed in this section with respect to I_v and I_{off} are summarised in Figure 7.13, with observed linear correlations for each group of samples. This shows schematically how factors such as yield and GSR interact with each other and with vegetation iodine.

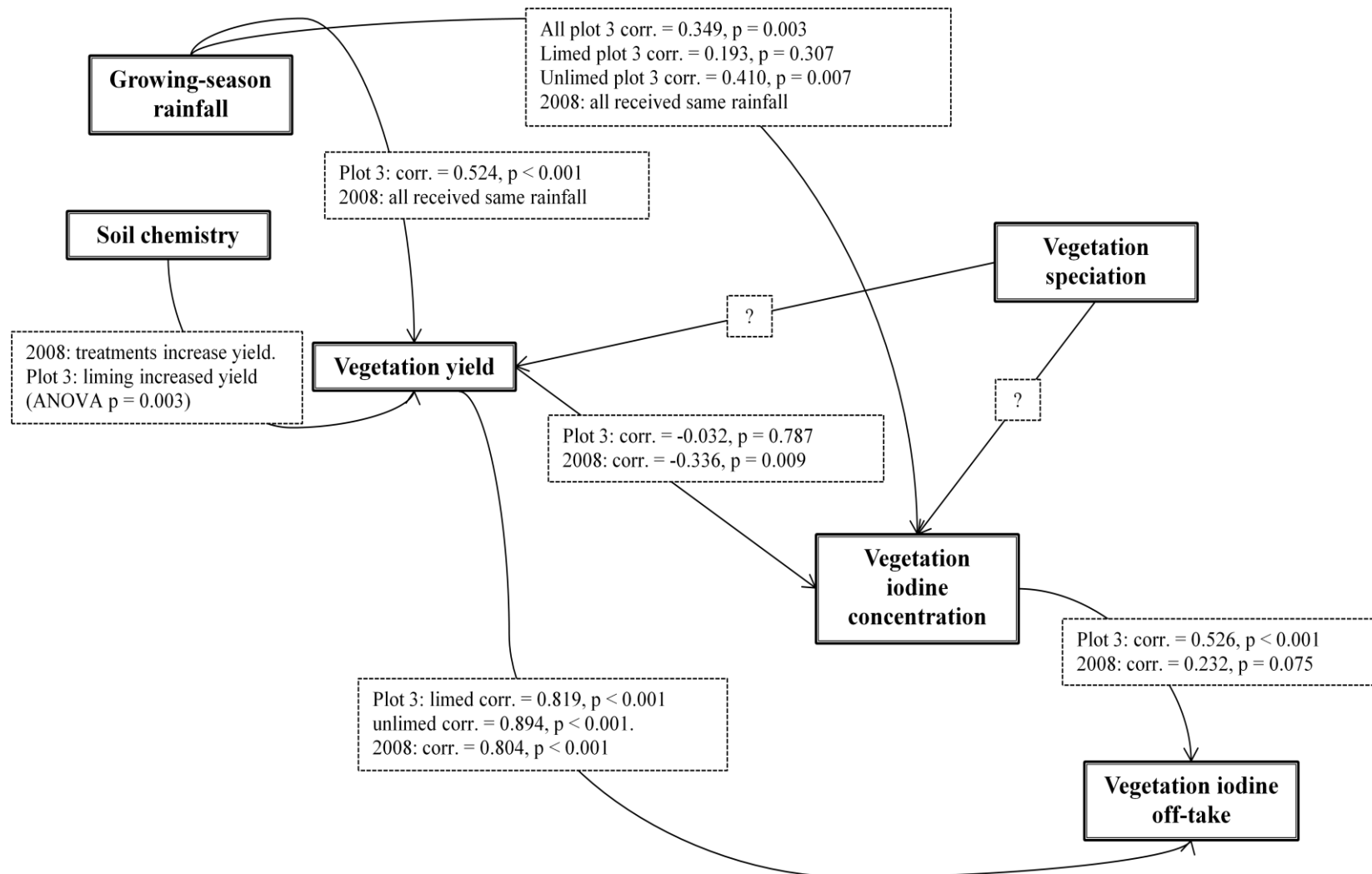


Figure 7.13. Schematic diagram of influences on vegetation iodine concentration and off-take, with linear correlations observed for the various sample groups.

7.4 STEPWISE REGRESSION TO PREDICT VEGETATION IODINE

Stepwise regression was undertaken on all samples to allow prediction of I_V and I_{off} . The effects of I_S , pH, SOC, Y and GSR on I_V or I_{off} were tested, and considered to have an effect if significance < 0.15 , where 0 = highly significant and 1 = not significant. Yield was excluded from the prediction of I_{off} as it is used in its calculation. Significant predictor variables are listed in order of their relative influence on response in Table 7.8. Figure 7.14 and Figure 7.15 show the relationships between measured values and those from regressed equations.

Table 7.8. Results of stepwise regression to predict iodine vegetation concentration (I_V) and off-take (I_{off}) from soil properties pH, SOC (%), I_S (mg I kg^{-1}) and GSR (mm) and Y ($\text{t ha}^{-1} \text{cut}^{-1}$). Includes all samples analysed. Any predictors not appearing in 'relative influence' column did not significantly influence the response; values in brackets are the significance of including that predictor.

Response	Predictors	Relative influence	r^2 of predicted vs measured
I_V	pH, SOC, Y, GSR, I_S	$I_S (< 0.001) > Y (< 0.001) > \text{GSR} (0.006)$	0.39 (Figure 7.14)
I_{off}	pH, SOC, GSR, I_S	$\text{GSR} (< 0.001) > I_S (< 0.001) > \text{pH} (< 0.001) > \text{SOC} (0.065)$	0.48 (Figure 7.15)

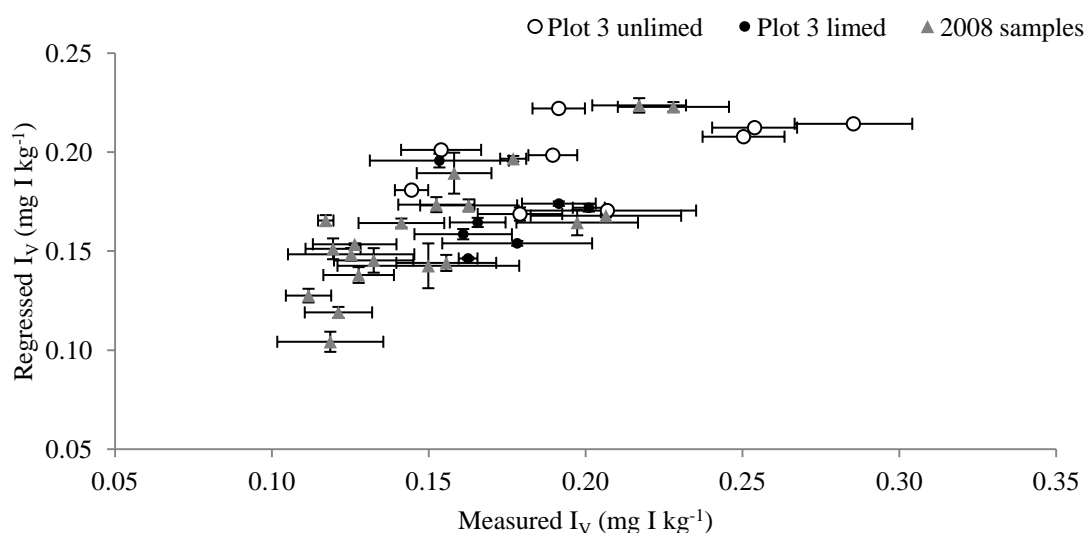


Figure 7.14. Relationship between regressed (predicted from regression results) and measured vegetation iodine concentrations (I_V). Error bars show the standard error of three replicates originating from I_V measurement. Samples shown are those where both soil and vegetation samples were available for analysis.

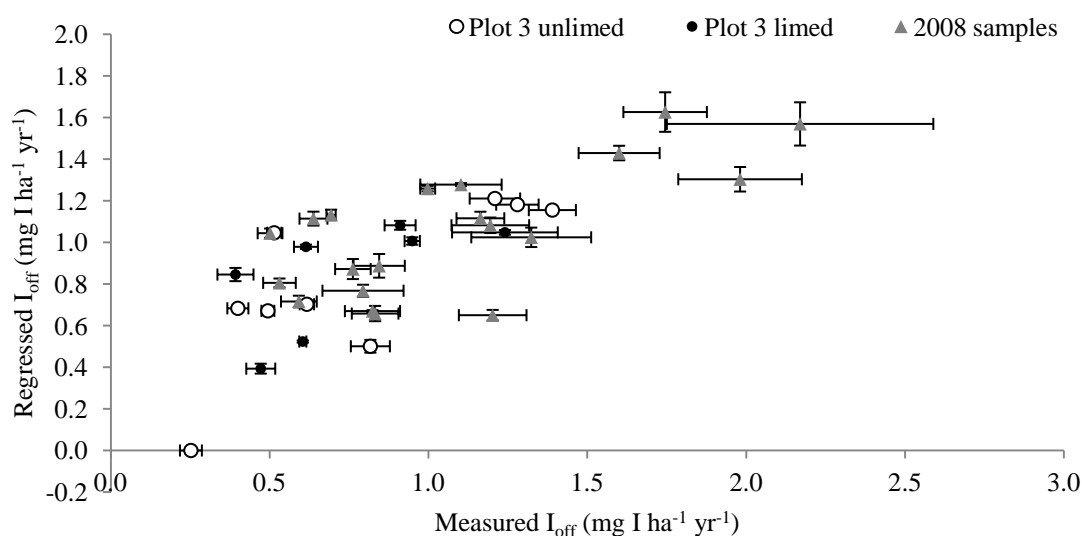


Figure 7.15. Relationship between regressed (predicted from regression results) and measured vegetation iodine off-take (I_{off}). Error bars show the standard error of three replicates originating from I_V measurement. Samples shown are those where both soil and vegetation samples were available for analysis.

The main predictors of I_V were I_S , Y and GSR , with pH and SOC having no significant effect. I_{off} was moderately predicted from GSR , I_S , pH and SOC . This is in broad agreement with the findings previously discussed, although experimental results showed that GSR was more influential on I_V than Y was. The regression confirms that the apparent effect of pH on I_V in the control samples is likely to manifest itself in its impact on Y , rather than on I_V directly. Soil pH and SOC were significant in the regression for I_{off} , which is likely to be due to their effect on Y . Remaining uncertainty in predicting I_V and I_{off} is likely to come from variations in plant species, and potentially other soil factors that have not been measured (Jenkinson et al., 1994).

7.5 CONCLUSIONS

Archived samples from the Rothamsted Park Grass control plots have been used to investigate the effect on vegetation and soil iodine, of changes to soil chemistry through time and due to rainfall; also soil and vegetation samples from a range of treated plots from 1876 and 2008 were compared, to determine the effect of applied fertilisers on iodine contents. The experiment provides samples with a range of soil chemistries which are uncomplicated by the effects of differences in underlying geology or coastal proximity, and it was hoped that the 2008 samples would allow comparison of soil chemistry without the added dimension of differences in rainfall. However, an underlying gradient in I_S was identified across the site in 1876 and

remained in 2008 samples. This meant that the effect of soil chemistry alone could not be elucidated using these samples.

The main factors in determining I_S in the control plot samples were input from rainfall and changes in retention due to pH. In contrast to the established view that SOC is important for controlling I_S , no correlation was observed. This may in part be due to the independence of pH from SOC in this study, in contrast to studies comparing soils from different sources, where high organic matter is often associated with low pH. There was also more variation in pH than in SOC in the control plots. Off-take of iodine by vegetation was negligible compared to reduction in I_S due to pH changes, so is unlikely to have influenced I_S in any of the plots. Vegetation iodine concentration was strongly influenced by I_S , as has been found in other studies, but the dominant influence was of GSR, which is likely to have affected I_V by increasing either foliar uptake or phyto-available iodine in soil solution. Secondary to the effect of GSR was Y , which caused a 'yield dilution' effect in plots where yield was high. This supports the theory of a pool of phyto-available iodine in soil solution which is replenished at a rate dependent on soil type, but more slowly than uptake by fast-growing vegetation. Also likely to be important in determining I_V and I_{off} is the vegetation type, which is known to vary considerably across the site. Despite these limitations, reasonable prediction of I_V and I_{off} were possible from soil properties, GSR and Y .

The effect of individual fertiliser treatments on soil chemistry could not be linked to I_S and I_V due to the underlying spatial gradient, however iodine inputs from chalk and fertilisers were estimated to be lower than, but of a similar order of magnitude to, the input from rainfall. They therefore have the potential to significantly impact I_S and I_V , both by increasing iodine input, and by affecting soil chemistry to determine retention. Further research into the role of plant species and specific soil chemistry would be valuable for predicting the phyto-availability of iodine applied as part of biofortification programmes.

8 CONCLUSIONS

Soil iodine dynamics and subsequent iodine uptake to plants have been investigated using soils from NI. The Rothamsted Park Grass experiment archive was also used to examine longer-term effects of soil chemistry on iodine retention. Experimental results and measured soil chemical characteristics have been combined in predictive models describing (i) the dynamics of iodine in soil, (ii) reactions with humic acid and (iii) uptake from soil to grass. The interpretation of these results provided new insights into relationships between soil properties, iodine geochemistry and phyto-availability.

8.1 IODINE INTERACTIONS WITH SOIL

Experiments have confirmed that sorption to, and storage on, soil solid phases is the dominant reaction of iodine with soil. SOC is the most important phase in long-term iodine retention, and in the rapid sorption of iodate. Some ^{127}I in HA was determined to be unavailable for isotopic mixing, suggesting that a proportion of native iodine in soil is also likely to be fixed in soil organic matter, thus unavailable for uptake. This highlights the importance of understanding iodine speciation and binding in soil when predicting availability. Organic matter also controlled speciation in soil solution; most iodine was bonded to DOC, and solution speciation at the conclusion of the pot experiment indicated that four individual organic species (not identified) were present in solutions with high iodine concentration.

In high-SOC soils ($\text{SOC} \geq 38\%$), both iodide and iodate were rapidly sorbed onto the solid phase. In low-SOC soils, iodate apparently followed a two-stage sorption process: initial instantaneous sorption was followed by slower incorporation into the soil. Modelling indicated that the initial sorption was onto metal oxides; larger rate constants were observed for soils with lower pH and higher Fe oxide content. Interaction of iodide with metal oxides in soil was not implied by modelling, and the instantaneous sorption term in low-SOC soils was negligible. Transformation of iodide to OrgI was slower in HA than in soil, suggesting that even in high-SOC soils, the reaction is not solely with organic matter. Modelling indicated that Al oxides may increase iodide binding to SOC, potentially by blocking negative charge on humus and thereby reducing electrostatic repulsion. Another important factor in determining the extent of soil iodine retention was pH: co-occurrence of low pH and high SOC

provides protons and electrons for iodate reduction to OrgI, and adsorption to metal oxides is promoted at lower pH.

Transformation to iodide was observed when iodate spike was added to highly organic soils and HA solution. This reaction was likely to be facilitated by electron and proton donation from SOC; there was no evidence that metal oxides were involved in the reduction from iodate to iodide (I^V to I^I). The reverse reaction, transformation of spiked iodide to iodate, was never observed. In HA solution there was evidence to support redox coupling of iodide and iodate, as reaction in mixed-spike systems was faster than in systems spiked with iodide or iodate alone. The reaction of iodate was also faster than that of iodide, which may have been due to the presence of native iodide coupling with spiked iodate; when iodide was added, no native iodate was present to fulfil the same role. No investigation was undertaken into whether this mechanism occurs in soil, however it is possible that in low-SOC soils the presence of native iodide could enhance reduction of spiked iodate to I_2 or HOI as precursors in the transformation to OrgI, in addition to redox coupling with oxides.

8.2 IODINE UPTAKE BY GRASS

In general, higher soil iodine concentrations were associated with higher vegetation iodine concentrations. This is likely to be a result of both higher phyto-available iodine concentrations, and greater direct inputs to soil and vegetation concurrently. Off-take by vegetation was shown to be negligible compared to total soil iodine. In the context of input from rainfall, vegetation uptake is unlikely to deplete soil iodine: estimated iodine rainfall input provided an average of c. 40 times the off-take by vegetation at Rothamsted, and 1 – 10 times for NI soils (excluding ‘coastal’ soils NI05 and NI08, where off-take was greater). The importance of incoming iodine in rainfall/irrigation to replenish the transient pool of phyto-available iodine was clear in the pot experiment, where the majority of iodine in grass was provided by irrigation water, despite this having very low iodine concentration. GSR was the main control on vegetation iodine in Rothamsted samples, overcoming the ‘yield dilution effect’ resulting from faster growth. Dilution was, however, evident in samples from the Rothamsted 2008 treatment plots, where increased yield due to fertilisation resulted in faster growth depleting the transient pool of iodine more rapidly than it could be replenished. Comparison of concentration ratios in pot and field situations for the NI

soils also supported the finding that irrigation water is an important source of iodine for vegetation.

Sorption to the soil solid phase controlled availability of spiked ^{129}I in the plant uptake experiment, with high SOC contents resulting in particularly rapid sorption and low uptake. In NI05 and NI08, which had been particularly exposed to coastal iodine input in their natural environment, spiked iodine remained in solution throughout the experimental period and irrigation water was not important in providing iodine to grass. Results from the soil incubation experiment (Chapter 4) showed that release of ^{127}I from the solid phase occurred through the course of the experiment in these soils and therefore replenishment of phyto-available iodine to soil solution was likely to be rapid. They also had reasonably low SOC contents, so after binding to the most thermodynamically favourable sites had occurred, more labile sites would have been filled. Due to the large amounts of iodine entering the system, there is likely to have been a high concentration of labile iodine.

No conclusions about uptake mechanisms could be made, as passive iodine uptake could not be ruled out, and no correlation between iodine concentration in soil solution and uptake by grass was found. The effect of aqueous iodine speciation on uptake by grass was also not determined. To elucidate this information, solution would need to be extracted from soil during the growth phase, rather than afterwards.

8.3 IMPLICATIONS FOR PROVISION OF DIETARY IODINE

Soil and vegetation iodine concentrations were typically positively correlated, however in most cases the main provision of iodine to vegetation was from irrigation rather than soil. Increasing soil iodine concentration by adding solid fertiliser may therefore be effective in improving the iodine content of foodstuffs, but providing consistent iodine inputs to the transient phyto-available pool via irrigation is likely to be more successful. Trials of this method have been productive in China and this work now elucidates some of the underlying mechanisms for this. The same method will not, however, be effective for all soil types; high SOC contents are likely to result in iodine being fixed in the solid phase and therefore unavailable to plants. In soils with high iodine concentrations but low SOC contents, iodine is likely to be naturally

more available, so these would be the most appropriate soils on which to grow food for iodine sufficiency without intervention.

No general soil management plan has been identified as being effective for improving crop iodine concentrations. Enhanced retention in soil could be achieved by adding organic matter or decreasing soil pH, however too much organic matter would result in iodine fixation within the soil but not the phyto-available pool, and too low a pH may adversely affect crop yields. The predictive models developed could be used to compare likely phyto-availability of already-present iodine in productive fields to inform choices as to where crops are grown, and to determine whether adding iodine to irrigation water is likely to be successful in raising vegetation concentrations in particular soils.

8.4 FUTURE WORK

The main areas that have been highlighted as requiring further investigation to improve knowledge about soil iodine dynamics and plant uptake are:

- identification of organically-bound species of iodine in soil solution;
- investigation of the effect of aqueous iodine speciation on availability to plant and whether uptake is active or passive;
- determination of whether the redox coupling inferred in humic acid systems also occurs in soils, and whether this increases the rate of iodate sorption;
- investigation of the reaction mechanism of iodate with organic matter, given the high density of negative charge on humus.

REFERENCES

- Aldahan, A., Persson, S., Possnert, G. and Hou, X.L., 2009. Distribution of I-127 and I-129 in precipitation at high European latitudes. *Geophysical Research Letters*, 36: 5.
- Alderman, H., 2010. The economic cost of a poor start to life. *Journal of Developmental Origins of Health and Disease*, 1(01): 19-25.
- Allard, B., 2006. A comparative study on the chemical composition of humic acids from forest soil, agricultural soil and lignite deposit. *Bound lipid, carbohydrate and amino acid distributions. Geoderma*, 130: 77 - 96.
- Allard, S., von Gunten, U., Sahli, E., Nicolau, R. and Gallard, H., 2009. Oxidation of iodide and iodine on birnessite (δ -MnO₂) in the pH range 4-8. *Water Research*, 43(14): 3417-3426.
- Amachi, S., 2008. Microbial Contribution to Global Iodine Cycling: Volatilization, Accumulation, Reduction, Oxidation, and Sorption of Iodine. *Microbes and Environments*, 23(4): 269-276.
- Amachi, S., Minami, K., Miyasaka, I. and Fukunaga, S., 2010. Ability of anaerobic microorganisms to associate with iodine: (¹²⁵I) tracer experiments using laboratory strains and enriched microbial communities from subsurface formation water. *Chemosphere*, 79(4): 349-354.
- Andersen, S., Guan, H.X., Teng, W.P. and Laurberg, P., 2009. Speciation of Iodine in High Iodine Groundwater in China Associated with Goitre and Hypothyroidism. *Biological Trace Element Research*, 128(2): 95-103.
- Andersen, S. et al., 2008. Naturally occurring iodine in humic substances in drinking water in Denmark is bioavailable and determines population iodine intake. *British Journal of Nutrition*, 99(2): 319-325.
- Andersson, A., de Benoist, B., Darnton-Hill, I. and Delange, F., 2007a. Iodine deficiency in Europe: A continuing public health problem.
- Andersson, M., de Benoist, B., Delange, F., Zupan, J. and W. H. O. Secretariat, 2007b. Prevention and control of iodine deficiency in pregnant and lactating women and in children less than 2-years-old: conclusions and recommendations of the Technical Consultation. *Public Health Nutrition*, 10(12A): 1606-1611.
- Anke, M., Groppe, B., Müller, M., Scholz, E. and Kramer, K., 1995. The Iodine supply of humans depending on site, food offer and water supply. *Fresenius Journal of Analytical Chemistry*, 352(1-2): 97-101.
- Anschutz, P., Sundby, B., Lefrançois, L., Luther, G.W. and Mucci, A., 2000. Interactions between metal oxides and species of nitrogen and iodine in bioturbated marine sediments. *Geochimica Et Cosmochimica Acta*, 64(16): 2751-2763.
- Anschutz, P., Zhong, S.J., Sundby, B., Mucci, A. and Gobeil, C., 1998. Burial efficiency of phosphorus and the geochemistry of iron in continental margin sediments. *Limnology and Oceanography*, 43(1): 53-64.
- Ashworth, D.J. and Shaw, G., 2006a. A comparison of the soil migration and plant uptake of radioactive chlorine and iodine from contaminated groundwater. *Journal of Environmental Radioactivity*, 89(1): 61-80.
- Ashworth, D.J. and Shaw, G., 2006b. Effects of moisture content and redox potential on in situ K-d values for radioiodine in soil. *Science of the Total Environment*, 359(1-3): 244-254.
- Assemi, S. and Erten, H.N., 1994. Sorption of radioiodine on organic-rich soil, clay-minerals and alumina. *Journal of Radioanalytical and Nuclear Chemistry-Articles*, 178(1): 193-204.

- Baker, A.R., Thompson, D., Campos, M.L.A.M., Parry, S.J. and Jickells, T.D., 2000. Iodine concentration and availability in atmospheric aerosol. *Atmospheric Environment*, 34(25): 4331-4336.
- Barry, T.N., Duncan, S.J., Sadler, W.A., Millar, K.R. and Sheppard, A.D., 1983. Iodine-metabolism and thyroid-hormone relationships in growing sheep fed on kale (*brassica-oleracea*) and ryegrass (*lolium-perenne*)-clover (*trifolium-repens*) fresh-forage diets. *British Journal of Nutrition*, 49(2): 241-253.
- Bath, S.C., Button, S. and Rayman, M.P., 2011. Iodine concentration of organic and conventional milk: implications for iodine intake. *British Journal of Nutrition*.
- Beals, D.M., Chastagner, P. and Turner, P., 1992. Analysis of iodine-129 in aqueous samples by inductively coupled plasma - mass spectrometry.
- Beresford, N.A. et al., 2012. Observations of Fukushima fallout in Great Britain. *Journal of Environmental Radioactivity*, 114: 48-53.
- Bird, G.A. and Schwartz, W., 1997. Distribution coefficients, K_ds, for iodide in Canadian Shield Lake sediments under oxic and anoxic conditions. *Journal of Environmental Radioactivity*, 35(3): 261-279.
- Blake, L. and Goulding, K.W.T., 2002. Effects of atmospheric deposition, soil pH and acidification on heavy metal contents in soils and vegetation of semi-natural ecosystems at Rothamsted Experimental Station, UK. *Plant and Soil*, 240(2): 235-251.
- Blasco, B. et al., 2011. Does Iodine Biofortification Affect Oxidative Metabolism in Lettuce Plants? *Biological Trace Element Research*, 142(3): 831-842.
- Blasco, B. et al., 2008. Iodine biofortification and antioxidant capacity of lettuce: potential benefits for cultivation and human health. *Annals of Applied Biology*, 152(3): 289-299.
- Bloss, W. and Ball, S., 2009. Iodine chemistry in the coastal marine atmosphere, *Royal Society of Chemistry Environmental Chemistry Group Bulletin*. Royal Society of Chemistry, pp. 3 - 8.
- Bostock, A.C., Shaw, G. and Bell, J.N.B., 2003. The volatilisation and sorption of ¹²⁹I in coniferous forest, grassland and frozen soils. *Journal of Environmental Radioactivity*, 70(1-2): 29-42.
- Bradley, P.M., Chapelle, F.H. and Lovley, D.R., 1998. Humic acids as electron acceptors for anaerobic microbial oxidation of vinyl chloride and dichloroethene. *Applied and Environmental Microbiology*, 64(8): 3102-3105.
- Brown, C.F., Geiszler, K.N. and Lindberg, M.J., 2007. Analysis of I-129 in groundwater samples: Direct and quantitative results below the drinking water standard. *Applied Geochemistry*, 22(3): 648-655.
- Buchberger, W., Czizsek, B., Hann, S. and Stingeder, G., 2003. Preliminary comparison of inductively coupled plasma mass spectrometry and electrospray mass spectrometry hyphenated with ion chromatography for trace analysis of iodide. *Journal of Analytical Atomic Spectrometry*, 18(5): 512-514.
- Caffagni, A. et al., 2011. Iodine Fortification Plant Screening Process and Accumulation in Tomato Fruits and Potato Tubers. *Communications in Soil Science and Plant Analysis*, 42(6): 706-718.
- Campos, M., Nightingale, P. and Jickells, T., 1996. A comparison of methyl iodide emissions from seawater and wet depositional fluxes of iodine over the southern North Sea. *Tellus B*, 48: 106-114.
- Cao, X.Y. et al., 1994. Iodination of irrigation water as a method of supplying iodine to a severely iodine-deficient population in Xinjiang, China. *Lancet*, 344(8915): 107-110.

- Carpenter, L.J. et al., 2013. Atmospheric iodine levels influenced by sea surface emissions of inorganic iodine. *Nature Geoscience*, 6(2): 108-111.
- Chance, R. et al., 2009. Release and transformations of inorganic iodine by marine macroalgae. *Estuarine Coastal and Shelf Science*, 82(3): 406-414.
- Chen, J.H., Wang, K.E. and Jiang, S.J., 2007. Determination of iodine and bromine compounds in foodstuffs by CE-inductively coupled plasma MS. *Electrophoresis*, 28(22): 4227-4232.
- Christiansen, J.V. and Carlsen, L., 1991. Enzymatically controlled iodination reactions in the terrestrial environment. *Radiochimica Acta*, 52-3: 327-333.
- Cohen, B.L., 1985. The Origin of I in Soil and the 129I Problem. *Health Physics*, 49(2): 279-285.
- Collins, C.D., Gravett, A.E. and Bell, J.N.B., 2004. The deposition and translocation of methyl iodide by crops. *Health Physics*, 87(5): 512-516.
- Cornish Seaweed Resources, 2010. Cornish Seaweed Resources.
- Cruickshank, J.G.E., 1997. Soil and Environment: Northern Ireland. Agricultural and Environmental Science Division, DANI; and The Agricultural and Environmental Science Department, The Queen's University of Belfast.
- Dahl, L., Opsahl, J.A., Meltzer, H.M. and Julshamn, K., 2003. Iodine concentration in Norwegian milk and dairy products. *British Journal of Nutrition*, 90(3): 679-685.
- Dai, J.L. et al., 2009. Adsorption and desorption of iodine by various Chinese soils: II. Iodide and iodate. *Geoderma*, 153(1-2): 130-135.
- Dai, J.L., Zhang, M. and Zhu, Y.G., 2004. Adsorption and desorption of iodine by various Chinese soils - I. Iodate. *Environment International*, 30(4): 525-530.
- Dai, J.L., Zhu, Y.G., Huang, Y.Z., Zhang, M. and Song, J.L., 2006. Availability of iodide and iodate to spinach (*Spinacia oleracea* L.) in relation to total iodine in soil solution. *Plant and Soil*, 289(1-2): 301-308.
- de Benoist, B., Andersson, M., Takkouche, B. and Egli, I., 2003. Prevalence of iodine deficiency worldwide. *The Lancet*, 362(9398): 1859-1860.
- de Benoist, B., McLean, E., Andersson, M. and Rogers, L., 2008. Iodine deficiency in 2007: Global progress since 2003. *Food and Nutrition Bulletin*, 29(3): 195-202.
- de Long, G.R., 2002. Iodine Dripping into Irrigation Water: Its Role in Correcting Iodine Deficiency. *ICCIDD Newsletter*, 2002(November): 60 - 61.
- DeLong, G.R., 2002. Iodine Dripping into Irrigation Water: Its Role in Correcting Iodine Deficiency. *ICCIDD Newsletter*, 2002(November): 60 - 61.
- Di Bonito, M., 2005. Trace elements in pore water: a comparison of sampling methods, University of Nottingham.
- Dodd, M.E., Silvertown, J., McConway, K., Potts, J. and Crawley, M., 1994. Stability in the plant-communities of the Park-Grass-experiment - the relationships between species richness, soil-pH and biomass variability. *Philosophical Transactions of the Royal Society of London Series B-Biological Sciences*, 346(1316): 185-193.
- Downs, A.J. and Adams, C.J., 1975. *The Chemistry of Chlorine, Bromine, Iodine and Astatine*. Pergamon Texts in Inorganic Chemistry, 7. Pergamon Press, Oxford.
- Dunn, J.T., 1993. Sources of Dietary Iodine in Industrialized Countries. *Iodine Deficiency in Europe*, 241: 17-23.
- Dyke, J.V., Dasgupta, P.K. and Kirk, A.B., 2009. Trace iodine quantitation in biological samples by mass spectrometric methods The optimum internal standard. *Talanta*, 79(2): 235-242.

- Eckhoff, K.M. and Maage, A., 1997. Iodine content in fish and other food products from East Africa analyzed by ICP-MS. *Journal of Food Composition and Analysis*, 10(3): 270-282.
- Endo, S. et al., 2012. Measurement of soil contamination by radionuclides due to the Fukushima Dai-ichi Nuclear Power Plant accident and associated estimated cumulative external dose estimation. *Journal of Environmental Radioactivity*, 111: 18-27.
- Fecher, P.A., Goldmann, I. and Nagengast, A., 1998. Determination of iodine in food samples by inductively coupled plasma mass spectrometry after alkaline extraction. *Journal of Analytical Atomic Spectrometry*, 13(9): 977-982.
- Fernandez-Sanchez, L. and Szpunar, J., 1999. Speciation analysis for iodine in milk by size-exclusion chromatography with inductively coupled plasma mass spectrometric detection (SEC-ICP MS). *Journal of Analytical Atomic Spectrometry*, 14(11): 1697-1702.
- Fordyce, 2003. Database of the iodine content of food and diets populated with data from published literature. In: Department for International Development (Editor).
- Fordyce, F.M., Stewart, A.G., Ge, X., Jiang, J.-Y. and Cave, M., 2003. Environmental Controls in IDD: A Case Study in the Xinjiang Province of China. British Geological Society.
- Fox, P.M., Davis, J.A. and Luther, G.W., 2009. The kinetics of iodide oxidation by the manganese oxide mineral birnessite. *Geochimica Et Cosmochimica Acta*, 73(10): 2850-2861.
- Francois, R., 1987. The influence of humic substances on the geochemistry of iodine in nearshore and hemipelagic marine sediments. *Geochimica et Cosmochimica Acta*, 51: 2417 - 2427.
- Franke, K., Meyer, U., Wagner, H., Hoppen, H.O. and Flachowsky, G., 2009. Effect of various iodine supplementations, rapeseed meal application and two different iodine species on the iodine status and iodine excretion of dairy cows. *Livestock Science*, 125(2-3): 223-231.
- Fuge, R., 1990. The Role of Volatility in the Distribution of Iodine in the Secondary Environment. *Applied Geochemistry*, 5(3): 357-360.
- Fuge, R., 1996. Geochemistry of iodine in relation to iodine deficiency diseases. In: J.D. Appleton, R. Fuge and G.J.H. McCall (Editors), *Environmental Geochemistry and Health, with Special Reference to Developing Countries*. Geological Society Special Publication. Geological Soc Publishing House, Bath, pp. 201-211.
- Fuge, R., 2005. Soils and Iodine Deficiency. In: O. Selinus (Editor), *Essentials of Medical Geology, Impacts of the Natural Environment on Public Health*. Elsevier Academic Press, pp. 417 - 424.
- Fuge, R. and Johnson, C.C., 1986. The Geochemistry of Iodine - a Review. *Environmental Geochemistry and Health*, 8(2): 31-54.
- Gallard, H., Allard, S., Nicolau, R., von Gunten, U. and Croue, J.P., 2009. Formation of Iodinated Organic Compounds by Oxidation of Iodide-Containing Waters with Manganese Dioxide. *Environmental Science & Technology*, 43(18): 7003-7009.
- Gerzabek, M.H., Muramatsu, Y., Strebl, F. and Yoshida, S., 1999. Iodine and bromine contents of some Austrian soils and relations to soil characteristics. *Journal of Plant Nutrition and Soil Science-Zeitschrift Fur Pflanzenernahrung Und Bodenkunde*, 162(4): 415-419.

- Gilfedder, B.S., Lai, S.C., Petri, M., Biester, H. and Hoffmann, T., 2008. Iodine speciation in rain, snow and aerosols. *Atmospheric Chemistry and Physics*, 8(20): 6069-6084.
- Gilfedder, B.S., Petri, M. and Biester, H., 2007. Iodine speciation in rain and snow: Implications for the atmospheric iodine sink. *Journal of Geophysical Research-Atmospheres*, 112(D7): 7.
- Gilfedder, B.S., Petri, M. and Biester, H., 2009. Iodine speciation and cycling in fresh waters: a case study from a humic rich headwater lake (Mummelsee). *Journal of Limnology*, 68(2): 396-408.
- Goldschmidt, V.M., 1958. *Geochemistry*. Oxford Clarendon Press, 602 - 620 pp.
- Goulding, K.W.T., McGrath, S.P. and Johnston, A.E., 1989. Predicting the lime requirements of soils under permanent grassland and arable crops. *Soil Use and Management*, 5(2): 54-58.
- Haldimann, M., Alt, A., Blanc, A. and Blondeau, K., 2005. Iodine content of food groups. *Journal of Food Composition and Analysis*, 18(6): 461-471.
- Haldimann, M., Eastgate, A. and Zimmerli, B., 2000. Improved measurement of iodine in food samples using inductively coupled plasma isotope dilution mass spectrometry. *Analyst*, 125(11): 1977-1982.
- Haldimann, M., Zimmerli, B., Als, C. and Gerber, H., 1998. Direct determination of urinary iodine by inductively coupled plasma mass spectrometry using isotope dilution with iodine-129. *Clinical Chemistry*, 44(4): 817-824.
- Hansen, V., Roos, P., Aldahan, A., Hou, X. and Possnert, G., 2011. Partition of iodine ((129)I and (127)I) isotopes in soils and marine sediments. *Journal of Environmental Radioactivity*, 102(12): 1096-1104.
- Hauschild, J. and Aumann, D.C., 1989. Iodine-129 in the environment of a nuclear fuel reprocessing plant: V. The transfer of I-129 and I-127 in the soil-pasture-cow-milk/meat pathway as obtained by field measurements. *J. Environ. Radioactivity*, 9: 145-162.
- Hercus, C.E. and Roberts, K.C., 1927. The iodine content of foods, manures and animal products in relation to the prophylaxis of endemic goitre in New Zealand. *Journal of Hygiene*, 26(1): 49-83.
- Heumann, K.G., 1992. Isotope-dilution mass-spectrometry (IDMS) of the elements. *Mass Spectrometry Reviews*, 11(1): 41-67.
- Heumann, K.G., Rottmann, L. and Vogl, J., 1994. Elemental speciation with liquid chromatography inductively-coupled plasma isotope-dilution mass spectrometry. *Journal of Analytical Atomic Spectrometry*, 9(12): 1351-1355.
- Hirsch, R., Ternes, T.A., Lindart, A., Haberer, K. and Wilken, R.D., 2000. A sensitive method for the determination of iodine containing diagnostic agents in aqueous matrices using LC-electrospray-tandem-MS detection. *Fresenius Journal of Analytical Chemistry*, 366(8): 835-841.
- Hong, C. et al., 2012. Evaluation of Iodide and Iodate for Adsorption-Desorption Characteristics and Bioavailability in Three Types of Soil. *Biological Trace Element Research*, 146(2): 262-271.
- Hong, C.L., Weng, H.X., Yan, A.L. and Islam, E.U., 2009. The fate of exogenous iodine in pot soil cultivated with vegetables. *Environmental Geochemistry and Health*, 31(1): 99-108.
- Hou, X.L. et al., 2009. A review on speciation of iodine-129 in the environmental and biological samples. *Analytica Chimica Acta*, 632(2): 181-196.

- Hu, Q.H., Zhao, P.H., Moran, J.E. and Seaman, J.C., 2005. Sorption and transport of iodine species in sediments from the Savannah River and Hanford Sites. *Journal of Contaminant Hydrology*, 78(3): 185-205.
- ICCIDD, 2009a. ICCIDD: About us.
- ICCIDD, 2009b. The need for iodine, pp. ICCIDD website briefly describing the need for iodine.
- Izmer, A.V., Boulyga, S.F. and Becker, J.S., 2003. Determination of I-129/I-127 isotope ratios in liquid solutions and environmental soil samples by ICP-MS with hexapole collision cell. *Journal of Analytical Atomic Spectrometry*, 18(11): 1339-1345.
- Izmer, A.V., Boulyga, S.F., Zoriy, M.V. and Becker, J.S., 2004. Improvement of the detection limit for determination of I-129 in sediments by quadrupole inductively coupled plasma mass spectrometer with collision cell. *Journal of Analytical Atomic Spectrometry*, 19: 1278 - 1280.
- Jenkinson, D.S. et al., 1994. Trends in herbage yields over the last century on the Rothamsted long-term continuous hay experiment. *Journal of Agricultural Science*, 122: 365-374.
- Johnson, C.C., 2003a. Database of the iodine content of soils populated with data from published literature. British Geological Survey Commissioned Report.
- Johnson, C.C., 2003b. The geochemistry of iodine and its application to environmental strategies for reducing the risks from iodine deficiency disorders (IDD). British Geological Survey Commissioned Report.
- Johnson, C.C., Fordyce, F.M. and Stewart, A.G., 1999. Environmental Controls in IDD - What do we really know? ICCIDD Newsletter, November: 56 - 57.
- Johnson, C.C., Fordyce, F.M. and Stewart, A.G., 2003. Environmental Controls in Iodine Deficiency Disorders Project Summary Report. British Geological Survey.
- Johnson, C.C., Strutt, M.H., Hmeurras, M. and Mounir, M., 2002. Iodine in the environment of the High Atlas Mountains, Morocco. British Geological Survey Commissioned Report.
- Johnston, A.E., Goulding, K.W.T. and Poulton, P.R., 1986. Soil acidification during more than 100 years under permanent grassland and woodland at Rothamsted. *Soil Use and Management*, 2(1): 3-10.
- Julshamn, K., Dahl, L. and Eckhoff, K., 2001. Determination of iodine in seafood by inductively coupled plasma/mass spectrometry. *Journal of Aoac International*, 84(6): 1976-1983.
- Kashparov, V. et al., 2005. Soil-to-plant halogens transfer studies 1. Root uptake of radioiodine by plants. *Journal of Environmental Radioactivity*, 79(2): 187-204.
- Kelly, F.C., 1961. Iodine in medicine and pharmacy since its discovery - 1811 - 1961. *Proceedings of the Royal Society of Medicine-London*, 54(10): 831-&.
- Kelly, F.C. and Snedden, W.W., 1960. Prevalence and geographical distribution of endemic goitre. *Monogr Ser World Health Organ*, 44: 27-233.
- Keppler, F. et al., 2003. Organoiodine formation during humification in peatlands. *Environmental Chemistry Letters*, 1(4): 219-223.
- Knapp, H.A., 1964. I-131 in fresh milk and human thyroids following a single deposition of nuclear test fallout. *Nature*, 202(9 May 1964): 534-537.
- Kodama, S., Takahashi, Y., Okumura, K. and Uruga, T., 2006. Speciation of iodine in solid environmental samples by iodine K-edge XANES: Application to soils and ferromanganese oxides. *Science of the Total Environment*, 363(1-3): 275-284.

- Kostka, J.E. and Luther, G.W., 1994. Partitioning and speciation of solid-phase iron in salt-marsh sediments. *Geochimica Et Cosmochimica Acta*, 58(7): 1701-1710.
- Krupp, G. and Aumann, D.C., 1999. The origin of iodine in soil: I. Iodine in rainfall over Germany. *Chemie Der Erde-Geochemistry*, 59(1): 57-67.
- Landini, M., Gonzali, S. and Perata, P., 2011. Iodine biofortification in tomato. *Journal of Plant Nutrition and Soil Science*, 174(3): 480-486.
- Leiterer, M., Truckenbrodt, D. and Franke, K., 2001. Determination of iodine species in milk using ion chromatographic separation and ICP-MS detection. *European Food Research and Technology*, 213(2): 150-153.
- Li, H.-P. et al., 2012. Bacterial Production of Organic Acids Enhances H₂O₂-Dependent Iodide Oxidation. *Environmental Science & Technology*, 46(9): 4837-4844.
- Lidiard, H.M., 1995. Iodine in the reclaimed upland soils of a farm in the Exmoor National Park, Devon, U.K. and its impact on livestock health. *Applied Geochemistry*, 10: 85 - 95.
- Lucia, M. and Campos, A.M., 1997. New approach to evaluating dissolved iodine speciation in natural waters using cathodic stripping voltammetry and a storage study for preserving iodine species. *Marine Chemistry*, 57(1-2): 107-117.
- Machado, E.C., Bellido, L.F. and Bellido, A.V., 2001. Separation of iodine species by adsorption chromatography. *Journal of Radioanalytical and Nuclear Chemistry*, 249(3): 653-656.
- Mackowiak, C.L. and Grossl, P.R., 1999. Iodate and iodide effects on iodine uptake and partitioning in rice (*Oryza sativa* L.) grown in solution culture. *Plant and Soil*, 212(2): 135-143.
- MacNaeidhe, F., 1995. Procedures and precautions used in sampling techniques and analysis of trace elements in plant matrices. *Science of the Total Environment*, 176(1-3): 25-31.
- Marshall, S., 1992. The complexation of aluminium by humic acids in fresh waters, University of Nottingham.
- Martino, M., Mills, G.P., Woeltjen, J. and Liss, P.S., 2009. A new source of volatile organoiodine compounds in surface seawater. *Geophysical Research Letters*, 36.
- Michalke, B., 2003. Element speciation definitions, analytical methodology, and some examples. *Ecotoxicology and Environmental Safety*, 56(1): 122-139.
- Michalke, B. and Schramel, P., 1999. Iodine speciation in biological samples by capillary electrophoresis - inductively coupled plasma mass spectrometry. *Electrophoresis*, 20(12): 2547-2553.
- Ming, C.A., 2004. Total organic carbon in soil - SSM5000A application note, Shimadzu.
- Moreda-Pineiro, A., Romaris-Hortas, V. and Bermejo-Barrera, P., 2011. A review on iodine speciation for environmental, biological and nutrition fields. *Journal of Analytical Atomic Spectrometry*, 26(11): 2107-2152.
- Morris, M.G., 1992. Responses of Auchenorrhyncha (Homoptera) to fertiliser and liming treatments at Park Grass, Rothamsted. *Agriculture Ecosystems and Environment*, 41(3-4): 263-283.
- Moulin, V., Reiller, P., Amekraz, B. and Moulin, C., 2001. Direct characterization of iodine covalently bound to fulvic acids by electrospray mass spectrometry. *Rapid communications in mass spectrometry*, 15: 2488 - 2496.

- Muramatsu, Y., Uchida, S., Sriyotha, P. and Sriyotha, K., 1990. Some considerations on the sorption and desorption phenomena of iodide and iodate on soil. *Water Air and Soil Pollution*, 49(1-2): 125-138.
- Muramatsu, Y. and Wedepohl, K.H., 1998. The distribution of iodine in the earth's crust. *Chemical Geology*, 147(3-4): 201-216.
- Muramatsu, Y. and Yoshida, S., 1995. Volatilization of methyl-iodide from the soil-plant system. *Atmospheric Environment*, 29(1): 21-25.
- Muramatsu, Y., Yoshida, S. and Bannai, T., 1994. Tracer experiments on the behavior of radioiodine in the soil-plant-atmosphere system, 3rd International Conference on Methods and Applications of Radioanalytical Chemistry (MARC-III). *Akademiai Kiado, Kailua Kona, Hi*, pp. 303-310.
- Muramatsu, Y., Yoshida, S., Fehn, U., Amachi, S. and Ohmomo, Y., 2004. Studies with natural and anthropogenic iodine isotopes: iodine distribution and cycling in the global environment. *Journal of Environmental Radioactivity*, 74(1-3): 221-232.
- Neal, C., Neal, M., Wickham, H., Hill, L. and Harman, S., 2007. Dissolved iodine in rainfall, cloud, stream and groundwater in the Plynlimon area of mid-Wales. *Hydrology and Earth System Sciences*, 11(2): 283-293.
- Nitschke, U., Ruth, A.A., Dixneuf, S. and Stengel, D.B., 2011. Molecular iodine emission rates and photosynthetic performance of different thallus parts of *Laminaria digitata* (Phaeophyceae) during emersion. *Planta*, 233(4): 737-748.
- Orr, J.B., Kelly, F.C. and Stuart, G.L., 1928. The effect of iodine manuring on the iodine content of plants. *Journal of Agricultural Science*, 18: 159-161.
- Pantsar-Kallio, M. and Manninen, P.K.G., 1998. Speciation of halogenides and oxyhalogens by ion chromatography inductively coupled plasma mass spectrometry. *Analytica Chimica Acta*, 360(1-3): 161-166.
- Phillips, D.I.W., 1997. Iodine, milk, and the elimination of endemic goitre in Britain: the story of an accidental public health triumph. *Journal of Epidemiology and Community Health*, 51(4): 391-393.
- Popp, M., Hann, S. and Koellensperger, G., 2010. Environmental application of elemental speciation analysis based on liquid or gas chromatography hyphenated to inductively coupled plasma mass spectrometry-A review. *Analytica Chimica Acta*, 668(2): 114-129.
- Radlinger, G. and Heumann, K.G., 2000. Transformation of iodide in natural and wastewater systems by fixation on humic substances. *Environmental Science & Technology*, 34(18): 3932-3936.
- Redeker, K.R. et al., 2000. Emissions of methyl halides and methane from rice paddies. *Science*, 290(5493): 966-969.
- Reid, H.J. et al., 2008. Determination of iodine and molybdenum in milk by quadrupole ICP-MS. *Talanta*, 75(1): 189-197.
- Reiller, P., Mercier-Bion, F., Gimenez, N., Barre, N. and Miserque, F., 2006. Iodination of humic acid samples from different origins. *Radiochimica Acta*, 94(9-11): 739-745.
- Ren, Q., Fan, J., Zhang, Z.Z., Zheng, X.Y. and DeLong, G.R., 2008. An environmental approach to correcting iodine deficiency: Supplementing iodine in soil by iodination of irrigation water in remote areas. *Journal of Trace Elements in Medicine and Biology*, 22(1): 1-8.
- Rengel, Z., Batten, G.D. and Crowley, D.E., 1999. Agronomic approaches for improving the micronutrient density in edible portions of field crops. *Field Crops Research*, 60(1-2): 27-40.

- Rodriguez-Gonzalez, P., Marchante-Gayon, J.M., Alonso, J.I.G. and Sanz-Medel, A., 2005. Isotope dilution analysis for elemental speciation: A tutorial review. *Spectrochimica Acta Part B-Atomic Spectroscopy*, 60(2): 151-207.
- Romaris-Hortas, V. et al., 2011. Bioavailability study using an in-vitro method of iodine and bromine in edible seaweed. *Food Chemistry*, 124(4): 1747-1752.
- Rose, M. et al., 2001. Bromine and iodine in 1997 UK total diet study samples. *Journal of Environmental Monitoring*, 3(4): 361-365.
- Rothamsted Research, 2006. Rothamsted Long-term Experiments.
- Royal Society of Chemistry, Iodine Factsheet.
- Rui, Y.-k., Jiang, S.-l., Zhang, F.-s. and Shen, J.-h., 2009. Effects of nitrogen fertilizer input on the composition of mineral elements in corn grain. *Agrociencia*, 43(1): 21-27.
- Saikat, S.Q., Carter, J.E., Mehra, A., Smith, B. and Stewart, A., 2004. Goitre and environmental iodine deficiency in the UK - Derbyshire: a review. *Environmental Geochemistry and Health*, 26(4): 395-401.
- Saiz-Lopez, A. et al., 2006. Modelling molecular iodine emissions in a coastal marine environment: the link to new particle formation. *Atmospheric Chemistry and Physics*, 6: 883-895.
- Sandell, E.B. and Kolthoff, I.M., 1937. Micro determination of iodine by a catalytic method. *Microchimica Acta*, 1(1): 9 - 25.
- Saunders, R.W., Kumar, R., MacDonald, S.M. and Plane, J.M.C., 2012. Insights into the Photochemical Transformation of Iodine in Aqueous Systems: Humic Acid Photosensitized Reduction of Iodate. *Environmental Science & Technology*, 46(21): 11854-11861.
- Schlegel, M.L., Reiller, P., Mercier-Bion, F., Barre, N. and Moulin, V., 2006. Molecular environment of iodine in naturally iodinated humic substances: Insight from X-ray absorption spectroscopy. *Geochimica et Cosmochimica Acta*, 70: 5536 - 5551.
- Schmitz, K. and Aumann, D.C., 1994. Why are the soil-to-pasture transfer-factors, as determined by field-measurements, for I-127 lower than for I-129. *Journal of Environmental Radioactivity*, 24(1): 91-100.
- Schmitz, K. and Aumann, D.C., 1995. A study on the association of two iodine isotopes, of natural I-127 and of the fission product I-129, with soil components using a sequential extraction procedure. *Journal of Radioanalytical and Nuclear Chemistry-Articles*, 198(1): 229-236.
- Schnell, D. and Aumann, D.C., 1999. The origin of iodine in soil: II. Iodine in soils of Germany. *Chemie Der Erde-Geochemistry*, 59(1): 69-76.
- Schone, F. et al., 2009. Iodine concentration of milk in a dose-response study with dairy cows and implications for consumer iodine intake. *Journal of Trace Elements in Medicine and Biology*, 23(2): 84-92.
- Schwehr, K.A. and Santschi, P.H., 2003. Sensitive determination of iodine species, including organo-iodine, for freshwater and seawater samples using high performance liquid chromatography and spectrophotometric detection. *Analytica Chimica Acta*, 482(1): 59-71.
- Schwehr, K.A., Santschi, P.H., Kaplan, D.I., Yeager, C.M. and Brinkmeyer, R., 2009. Organo-Iodine Formation in Soils and Aquifer Sediments at Ambient Concentrations. *Environmental Science & Technology*, 43(19): 7258-7264.
- Seki, M. et al., 2013. Laccase-catalyzed oxidation of iodide and formation of organically bound iodine in soils. *Environmental science & technology*, 47(1): 390-7.

- Shaw, G., Scott, L.K. and Kinnersley, R.P., 2007. Sorption of caesium, iodine and sulphur in solution to the adaxial leaf surface of broad bean (*Vicia faba* L.). *Environmental and Experimental Botany*, 59(3): 361-370.
- Sheppard, M.I., Hawkins, J.L. and Smith, P.A., 1996. Linearity of iodine sorption and sorption capacities for seven soils. *Journal of Environmental Quality*, 25(6): 1261-1267.
- Sheppard, M.I. and Thibault, D.H., 1992. Chemical Behaviour of Iodine in Organic and Mineral Soils. *Applied Geochemistry*, 7(3): 265-272.
- Sheppard, M.I., Thibault, D.H., Smith, P.A. and Hawkins, J.L., 1994. Volatilization - a soil gassing coefficient for iodine. *Journal of Environmental Radioactivity*, 25(3): 189-203.
- Sheppard, S.C. and Evenden, W.G., 1988. The assumption of linearity in soil and plant concentration ratios - an experimental evaluation. *Journal of Environmental Radioactivity*, 7(3): 221-247.
- Sheppard, S.C., Evenden, W.G. and Amiro, B.D., 1993. Investigation of the soil-to-plant pathway for I, Br, Cl and F. *Journal of Environmental Radioactivity*, 21(1): 9-32.
- Sheppard, S.C., Long, J.M. and Sanipelli, B., 2010. Plant/soil concentration ratios for paired field and garden crops, with emphasis on iodine and the role of soil adhesion. *Journal of Environmental Radioactivity*, 101(12): 1032-1037.
- Sheppard, S.C., Sheppard, M.I., Tait, J.C. and Sanipelli, B.L., 2006. Revision and meta-analysis of selected biosphere parameter values for chlorine, iodine, neptunium, radium, radon and uranium. *Journal of Environmental Radioactivity*, 89(2): 115-137.
- Shetaya, W.H., Young, S.D., Watts, M.J., Ander, E.L. and Bailey, E.H., 2012. Iodine dynamics in soils. *Geochimica et Cosmochimica Acta*, 77(0): 457-473.
- Shimamoto, Y.S., Itai, T. and Takahashi, Y., 2010. Soil column experiments for iodate and iodide using K-edge XANES and HPLC-ICP-MS. *Journal of Geochemical Exploration*, 107(2): 117-123.
- Shimamoto, Y.S. and Takahashi, Y., 2008. Superiority of K-edge XANES over L-III-edge XANES in the speciation of iodine in natural soils. *Analytical Sciences*, 24(3): 405-409.
- Shimamoto, Y.S., Takahashi, Y. and Terada, Y., 2011. Formation of Organic Iodine Supplied as Iodide in a Soil-Water System in Chiba, Japan. *Environmental Science & Technology*, 45(6): 2086-2092.
- Silvertown, J. et al., 2006. The Park Grass Experiment 1856-2006: Its contribution to ecology. *Journal of Ecology*, 94(4): 801-814.
- Smith, L.C., Morton, J.D. and Catto, W.D., 1999. The effects of fertiliser iodine application on herbage iodine concentration and animal blood levels. *New Zealand Journal of Agricultural Research*, 42(4): 433-440.
- Smith, L.C., Morton, J.D., Longhurst, R.D., O'Connor, M.B. and Catto, W.D., 2006. Fortification of silage and hay crops with trace elements. *New Zealand Journal of Agricultural Research*, 49(3): 273-284.
- Smoleń, S., Rozek, S., Strzetelski, P. and Ledwozyw-Smolen, I., 2011. Preliminary evaluation of the influence of soil fertilization and foliar nutrition with iodine on the effectiveness of iodine biofortification and mineral composition of carrot. *Journal of Elementology*, 16(1): 103-113.
- Smyth, D. and Johnson, C.C., 2011. Distribution of iodine in soils of Northern Ireland. *Geochemistry-Exploration Environment Analysis*, 11(1): 25-39.

- Smyth, P.P.A. et al., 2011. Does iodine gas released from seaweed contribute to dietary iodine intake? *Environmental Geochemistry and Health*, 33(4): 389-397.
- Stark, H.J., Mattusch, J., Wennrich, R. and Mroczek, A., 1997. Investigation of the IC-ICP-MS determination of iodine species with reference to sample digestion procedures. *Fresenius Journal of Analytical Chemistry*, 359(4-5): 371-374.
- Stewart, A.G., 1990. For debate: Drifting continents and endemic goitre in northern Pakistan. *BMJ*, 300: 1507-1512.
- Stewart, A.G., Carter, J., Parker, A. and Alloway, B.J., 2003. The Illusion of Environmental Iodine Deficiency. *Environmental Geochemistry and Health*, 25(1): 165 - 170.
- Stewart, A.G. and Pharoah, P.O.D., 1996. Clinical and epidemiological correlates of iodine deficiency disorders. *Environmental Geochemistry and Health*(113): 223-230.
- Striegel, A.M., Yau, W.W., Kirkland, J.J. and Bly, D.D., 2009. *Modern Size-Exclusion Liquid Chromatography*. Wiley.
- Sutton, R. and Sposito, G., 2005. Molecular structure in soil humic substances: The new view. *Environmental Science & Technology*, 39(23): 9009-9015.
- Tagami, K., Uchida, S., Hirai, I., Tsukada, H. and Takeda, H., 2006. Determination of chlorine, bromine and iodine in plant samples by inductively coupled plasma-mass spectrometry after leaching with tetramethyl ammonium hydroxide under a mild temperature condition. *Analytica Chimica Acta*, 570(1): 88-92.
- Tagami, K., Uchida, S., Takeda, A., Yamasaki, S. and Tsuchiya, N., 2010. Estimation of Plant-Unavailable Iodine Concentrations in Agricultural Fields. *Soil Science Society of America Journal*, 74(5): 1562-1567.
- Tilman, D. et al., 1994. The Park Grass Experiment: Insights from the most long-term ecological study. In: R.A. Leigh and A.E. Johnston (Editors), *Long-term experiments in agricultural and ecological sciences*. CAB International, Wallingford, pp. 287 - 303.
- Truesdale, V.W. and Jones, S.D., 1996. The variation of iodate and total iodine in some UK rainwaters during 1980-1981. *Journal of Hydrology*, 179(1-4): 67-86.
- Tschiersch, J., Shinonaga, T. and Heuberger, H., 2009. Dry deposition of gaseous radioiodine and particulate radiocaesium onto leafy vegetables. *Science of the Total Environment*, 407(21): 5685-5693.
- Tsukada, H., Takeda, A., Tagami, K. and Uchida, S., 2008. Uptake and Distribution of Iodine in Rice Plants. *Journal of Environmental Quality*, 37(6): 2243-2247.
- Tye, A.M., Kemp, S.J. and Poulton, P.R., 2009. Responses of soil clay mineralogy in the Rothamsted Classical Experiments in relation to management practice and changing land use. *Geoderma*, 153(1-2): 136-146.
- Vanderpump, M.P.J. et al., 2011. Iodine status of UK schoolgirls: a cross-sectional survey. *The Lancet*, 377(9782): 2007 - 2012.
- Voogt, W., Holwerda, H.T. and Khodabaks, R., 2010. Biofortification of lettuce (*Lactuca sativa* L.) with iodine: the effect of iodine form and concentration in the nutrient solution on growth, development and iodine uptake of lettuce grown in water culture. *Journal of the Science of Food and Agriculture*, 90(5): 906-913.
- Wang, K.E. and Jiang, S.J., 2008. Determination of iodine and bromine compounds by ion chromatography/dynamic reaction cell inductively coupled plasma mass spectrometry. *Analytical Sciences*, 24(4): 509-514.

- Warner, J.A., Casey, W.H. and Dahlgren, R.A., 2000. Interaction kinetics of I⁻²(aq) with substituted phenols and humic substances. *Environmental Science & Technology*, 34(15): 3180-3185.
- Warren, R.G. and Johnston, A.E., 1963. The Park Grass Experiment; Rothamsted experimental station report.
- Warwick, P., Zhao, R., Higgo, J.J.W., Smith, B. and Williams, G.M., 1993. The mobility and stability of iodine-humic and iodine-fulvic complexes through sand. *Science of the Total Environment*, 130: 459-465.
- Watts, M.J. and Mitchell, C.J., 2009. A pilot study on iodine in soils of Greater Kabul and Nangarhar provinces of Afghanistan. *Environmental Geochemistry and Health*, 31(4): 503-509.
- Watts, M.J. et al., 2010. A snapshot of environmental iodine and selenium in La Pampa and San Juan provinces of Argentina. *Journal of Geochemical Exploration*, 107(2): 87-93.
- Weng, H.X. et al., 2008a. Mechanism of iodine uptake by cabbage: Effects of iodine species and where it is stored. *Biological Trace Element Research*, 125(1): 59-71.
- Weng, H.X. et al., 2008b. Increment of iodine content in vegetable plants by applying iodized fertilizer and the residual characteristics of iodine in soil. *Biological Trace Element Research*, 123(1-3): 218-228.
- Weng, H.X. et al., 2009. Biogeochemical transfer and dynamics of iodine in a soil-plant system. *Environmental Geochemistry and Health*, 31(3): 401-411.
- White, P.J. et al., 2012. Testing the distinctness of shoot ionomes of angiosperm families using the Rothamsted Park Grass Continuous Hay Experiment. *New Phytologist*.
- Whitehead, D.C., 1973a. Sorption of iodide by soils as influenced by equilibrium conditions and soil properties. *Journal of the Science of Food and Agriculture*, 24(5): 547-556.
- Whitehead, D.C., 1973b. Studies on iodine in British soils. *Journal of Soil Science*, 24(2): 260-270.
- Whitehead, D.C., 1973c. Uptake and distribution of iodine in grass and clover plants grown in solution culture. *Journal of the Science of Food and Agriculture*, 24(1): 43-50.
- Whitehead, D.C., 1974a. Influence of organic matter, chalk, and sesquioxides on solubility of iodine, elemental iodine, and iodate incubated with soil. *Journal of Soil Science*, 25(4): 461-470.
- Whitehead, D.C., 1974b. Sorption of iodide by soil components. *Journal of the Science of Food and Agriculture*, 25(1): 73-79.
- Whitehead, D.C., 1975. Uptake of perennial ryegrass of iodide, elemental iodine and iodate added to soil as influenced by various amendments. *Journal of the Science of Food and Agriculture*, 26(3): 361-367.
- Whitehead, D.C., 1978. Iodine in soil profiles in relation to iron and aluminium-oxides and organic-matter. *Journal of Soil Science*, 29(1): 88-94.
- Whitehead, D.C., 1979. Iodine in the environment with particular reference to agriculture. *Journal of Applied Ecology*, 16(1): 269-279.
- Whitehead, D.C., 1984. The Distribution and Transformations of Iodine in the Environment. *Environment International*, 10(4): 321-339.
- Wong, G.T.F. and Cheng, X.H., 2008. Dissolved inorganic and organic iodine in the Chesapeake Bay and adjacent Atlantic waters: Speciation changes through an estuarine system. *Marine Chemistry*, 111(3-4): 221-232.

- World Health Organisation, 2009. Micronutrient deficiencies: Iodine deficiency disorders (web page), pp. WHO website about iodine deficiency disorders.
- Xu, C. et al., 2011a. Sequestration and Remobilization of Radioiodine (^{129}I) by Soil Organic Matter and Possible Consequences of the Remedial Action at Savannah River Site. *Environmental Science & Technology*, 45(23): 9975-9983.
- Xu, C. et al., 2011b. Is soil natural organic matter a sink or source for mobile radioiodine (^{129}I) at the Savannah River Site? *Geochimica Et Cosmochimica Acta*, 75(19): 5716-5735.
- Xu, C. et al., 2012. Molecular environment of stable iodine and radioiodine (I-129) in natural organic matter: Evidence inferred from NMR and binding experiments at environmentally relevant concentrations. *Geochimica Et Cosmochimica Acta*, 97: 166-182.
- Yamada, H., Hisamori, I. and Yonebayashi, K., 2002. Identification of organically bound iodine in soil humic substances by size exclusion chromatography/inductively coupled plasma mass spectrometry (SEC/ICP-MS). *Soil Science and Plant Nutrition*, 48(3): 379-385.
- Yamaguchi, N., Nakano, M., Takamatsu, R. and Tanida, H., 2010. Inorganic iodine incorporation into soil organic matter: evidence from iodine K-edge X-ray absorption near-edge structure. *Journal of Environmental Radioactivity*, 101(6): 451-457.
- Yang, H.X. et al., 2007. Speciation analysis for iodine in groundwater using high performance liquid chromatography-inductively coupled plasma-mass spectrometry (HPLC-ICP-MS). *Geostandards and Geoanalytical Research*, 31(4): 345-351.
- Yoshida, S., Muramatsu, Y., Katou, S. and Sekimoto, H., 2007. Determination of the chemical forms of iodine with IC-ICP-MS and its application to environmental samples. *Journal of Radioanalytical and Nuclear Chemistry*, 273(1): 211-214.
- Yoshida, S., Muramatsu, Y. and Uchida, S., 1992. Studies on the sorption of iodide and iodate onto Andosols. *Water air & soil pollution*, 63(3-4): 321 - 329.
- Young, S.D. et al., 2006. Characterizing the availability of metals in contaminated soils. I. The solid phase: sequential extraction and isotopic dilution. *Soil Use and Management*, 21: 450-458.
- Yuita, K. et al., 2005. Behavior of iodine in a forest plot, an upland field and a paddy field in the upland area of Tsukuba, Japan. Iodine concentration in precipitation, irrigation water, ponding water and soil water to a depth of 2.5 m. *Soil Science and Plant Nutrition*, 51(7): 1011-1021.
- Zhu, Y.G., Huang, Y.Z., Hu, Y. and Liu, Y.X., 2003. Iodine uptake by spinach (*Spinacia oleracea* L.) plants grown in solution culture: effects of iodine species and solution concentrations. *Environment International*, 29(1): 33-37.
- Zimmermann, M.B., 2008. Iodine requirements and the risks and benefits of correcting iodine deficiency problems. *Journal of Trace Elements in Medicine and Biology*, 22: 81 - 92.
- Zimmermann, M.B., 2010. Iodine deficiency in industrialised countries. *Proceedings of the Nutrition Society*, 69(1): 133-143.
- Zimmermann, M.B. et al., 2006. Iodine supplementation improves cognition in iodine-deficient schoolchildren in Albania: a randomized, controlled, double-blind study. *American Journal of Clinical Nutrition*, 83(1): 108-114.
- Zimmermann, M.B., Jooste, P.L. and Pandav, C.S., 2008. Iodine-deficiency disorders. *Lancet*, 372(9645): 1251-1262.

APPENDIX 1: NORTHERN IRELAND SAMPLING INFORMATION

This appendix includes details of sampling sites, including site observations and land-use, and photographs of individual soil samples.

Table A1. Sampling site location details

Site no	Date sampled	Easting	Northing	Land use	Drift	Slope	Contamination	Soil texture	Moisture	Organic matter	Weather
NI01	07/10/10	289157	331808	Pasture	Soil	Gentle slope (5-20°)	N	Silty clay	Low	Low	c
NI02	07/10/10	309491	341214	Pasture	Soil	Gentle slope (5-20°)	N	Silty clay	Low	Low	c
NI03	07/10/10	331233	345535	Heather moor	Soil	Gentle slope (5-20°)	N	Silt	Moderate	High	c
NI04	08/10/10	356382	368078	Arable	Soil	Level field, flood plain	N	Sandy clay	Moderate	Low	c
NI05	08/10/10	364034	364963	Pasture & arable	Soil	Gentle slope (5-20°)	N	Silty sand	Low	Low	b
NI06	08/10/10	353510	344149	Pasture	Soil	Steep slope (>20°)	N	Silt	Low	Low	b
NI07	08/10/10	352386	339070	Pasture	Soil	Gentle slope (5-20°)	Cow faeces.	Silt	Low	Low	b
NI08	09/10/10	335476	318467	Pasture	Soil	Level field, flood plain	Some cow faeces.	Sandy silt	Low	Low	b
NI09	09/10/10	335948	326762	Heather moor	Peat	Gentle slope (5-20°)	N	Silt	Moderate	High	b
NI10	10/10/10	312014	430266	Heather Moor	Peat	Gentle slope (5-20°)	N	Peat	High	High	b
NI11	11/10/10	286458	424749	Pasture	Soil	Level field, flood plain	Some cow faeces.	Clayey silt	Low	Low	b
NI12	11/10/10	276524	434574	Pasture	Soil	Gentle slope (5-20°)	Occasional cow faeces	Sandy clay	Low	Low	a
NI13	11/10/10	282682	430463	Pasture	Soil	Gentle slope (5-20°)	N	Sandy clay	Low	Low	a

Site no	Date sampled	Easting	Northing	Land use	Drift	Slope	Contamination	Soil texture	Moisture	Organic matter	Weather
NI14	11/10/10	296721	422071	Pasture & arable	Soil	Gentle slope (5-20°)	N	Silty clay	Moderate	Low	a
NI15	12/10/10	324717	412989	Pasture	Soil	Gentle slope (5-20°)	Minor cow faeces. Nutrient lick-bucket in adjoining field.	Silt	Low	Moderate	a
NI16	12/10/10	319976	418555	Heather moor	Peat	Bog	N	Peat	High	High	a
NI17	12/10/10	324649	436176	Heather moor	Peat	Hill top	Potential areas of cut peat: sample taken from above.	Peat	Moderate	High	a
NI18	13/10/10	296307	395723	Pasture	Soil	Level field, flood plain	N	Clayey silt	Low	Low	c
NI19	13/10/10	306435	398967	Pasture	Soil	Gentle slope (5-20°)	Some cow faeces.	Clayey silt	Low	Low	c
NI20	13/10/10	324425	400822	Pasture	Soil	Gentle slope (5-20°)	Supplement bucket observed nearby (contains iodine)	Silt	Low	Moderate	c

Key to weather observations: a – no rain within a week; b – rain heavy 2 – 7 days before sampling; c – rain heavy within twelve hours before sampling.

Table A2. Site observations: soil, vegetation and land-use

Site no	Additional land use?	Site notes	Soil notes	Vegetation notes
NI01	Cattle grazing: beef, 2 cows, 1 calf.		Red iron oxide streaks (<2mm) abundant. Worms abundant. Top few cm soil moister than further down. Grass roots to approx. 3 cm	Vegetation mainly grass with lots of clover. Grass not lush. All sampled. Longer, dead grass avoided as obviously not being eaten by cattle. Most sward 3 - 5 cm long.
NI02	Cattle for beef: young males reared to be sold.		Coal fragment (single) found in soil. Grass roots to approx. 3 cm. Rare greywacke clasts < 2 cm. Red Fe mottling observed below 5 cm depth. Rare worms.	Grass 10 - 15 cm long. Reasonably lush although patchy. Rare dandelions present but only grass sampled.
NI03	Rough, low density sheep grazing	Boulders scattered around but not where sampled. Prob not in situ. Very misty so sampled close to (above) road. On Slieve Croob.	Fine roots to 10 cm. Matted vegetation (approx. 3 cm) on top of soil was discarded.	Vegetation some heather, mostly rank grass and moss. All sampled.
NI04	Silage field, recently cut. Frequently flooded until sea wall built approx. 1990. Stewardship scheme in place for geese and	Laminated thick red clay and red sand have been excavated in neighbouring field. FORMER flood plain. Water table approx. 1 m deep. 2 cuts for silage per year. Geese overwinter on this field and eat local seaweed: iodine input. Just over sea wall from Strangford Lough. Stewardship scheme.	Mod. Fe staining at 8-10cm depth. Abundant sand throughout depth. Abundant worms. Marginal darkening of top 2cm. 0.3 - 1.0 m silty marine deposited clay. Sandy, silty clay.	Grass patchy green/brown. Length up to 10 cm. Some docks. Only live, green, grass sampled.
NI05	Silage then grazing for dairy cattle.	Iodophore teat cleaner used. Hit rocks/stones at 0.10 - 0.15 m, so soil temp likely to be unreliable since could not achieve full depth. Previously used for silage. This year grazed dairy herd. Very near sea and therefore strong sea wind/sea spray input.	Clasts of greywacke present at ~10 cm. Clast size up to 3 cm. Some worms.	Abundant clover and other herbs in grass, both sampled. Louise requests total iodine on grass and clover separately. Height ~10 cm.

Site no	Additional land use?	Site notes	Soil notes	Vegetation notes
NI06	Grass field, grazing horses (in other part of field at present), cut for hay. Unfertilised. Grazes sheep in winter.	Under stewardship scheme.	Greywacke clasts. Occasional Fe-ox staining where mudstone weathering evident. Abundant worms. Abundant clasts. Light, well drained soil. Most clasts 2-3mm but occasional up to 2cm.	Grass long (0.20 m) and lush with abundant clover and other herbs. Not patchy. Both clover and grass sampled.
NI07	Dairy grazing ~200 head in field until beginning of this week. No iodophores used.	Dose for Co, Cu, Se, I where deficiency evident. Abundant cow faeces therefore likely abundant cow urine in soil.	Rare worms. Rare greywacke clasts.	Mixed strong grass and clover up to 20 cm tall. Few herbs.
NI08	Cows currently grazing in field, low density.	Close to sea, with strong sea wind. Site on Mourne Plain. No iodophores: beef sucklers in field. Shell debris historically sold to farmers from local shell fish factory & applied to land. Discussion with land owner about seaweed being used approx. 30 - 50 years ago.	Soil clast lithology: weathered granite inc. weathered feldspar quartz, all less than 3 mm and moderately abundant. Weathered sandstone also present.	Grass with abundant clover - both sampled. Height up to 15 cm, quite green but patchy in shorter areas. Occasional dock and ragwort present but not sampled.
NI09	Low density mountain sheep grazing.	Site was in mountain cloud therefore cloud-deposition of iodine likely. Granite observed in quarry and stream course. Wind chill significant: very windy.	Could have been any 'black' chosen from Munsell chart. At 3 - 20 cm deep, mineral horizon appeared (not sampled). Within mineral horizon were abundant, mm-size weathered granite, with especially visible feldspar minerals. Peaty soil but not deep enough to be peat.	Moor grass turning yellow, ~30cm tall. Heather also present (finished flowering) but no sphagnum.
NI10	Heather moor, no evidence of any grazing animals. Historical peat cutting evident lower down slope from sample site.	Sunny, windy day. Boggy moor but sampling site chosen to be slightly drier area to avoid sinking.	Colour called 'black' in Munsell chart, but colour actually not black: is v dark brown due to plant matter. No clasts: is peat.	Thin, wiry moor grass sampled from among heather. Some mosses. Grass up to 30 cm long.
NI11	Grass field with 14 suckler cows. No dairy so no iodophores used.	Quite flat field.	No soil clasts observed. Moderate worms. Colour dark reddish brown. At 0.2m, soil becomes orangey clay.	Good density grass, very occasional clover. Few herbs.

Site no	Additional land use?	Site notes	Soil notes	Vegetation notes
NI12	Grass field currently used for beef cattle: only 2 cattle so very low density. Before this year, used for silage for 4 - 5 years.	No iodophors used.	Occasional worms. Trace basalt clasts approx. 2 cm diameter. Plastic bottle top found while processing soil.	Grass up to 20 cm long: patchy long due to cow faeces. Occasional herbs. Occasional fungi. Many dead, quite short stalks, not sampled.
NI13	Beef cattle recently put into field and still present.	Sample taken from same field as Tellus sample. Sampled on slope above floodplain, which is approx. 50 m away in same field.	No clasts. 1 auger showed Fe streaks at approx. 8 cm depth: not sampled. Abundant worms.	Thick grass, no clover, few herbs.
NI14	Grass in field cut twice annually for silage then grazed by dairy cows.	Ground v wet.	Minor clasts of basalt and quartz, <0.5 cm. At 0.20 m, stiffer clay, more grey with minor Fe staining. Gley soil. Mod Fe staining below 2 cm; below 2cm rare Fe staining. Abundant worms.	Grass approx. 15 cm long, very green. Abundant creeping buttercup. Slightly patchy vegetation due to very wet ground and cattle feet. Rare clover. All vegetation sampled.
NI15	Beef cattle. Rough ground.	Sampled just above marshy (juncus) area alongside stream: hillside of valley. Hummocky with visible boulders in places: avoided as look like debris in places. Young conifer plantation on opposite side of valley. Bedrock observed ~50 m away: basalt. High pressure weather continued. Cold night, misty start, sun now breaking through. No wind. Heavy dew.	1 x basalt clast < 1 cm diameter. At 0.10 - 0.15 m, rock hit so no deeper sampling. Trace worms. Possible rabbit burrows. Where 0.15m hit, soil more yellow-brown and clayey.	Dense grass, abundant clover and lots of thistles
NI16	Quite flat, boggy, standing water present.	Is moorland but not heather. Sample taken approx. 200 m from coniferous forest. Cloudy, mild. Sample site accessed from footpath (towards forest) off road. Sample site ~100m from f/path. Potentially cut edge ~50-100m away: avoided.	Colour called 'black' in Munsell chart, but colour actually not black: is v dark brown due to plant matter. No clasts: is peat. Auger easily sunk up to handles in peat so depth >1.5m.	Vegetation is mainly grass ~30cm long, yellowing for winter. Some thin & wiry, some broader bladed. Abundant mosses of various sorts.

Site no	Additional land use?	Site notes	Soil notes	Vegetation notes
NI17	Heather moor, heather ~50cm high. Localised areas of cut/drainage avoided. No sheep observed at site but surround site on all sides.	Outcrop ~150m away observed. Weather very still, with high level mists but good visibility at site.	Colour labelled 'black' but actually a dark brown. No clasts, but some carbonaceous material resembling charcoal (burnt heather?) was observed in some augers around 15cm. This was not sampled.	Moss and grass sampled separately. Some thin wiry grass and mosses present but heather dominant vegetation.
NI18	Field used for grazing beef cattle, but no evidence of cattle being recently present. Muck spread in area last year. Field edged by deciduous trees. Field ~70m x ~100m	Very misty for 2 days, plus heavy dew. Low lying land near lough. Not boggy.	Colour dark yellowy brown. Clayey silt with minor Fe staining and trace sand observed. No worms obs. 1 x charcoal piece (~0.5cm dia.) observed. Trace basalt(?) <1 cm dia. observed at 10 cm depth. At 30 cm, hit stones.	Thick grass up to 20cm tall. Moderate other plants present inc. Dock, cranesbill, dandelion, clover (minor), plantain. Only grass sampled.
NI19	Site regularly used by dairy herd grazing; moderate cow faeces present. Iodophor disinfectant used at milking.	Sampled on house-side of field away from direct path between 2 gates and quite modern barns. Farm has 'wet' and 'dry' fields; dry field sampled as best for dairy herd. Weather as NI18, including heavy dew.	Colour dark yellowy brown. Very friable. Rare worms. Moderately abundant basalt(?) clasts <1cm dia. Soil becoming lighter, more sandy colour below 0.20m, also slightly more clayey.	Long (up to 30cm) grass, wide-blade pasture. Moderate docks, few other species. Good growth density. Minor clover obs.
NI20	Improved pasture: clear boundary with unimproved pasture. Juncus grass growing: wet although local hill top. Not currently boggy.	Potential sheep grazing, evidence of recent cows present but no animals seen at site.	Colour 7.5YR 3/2. Rare Fe oxide staining observed. At bottom of soil, rotting basalt observed. Depth 8 - 20 cm. Moderate worms.	Very dense, lush, bright green grass with moderate clover. Some juncus growing but not sampled.

Figure A1. Soil Comparison Photos



APPENDIX 2: RESULTS OF SOIL IODINE DYNAMICS EXPERIMENT

Concentrations of ^{129}I , ^{127}I and DOC in solution measured during short-term dynamics experiments in soils. Values measured as concentration in solution then expressed as mg I kg^{-1} soil. Values underlined were below LOD when measured in solution. Negative values occurred either due to negative concentration measured in solution, or due to correction for ^{127}I in ^{129}I spike. Values are mean and standard error of triplicate measurements.

Table A3. Results of soil iodine dynamics experiments

Soil	Species added	Time (hr)	¹²⁷ Iodine (µg I kg ⁻¹)		¹²⁷ IO ₃ ⁻ (µg I kg ⁻¹)		¹²⁷ I ⁻ (µg I kg ⁻¹)		¹²⁹ Iodine (µg I kg ⁻¹)		¹²⁹ IO ₃ ⁻ (µg I kg ⁻¹)		¹²⁹ I ⁻ (µg I kg ⁻¹)		DOC (mg kg ⁻¹)	
			Mean	S. E.	Mean	S. E.	Mean	S. E.	Mean	S. E.	Mean	S. E.	Mean	S. E.	Mean	S. E.
NI01	Iodate	1	7.41	1.23	4.65	1.11	<u>0.000</u>	0.000	184	4.52	156	3.49	<u>0.000</u>	0.000	288	8.92
		3	5.63	0.788	2.98	0.617	<u>1.31</u>	0.797	129	3.54	106	1.04	<u>0.000</u>	0.000	161	24.4
		7	6.50	0.663	1.50	0.412	<u>0.344</u>	0.344	93.4	1.29	73.6	0.906	<u>0.000</u>	0.000	156	11.7
		24	8.01	0.287	1.71	0.200	2.21	0.181	56.9	0.699	36.3	0.370	2.13	0.393	177	5.65
	Iodide	1	19.8	0.509	0.000	0.000	16.1	1.20	478	2.07	<u>0.000</u>	0.000	443	3.98	160	30.3
		3	18.2	0.732	0.000	0.000	11.2	1.59	238	2.04	<u>0.000</u>	0.000	199	2.20	180	32.3
		7	9.35	0.566	0.000	0.000	5.78	2.45	53.2	0.427	<u>0.000</u>	0.000	28.8	1.05	166	10.1
		24	12.4	0.904	0.000	0.000	1.22	0.295	17.6	0.625	<u>0.000</u>	0.000	2.27	0.123	194	8.52
NI02	Iodate	1	4.15	0.487	3.24	0.203	<u>0.000</u>	0.000	112	2.68	127	2.48	<u>0.000</u>	0.000	190	48.4
		3	4.52	0.214	2.44	0.0624	<u>1.27</u>	0.815	79.6	0.656	84.4	0.726	<u>0.000</u>	0.000	144	23.5
		7	6.01	0.929	1.54	0.194	<u>0.878</u>	0.525	63.0	1.17	61.1	0.710	<u>0.000</u>	0.000	142	18.1
		24	7.92	0.449	1.73	0.438	1.92	0.992	45.2	1.14	32.3	0.665	<u>0.520</u>	0.471	135	4.56
	Iodide	1	19.3	0.978	<u>0.000</u>	0.000	17.0	1.25	468	1.50	<u>0.000</u>	0.000	403	2.33	135	11.0
		3	15.9	0.995	<u>0.000</u>	0.000	15.1	1.29	233	1.96	<u>0.000</u>	0.000	148	2.83	155	23.8
		7	9.78	1.56	<u>0.000</u>	0.000	4.23	0.592	51.9	0.371	<u>0.000</u>	0.000	13.6	1.16	167	25.5
		24	11.0	1.43	<u>0.000</u>	0.000	16.4	8.23	17.1	0.601	<u>0.000</u>	0.000	2.46	0.270	134	3.27
NI03	Iodate	1	58.1	9.30	9.93	1.62	<u>-0.910</u>	0.000	426	3.12	345	3.77	8.36	0.362	487	86.1
		3	126	9.81	3.52	1.04	3.45	0.897	195	4.70	142	3.24	21.4	0.259	678	46.4
		7	175	2.91	<u>0.170</u>	0.0657	3.89	0.952	47.6	1.67	15.9	1.61	12.9	0.619	1690	30.2
		24	406	12.2	<u>0.000</u>	0.000	<u>1.48</u>	1.48	17.5	0.947	<u>0.000</u>	0.000	<u>0.000</u>	0.000	3100	81.2
	Iodide	1	71.9	7.75	<u>0.000</u>	0.000	19.1	1.67	463	4.81	<u>0.000</u>	0.000	408	9.03	470	35.7
		3	111	5.69	<u>0.000</u>	0.000	19.9	1.31	232	1.44	<u>0.000</u>	0.000	215	2.39	588	43.8

Soil	Species added	Time (hr)	¹²⁷ Iodine (µg I kg ⁻¹)		¹²⁷ IO ₃ ⁻ (µg I kg ⁻¹)		¹²⁷ I ⁻ (µg I kg ⁻¹)		¹²⁹ Iodine (µg I kg ⁻¹)		¹²⁹ IO ₃ ⁻ (µg I kg ⁻¹)		¹²⁹ I ⁻ (µg I kg ⁻¹)		DOC (mg kg ⁻¹)	
			Mean	S. E.	Mean	S. E.	Mean	S. E.	Mean	S. E.	Mean	S. E.	Mean	S. E.	Mean	S. E.
NI04	Iodate	7	232	17.4	<u>0.000</u>	0.000	13.7	3.00	64.9	0.410	<u>0.000</u>	0.000	44.4	0.492	1790	25.4
		24	430	13.9	<u>0.003</u>	0.003	2.98	0.682	20.8	1.07	<u>0.000</u>	0.000	<u>0.000</u>	0.000	3100	90.2
		1	82.3	9.46	13.7	0.729	<u>0.000</u>	0.000	494	46.8	330	3.93	<u>0.000</u>	0.000	426	80.3
		3	67.3	2.12	11.9	1.26	<u>0.894</u>	0.946	388	33.2	273	6.27	<u>0.474</u>	0.430	435	23.9
	Iodide	7	74.7	3.81	9.23	0.230	<u>0.641</u>	0.718	305	31.2	202	3.26	<u>0.701</u>	0.635	175	8.67
		24	113	9.60	98.1	2.45	1.72	0.006	198	17.1	125	2.49	2.24	0.006	222	8.36
		1	83.1	5.67	<u>0.000</u>	0.000	19.0	2.18	670	56.5	<u>0.000</u>	0.000	490	4.19	388	50.1
		3	76.3	0.869	<u>0.000</u>	0.000	24.0	1.11	437	37.1	<u>0.000</u>	0.000	265	36.0	424	55.2
NI05	Iodate	7	89.2	1.48	<u>0.000</u>	0.000	18.1	9.68	180	15.5	<u>0.000</u>	0.000	54.2	14.6	178	7.55
		24	112	5.76	<u>0.000</u>	0.000	2.98	0.374	62.0	7.39	<u>0.000</u>	0.000	3.87	0.386	246	6.61
		1	1208	63.9	14.1	0.440	15.7	1.55	449	29.3	314	2.13	<u>0.000</u>	0.000	423	94.2
		3	1390	85.2	9.30	1.08	55.0	17.7	371	25.7	274	8.23	<u>0.990</u>	0.898	439	41.5
	Iodide	7	1842	60.5	7.29	0.672	55.9	20.4	304	15.0	220	1.94	<u>1.06</u>	0.963	194	7.60
		24	3626	153	130	3.67	2.33	0.0288	214	4.62	167	3.74	3.04	0.0298	261	3.15
		1	1277	96.4	<u>0.000</u>	0.000	112	20.0	351	26.6	<u>0.000</u>	0.000	234	7.66	403	29.8
		3	1487	121	<u>0.000</u>	0.000	81.2	23.8	105	10.5	<u>0.000</u>	0.000	36.2	3.11	416	53.0
NI06	Iodate	7	1989	162	<u>0.000</u>	0.000	50.8	11.2	61.4	5.58	<u>0.000</u>	0.000	6.29	0.664	204	8.24
		24	3855	250	<u>0.000</u>	0.000	3.70	0.235	50.2	1.53	<u>0.000</u>	0.000	4.81	0.243	282	0.721
		1	-4.79	2.83	2.22	0.351	<u>0.671</u>	0.671	160	2.70	138	2.12	<u>0.000</u>	0.000	119	9.30
		3	1.10	6.18	1.92	0.222	3.87	0.0778	115	2.06	97.9	1.02	<u>0.000</u>	0.000	128	5.68
	Iodide	7	8.99	1.00	1.50	0.429	3.81	0.492	90.5	0.225	80.4	3.48	<u>0.000</u>	0.000	115	5.07
		24	15.6	2.44	-0.139	0.250	2.60	0.396	59.8	1.01	53.0	0.645	<u>0.0381</u>	0.0346	138	2.49

Soil	Species added	Time (hr)	¹²⁷ Iodine (µg I kg ⁻¹)		¹²⁷ IO ₃ ⁻ (µg I kg ⁻¹)		¹²⁷ I ⁻ (µg I kg ⁻¹)		¹²⁹ Iodine (µg I kg ⁻¹)		¹²⁹ IO ₃ ⁻ (µg I kg ⁻¹)		¹²⁹ I ⁻ (µg I kg ⁻¹)		DOC (mg kg ⁻¹)	
			Mean	S. E.	Mean	S. E.	Mean	S. E.	Mean	S. E.	Mean	S. E.	Mean	S. E.	Mean	S. E.
NI07	Iodate	7	10.4	6.06	<u>0.000</u>	0.000	8.28	0.381	56.1	0.703	<u>0.000</u>	0.000	24.7	0.599	101	2.78
		24	14.8	6.60	<u>-0.001</u>	0.000	4.09	0.216	20.0	0.528	<u>0.0113</u>	0.0103	3.61	0.833	121	2.09
		1	42.8	2.92	5.26	0.702	<u>0.000</u>	0.000	428	9.50	359	2.58	<u>0.000</u>	0.000	151	4.44
		3	118	55.9	4.84	0.336	4.20	0.236	365	3.78	312	3.80	<u>0.000</u>	0.000	178	11.9
	Iodide	7	66.3	1.56	5.27	1.30	<u>0.597</u>	0.597	323	2.06	292	12.9	<u>0.000</u>	0.000	172	6.62
		24	78.3	1.62	1.53	0.294	0.896	0.448	221	5.05	202	1.17	<u>0.000</u>	0.000	202	7.51
		1	48.7	7.60	<u>0.000</u>	0.000	46.1	22.0	563	2.52	<u>0.000</u>	0.000	461	6.64	153	2.67
		3	50.9	2.85	<u>0.000</u>	0.000	29.4	0.913	460	6.77	<u>0.000</u>	0.000	360	5.08	174	12.9
NI08	Iodate	7	73.4	17.9	<u>0.000</u>	0.000	20.8	1.25	292	4.79	<u>0.000</u>	0.000	220	3.60	161	8.61
		24	78.2	15.8	<u>0.000</u>	0.000	5.83	0.666	59.8	1.74	<u>0.000</u>	0.000	9.22	0.666	186	7.60
		1	428	42.5	4.03	0.506	<u>0.000</u>	0.000	347	2.52	299	2.29	<u>0.000</u>	0.000	166	13.0
		3	444	38.8	3.87	0.468	15.6	1.24	303	2.25	259	1.64	<u>0.000</u>	0.000	186	1.49
	Iodide	7	695	58.9	4.54	1.08	7.65	0.388	273	1.65	248	13.3	<u>0.000</u>	0.000	219	8.25
		24	2042	118	1.03	0.165	9.83	2.59	219	4.92	197	6.01	<u>0.000</u>	0.000	328	20.5
		1	373	56.7	<u>0.000</u>	0.000	31.3	0.663	234	6.10	<u>0.000</u>	0.000	146	3.72	172	9.63
		3	486	31.2	<u>0.000</u>	0.000	28.3	0.559	83.6	1.61	<u>0.000</u>	0.000	26.0	0.589	193	9.38
NI09	Iodate	7	573	12.4	<u>0.000</u>	0.000	7.85	0.574	47.7	0.626	<u>0.000</u>	0.000	<u>0.000</u>	0.000	225	20.3
		24	1798	97.5	<u>0.000</u>	0.000	9.47	2.08	48.0	0.608	<u>0.000</u>	0.000	<u>0.000</u>	0.000	321	4.73
		1	252	4.96	10.4	2.14	<u>-1.11</u>	0.000	328	14.7	253	7.28	10.2	1.94	1180	144
		3	245	18.4	1.70	1.46	4.07	0.314	112	5.69	75.6	7.95	10.6	1.56	1290	95.0
	Iodide	7	394	42.6	<u>-0.0944</u>	0.684	<u>1.49</u>	1.66	21.5	2.65	7.15	1.34	<u>1.56</u>	1.42	1200	69.6
		24	759	60.0	<u>0.000</u>	0.000	<u>0.000</u>	0.000	11.2	1.76	<u>0.000</u>	0.000	<u>0.000</u>	0.000	2030	48.7
		1	257	20.4	<u>0.000</u>	0.000	25.5	6.03	407	21.9	<u>0.000</u>	0.000	305	31.8	1200	62.8
		3	243	21.2	<u>0.000</u>	0.000	35.0	0.384	154	5.38	<u>0.000</u>	0.000	110	9.10	1200	61.0

Soil	Species added	Time (hr)	¹²⁷ Iodine (µg I kg ⁻¹)		¹²⁷ IO ₃ ⁻ (µg I kg ⁻¹)		¹²⁷ I ⁻ (µg I kg ⁻¹)		¹²⁹ Iodine (µg I kg ⁻¹)		¹²⁹ IO ₃ ⁻ (µg I kg ⁻¹)		¹²⁹ I ⁻ (µg I kg ⁻¹)		DOC (mg kg ⁻¹)	
			Mean	S. E.	Mean	S. E.	Mean	S. E.	Mean	S. E.	Mean	S. E.	Mean	S. E.	Mean	S. E.
NI10	Iodate	7	401	24.0	<u>0.000</u>	0.000	11.0	3.00	21.8	2.50	<u>0.000</u>	0.000	6.60	1.53	1200	46.0
		24	713	31.4	<u>0.000</u>	0.000	<u>0.830</u>	0.947	13.7	2.18	<u>0.000</u>	0.000	<u>1.08</u>	0.979	2000	22.0
		1	51.4	11.4	7.48	3.00	4.52	2.37	392	7.84	247	3.10	31.1	2.18	1200	72.7
		3	107	10.4	1.07	1.29	9.52	1.87	162	4.95	75.4	1.53	68.3	2.05	1630	37.7
	Iodide	7	232	12.7	<u>-0.971</u>	0.000	19.0	9.77	51.4	3.17	8.92	0.769	35.8	3.42	2130	25.0
		24	475	49.3	<u>0.000</u>	0.000	<u>3.42</u>	1.73	18.5	0.751	<u>0.000</u>	0.000	<u>0.000</u>	0.000	3680	214
		1	61.8	11.0	<u>0.000</u>	0.000	1.32	4.40	483	4.80	<u>0.000</u>	0.000	589	7.61	1170	40.8
		3	127	11.5	<u>0.000</u>	0.000	21.5	16.3	277	2.46	<u>0.000</u>	0.000	334	7.99	1630	39.1
NI11	Iodate	7	145	5.54	<u>0.000</u>	0.000	23.7	18.4	114	3.59	<u>0.000</u>	0.000	123	3.34	1660	43.4
		24	423	46.4	<u>0.000</u>	0.000	5.41	2.95	20.2	1.26	<u>0.000</u>	0.000	<u>0.000</u>	0.000	3470	107
		1	-1.11	1.64	4.33	0.721	<u>0.000</u>	0.000	105	1.00	82.1	0.123	<u>0.000</u>	0.000	142	4.49
		3	1.24	0.654	2.19	0.442	<u>8.84</u>	8.84	78.7	1.78	61.1	1.20	<u>0.000</u>	0.000	162	1.13
	Iodide	7	5.05	1.69	1.17	0.496	1.98	0.378	58.5	1.35	43.1	0.435	<u>0.000</u>	0.000	169	0.460
		24	15.3	1.08	0.353	0.479	4.34	4.34	43.2	0.657	28.3	0.482	<u>0.000</u>	0.000	222	3.76
		1	18.2	0.707	<u>0.000</u>	0.000	-0.277	0.316	388	1.76	<u>0.000</u>	0.000	465	7.49	134	2.25
		3	12.0	1.40	<u>0.000</u>	0.000	6.74	2.15	129	2.88	<u>0.000</u>	0.000	132	1.50	165	1.68
NI12	Iodate	7	3.51	0.968	<u>0.000</u>	0.000	1.81	0.705	22.2	0.520	<u>0.000</u>	0.000	6.74	0.598	147	54.8
		24	14.4	1.54	<u>0.000</u>	0.000	<u>0.000</u>	0.000	13.5	0.479	<u>0.000</u>	0.000	<u>0.000</u>	0.000	223	4.47
		1	18.3	2.16	0.554	0.720	<u>0.000</u>	0.000	72.7	2.34	84.9	2.80	<u>0.000</u>	0.000	114	9.34
		3	30.5	1.61	0.671	0.217	3.68	0.675	49.9	1.29	49.4	2.46	<u>0.000</u>	0.000	91.7	7.90
	Iodide	7	22.6	0.539	-0.0635	0.0634	<u>0.000</u>	0.000	37.7	0.264	36.0	0.628	<u>0.000</u>	0.000	114	9.00
		24	21.4	0.248	-0.298	0.0889	<u>0.735</u>	0.735	29.2	0.335	22.6	0.738	<u>0.000</u>	0.000	122	8.98
		1	41.2	0.574	<u>0.000</u>	0.000	11.3	1.67	459	7.43	<u>0.000</u>	0.000	369	23.5	88.6	10.8
		3	30.4	1.05	<u>0.000</u>	0.000	23.7	4.61	228	2.67	<u>0.000</u>	0.000	164	12.0	106	2.31

Soil	Species added	Time (hr)	¹²⁷ Iodine (µg I kg ⁻¹)		¹²⁷ IO ₃ ⁻ (µg I kg ⁻¹)		¹²⁷ I ⁻ (µg I kg ⁻¹)		¹²⁹ Iodine (µg I kg ⁻¹)		¹²⁹ IO ₃ ⁻ (µg I kg ⁻¹)		¹²⁹ I ⁻ (µg I kg ⁻¹)		DOC (mg kg ⁻¹)	
			Mean	S. E.	Mean	S. E.	Mean	S. E.	Mean	S. E.	Mean	S. E.	Mean	S. E.	Mean	S. E.
NI13	Iodate	7	16.0	0.785	<u>0.000</u>	0.000	2.00	0.300	36.1	0.828	<u>0.000</u>	0.000	14.9	0.474	116	4.99
		24	12.5	0.267	<u>0.000</u>	0.000	<u>0.000</u>	0.000	13.5	0.311	<u>0.000</u>	0.000	<u>0.000</u>	0.000	129	12.5
		1	-3.82	1.98	7.81	0.882	<u>4.38</u>	4.38	192	4.18	141	1.35	<u>0.000</u>	0.000	163	19.9
		3	-4.12	0.377	5.45	1.04	5.29	2.65	147	1.96	111	1.74	<u>0.000</u>	0.000	168	2.30
	Iodide	7	-3.50	0.302	3.44	0.316	<u>0.000</u>	0.000	109	2.18	80.8	0.959	<u>0.000</u>	0.000	176	2.62
		24	1.31	0.528	2.57	0.174	2.30	1.15	74.4	0.733	54.1	0.438	<u>0.000</u>	0.000	231	13.4
		1	10.9	1.49	<u>0.000</u>	0.000	-2.79	0.352	489	4.40	<u>0.000</u>	0.000	610	6.85	146	8.82
		3	7.50	0.475	<u>0.000</u>	0.000	1.02	2.23	263	2.50	<u>0.000</u>	0.000	314	2.49	170	5.74
NI14	Iodate	7	-0.859	0.822	<u>0.000</u>	0.000	5.99	3.48	68.6	0.560	<u>0.000</u>	0.000	67.2	2.30	169	10.2
		24	-0.424	1.35	<u>0.000</u>	0.000	1.78	0.950	8.72	0.229	<u>0.000</u>	0.000	<u>0.000</u>	0.000	215	7.75
		1	2.48	1.83	4.97	0.477	<u>0.000</u>	0.000	171	3.45	135	2.69	<u>0.000</u>	0.000	101	3.46
		3	1.70	1.38	4.05	0.788	<u>0.000</u>	0.000	110	1.44	84.5	1.89	<u>0.000</u>	0.000	122	2.36
	Iodide	7	6.25	3.82	2.48	0.659	<u>0.000</u>	0.000	77.9	2.39	65.2	3.22	<u>0.000</u>	0.000	113	20.8
		24	25.2	2.78	1.64	0.508	<u>0.000</u>	0.000	34.8	2.63	38.4	3.17	<u>0.000</u>	0.000	151	16.0
		1	7.00	1.39	<u>0.000</u>	0.000	2.83	2.38	459	11.0	<u>0.000</u>	0.000	171	14.2	101	3.95
		3	5.13	1.05	<u>0.000</u>	0.000	0.277	1.08	210	3.25	<u>0.000</u>	0.000	74.1	9.97	115	1.94
NI15	Iodate	7	<u>0.201</u>	0.654	<u>0.000</u>	0.000	-0.636	0.000	27.0	1.09	<u>0.000</u>	0.000	5.85	0.417	134	18.2
		24	18.8	1.12	<u>0.000</u>	0.000	0.000	0.000	<u>-3.04</u>	0.487	<u>0.000</u>	0.000	<u>0.000</u>	0.000	194	14.0
		1	50.6	4.92	0.0753	0.443	<u>0.000</u>	0.000	71.8	4.39	77.3	1.22	<u>0.000</u>	0.000	174	5.18
		3	87.7	28.1	0.671	0.119	5.37	0.472	51.7	3.02	50.2	2.57	<u>0.000</u>	0.000	176	1.19
	Iodide	7	48.8	0.438	0.245	0.186	<u>0.000</u>	0.000	41.7	0.292	36.1	0.764	<u>0.000</u>	0.000	238	10.6
		24	69.5	2.93	-0.333	0.172	<u>0.000</u>	0.000	27.7	0.460	16.7	0.385	<u>0.000</u>	0.000	388	4.89
		1	95.4	11.6	<u>0.000</u>	0.000	16.8	2.35	286	7.29	<u>0.000</u>	0.000	175	13.8	142	6.58
		3	82.5	28.8	<u>0.000</u>	0.000	34.7	4.47	64.5	2.62	<u>0.000</u>	0.000	27.2	5.11	223	20.3

Soil	Species added	Time (hr)	¹²⁷ Iodine (µg I kg ⁻¹)		¹²⁷ IO ₃ ⁻ (µg I kg ⁻¹)		¹²⁷ I ⁻ (µg I kg ⁻¹)		¹²⁹ Iodine (µg I kg ⁻¹)		¹²⁹ IO ₃ ⁻ (µg I kg ⁻¹)		¹²⁹ I ⁻ (µg I kg ⁻¹)		DOC (mg kg ⁻¹)	
			Mean	S. E.	Mean	S. E.	Mean	S. E.	Mean	S. E.	Mean	S. E.	Mean	S. E.	Mean	S. E.
NI16	Iodate	7	45.2	1.82	<u>0.000</u>	0.000	<u>0.000</u>	0.000	14.9	0.394	<u>0.000</u>	0.000	<u>0.000</u>	0.000	234	12.4
		24	53.1	3.96	<u>0.000</u>	0.000	<u>0.000</u>	0.000	10.7	0.287	<u>0.000</u>	0.000	<u>0.000</u>	0.000	347	5.32
		1	456	82.7	6.41	2.74	24.7	3.45	390	13.3	292	14.4	20.7	2.75	2980	279
		3	590	22.2	0.991	3.72	22.0	2.16	250	18.8	161	21.6	29.3	3.61	4030	274
	Iodide	7	778	59.3	<u>-0.374</u>	3.23	25.7	4.42	108	14.2	56.8	15.9	4.13	3.75	4570	512
		24	2000	225	<u>-0.447</u>	0.000	<u>7.76</u>	7.76	<u>-3.40</u>	10.8	<u>4.11</u>	3.72	<u>0.000</u>	0.000	7890	437
		1	394	91.6	<u>0.000</u>	0.000	30.7	2.57	399	12.9	<u>0.000</u>	0.000	291	2.31	2850	326
		3	563	118	<u>0.000</u>	0.000	27.4	1.88	205	12.6	<u>0.000</u>	0.000	130	10.7	3840	397
NI17	Iodate	7	791	119	<u>0.000</u>	0.000	35.1	5.67	57.2	5.24	<u>0.000</u>	0.000	22.4	2.27	4430	420
		24	1640	189	<u>0.000</u>	0.000	73.3	28.0	<u>-14.8</u>	4.03	<u>0.000</u>	0.000	<u>2.66</u>	2.41	7270	583
		1	128	3.53	5.86	1.05	5.64	1.36	215	1.36	157	0.669	32.0	0.674	611	7.20
		3	170	6.11	<u>-0.541</u>	0.686	4.95	0.704	53.3	2.02	17.6	0.731	37.4	1.31	1240	42.8
	Iodide	7	263	1.48	<u>0.000</u>	0.000	14.7	5.94	<u>-5.03</u>	1.42	<u>0.000</u>	0.000	13.0	0.592	1820	18.2
		24	430	6.33	<u>0.000</u>	0.000	5.07	0.269	<u>-17.9</u>	1.40	<u>0.000</u>	0.000	<u>0.000</u>	0.000	3130	33.1
		1	145	7.23	<u>0.000</u>	0.000	32.1	2.11	467	8.04	<u>0.000</u>	0.000	412	4.58	560	13.0
		3	216	5.59	<u>0.000</u>	0.000	36.7	4.80	313	4.53	<u>0.000</u>	0.000	274	3.60	1480	86.6
NI18	Iodate	7	264	5.43	<u>0.000</u>	0.000	28.2	6.24	143	3.95	<u>0.000</u>	0.000	133	3.81	1690	55.8
		24	483	20.5	<u>0.000</u>	0.000	10.5	1.42	<u>-3.99</u>	0.410	<u>0.000</u>	0.000	9.66	0.912	3500	158
		1	22.1	3.22	0.117	0.268	<u>0.000</u>	0.000	49.2	0.356	44.0	0.800	<u>0.000</u>	0.000	120	7.46
		3	27.6	2.94	0.0233	0.274	6.61	0.390	34.4	0.741	27.3	1.65	<u>0.000</u>	0.000	133	28.1
	Iodide	7	25.8	1.43	-0.307	0.0150	<u>0.282</u>	0.282	26.8	0.800	18.8	0.180	<u>0.000</u>	0.000	125	6.65
		24	25.9	1.34	-0.208	0.274	<u>0.662</u>	0.662	20.2	0.520	12.8	0.369	<u>0.000</u>	0.000	140	3.62
		1	364	181	<u>0.000</u>	0.000	13.2	3.14	240	5.63	<u>0.000</u>	0.000	191	13.4	83.1	1.47
		3	31.0	13.1	<u>0.000</u>	0.000	18.9	1.69	37.7	0.702	<u>0.000</u>	0.000	17.1	1.09	112	3.37

Soil	Species added	Time (hr)	¹²⁷ Iodine (µg I kg ⁻¹)		¹²⁷ IO ₃ ⁻ (µg I kg ⁻¹)		¹²⁷ I ⁻ (µg I kg ⁻¹)		¹²⁹ Iodine (µg I kg ⁻¹)		¹²⁹ IO ₃ ⁻ (µg I kg ⁻¹)		¹²⁹ I ⁻ (µg I kg ⁻¹)		DOC (mg kg ⁻¹)	
			Mean	S. E.	Mean	S. E.	Mean	S. E.	Mean	S. E.	Mean	S. E.	Mean	S. E.	Mean	S. E.
NI19	Iodate	7	15.8	1.20	<u>0.000</u>	0.000	<u>0.740</u>	0.740	11.8	0.382	<u>0.000</u>	0.000	<u>0.000</u>	0.000	113	2.87
		24	17.6	1.05	<u>0.000</u>	0.000	<u>0.000</u>	0.000	8.77	0.259	<u>0.000</u>	0.000	<u>0.000</u>	0.000	134	4.09
		1	39.8	2.09	3.14	0.184	<u>3.51</u>	3.51	67.1	0.451	84.6	1.58	<u>0.000</u>	0.000	108	9.35
		3	40.8	1.55	1.66	0.156	2.31	1.30	16.6	0.620	51.0	0.389	<u>0.000</u>	0.000	125	3.75
	Iodide	7	39.5	0.347	1.34	0.311	<u>0.000</u>	0.000	<u>-1.55</u>	0.439	33.3	0.865	<u>0.000</u>	0.000	112	3.53
		24	40.6	0.723	0.516	0.160	<u>0.000</u>	0.000	<u>-5.51</u>	0.432	20.5	0.165	<u>0.000</u>	0.000	173	21.2
		1	66.2	1.18	<u>0.000</u>	0.000	20.9	3.35	344	7.30	<u>0.000</u>	0.000	287	4.42	101	2.61
		3	60.2	12.2	<u>0.000</u>	0.000	16.4	8.59	93.1	5.45	<u>0.000</u>	0.000	71.6	4.45	129	3.94
NI20	Iodate	7	38.2	1.27	<u>0.000</u>	0.000	1.18	1.42	4.76	0.196	<u>0.000</u>	0.000	2.24	0.287	124	8.23
		24	47.8	1.72	<u>0.000</u>	0.000	<u>0.000</u>	0.000	<u>0.198</u>	0.525	<u>0.000</u>	0.000	<u>0.000</u>	0.000	153	3.85
		1	18.9	3.92	9.01	2.12	<u>0.000</u>	0.000	237	8.84	182	2.22	<u>0.000</u>	0.000	379	15.7
		3	23.3	5.55	6.42	0.778	<u>0.000</u>	0.000	157	0.531	120	1.26	<u>0.000</u>	0.000	518	21.1
	Iodide	7	28.8	4.14	3.34	0.656	<u>0.000</u>	0.000	104	1.01	87.4	3.65	<u>0.000</u>	0.000	594	41.1
		24	144	6.78	1.54	0.732	<u>1.01</u>	1.01	30.1	1.32	37.3	1.63	<u>0.000</u>	0.000	1040	74.6
		1	9.20	1.88	<u>0.000</u>	0.000	-5.43	2.97	383	2.71	<u>0.000</u>	0.000	212	12.2	386	14.8
		3	6.44	2.89	<u>0.000</u>	0.000	-1.92	1.97	113	6.18	<u>0.000</u>	0.000	53.8	2.89	512	7.87
		7	14.4	2.11	<u>0.000</u>	0.000	<u>0.000</u>	0.000	9.05	0.262	<u>0.000</u>	0.000	<u>0.000</u>	0.000	616	36.2
		24	129	5.68	<u>0.000</u>	0.000	<u>1.00</u>	1.00	<u>-11.5</u>	1.11	<u>0.000</u>	0.000	<u>0.000</u>	0.000	1000	51.1

APPENDIX 3: SOIL IODINE DYNAMICS MODEL

This appendix describes all model details using the format of the OpenModel software, for the model describing iodine dynamics for individual soils, the precursor to the ‘array’ model. Parameters $k_1 - k_5$ and $kd - kd_3$ produced by this model are the ‘fitted’ parameters described in the text. Symbols used for concentrations of species in solution are different from thesis text due to requirements of OpenModel for formatting.

SYMBOLS

Table A4. Variables

Symbol	Meaning
Ide_N_sltn	Concentration of $^{127}\text{I}^-$ in solution ($\mu\text{g I L}^{-1}$)
Ine_N_sltn	Concentration of ^{127}I in solution ($\mu\text{g I L}^{-1}$)
Ine_N_solid	Concentration of ^{127}I on solution ($\mu\text{g I kg}^{-1}$)
Ine_S_sltn_I	Concentration of ^{129}I in solution ($\mu\text{g I L}^{-1}$) after addition of $^{129}\text{I}^-$
Ine_S_sltn_IO	Concentration of ^{129}I in solution ($\mu\text{g I L}^{-1}$) after addition of $^{129}\text{IO}_3^-$
k2	Rate of movement of iodine from Ine_S_solid to Ide_S_sltn ($\text{L kg}^{-1} \text{hr}^{-1}$)
k4	Rate of movement of iodine from OrgI_S_sltn to Ide_S_sltn (hr^{-1})
m	Mass of soil (oven-dry weight) in system (kg). Unique soil value, calculated as mean of 3 replicates when iodate added.
OrgI_N_sltn	Concentration Org ^{127}I in solution ($\mu\text{g I L}^{-1}$)
SIC	Soil iodine concentration (mg/kg). Unique soil value, calculated from triplicate analysis of NI soils.
Tot_S_I	Total spike in system (μg) after addition of $^{129}\text{I}^-$. Same amount added to all soils: iodide – $2.002 \mu\text{g } ^{129}\text{I} \equiv 2.207 \mu\text{g}$ spike.
Tot_S_IO	Total spike in system (μg) after addition of $^{129}\text{IO}_3^-$. Same amount added to all soils: iodate – $2.000 \mu\text{g } ^{129}\text{I} \equiv 2.205 \mu\text{g}$ spike.
v	Volume of liquid in system (l). Unique value per soil, calculated as mean of four sampling times and 3 replicates.

Table A5. ODEs

Symbol	Meaning
Ide_S_sltn_I	Concentration of $^{129}\text{I}^-$ in solution ($\mu\text{g L}^{-1}$) after addition of $^{129}\text{I}^-$
Ide_S_sltn_IO	Concentration of $^{129}\text{I}^-$ in solution ($\mu\text{g L}^{-1}$) after addition of $^{129}\text{IO}_3^-$
Ine_S_solid_I	Concentration of ^{129}I on solid ($\mu\text{g kg}^{-1}$) after addition of $^{129}\text{I}^-$
Ine_S_solid_IO	Concentration of ^{129}I on solid ($\mu\text{g kg}^{-1}$) after addition of $^{129}\text{IO}_3^-$
Ite_S_sltn_I	Concentration of $^{129}\text{IO}_3^-$ in solution ($\mu\text{g L}^{-1}$) after addition of $^{129}\text{I}^-$
Ite_S_sltn_IO	Concentration of $^{129}\text{IO}_3^-$ in solution ($\mu\text{g L}^{-1}$) after addition of $^{129}\text{IO}_3^-$
OrgI_S_sltn_I	Concentration of Org ^{129}I in solution ($\mu\text{g L}^{-1}$) after addition of $^{129}\text{I}^-$
OrgI_S_sltn_IO	Concentration of Org ^{129}I in solution ($\mu\text{g L}^{-1}$) after addition of $^{129}\text{IO}_3^-$

Table A6. Parameters

Symbol	Meaning
k1	Rate of movement of iodine from Ide_S_sltn to Ine_S_solid (L kg ⁻¹ hr ⁻¹)
k3	Rate of movement of iodine from Ide_S_sltn to OrgI_S_sltn (hr ⁻¹)
k5	Rate of movement of iodine from Ite_S_sltn to Ide_S_sltn (hr ⁻¹)
kd	Instantaneous partition coefficient from Ide_S_sltn to Ine_S_solid (L kg ⁻¹)
kd2	Instantaneous partition coefficient from Ite_S_sltn to Ine_S_solid (L kg ⁻¹)
kd3	Instantaneous partition coefficient from Ite_S_sltn to OrgI_S_solid (dimensionless)

MODEL SET-UP**Initial**

m = unique soil value

v = unique soil value

SIC = unique soil value

Ine_N_sltn = 1.85

Ide_N_sltn = 0.87

OrgI_N_sltn = 0.94

$Ine_N_solid = ((m * SIC * 1000) - (Ine_N_sltn * v)) / m$

$k2 = (k1 * Ide_N_sltn) / (Ine_N_solid * (m/v))$

$k4 = (k3 * Ide_N_sltn) / OrgI_N_sltn$

//Iodide added

Tot_S_I = 2.207

Ite_S_sltn_I = 0

$Ide_S_sltn_I = Tot_S_I / ((kd * m) + v)$

$Ine_S_solid_I = kd * Ide_S_sltn_I$

//Iodate added

Tot_S_IO = 2.205

$Ite_S_sltn_IO = Tot_S_IO / (kd3 * v + v + kd2 * m)$

Ide_S_sltn_IO = 0

$OrgI_S_sltn_IO = Ite_S_sltn_IO * kd3$

$Ine_S_solid_IO = kd2 * Ite_S_sltn_IO$

Main

$k2 = (k1 * Ide_N_sltn) / (Ine_N_solid * (m/v))$

$k4 = (k3 * Ide_N_sltn) / OrgI_N_sltn$


```
//Iodide added
OrgI_S_sltn_I.rate = (k3*Ide_S_sltn_I) - (k4*OrgI_S_sltn_I)
Ite_S_sltn_I.rate = - (k5 * Ite_S_sltn_I)
Ide_S_sltn_I.rate = (k5 * Ite_S_sltn_I) + (k2 * Ine_S_solid_I * (m/v)) - (k1 * Ide_S_sltn_I) + (k4 *
OrgI_S_sltn_I) - (k3 * Ide_S_sltn_I)
Ine_S_solid_I.rate = (k1*Ide_S_sltn_I*(v/m)) - (k2*Ine_S_solid_I)

Ine_S_sltn_I = Ide_S_sltn_I + OrgI_S_sltn_I + Ite_S_sltn_I
Tot_S_I = (Ine_S_sltn_I * v) + (Ine_S_solid_I * m)
```

```
//Iodate added
Ite_S_sltn_IO.rate = - (k5 * Ite_S_sltn_IO)
Ide_S_sltn_IO.rate = (k5 * Ite_S_sltn_IO) + (k2 * Ine_S_solid_IO * (m/v)) - (k1 * Ide_S_sltn_IO) +
(k4 * OrgI_S_sltn_IO) - (k3 * Ide_S_sltn_IO)
OrgI_S_sltn_IO.rate = (k3*Ide_S_sltn_IO) - (k4*OrgI_S_sltn_IO)
Ine_S_solid_IO.rate = (k1*Ide_S_sltn_IO*(v/m)) - (k2*Ine_S_solid_IO)

Ine_S_sltn_IO = Ide_S_sltn_IO + OrgI_S_sltn_IO + Ite_S_sltn_IO
Tot_S_IO = (Ine_S_sltn_IO * v) + (Ine_S_solid_IO * m)
```

DATA SHEETS

Data sheets for mean and standard error at each measured time point, e.g. Tables A7 and A8.

Table A7. Example data sheet: mean values for NI01.

Time (hr)	Ine_S_sltn_IO ($\mu\text{g L}^{-1}$)	Ide_S_sltn_IO ($\mu\text{g L}^{-1}$)	Ite_S_sltn_IO ($\mu\text{g L}^{-1}$)	Ine_S_sltn_I ($\mu\text{g L}^{-1}$)	Ide_S_sltn_I ($\mu\text{g L}^{-1}$)
1	27.6	0.14	23.35	71.51	66.21
3	20.72	0.14	17.08	38.15	31.84
7	16.15	0.14	12.73	9.19	4.98
24	10.66	0.4	6.81	3.29	0.43

Table A8. Example data sheet: standard error values for NI01.

Time (hr)	Ine_S_sltn_IO ($\mu\text{g L}^{-1}$)	Ide_S_sltn_IO ($\mu\text{g L}^{-1}$)	Ite_S_sltn_IO ($\mu\text{g L}^{-1}$)	Ine_S_sltn_I ($\mu\text{g L}^{-1}$)	Ide_S_sltn_I ($\mu\text{g L}^{-1}$)
1	0.03	0.14	0.03	0.03	0.03
3	0.03	0.14	0.03	0.03	0.03
7	0.03	0.14	0.03	0.03	0.03
24	0.03	0.03	0.03	0.03	0.03

APPENDIX 4: SOIL IODINE DYNAMICS ARRAY MODEL

This appendix describes all model details using the format of the OpenModel software, for the final ‘array’ model describing iodine dynamics in terms of soil properties. Parameters $k_1 - k_5$ and $kd - kd_3$ produced by this model are the ‘optimised’ parameters described in the text. Symbols used for concentrations of species in solution are different from thesis text due to requirements of OpenModel for formatting

All variables and ODEs (ordinary differential equations) are followed by ‘(1..20)’. This means that the model chooses/calculates the values for the soils NI01 – NI20 using the appropriate values from the data sheets as an ‘array’.

SYMBOLS

Table A9. Variables

Symbol	Meaning
Al(1..20)	Measured aluminium oxide content (g kg^{-1})
Fe(1..20)	Measured iron oxide content (g kg^{-1}) for soils NI01 – NI20
Ide_N_sltn(1..20)	Concentration of ^{127}I in solution ($\mu\text{g I L}^{-1}$)
Ine_N_sltn(1..20)	Concentration of ^{127}I in solution ($\mu\text{g I L}^{-1}$)
Ine_N_solid(1..20)	Concentration of ^{127}I on solution ($\mu\text{g I kg}^{-1}$)
Ine_S_sltn_I(1..20)	Concentration of ^{129}I in solution ($\mu\text{g I L}^{-1}$) after addition of ^{129}I
Ine_S_sltn_IO(1..20)	Concentration of ^{129}I in solution ($\mu\text{g I L}^{-1}$) after addition of $^{129}\text{IO}_3^-$
k1(1..20)	Rate of movement of iodine from Ide_S_sltn to Ine_S_solid ($\text{L kg}^{-1} \text{hr}^{-1}$)
k2(1..20)	Rate of movement of iodine from Ine_S_solid to Ide_S_sltn ($\text{L kg}^{-1} \text{hr}^{-1}$)
k3(1..20)	Rate of movement of iodine from Ide_S_sltn to OrgI_S_sltn (hr^{-1})
k4(1..20)	Rate of movement of iodine from OrgI_S_sltn to Ide_S_sltn (hr^{-1})
k5(1..20)	Rate of movement of iodine from Ite_S_sltn to Ide_S_sltn (hr^{-1})
kd(1..20)	Instantaneous partition coefficient from Ide_S_sltn to Ine_S_solid (L kg^{-1})
kd2(1..20)	Instantaneous partition coefficient from Ite_S_sltn to Ine_S_solid (L kg^{-1})
kd3(1..20)	Instantaneous partition coefficient from Ite_S_sltn to OrgI_S_solid (dimensionless)
m(1..20)	Mass of soil (oven-dry weight) in system (kg). Unique soil value, calculated as mean of 3 replicates when iodate added.
OrgI_N_sltn(1..20)	Concentration Org ^{127}I in solution ($\mu\text{g I L}^{-1}$)
pH(1..20)	Measured soil pH

Symbol	Meaning
SIC(1..20)	Soil iodine concentration (mg/kg). Unique soil value, calculated from triplicate analysis of NI soils.
SOC(1..20)	Measured soil organic carbon content (%)
Tot_S_I(1..20)	Total spike in system (μg) after addition of $^{129}\text{I}^-$. Same amount added to all soils: iodide – $2.002 \mu\text{g } ^{129}\text{I} \equiv 2.207 \mu\text{g}$ spike.
Tot_S_IO(1..20)	Total spike in system (μg) after addition of $^{129}\text{IO}_3^-$. Same amount added to all soils: iodate – $2.000 \mu\text{g } ^{129}\text{I} \equiv 2.205 \mu\text{g}$ spike.
v(1..20)	Volume of liquid in system (l). Unique value per soil, calculated as mean of four sampling times and 3 replicates.

Table A10. ODEs

Symbol	Meaning
Ide_S_sltn_I(1..20)	Concentration of $^{129}\text{I}^-$ in solution ($\mu\text{g L}^{-1}$) after addition of $^{129}\text{I}^-$
Ide_S_sltn_IO(1..20)	Concentration of $^{129}\text{I}^-$ in solution ($\mu\text{g L}^{-1}$) after addition of $^{129}\text{IO}_3^-$
Ine_S_solid_I(1..20)	Concentration of ^{129}I on solid ($\mu\text{g kg}^{-1}$) after addition of $^{129}\text{I}^-$
Ine_S_solid_IO(1..20)	Concentration of ^{129}I on solid ($\mu\text{g kg}^{-1}$) after addition of $^{129}\text{IO}_3^-$
Ite_S_sltn_I(1..20)	Concentration of $^{129}\text{IO}_3^-$ in solution ($\mu\text{g L}^{-1}$) after addition of $^{129}\text{I}^-$
Ite_S_sltn_IO(1..20)	Concentration of $^{129}\text{IO}_3^-$ in solution ($\mu\text{g L}^{-1}$) after addition of $^{129}\text{IO}_3^-$
OrgI_S_sltn_I(1..20)	Concentration of Org ^{129}I in solution ($\mu\text{g L}^{-1}$) after addition of $^{129}\text{I}^-$
OrgI_S_sltn_IO(1..20)	Concentration of Org ^{129}I in solution ($\mu\text{g L}^{-1}$) after addition of $^{129}\text{IO}_3^-$

Parameters

Parameters a, b, c, cc, d, dd, e, ee, f, ff, g, gg, h, jj, kk, ll, mm, w are used in ‘initial’ and ‘main’ scripts to link measured soil properties to rate parameters k1 – k5 and kd – kd3.

MODEL SET-UP

Initial

for i = 1,20

// Soil properties, measured experimentally and defined in 'input' data table.

m(i) = input.m(i)

v(i) = input.v(i)

SIC(i) = input.SIC(i)

pH(i) = input.pH(i)

SOC(i) = input.SOC(i)

Al(i) = input.Al(i)

```

Fe(i) = input.Fe(i)
Ine_N_sltn(i) = input.Ine_N_sltn(i)
Ide_N_sltn(i) = input.Ide_N_sltn(i)
OrgI_N_sltn(i) = input.OrgI_N_sltn(i)

// Define rate parameters and variables not measured experimentally.
Ine_N_solid(i) = ((m(i)*SIC(i)*1000) - (Ine_N_sltn(i)*v(i))) / m(i)
k1(i) = a + (b * Al(i))
k2(i) = (k1(i)*Ide_N_sltn(i)) / (Ine_N_solid(i)*(m(i)/v(i)))
k3(i) = c + (d * Al(i)) + (e * SIC(i))
k4(i) = (k3(i) * Ide_N_sltn(i)) / OrgI_N_sltn(i)
k5(i) = f + (g * SOC(i)) - (h * Al(i))

// Calculate instantaneous partition coefficients. Note that kd3 is mean of all soils due to large
uncertainty. SOC cutoff works for my soils' observations, but I have no soils with 30 > SOC < 38 %.
if SOC(i) < 38
    kd(i) = 10^(-26.17+(3.8*pH(i)))
    kd2(i) = 10^(cc + (dd*Fe(i)) - (ee*pH(i)) + (ff*Al(i)))
else
    kd(i) = 10^(gg - (hh*pH(i)) - (jj*Al(i)))
    kd2(i) = 10^(kk - (ll*Al(i)) - (mm*pH(i)))
endif
kd3(i) = w

// Iodide added - application of instantaneous partition coefficients.
Tot_S_I(i) = 2.207
Ite_S_sltn_I(i) = 0
Ide_S_sltn_I(i) = Tot_S_I(i)/((kd(i)*m(i))+v(i))
Ine_S_solid_I(i) = kd(i) * Ide_S_sltn_I(i)

// Iodate added - application of instantaneous partition coefficients.
Tot_S_IO(i) = 2.205
Ite_S_sltn_IO(i) = Tot_S_IO(i)/(kd3(i)*v(i) + v(i) + kd2(i)*m(i))
Ide_S_sltn_IO(i) = 0
OrgI_S_sltn_IO(i) = Ite_S_sltn_IO(i) * kd3(i)
Ine_S_solid_IO(i) = kd2(i) * Ite_S_sltn_IO(i)

endfor

```

Main

for i = 1,20

// Define rate parameters. k2 and k4 are defined by equilibrium (native) ratios in solution.

$$k1(i) = a + (b * Al(i))$$

$$k2(i) = (k1(i)*Ide_N_sltn(i)) / (Ine_N_solid(i)*(m(i)/v(i)))$$

$$k3(i) = c + (d * Al(i)) + (e * SIC(i))$$

$$k4(i) = (k3(i) * Ide_N_sltn(i)) / OrgI_N_sltn(i)$$

$$k5(i) = f + (g * SOC(i)) - (h * Al(i))$$

// Iodide added - implement rate parameters.

$$OrgI_S_sltn_I(i).rate = (k3(i)*Ide_S_sltn_I(i)) - (k4(i)*OrgI_S_sltn_I(i))$$

$$Ite_S_sltn_I(i).rate = - (k5(i) * Ite_S_sltn_I(i))$$

$$Ide_S_sltn_I(i).rate = (k5(i) * Ite_S_sltn_I(i)) + (k2(i) * Ine_S_solid_I(i) * (m(i)/v(i))) - (k1(i) * Ide_S_sltn_I(i)) + (k4(i) * OrgI_S_sltn_I(i)) - (k3(i) * Ide_S_sltn_I(i))$$

$$Ine_S_solid_I(i).rate = (k1(i)*Ide_S_sltn_I(i)*(v(i)/m(i))) - (k2(i)*Ine_S_solid_I(i))$$

$$Ine_S_sltn_I(i) = Ide_S_sltn_I(i) + OrgI_S_sltn_I(i) + Ite_S_sltn_I(i)$$

$$Tot_S_I(i) = (Ine_S_sltn_I(i) * v(i)) + (Ine_S_solid_I(i) * m(i))$$

// Iodate added - implement rate parameters

$$Ite_S_sltn_IO(i).rate = - (k5(i) * Ite_S_sltn_IO(i))$$

$$Ide_S_sltn_IO(i).rate = (k5(i) * Ite_S_sltn_IO(i)) + (k2(i) * Ine_S_solid_IO(i) * (m(i)/v(i))) - (k1(i) * Ide_S_sltn_IO(i)) + (k4(i) * OrgI_S_sltn_IO(i)) - (k3(i) * Ide_S_sltn_IO(i))$$

$$OrgI_S_sltn_IO(i).rate = (k3(i)*Ide_S_sltn_IO(i)) - (k4(i)*OrgI_S_sltn_IO(i))$$

$$Ine_S_solid_IO(i).rate = (k1(i)*Ide_S_sltn_IO(i)*(v(i)/m(i))) - (k2(i)*Ine_S_solid_IO(i))$$

$$Ine_S_sltn_IO(i) = Ide_S_sltn_IO(i) + OrgI_S_sltn_IO(i) + Ite_S_sltn_IO(i)$$

$$Tot_S_IO(i) = (Ine_S_sltn_IO(i) * v(i)) + (Ine_S_solid_IO(i) * m(i))$$

endfor

DATA SHEETS

Data sheets for input values, and mean and standard error for each measured time point, for all soils.

Table A11. 'Input' data sheet, containing information about all soils, referenced by the model for $i = 1$ to $i = 20$, where 'i' is the soil number.

Soil	m	v	SIC	Ine_N_slt	Ide_N_slt	OrgI_N_slt	Al	Mn	Fe	pH	SOC
1	0.004	0.024	2.89	1.85	0.87	0.94	1.25	0.132	9.01	4.71	4.81
2	0.004	0.0235	4.29	1.92	1.29	0.84	1.57	0.32	10.1	4.54	3.64
3	0.002	0.0262	20.81	16.25	0.67	14.68	3.8	0.0103	1.34	3.72	47.7
4	0.004	0.0236	9.29	15.19	1.49	13.7	0.573	0.0547	4.55	4.96	3.28
5	0.004	0.0233	274.2	374.65	7.81	366.84	1.72	0.162	8.11	5.49	4.76
6	0.004	0.0234	9.38	1.88	1.41	0.88	1.74	0.526	13	4.78	3.59
7	0.004	0.0235	13.98	12.59	2.29	14.41	1.29	0.23	10.2	5.89	3.98
8	0.004	0.0235	127.15	154.83	2.32	152.51	2.07	0.0757	9.29	5.9	6.01
9	0.002	0.0271	31.99	31.86	0.71	38.05	3.46	0.0107	2.01	3.7	38.5
10	0.001	0.0266	16.56	8.07	0.46	7.61	0.416	0.00704	1.14	3.52	52.1
11	0.004	0.0247	10.03	1.52	0.58	1.1	4.03	0.358	18.2	4.8	9.58
12	0.004	0.024	4.15	3.99	0.93	3.08	1.7	0.155	14.7	4.7	5.05
13	0.004	0.0251	7.46	0.54	0.49	0.41	2.56	0.372	18.7	5.74	12.1
14	0.004	0.0246	5.16	1.55	0.23	1.41	2.39	0.312	20.7	5.37	8.11
15	0.004	0.0263	27.36	10.09	1.17	8.93	8.34	0.619	18.6	4.28	22.9
16	0.0007	0.0273	21.57	23.01	0.78	22.23	0.74	0.00649	1.75	2.84	50.1
17	0.0013	0.0267	13.16	13.6	0.86	12.74	0.295	-1E308	0.358	3.49	53.4
18	0.004	0.0247	9.64	4.26	0.89	9.18	4.13	0.841	20.1	4.86	8.43
19	0.004	0.0248	11.11	7.35	1.03	6.27	3.61	0.966	23.9	4.85	8.33
20	0.002	0.0259	9.6	3.9	0.17	3.74	10.7	0.0418	10.1	4.73	29.7

Table A12. Part of 'Mean_measured' data sheet. This table shows only information for NI01 and part of NI02; actual data sheet continues with columns for all ODEs for all soils.

Time (hr)	Ine_S_slt_n_IO(1)	Ide_S_slt_n_IO(1)	Ite_S_slt_n_IO(1)	Ine_S_slt_n_I(1)	Ide_S_slt_n_I(1)	Ine
1	27.6	0.14	23.35	71.51	66.21	
3	20.72	0.14	17.08	38.15	31.84	
7	16.15	0.14	12.73	9.19	4.98	
24	10.66	0.4	6.81	3.29	0.43	

Table A13. Part of 'standard_error_measured' data sheet. This table shows only information for NI01 and part of NI02; actual data sheet continues with columns for all ODEs for all soils.

Time (hr)	Ine_S_slt_n_IO(1)	Ide_S_slt_n_IO(1)	Ite_S_slt_n_IO(1)	Ine_S_sltn_I(1)	Ide_S_sltn_I(1)	Ine_S_slt_n_IO(2)	Ide_S_slt_n_IO(2)	Ite_S_slt_n_IO(2)
1	0.03	0.14	0.03	0.03	0.03	0.03	0.14	0.03
3	0.03	0.14	0.03	0.03	0.03	0.03	0.14	0.03
7	0.03	0.14	0.03	0.03	0.03	0.03	0.14	0.03
24	0.03	0.03	0.03	0.03	0.03	0.03	0.14	0.03

APPENDIX 5: RESULTS OF IODINE DYNAMICS EXPERIMENT IN HUMIC ACID

Key to sample names:

Concentration added – species added – day spiked.

e.g. 20-I-73 had $22.1 \mu\text{g } ^{129}\text{I L}^{-1}$ added as iodide and was incubated for 1 day.

20 – $22.1 \mu\text{g I L}^{-1}$ added

40 – $44.1 \mu\text{g I L}^{-1}$ added

80 – $88.2 \mu\text{g I L}^{-1}$ added

I – only iodide added

IO – only iodate added

Mix – equal proportions of iodide and iodate added

Days spiked: between

1 - incubated for 73 days (1400 hr)

and

73 - incubated for 1 day (24 hr)

Table A14. Concentrations of ^{129}I and ^{127}I in solution for spiked, incubated humic acid samples. Values are mean and standard error of triplicate measurements.

Sample	Hours incubated	$^{129}\text{I total}$ ($\mu\text{g I L}^{-1}$)		$^{129}\text{OrgI}$ ($\mu\text{g I L}^{-1}$)		$^{129}\text{IO}_3^-$ ($\mu\text{g I L}^{-1}$)		$^{129}\text{I}^-$ ($\mu\text{g I L}^{-1}$)		$^{127}\text{I total}$ ($\mu\text{g I L}^{-1}$)		$^{127}\text{OrgI}$ ($\mu\text{g I L}^{-1}$)		$^{127}\text{IO}_3^-$ ($\mu\text{g I L}^{-1}$)		$^{127}\text{I}^-$ ($\mu\text{g I L}^{-1}$)	
		Mean	S. E.	Mean	S. E.	Mean	S. E.	Mean	S. E.	Mean	S. E.	Mean	S. E.	Mean	S. E.	Mean	S. E.
20-I-73	24.5	20.5	0.594	0.000	0.000	0.000	0.000	20.5	0.594	108	6.75	84.3	6.51	0.000	0.000	23.3	0.327
20-I-71	77.4	20.6	0.0689	0.000	0.000	0.000	0.000	20.6	0.0689	113	2.20	90.5	2.08	0.000	0.000	23.0	0.137
20-I-68	153	22.3	1.18	1.40	0.360	0.000	0.000	20.9	1.11	118	2.61	94.8	2.03	0.000	0.000	22.9	0.612
20-I-61	326	21.6	1.18	2.04	0.425	0.000	0.000	19.6	1.04	118	1.56	96.2	1.22	0.000	0.000	21.4	0.733
20-I-50	594	21.8	0.940	3.37	0.141	0.000	0.000	18.4	0.000	118	0.455	98.2	2.45	0.000	0.000	20.1	0.000
20-I-36	990	20.2	0.687	3.18	0.159	0.000	0.000	17.1	0.645	113	4.78	95.7	4.12	0.000	0.000	17.5	0.655
20-I-19	1403	20.5	0.123	3.36	0.104	0.000	0.000	17.1	0.104	115	5.95	98.0	5.35	0.000	0.000	16.8	0.785
20-I-1	1854	21.6	0.495	4.67	0.112	0.000	0.000	16.9	0.385	115	5.06	99.6	4.79	0.000	0.000	15.9	0.411
20-IO3-73	24.9	24.0	1.26	1.28	0.826	21.6	0.500	1.20	0.151	103	4.44	88.1	4.16	0.541	0.0930	14.6	0.388
20-IO3-71	77.8	24.3	0.672	3.35	0.867	17.7	0.637	3.31	0.271	110	2.82	94.9	2.70	0.659	0.227	14.6	0.122
20-IO3-68	154	24.7	1.17	6.30	1.32	12.5	0.595	5.94	0.376	113	1.55	98.4	1.25	0.294	0.0346	14.4	0.271
20-IO3-61	326	24.1	1.62	8.89	1.37	4.80	0.103	10.4	0.565	113	1.94	97.8	1.06	0.293	0.140	14.6	0.903
20-IO3-50	594	23.6	0.311	9.51	0.847	1.34	0.0472	12.8	0.0521	115	0.538	99.6	0.758	0.000	0.000	15.3	0.000
20-IO3-36	991	22.9	0.957	9.90	0.696	0.812	0.0414	12.2	0.516	111	3.44	98.8	3.03	0.000	0.000	12.3	0.423
20-IO3-19	1403	23.0	0.791	8.47	0.452	0.124	0.124	14.4	0.517	113	5.40	99.7	4.82	0.000	0.000	13.5	0.591
20-IO3-1	1854	24.5	0.167	8.75	0.207	0.000	0.000	15.7	0.374	116	2.26	102	2.02	0.000	0.000	14.0	0.575
20-mix-73	25.3	21.8	1.06	1.66	0.505	10.8	0.268	9.32	0.442	107	6.22	88.4	5.50	0.371	0.0915	18.4	0.732
20-mix-71	78.2	22.6	0.738	3.15	0.902	8.83	0.199	10.6	0.0462	113	1.49	93.8	1.36	0.449	0.0661	19.0	0.229
20-mix-68	154	23.8	1.14	5.68	1.24	5.72	0.381	12.4	0.361	115	1.92	96.8	1.36	0.298	0.164	18.3	0.623
20-mix-61	327	23.4	1.47	6.91	1.24	2.00	0.0667	14.5	0.686	119	2.10	100.0	1.45	0.0103	0.0103	18.8	0.634
20-mix-50	595	22.9	0.303	7.42	0.373	0.614	0.0338	14.8	0.0373	115	0.309	97.6	1.13	0.000	0.000	17.5	0.000
20-mix-36	991	21.0	0.832	6.97	0.601	0.221	0.113	13.8	0.508	110	5.36	94.9	4.89	0.000	0.000	14.6	0.467

Sample	Hours incubated	¹²⁹ I total (µg I L ⁻¹)		¹²⁹ OrgI (µg I L ⁻¹)		¹²⁹ IO ₃ ⁻ (µg I L ⁻¹)		¹²⁹ I ⁻ (µg I L ⁻¹)		¹²⁷ I total (µg I L ⁻¹)		¹²⁷ OrgI (µg I L ⁻¹)		¹²⁷ IO ₃ ⁻ (µg I L ⁻¹)		¹²⁷ I ⁻ (µg I L ⁻¹)	
		Mean	S. E.	Mean	S. E.	Mean	S. E.	Mean	S. E.	Mean	S. E.	Mean	S. E.	Mean	S. E.	Mean	S. E.
20-mix-19	1404	21.5	0.192	6.11	0.254	0.193	0.193	15.2	0.486	115	5.35	99.5	4.77	0.000	0.000	15.1	0.573
20-mix-1	1854	23.1	0.404	6.89	0.168	0.000	0.000	16.2	0.274	114	4.13	99.7	4.05	0.000	0.000	14.7	0.516
40-I-73	25.7	41.0	0.525	0.000	0.000	0.000	0.000	41.0	0.525	111	4.36	87.6	3.74	0.000	0.000	23.5	0.624
40-I-71	78.6	42.0	0.623	0.293	0.293	0.000	0.000	41.7	0.512	116	1.37	92.8	1.04	0.000	0.000	23.3	0.329
40-I-68	154	43.3	1.95	2.70	0.471	0.000	0.000	40.6	2.00	117	1.95	94.5	1.53	0.000	0.000	22.6	0.470
40-I-61	327	43.5	1.66	4.48	0.809	0.000	0.000	39.0	1.62	120	2.78	98.2	2.07	0.000	0.000	22.0	0.740
40-I-50	595	41.9	1.01	6.25	0.573	0.000	0.000	35.6	0.000	113	0.772	93.2	3.22	0.000	0.000	20.1	0.000
40-I-36	992	40.3	1.32	5.74	0.437	0.000	0.000	34.6	1.00	113	5.77	95.3	5.10	0.000	0.000	17.7	0.732
40-I-19	1404	40.8	0.945	7.09	0.549	0.000	0.000	33.7	0.661	115	5.80	97.8	5.34	0.000	0.000	16.9	0.597
40-I-1	1855	41.6	0.896	8.14	0.191	0.000	0.000	33.4	0.706	116	3.97	99.6	3.72	0.000	0.000	16.7	0.265
40-IO3-73	26.2	49.4	1.15	1.85	0.725	45.7	0.536	1.83	0.267	106	5.07	93.9	5.12	1.08	0.226	10.8	0.445
40-IO3-71	79.1	48.7	0.564	5.12	1.28	38.9	1.08	4.63	0.441	110	2.30	99.7	2.37	1.07	0.358	9.58	0.361
40-IO3-68	155	49.0	1.32	8.62	1.41	32.0	1.18	8.41	0.486	112	1.73	102	1.47	0.688	0.0491	9.23	0.243
40-IO3-61	328	47.3	2.05	14.6	1.86	17.1	0.682	15.6	0.752	113	1.56	103	0.923	0.300	0.0879	9.89	0.597
40-IO3-50	596	45.0	0.222	17.1	1.13	6.93	0.557	21.0	0.614	113	0.752	102	0.506	0.306	0.0308	11.0	0.0360
40-IO3-36	992	44.0	1.99	18.5	1.26	4.14	0.603	21.4	1.53	111	6.95	102	6.43	0.329	0.0635	9.31	0.503
40-IO3-19	1404	44.5	0.964	17.3	0.423	1.18	0.153	26.0	1.13	112	4.95	101	4.48	0.211	0.211	11.1	0.379
40-IO3-1	1855	46.4	0.796	17.3	0.680	0.000	0.000	29.0	0.116	117	5.46	105	5.32	0.282	0.282	12.2	0.507
40-mix-73	26.6	43.3	1.34	4.72	1.17	22.6	0.235	16.0	0.194	109	5.03	92.1	4.78	0.638	0.0446	16.5	0.213
40-mix-71	79.5	43.7	0.620	6.43	0.689	19.3	0.568	18.0	0.296	112	0.672	95.7	0.354	0.666	0.101	15.8	0.402
40-mix-68	155	45.2	1.61	10.2	1.47	14.9	0.556	20.1	0.864	115	1.96	98.5	1.49	0.528	0.140	15.6	0.485
40-mix-61	328	44.8	1.51	13.4	1.18	7.30	0.303	24.1	0.860	114	2.08	98.1	1.70	0.360	0.171	15.7	0.354
40-mix-50	596	42.1	0.0272	14.1	1.12	2.54	0.180	25.4	0.198	113	0.690	97.1	4.40	0.407	0.0961	15.0	0.0745

Sample	Hours incubated	¹²⁹ I total (µg I L ⁻¹)		¹²⁹ OrgI (µg I L ⁻¹)		¹²⁹ IO ₃ ⁻ (µg I L ⁻¹)		¹²⁹ I ⁻ (µg I L ⁻¹)		¹²⁷ I total (µg I L ⁻¹)		¹²⁷ OrgI (µg I L ⁻¹)		¹²⁷ IO ₃ ⁻ (µg I L ⁻¹)		¹²⁷ I ⁻ (µg I L ⁻¹)	
		Mean	S. E.	Mean	S. E.	Mean	S. E.	Mean	S. E.	Mean	S. E.	Mean	S. E.	Mean	S. E.	Mean	S. E.
40-mix-36	992	42.0	1.36	15.0	0.702	1.66	0.258	25.4	0.995	110	6.21	97.1	5.74	0.000	0.000	12.8	0.528
40-mix-19	1405	43.0	1.32	14.5	0.601	0.419	0.210	28.0	1.03	114	5.13	100.0	4.50	0.000	0.000	14.1	0.628
40-mix-1	1856	43.9	1.01	13.9	0.0456	0.142	0.142	29.9	1.00	115	2.48	101	1.93	0.000	0.000	14.8	0.618
80-I-73	27.0	83.6	0.298	1.40	0.424	0.000	0.000	82.2	0.720	112	2.79	87.6	2.54	0.000	0.000	24.1	0.285
80-I-71	79.9	85.3	2.04	2.88	0.467	0.000	0.000	82.4	2.01	117	1.35	92.6	1.01	0.000	0.000	23.9	0.424
80-I-68	156	85.1	3.17	5.27	0.608	0.000	0.000	79.9	3.36	115	1.56	92.2	1.21	0.000	0.000	23.0	0.364
80-I-61	329	84.4	3.41	7.89	1.23	0.000	0.000	76.5	3.30	119	1.00	96.4	0.636	0.000	0.000	23.0	0.379
80-I-50	597	79.8	1.79	10.8	1.24	0.000	0.000	69.0	0.000	114	0.427	93.2	4.37	0.000	0.000	20.3	0.000
80-I-36	993	79.3	2.68	12.3	0.742	0.000	0.000	66.9	2.14	112	5.69	93.9	4.70	0.000	0.000	18.5	0.993
80-I-19	1405	79.7	1.58	14.9	0.547	0.000	0.000	64.8	1.16	114	3.76	97.0	3.25	0.000	0.000	17.4	0.617
80-I-1	1856	82.1	1.31	17.0	0.224	0.000	0.000	65.0	1.38	118	4.34	100	3.84	0.000	0.000	17.5	0.51
80-IO3-73	27.4	98.1	1.27	3.10	1.20	92.5	0.213	2.51	0.0295	111	3.38	95.6	3.72	2.58	0.309	12.4	0.842
80-IO3-71	80.3	98.9	2.52	6.97	1.23	86.5	2.40	5.46	0.406	112	1.68	102	2.27	2.31	0.269	7.70	0.725
80-IO3-68	156	98.6	3.07	11.2	1.72	77.6	3.32	9.83	0.677	115	0.766	107	0.937	1.67	0.271	6.27	0.435
80-IO3-61	329	87.5	10.6	17.7	1.14	50.6	10.7	19.3	1.01	113	2.44	105	2.13	1.15	0.0984	7.24	0.382
80-IO3-50	597	63.0	0.431	21.6	1.99	16.2	0.512	25.2	0.564	109	0.562	100	5.17	0.289	0.0925	8.94	0.154
80-IO3-36	993	91.1	3.06	28.8	2.07	28.7	1.15	33.5	2.46	110	6.48	102	6.19	0.753	0.277	7.76	0.191
80-IO3-19	1406	90.4	3.01	33.7	1.90	13.5	0.913	43.2	2.63	114	4.27	104	3.94	0.477	0.151	9.02	0.405
80-IO3-1	1857	92.7	1.44	35.1	0.800	4.56	0.159	53.0	1.55	116	3.87	105	3.20	0.153	0.121	11.3	0.657
80-mix-73	27.9	87.9	1.09	8.78	1.85	46.5	0.539	32.6	0.866	112	1.74	93.4	1.91	1.19	0.207	17.5	0.282
80-mix-71	80.8	88.2	1.71	14.1	2.18	42.7	1.15	31.3	0.958	113	2.65	96.7	2.49	1.10	0.266	14.9	0.145
80-mix-68	157	88.6	1.86	19.0	2.46	37.5	1.24	32.0	1.15	115	1.42	99.9	1.76	0.955	0.127	13.8	0.304
80-mix-61	329	82.9	5.39	22.9	0.665	23.5	4.15	36.4	1.19	115	3.51	100.0	3.19	0.679	0.147	13.9	0.466

Sample	Hours incubated	¹²⁹ I total (µg I L ⁻¹)		¹²⁹ OrgI (µg I L ⁻¹)		¹²⁹ IO ₃ ⁻ (µg I L ⁻¹)		¹²⁹ I ⁻ (µg I L ⁻¹)		¹²⁷ I total (µg I L ⁻¹)		¹²⁷ OrgI (µg I L ⁻¹)		¹²⁷ IO ₃ ⁻ (µg I L ⁻¹)		¹²⁷ I ⁻ (µg I L ⁻¹)	
		Mean	S. E.	Mean	S. E.	Mean	S. E.	Mean	S. E.	Mean	S. E.	Mean	S. E.	Mean	S. E.	Mean	S. E.
80-mix-50	597	68.6	1.00	22.1	2.42	7.88	0.141	38.7	0.155	112	1.56	96.6	5.30	0.573	0.121	14.3	0.138
80-mix-36	994	84.1	3.45	29.8	2.08	10.8	0.574	43.5	2.04	111	5.87	99.0	5.34	0.252	0.174	12.3	0.471
80-mix-19	1406	85.0	2.18	31.8	1.14	4.49	0.563	48.7	1.89	117	6.65	104	6.03	0.208	0.172	12.9	0.589
80-mix-1	1857	86.3	2.15	30.0	0.294	1.63	0.197	54.6	2.17	115	3.34	101	2.91	0.000	0.000	13.8	0.429

APPENDIX 6: HUMIC ACID IODINE DYNAMICS MODEL

This appendix describes all model details using the format of the OpenModel software, for the model describing iodine dynamics in humic acid. Parameters k1 – k8 were fitted, as described in the main text. Symbols used for concentrations of species in solution are different from thesis text due to requirements of OpenModel for formatting

The use of ‘_x’ as a symbol suffix indicates that the symbol was produced for all nine solutions (+20, +40, +80 ppb; added iodide, iodate or mix; Table 5.1), for example Sum_Ide_x represents Sum_Ide_1 for +20 ppb iodide, Sum_Ide_2 for +40 ppb iodide, Sum_Ide_3 for +80 ppb iodide, etc.

SYMBOLS

Table A15. Variables

Symbol	Meaning
Sum_Ide_x	Sum of iodide-127 and iodide-129 ($\mu\text{g L}^{-1}$)
Sum_OrgI_x	Sum of Org ¹²⁷ I + Org ¹²⁹ I ($\mu\text{g L}^{-1}$)
Tot_N_x	Total ¹²⁷ I (native iodine) in system ($\mu\text{g L}^{-1}$)
Tot_S_x	Total ¹²⁹ I (spike iodine) in system ($\mu\text{g L}^{-1}$)

Table A16. ODEs

Symbol	Meaning
Ide_N_x	Iodide-127 ($\mu\text{g L}^{-1}$)
Ide_S_x	Iodide-129 ($\mu\text{g L}^{-1}$)
Ite_N_x	Iodate-127 ($\mu\text{g L}^{-1}$)
Ite_S_x	Iodate-129 ($\mu\text{g L}^{-1}$)
OrgI_N_x	Org ¹²⁷ I ($\mu\text{g L}^{-1}$)
OrgI_S_x	Org ¹²⁹ I ($\mu\text{g L}^{-1}$)

Parameters

Rate parameters k1 – k8 (hr^{-1}).

MODEL SET-UP

Initial

OrgI_N_1 = 93.072
OrgI_N_2 = 93.072
OrgI_N_3 = 93.072
OrgI_N_4 = 93.072
OrgI_N_5 = 93.072
OrgI_N_6 = 93.072
OrgI_N_7 = 93.072
OrgI_N_8 = 93.072
OrgI_N_9 = 93.072

Ide_N_1 = 20.930
Ide_N_2 = 20.930
Ide_N_3 = 20.930
Ide_N_4 = 20.930
Ide_N_5 = 20.930
Ide_N_6 = 20.930
Ide_N_7 = 20.930
Ide_N_8 = 20.930
Ide_N_9 = 20.930

Ite_N_1 = 0
Ite_N_2 = 0
Ite_N_3 = 0
Ite_N_4 = 0
Ite_N_5 = 0
Ite_N_6 = 0
Ite_N_7 = 0
Ite_N_8 = 0
Ite_N_9 = 0

Ide_S_1 = 22.053
Ite_S_1 = 0
OrgI_S_1 = 0

Ide_S_2 = 44.105
Ite_S_2 = 0
OrgI_S_2 = 0

Ide_S_3 = 88.211
Ite_S_3 = 0
OrgI_S_3 = 0

Ide_S_4 = 0
Ite_S_4 = 22.053
OrgI_S_4 = 0

Ide_S_5 = 0
Ite_S_5 = 44.105
OrgI_S_5 = 0

Ide_S_6 = 0
Ite_S_6 = 88.211
OrgI_S_6 = 0

Ide_S_7 = 11.026
Ite_S_7 = 11.026
OrgI_S_7 = 0

Ide_S_8 = 22.053
Ite_S_8 = 22.053
OrgI_S_8 = 0

Ide_S_9 = 44.105
Ite_S_9 = 44.105
OrgI_S_9 = 0

Sum_OrgI_1 = OrgI_N_1 + OrgI_S_1
Sum_OrgI_2 = OrgI_N_2 + OrgI_S_2
Sum_OrgI_3 = OrgI_N_3 + OrgI_S_3
Sum_OrgI_4 = OrgI_N_4 + OrgI_S_4
Sum_OrgI_5 = OrgI_N_5 + OrgI_S_5
Sum_OrgI_6 = OrgI_N_6 + OrgI_S_6
Sum_OrgI_7 = OrgI_N_7 + OrgI_S_7
Sum_OrgI_8 = OrgI_N_8 + OrgI_S_8
Sum_OrgI_9 = OrgI_N_9 + OrgI_S_9

Sum_Ide_1 = Ide_N_1 + Ide_S_1
Sum_Ide_2 = Ide_N_2 + Ide_S_2
Sum_Ide_3 = Ide_N_3 + Ide_S_3
Sum_Ide_4 = Ide_N_4 + Ide_S_4
Sum_Ide_5 = Ide_N_5 + Ide_S_5
Sum_Ide_6 = Ide_N_6 + Ide_S_6
Sum_Ide_7 = Ide_N_7 + Ide_S_7
Sum_Ide_8 = Ide_N_8 + Ide_S_8
Sum_Ide_9 = Ide_N_9 + Ide_S_9

Main

$Ite_S_1.rate = (k5 * OrgI_S_1) - (k4 * Ite_S_1) - (k1 * Ite_S_1)$
 $Ide_S_1.rate = (k1 * Ite_S_1) + (k2 * OrgI_S_1) - (k3 * Ide_S_1)$
 $OrgI_S_1.rate = (k3 * Ide_S_1) - (k2 * OrgI_S_1) + (k4 * Ite_S_1) - (k5 * OrgI_S_1)$

$Ide_N_1.rate = (k8 * OrgI_N_1) - (k7 * Ide_N_1)$
 $OrgI_N_1.rate = (k7 * Ide_N_1) - (k8 * OrgI_N_1)$

$Ite_S_2.rate = (k5 * OrgI_S_2) - (k4 * Ite_S_2) - (k1 * Ite_S_2)$
 $Ide_S_2.rate = (k1 * Ite_S_2) + (k2 * OrgI_S_2) - (k3 * Ide_S_2)$
 $OrgI_S_2.rate = (k3 * Ide_S_2) - (k2 * OrgI_S_2) + (k4 * Ite_S_2) - (k5 * OrgI_S_2)$

$Ide_N_2.rate = (k8 * OrgI_N_2) - (k7 * Ide_N_2)$
 $OrgI_N_2.rate = (k7 * Ide_N_2) - (k8 * OrgI_N_2)$

$Ite_S_3.rate = (k5 * OrgI_S_3) - (k4 * Ite_S_3) - (k1 * Ite_S_3)$

$$\begin{aligned} \text{Ide_S_3.rate} &= (k1 * \text{Ite_S_3}) + (k2 * \text{OrgI_S_3}) - (k3 * \text{Ide_S_3}) \\ \text{OrgI_S_3.rate} &= (k3 * \text{Ide_S_3}) - (k2 * \text{OrgI_S_3}) + (k4 * \text{Ite_S_3}) - (k5 * \text{OrgI_S_3}) \end{aligned}$$

$$\begin{aligned} \text{Ide_N_3.rate} &= (k8 * \text{OrgI_N_3}) - (k7 * \text{Ide_N_3}) \\ \text{OrgI_N_3.rate} &= (k7 * \text{Ide_N_3}) - (k8 * \text{OrgI_N_3}) \end{aligned}$$

$$\begin{aligned} \text{Ite_S_4.rate} &= (k5 * \text{OrgI_S_4}) - (k4 * \text{Ite_S_4}) - (k1 * \text{Ite_S_4}) \\ \text{Ide_S_4.rate} &= (k1 * \text{Ite_S_4}) + (k2 * \text{OrgI_S_4}) - (k3 * \text{Ide_S_4}) \\ \text{OrgI_S_4.rate} &= (k3 * \text{Ide_S_4}) - (k2 * \text{OrgI_S_4}) + (k4 * \text{Ite_S_4}) - (k5 * \text{OrgI_S_4}) \end{aligned}$$

$$\begin{aligned} \text{Ide_N_4.rate} &= (k8 * \text{OrgI_N_4}) - (k7 * \text{Ide_N_4}) \\ \text{OrgI_N_4.rate} &= (k7 * \text{Ide_N_4}) - (k8 * \text{OrgI_N_4}) \end{aligned}$$

$$\begin{aligned} \text{Ite_S_5.rate} &= (k5 * \text{OrgI_S_5}) - (k4 * \text{Ite_S_5}) - (k1 * \text{Ite_S_5}) \\ \text{Ide_S_5.rate} &= (k1 * \text{Ite_S_5}) + (k2 * \text{OrgI_S_5}) - (k3 * \text{Ide_S_5}) \\ \text{OrgI_S_5.rate} &= (k3 * \text{Ide_S_5}) - (k2 * \text{OrgI_S_5}) + (k4 * \text{Ite_S_5}) - (k5 * \text{OrgI_S_5}) \end{aligned}$$

$$\begin{aligned} \text{Ide_N_5.rate} &= (k8 * \text{OrgI_N_5}) - (k7 * \text{Ide_N_5}) \\ \text{OrgI_N_5.rate} &= (k7 * \text{Ide_N_5}) - (k8 * \text{OrgI_N_5}) \end{aligned}$$

$$\begin{aligned} \text{Ite_S_6.rate} &= (k5 * \text{OrgI_S_6}) - (k4 * \text{Ite_S_6}) - (k1 * \text{Ite_S_6}) \\ \text{Ide_S_6.rate} &= (k1 * \text{Ite_S_6}) + (k2 * \text{OrgI_S_6}) - (k3 * \text{Ide_S_6}) \\ \text{OrgI_S_6.rate} &= (k3 * \text{Ide_S_6}) - (k2 * \text{OrgI_S_6}) + (k4 * \text{Ite_S_6}) - (k5 * \text{OrgI_S_6}) \end{aligned}$$

$$\begin{aligned} \text{Ide_N_6.rate} &= (k8 * \text{OrgI_N_6}) - (k7 * \text{Ide_N_6}) \\ \text{OrgI_N_6.rate} &= (k7 * \text{Ide_N_6}) - (k8 * \text{OrgI_N_6}) \end{aligned}$$

$$\begin{aligned} \text{Ite_S_7.rate} &= (k5 * \text{OrgI_S_7}) - (k4 * \text{Ite_S_7}) - (k1 * \text{Ite_S_7}) \\ \text{Ide_S_7.rate} &= (k1 * \text{Ite_S_7}) + (k2 * \text{OrgI_S_7}) - (k3 * \text{Ide_S_7}) \\ \text{OrgI_S_7.rate} &= (k3 * \text{Ide_S_7}) - (k2 * \text{OrgI_S_7}) + (k4 * \text{Ite_S_7}) - (k5 * \text{OrgI_S_7}) \end{aligned}$$

$$\begin{aligned} \text{Ide_N_7.rate} &= (k8 * \text{OrgI_N_7}) - (k7 * \text{Ide_N_7}) \\ \text{OrgI_N_7.rate} &= (k7 * \text{Ide_N_7}) - (k8 * \text{OrgI_N_7}) \end{aligned}$$

$$\begin{aligned} \text{Ite_S_8.rate} &= (k5 * \text{OrgI_S_8}) - (k4 * \text{Ite_S_8}) - (k1 * \text{Ite_S_8}) \\ \text{Ide_S_8.rate} &= (k1 * \text{Ite_S_8}) + (k2 * \text{OrgI_S_8}) - (k3 * \text{Ide_S_8}) \\ \text{OrgI_S_8.rate} &= (k3 * \text{Ide_S_8}) - (k2 * \text{OrgI_S_8}) + (k4 * \text{Ite_S_8}) - (k5 * \text{OrgI_S_8}) \end{aligned}$$

$$\begin{aligned} \text{Ide_N_8.rate} &= (k8 * \text{OrgI_N_8}) - (k7 * \text{Ide_N_8}) \\ \text{OrgI_N_8.rate} &= (k7 * \text{Ide_N_8}) - (k8 * \text{OrgI_N_8}) \end{aligned}$$

$$\begin{aligned} \text{Ite_S_9.rate} &= (k5 * \text{OrgI_S_9}) - (k4 * \text{Ite_S_9}) - (k1 * \text{Ite_S_9}) \\ \text{Ide_S_9.rate} &= (k1 * \text{Ite_S_9}) + (k2 * \text{OrgI_S_9}) - (k3 * \text{Ide_S_9}) \\ \text{OrgI_S_9.rate} &= (k3 * \text{Ide_S_9}) - (k2 * \text{OrgI_S_9}) + (k4 * \text{Ite_S_9}) - (k5 * \text{OrgI_S_9}) \end{aligned}$$

$$\begin{aligned} \text{Ide_N_9.rate} &= (k8 * \text{OrgI_N_9}) - (k7 * \text{Ide_N_9}) \\ \text{OrgI_N_9.rate} &= (k7 * \text{Ide_N_9}) - (k8 * \text{OrgI_N_9}) \end{aligned}$$

$$\begin{aligned} \text{Sum_OrgI_1} &= \text{OrgI_N_1} + \text{OrgI_S_1} \\ \text{Sum_OrgI_2} &= \text{OrgI_N_2} + \text{OrgI_S_2} \\ \text{Sum_OrgI_3} &= \text{OrgI_N_3} + \text{OrgI_S_3} \\ \text{Sum_OrgI_4} &= \text{OrgI_N_4} + \text{OrgI_S_4} \\ \text{Sum_OrgI_5} &= \text{OrgI_N_5} + \text{OrgI_S_5} \\ \text{Sum_OrgI_6} &= \text{OrgI_N_6} + \text{OrgI_S_6} \\ \text{Sum_OrgI_7} &= \text{OrgI_N_7} + \text{OrgI_S_7} \\ \text{Sum_OrgI_8} &= \text{OrgI_N_8} + \text{OrgI_S_8} \\ \text{Sum_OrgI_9} &= \text{OrgI_N_9} + \text{OrgI_S_9} \end{aligned}$$

$$\begin{aligned} \text{Sum_Ide_1} &= \text{Ide_N_1} + \text{Ide_S_1} \\ \text{Sum_Ide_2} &= \text{Ide_N_2} + \text{Ide_S_2} \\ \text{Sum_Ide_3} &= \text{Ide_N_3} + \text{Ide_S_3} \\ \text{Sum_Ide_4} &= \text{Ide_N_4} + \text{Ide_S_4} \end{aligned}$$

$$\begin{aligned} \text{Sum_Ide_5} &= \text{Ide_N_5} + \text{Ide_S_5} \\ \text{Sum_Ide_6} &= \text{Ide_N_6} + \text{Ide_S_6} \\ \text{Sum_Ide_7} &= \text{Ide_N_7} + \text{Ide_S_7} \\ \text{Sum_Ide_8} &= \text{Ide_N_8} + \text{Ide_S_8} \\ \text{Sum_Ide_9} &= \text{Ide_N_9} + \text{Ide_S_9} \end{aligned}$$

$$\begin{aligned} \text{Tot_S_1} &= \text{Ite_S_1} + \text{Ide_S_1} + \text{OrgI_S_1} \\ \text{Tot_N_1} &= \text{Ite_N_1} + \text{Ide_N_1} + \text{OrgI_N_1} \end{aligned}$$

$$\begin{aligned} \text{Tot_S_9} &= \text{Ite_S_9} + \text{Ide_S_9} + \text{OrgI_S_9} \\ \text{Tot_N_9} &= \text{Ite_N_9} + \text{Ide_N_9} + \text{OrgI_N_9} \end{aligned}$$

$$\begin{aligned} \text{Tot_S_2} &= \text{Ite_S_2} + \text{Ide_S_2} + \text{OrgI_S_2} \\ \text{Tot_N_2} &= \text{Ite_N_2} + \text{Ide_N_2} + \text{OrgI_N_2} \end{aligned}$$

DATA SHEETS

Data sheets containing mean and standard error for each measured time point, for all solutions (1-9, Table 5.1) produced. Data for solution 6 were in separate tables which had one less time point but were otherwise the same.

Table A17. Part of ‘mean_most’ input data sheet, containing mean concentrations for solutions 1 – 5 and 7 – 9. This table shows only information for solutions one and two; actual data sheet continues with columns for all solutions.

Time (hr)	Ide_S_1	Ite_S_1	OrgI_S_1	Ide_N_1	OrgI_N_1	Sum_Ide_1	Sum_OrgI_1	Ide_S_2	Ite_S_2	OrgI_S_2	Ide_N_2	OrgI_N_2
26	20.53	0.007	0.007	23.27	84.26	43.8	84.27	41.02	0.007	0.007	23.55	87.61
79	20.62	0.007	0.007	22.96	90.46	43.58	90.46	41.73	0.007	0.29	23.28	92.77
155	20.86	0.007	1.4	22.9	94.81	43.76	96.2	40.64	0.007	2.7	22.61	94.52
328	19.6	0.007	2.04	21.43	96.17	41.04	98.21	39.05	0.007	4.48	22.03	98.24
596	18.39	0.007	3.37	20.12	98.19	38.52	101.56	35.63	0.007	6.25	20.14	93.23
992	17.06	0.007	3.18	17.48	95.7	34.54	98.88	34.59	0.007	5.74	17.67	95.3
1404	17.15	0.007	3.36	16.77	97.99	33.92	101.34	33.69	0.007	7.09	16.93	97.82
1855	16.91	0.007	4.67	15.86	99.6	32.77	104.27	33.44	0.007	8.14	16.74	99.63

Table A18. Part of ‘std_error_most’ input data sheet, containing standard errors for concentrations in solutions 1 – 5 and 7 – 9. This table shows only information for solutions one and two; actual data sheet continues with columns for all solutions.

Time (hr)	Ide_S_1	Ite_S_1	OrgI_S_1	Ide_N_1	OrgI_N_1	Sum_Ide_1	Sum_OrgI_1	Ide_S_2	Ite_S_2	OrgI_S_2	Ide_N_2	OrgI_N_2	Sum_Ide_2	Sum_OrgI_2
26	0.0439	0.007	0.007	0.0439	0.0439	0.0439	0.0439	0.0423	0.007	0.007	0.0423	0.0423	0.0423	0.0423
79	0.0439	0.007	0.007	0.0439	0.0439	0.0439	0.0439	0.0423	0.007	0.0423	0.0423	0.0423	0.0423	0.0423
155	0.0439	0.007	0.0439	0.0439	0.0439	0.0439	0.0439	0.0423	0.007	0.0423	0.0423	0.0423	0.0423	0.0423
328	0.0439	0.007	0.0439	0.0439	0.0439	0.0439	0.0439	0.0423	0.007	0.0423	0.0423	0.0423	0.0423	0.0423
596	0.0439	0.007	0.0439	0.0439	0.0439	0.0439	0.0439	0.0423	0.007	0.0423	0.0423	0.0423	0.0423	0.0423
992	0.0439	0.007	0.0439	0.0439	0.0439	0.0439	0.0439	0.0423	0.007	0.0423	0.0423	0.0423	0.0423	0.0423
1404	0.0439	0.007	0.0439	0.0439	0.0439	0.0439	0.0439	0.0423	0.007	0.0423	0.0423	0.0423	0.0423	0.0423
1855	0.0439	0.007	0.0439	0.0439	0.0439	0.0439	0.0439	0.0423	0.007	0.0423	0.0423	0.0423	0.0423	0.0423

APPENDIX 7: GRASS UPTAKE MODEL

This appendix describes all model details using the format of the OpenModel software, for the model describing iodine uptake by grass. The model was set up individually for uptake from all soils. Parameters k_6 , k_7 and kp_N (kp_N) and kp_s (kp_s) were fitted, as described in the main text. Symbols used for concentrations of species in solution are different from thesis text due to requirements of OpenModel for formatting

SYMBOLS

Table A19. Variables

Symbol	Meaning
Ide_N_sltn	Iodide-127 in solution ($\mu\text{g L}^{-1}$)
Ine_N_irri	Input of iodine-127 from irrigation water ($\mu\text{g hr}^{-1}$)
Ine_S_sltn_I	Iodine-129 in solution after addition of iodide-129 ($\mu\text{g L}^{-1}$)
Ine_S_sltn_IO	Iodine-129 in solution after addition of iodate-129 ($\mu\text{g L}^{-1}$)
k1	Optimised rate constant for ^{129}I -soil dynamics (Ch. 4) (hr^{-1}) Unique soil value
k2	Optimised rate constant for ^{129}I -soil dynamics (Ch. 4) (hr^{-1}) Unique soil value
k3	Optimised rate constant for ^{129}I -soil dynamics (Ch. 4) (hr^{-1}) Unique soil value
k4	Optimised rate constant for ^{129}I -soil dynamics (Ch. 4) (hr^{-1}) Unique soil value
k5	Optimised rate constant for ^{129}I -soil dynamics (Ch. 4) (hr^{-1}) Unique soil value
kd	Optimised instant partitioning coefficient for ^{129}I -soil dynamics (Ch. 4) (L kg^{-1}) Unique soil value
k2	Optimised instant partitioning coefficient for ^{129}I -soil dynamics (Ch. 4) (L kg^{-1}) Unique soil value
kd3	Optimised instant partitioning coefficient for ^{129}I -soil dynamics (Ch. 4) (L kg^{-1}) Unique soil value
m	Oven-dry mass of soil in system (kg) Unique soil value
OrgI_N_sltn	Org ^{127}I in solution ($\mu\text{g L}^{-1}$) Unique soil value
SIC	Soil iodine concentration (mg kg^{-1}) Unique soil value
Tot_S_I	Total iodine-129 in solution after addition of iodide-129 ($\mu\text{g L}^{-1}$)
Tot_S_IO	Total iodine-129 in solution after addition of iodate-129 ($\mu\text{g L}^{-1}$)
v	Volume of solution in system (L) Unique soil value

Table A20. ODEs

Symbol	Meaning
Ide_S_sltn_I	Iodide-129 in solution after addition of iodide-129 ($\mu\text{g L}^{-1}$)
Ide_S_sltn_IO	Iodide-129 in solution after addition of iodate-129 ($\mu\text{g L}^{-1}$)
Ine_N_plant	Iodine-127 in grass, cumulative weight; $^{127}\text{I}_{\text{G,C}}$ in main text (μg)
Ine_N_sltn	Iodine-127 in solution ($\mu\text{g L}^{-1}$)
Ine_N_solid	Iodine-127 on soil solid phase ($\mu\text{g kg}^{-1}$)
Ine_S_plant	Iodine-129 in grass, cumulative weight; $^{129}\text{I}_{\text{G,C}}$ in main text (μg)
Ine_S_solid_I	Iodine-129 on soil solid phase after addition of iodide ($\mu\text{g kg}^{-1}$)
Ine_S_solid_IO	Iodine-129 on soil solid phase after addition of iodate ($\mu\text{g kg}^{-1}$)
Ite_S_sltn_I	Iodate-129 in solution after addition of iodide-129 ($\mu\text{g L}^{-1}$)
Ite_S_sltn_IO	Iodate-129 in solution after addition of iodate-129 ($\mu\text{g L}^{-1}$)
OrgI_S_sltn_I	Org ^{129}I in solution after addition of iodide-129 ($\mu\text{g L}^{-1}$)
OrgI_S_sltn_IO	Org ^{129}I in solution after addition of iodate-129 ($\mu\text{g L}^{-1}$)

Parameters

Rate parameters k_6 , k_7 , kp_N (kp_N in main text) and kp_s (kp_s in main text) (hr^{-1}).

MODEL SET-UP

Initial

$$m = 0.0040$$

$$v = 0.02403$$

$$\text{SIC} = 2.89$$

$$k_2 = (k_1 * \text{Ide_N_sltn}) / (\text{Ine_N_solid} * (m/v))$$

$$k_4 = (k_3 * \text{Ide_N_sltn}) / \text{OrgI_N_sltn}$$

$$\text{Ine_N_sltn} = 1.85$$

$$\text{Ide_N_sltn} = 0.87$$

$$\text{OrgI_N_sltn} = 0.94$$

//Iodide added

$$\text{Tot_S_I} = 2.207$$

$$\text{Ite_S_sltn_I} = 0$$

$$\text{Ide_S_sltn_I} = \text{Tot_S_I} / ((kd * m) + v)$$

$$\text{Ine_S_solid_I} = kd * \text{Ide_S_sltn_I}$$

$$\text{Ine_N_irri} = 0.000734$$

$$k_1 = 0.3334$$

$$k_3 = 0.0157$$

$$k_5 = 0.060290$$

$$kd = 0.0000000001$$

$$kd_2 = 18.33$$

$$kd_3 = 0.08982$$

//Iodate added

$$\text{Tot_S_IO} = 2.205$$

$$\text{Ite_S_sltn_IO} = \text{Tot_S_IO} / (kd_3 * v + v + kd_2 * m)$$

$$\text{Ide_S_sltn_IO} = 0$$

$$\text{OrgI_S_sltn_IO} = \text{Ite_S_sltn_IO} * kd_3$$

$$\text{Ine_S_solid_IO} = kd_2 * \text{Ite_S_sltn_IO}$$

$$\text{Ine_S_plant} = 0$$

$$\text{Ine_N_solid} = ((m * \text{SIC} * 1000) - (\text{Ine_N_sltn} * v)) / m$$

Main

$$k_1 = 0.3334$$

$$k_3 = 0.0157$$

$$k_5 = 0.060290$$

$$kd = 0.0000000001$$

$$kd_2 = 18.33$$

$$kd_3 = 0.08982$$

$$k_4 = (k_3 * \text{Ide_N_sltn}) / \text{OrgI_N_sltn}$$

$$k_2 = (k_1 * \text{Ide_N_sltn}) / (\text{Ine_N_solid} * (m/v))$$

```
//Iodide added
OrgI_S_sltn_I.rate = (k3*Ide_S_sltn_I) - (k4*OrgI_S_sltn_I)
Ite_S_sltn_I.rate = - (k5 * Ite_S_sltn_I)
Ide_S_sltn_I.rate = (k5 * Ite_S_sltn_I) + (k2 * Ine_S_solid_I * (m/v)) - (k1 * Ide_S_sltn_I) + (k4 *
OrgI_S_sltn_I) - (k3 * Ide_S_sltn_I)
Ine_S_solid_I.rate = (k1*Ide_S_sltn_I*(v/m)) - (k2*Ine_S_solid_I)
```

```
Ine_S_sltn_I = Ide_S_sltn_I + OrgI_S_sltn_I + Ite_S_sltn_I
Tot_S_I = (Ine_S_sltn_I * v) + (Ine_S_solid_I * m)
```

```
//Iodate added
Ite_S_sltn_IO.rate = - (k5 * Ite_S_sltn_IO) - (kp_S * Ite_S_sltn_IO)
Ide_S_sltn_IO.rate = (k5 * Ite_S_sltn_IO) + (k2 * Ine_S_solid_IO * (m/v)) - (k1 * Ide_S_sltn_IO) +
(k4 * OrgI_S_sltn_IO) - (k3 * Ide_S_sltn_IO) - (kp_S * Ide_S_sltn_IO)
OrgI_S_sltn_IO.rate = (k3*Ide_S_sltn_IO) - (k4*OrgI_S_sltn_IO) - (kp_S * OrgI_S_sltn_IO)
Ine_S_solid_IO.rate = (k1*Ide_S_sltn_IO*(v/m)) - (k2*Ine_S_solid_IO)
```

```
Ine_S_sltn_IO = Ide_S_sltn_IO + OrgI_S_sltn_IO + Ite_S_sltn_IO
Tot_S_IO = (Ine_S_sltn_IO * v) + (Ine_S_solid_IO * m)
```

```
Ine_S_plant.rate = kp_S * Ine_S_sltn_IO * v
```

```
//Native iodine
Ine_N_solid.rate = (k7 * Ine_N_sltn) - (k6 * Ine_N_solid)
Ine_N_sltn.rate = (Ine_N_irri/v) - (kp_N/(t+1) * Ine_N_sltn) + (k6 * Ine_N_solid) - (k7 * Ine_N_sltn)
Ine_N_plant.rate = (kp_N/(t+1)) * Ine_N_sltn * v
```

DATA SHEETS

Data sheets containing mean and standard error for each measured time point were included for each soil's model. These sheets are for NI01 as an example.

Table A21. Input data sheet 'NI01_plant_means', containing mean Ine_S_plant (129IG,C) and Ine_N_plant (127IG,C) for NI01.

Time (hr)	Ine_S_plant	Ine_N_plant
672	0.002943	0.05233
1032	0.004099	0.06061
1560	0.004821	0.06375
2448	0.005722	0.0705

Table A22. Input data sheet 'NI01_plant_weight', containing weightings for Ine_S_plant (129IG,C) and Ine_N_plant (127IG,C) for NI01.

Time (hr)	Ine_S_plant	Ine_N_plant
672	0.287	0.295
1032	0.287	0.295
1560	0.287	0.295
2448	0.287	0.295